Entanglement between Quarks in Hadrons

Peter John Ehlers

A dissertation
submitted in partial fulfillment of the
requirements for the degree of

Doctor of Philosophy

University of Washington

2022

Reading Committee:
Silas Beane, Chair
David Kaplan
Martin Savage

Program Authorized to Offer Degree:
Physics

University of Washington

Abstract

Entanglement between Quarks in Hadrons

Peter John Ehlers

Chair of the Supervisory Committee:
Silas Beane
Department of Physics

Entanglement between valence quarks and the sea in hadrons is shown to be deeply connected to important features of QCD, namely chiral symmetry breaking and confinement. The sea degrees of freedom can be traced over to give a reduced density matrix, and it is shown that the resulting entanglement entropy acts as an order parameter of chiral symmetry breaking and potentially confinement in the nucleon. A general decomposition of the nucleon state in components labeled by definite chiral transformation properties is considered. In particular, the most general expression of the nucleon state in the chiral basis with three valence quarks is constructed, consistent with known QCD constraints, and its properties are studied. In the chiral basis, the nucleon state is naturally a bipartite system where all non-valence spin can be traced over to give a reduced density matrix for the valence spin. It is shown that the resulting entanglement entropy acts as an order parameter of chiral symmetry breaking on the null-plane. In the large-N_c limit, the entanglement entropy is minimized and the valence spin accounts for all of the nucleon spin, while in the limit of maximal entanglement entropy, the nucleon loses all memory of the valence spin and is therefore entirely accounted for by the non-valence spin. This suggests that the small observed valence content of the proton spin is a signature of strong entanglement in the nucleon between the valence quarks and the sea. The nucleon state vector in the chiral basis, fit to low-energy data, gives a valence spin content consistent with experiment and lattice QCD determinations, and has

large entanglement entropy.

Entanglement between valence and sea quarks in 1+1d QCD is also considered. While predecessors to QCD such as the parton model had a clear distinction between valence and sea particles, the Fock state expansion of a hadron gives no unambiguous definition of which quarks are valence quarks and which belong to the parton sea aside from their flavor. A rigorous definition of valence-sea (VS) entanglement in QCD is developed, which is consistent with the observation that it vanishes in the large-N_c limit and will remain low when finite-N_c states resemble their large-N_c counterparts. We perform a numerical study of VS entanglement in 1+1 dimensional discrete light-cone quantized QCD, and in the process develop a method for building the color-singlet basis of 1+1d QCD that is manifestly complete and orthogonal by construction. We find that the VS entanglement entropy for the first few excited states of both mesons and baryons is relatively low compared to all other states in the spectrum, with the VS entropy of ground state hadrons providing a minimum. We also see that for ground state mesons the entropy is well described in the $1/N_c$ approximation. These results suggest that low energy hadrons may be the only QCD bound states for which the large-N_c expansion, and perhaps the parton model, provide an accurate description. This work also provides evidence that the VS entanglement entropy of QCD in 3+1d, which would likely serve as an order parameter for the QCD phase transition, may be perturbatively accessible through a large-N_c expansion, and we develop a qualitative picture of what the VS entanglement entropy of nucleons in real QCD may look like.

TABLE OF CONTENTS

LIST OF FIGURES

LIST OF TABLES

DEDICATION

To my parents

Chapter 1

INTRODUCTION

The study of nuclear physics is the study of the strong nuclear force. It is called the "strong" nuclear force because at a distance of 1 femtometer or more it is orders of magnitude larger than the other three fundamental forces. This interaction is relevant for a class of subatomic particles called hadrons, which includes protons, neutrons, and pions. All atomic nuclei are composed of hadrons, and the vast majority of the mass of any atom comes from this nucleus. In turn, hadrons themselves are composite states which are bound together due to the strong interaction, and the masses of hadrons are primarily due to the energy stored in the interactions. The forces that bind atomic nuclei together are also described by this interaction, as a residual force mediated by light hadrons called pions [1].

In the theory of the strong interactions, fundamental particles called quarks interact via a fundamental force that is mediated by particles called gluons. These are the only particles that interact this way because they carry a color charge, which is similar to how particles with electric charge interact through exchanges of photons. One big difference between the strong force and electromagnetism are that quarks have three different types of color charge, simply called "colors", along with another three anti-charges of anti-quarks, whereas the electric charge has just one type along with its opposite. In addition, when the three colors are brought together, they form a color neutral combination called a "singlet" which is largely inert under the strong interaction.

Another difference is that the gluons that mediate the interaction have color charge and will interact with other gluons, while the photons that mediate electromagnetism have no electric charge. This leads to the strong interaction building up with distance instead of tapering off, causing the quarks to bind into color neutral combinations, forming the hadrons

we observe in nature. These differences are the reason why the strongest fundamental force only seems to matter at subatomic scales; the different charges necessarily form singlets and cancel each other out, leaving a residual interaction between hadrons that falls off very quickly with distance [1]. Additionally, there is no way to isolate a quark from other quarks at large distances, as an attempt to do so would generate enough energy to create quark-antiquark pairs that form more singlet hadrons. Consequently, The existence of quarks is inferred from the properties of hadrons.

There are many different types of hadrons, and each one can be defined by a handful of the constituent quarks called valence quarks. There is a heavier class of hadrons, called baryons, which have three valence quarks, and a lighter class called mesons that have one quark and one antiquark as valence particles. There are six flavors of quark, and different combinations of these create the different kinds of hadrons in nature. However, only the up and down quarks, which are the two lightest flavors, are abundant in nature. As an example, the proton always has two up quarks and one down quark as its valence quarks, while the neutron has two downs and one up. The up quark has an electric charge of $\frac{2}{3}e$, where e is the magnitude of charge of the electron, while the down quark has a charge of $-\frac{1}{3}e$. This results in the proton having a total charge of e and the neutron having no charge at all. This shows how the intrinsic properties of the valence quarks determine the same quantities of the hadrons they represent.

The valence quarks are not the only particles that make up hadrons. There are also a myriad of sea quarks and gluons, which have significant contributions to some hadron properties such as their mass and helicity [2]. This suggests that there could be a significant degree of connection between the valence and sea contributions inside of hadrons. To be more specific, the hadrons exist as definite quantum states that are superpositions of valence and sea quark states. A quantum superposition means that measuring the valence and sea quarks in the hadron states will not give a deterministic answer, it will be a probabilistic outcome. Since the quarks are in superposition when the hadron is not, this implies that there is some information in the hadron state that cannot be obtained from measuring the

quark states alone. This is what is referred to as quantum entanglement, and it can be quantified using what is known as entanglement entropy. Many of the chief results of this work revolve around the presence of entanglement between quarks inside of hadrons.

In the rest of Chapter 1, we will explain a bit more about theory of the strong interactions as well as a description of quantum entanglement and entropy. The theory of the strong interactions, known as quantum chromodynamics (QCD), has a number of key features that are central topics in nuclear physics, and we will briefly discuss them here as they are motivating factors for our research. We will also overview some of the background related to QCD that will be relevant for our research in later chapters. We will also describe information theory, entropy, and entanglement to establish these concepts, as they can be difficult to understand yet are similarly central to this work.

1.1 Quantum Chromodynamics

Quantum chromodynamics, or QCD, is currently the best theory of the strong interactions, and it is part of the Standard Model of particle physics. The Standard Model is currently the most accurate and most complete description of particle physics available to us. It incorporates the strong nuclear force, electromagnetism, and the weak nuclear force all in one theory, and describes how matter interacts under these forces. Since this is the strongest of the four fundamental forces by several orders of magnitude, it makes sense to look at this theory separately from the rest of the Standard Model. It is a quantum field theory, so describing QCD will necessarily require an overview of what that is and how we use it. The majority of this section will be devoted to establishing the building blocks of quantum field theories, specifically those that are relevant for QCD. Much of the material in this section is also covered in standard textbooks on quantum field theory, such as [3].

The fundamental element of a quantum field theory is, as the name implies, the quantum fields corresponding to the kinds of particles found in the theory. In QCD, we have the fields $q_{c,f,s}(x)$ representing a quark with one of three color charges c, one of six flavors f, and one of four spinor indices s at a point in spacetime x. Also, we have the fields $A^a_\mu(x)$ that represent

a gluon with four-vector component μ and adjoint color charge a at a point in spacetime x.

A quantum field theory can be defined by its action S, which is a quantity made up of field operators that ultimately contains all of the information about the dynamics of a given quantum field theory. In QCD, the action splits into two parts, the part with quark fields S_q and the part with only gluons S_g. The quark part of the action is given by

$$S_q = \int d^4x \sum_{f=1}^{6} \left(\sum_{c=1}^{3} \bar{q}_{c,f}(x) \left(i\partial_\mu \gamma^\mu - m_f \right) q_{c,f}(x) + \sum_{a=1}^{8} g A^a_\mu(x) \left(\sum_{c,c'=1}^{3} \bar{q}_{c,f}(x) \gamma^\mu T^a_{cc'} q_{c',f}(x) \right) \right) \tag{1.1}$$

Here we have made the spinor indices implicit, so that the quark fields are effectively vectors in spin space, with the γ^μ's as matrices in spinor space. There are also matrices in color space T^a, quark masses for each flavor given by m_f, and the coupling constant g of the strong interactions. The first term under the integral, called the kinetic term, determines the dynamics of the quarks in the absence of all interactions, and the second term proportional to g determines how the quarks interact with gluons. In particular, it shows that a quark or antiquark can emit or absorb a gluon, a quark and antiquark can annihilate and become a gluon, or a gluon could become and quark-antiquark pair.

The gluon-only part of the action S_g can also be separated into kinetic and interaction terms. With $A_\mu(x) = \sum_{a=1}^{8} A^a_\mu(x) T^a$ as a matrix in color space, we have for the kinetic term

$$S_{g,kin} = \int d^4x \, \frac{1}{2} \mathrm{Tr} \left[\left(\partial_\mu A_\nu(x) - \partial_\mu A_\nu(x) \right) \partial^\mu A^\nu(x) \right]. \tag{1.2}$$

This also encodes how the gluons behave without interaction. The interaction term looks like

$$S_{g,int} = \int d^4x \, \left(-ig \, \mathrm{Tr} \left[[A_\mu(x), A_\nu(x)] \, \partial^\nu A^\mu(x) \right] + \frac{g^2}{2} \mathrm{Tr} \left[[A_\mu(x), A_\nu(x)] \, A^\mu(x) A^\nu(x) \right] \right) \tag{1.3}$$

Where $[A_\mu(x), A_\nu(x)] = A_\mu(x)A_\nu(x) - A_\nu(x)A_\mu(x)$ and g is yet again the strong coupling constant. These interactions show that a single gluon can absorb and emit one or two other gluons at a time, or two gluons can directly exchange properties when they meet.

The action as a whole can be made much simpler if we consider what is known as gauge symmetry. A symmetry of the action describes a transformation of the quark and gluon fields that does not modify the action, and a gauge symmetry describes a transformation that depends on space and time. The presence of a gauge symmetry implies that parts of the fields are not physical, so all measurable quantities in the theory must also exhibit this symmetry. The gauge symmetry transformation of the QCD action is given by

$$q_f(x) \to U(x)q_f(x) \qquad A_\mu(x) \to U(x)A_\mu(x)U^\dagger(x) + \frac{i}{g}U(x)\partial_\mu U^\dagger(x), \tag{1.4}$$

where $U(x)$ can be any 3×3 special unitary matrix in color space. This gauge symmetry is ultimately what defines QCD from a theoretical perspective, as it is the most basic theory of quarks and gluons that transform under the Lie group $SU(3)$. It turns out that the quark and gluon terms in the action are separately gauge invariant. To see this, we can define the operator $D_\mu = \partial_\mu - igA_\mu(x)$, which transforms as $D_\mu \to U(x)D_\mu U^\dagger(x)$, with the $U^\dagger(x)$ being applied *before* the derivative. With this, the quark part of the action can be written as simply

$$S_q = \int d^4x \ \sum_{f=1}^{6} \bar{q}_f(x) \left(iD_\mu\gamma^\mu - m_f\right) q_f(x). \tag{1.5}$$

Likewise, we can simplify the gluon-only term by defining the field strength tensor $F_{\mu\nu}(x) = (\partial_\mu A_\nu(x) - \partial_\mu A_\nu(x) - ig\left[A_\mu(x), A_\nu(x)\right])$ which transforms as $F_{\mu\nu} \to U(x)F_{\mu\nu}U^\dagger(x)$. The action then becomes

$$S_g = \int d^4x \ \frac{-1}{4}\mathrm{Tr}\left[F_{\mu\nu}F^{\mu\nu}\right]. \tag{1.6}$$

This gives us a fairly simple expression for the full action

$$S = \int d^4x \ \left(\sum_{f=1}^{6} \bar{q}_f(x) \left(iD_\mu\gamma^\mu - m_f\right) q_f(x) - \frac{1}{4}\mathrm{Tr}\left[F_{\mu\nu}F^{\mu\nu}\right]\right). \tag{1.7}$$

In fact, the gauge symmetry helps explain why all three interactions use the same coupling constant g, as there would be no symmetry if they we allowed to be different.

While the action itself is fairly simple to formulate, using it as a starting point to calculate a physical quantity can be a long and arduous process. The action is used as part of a weight

function within a path integral, where the quark and gluons fields at each position treated as variables that are integrated over to get physical quantities. We do not know how to do these path integrals by hand for nearly all interacting theories, but perturbative methods exist where the interactions are expanded out into an infinite series of calculable terms. If the series converges for a given physical quantity, only the first few terms in the series will be needed to get an accurate result. Unfortunately, this expansion does not converge for QCD in the low energy regime where hadrons form. This is because the coupling constant g turns out to not be constant at all. Due to subtleties of the quantum field theory, it acquires a dependence on the energy scale of the physical quantity, with g decreasing as the scale increases and vice-versa [4, 5]. This is the reason why QCD exhibits both asymptotic freedom at high energies and confinement at low energies, but it also makes the theory much more difficult to work with, and the complete description of a hadron in terms of quark and gluon degrees of freedom is generally very difficult to obtain.

There are other approaches to working with QCD that do not involve perturbation theory. Chief among them are lattice methods, where spacetime is split up into discrete points, which renders the path integral calculable numerically by computers. Lattice calculations can be very resource intensive, however, and the precision of such calculations is limited by the technological capabilities of modern supercomputers. A promising future alternative would be lattice calculations done on quantum computers [6]. These simulations would use QCD in the Hamiltonian formalism, where the quark and gluon fields are rendered as operators that act on states in a Hilbert space. These states represent possible configurations of particles in the universe at a given time, and states at all other times are obtained from the Hamiltonian operator H. This operator is the generator of time translations in the theory, and it also determines the energy spectrum of the theory. The time translation operator is unitary, and quantum computers are much better suited to performing unitary operations than classical ones. The vast majority of this work will deal with QCD in the Hamiltonian formalism.

There is another important symmetry to consider in QCD, which is chiral symmetry. Chirality is another property of spin-$\frac{1}{2}$ fermions that, like its spin, can take one of two values,

dubbed "left-handed" and "right-handed". In fact, the spinor field ψ that represents such a fermion can be thought of in a particular basis as a 4-component vector, where each component corresponds to a specific choice of both spin and chirality simultaneously. Chirality originates from the representation theory of the Lorentz group, which is the symmetry group for the changing of reference frames in special relativity. The generators of spatial rotations J^i and the generators of boosts K^i can be reorganized into the operators $N^i_\pm = \frac{1}{\sqrt{2}}(J^i \pm iK^i)$, which have the commutation relations $[N^i_\pm, N^j_\pm] = i\epsilon_{ijk}N^k_\pm$ and $[N^i_+, N^j_-] = 0$. These are exactly the same relations as the generators of an $SU(2) \times SU(2)$ symmetry group, where each different $SU(2)$ factor allies to the two different chiralities. Chiral symmetry specifically refers to the symmetry group $SU_L(N_f) \times SU_R(N_f)$ for N_f quark flavors, where we apply unitary transformation to the quarks that may rearrange the flavors, and we can do completely different transformations to the two different chiralities.

However, QCD is not actually symmetric under the full chiral symmetry group for a couple of reasons. First, the quark masses break chiral symmetry explicitly as the mass term in the action couples the left- and right-handed quarks and is flavor dependent. Also, and perhaps more importantly, the QCD vacuum state does not exhibit full chiral symmetry, which is a phenomenon known as spontaneous symmetry breaking. It is known that when this occurs on its own, there will be single particle excitations above the vacuum known as Nambu-Goldstone bosons which have no mass [7, 8]. If the quark masses were zero, then this mechanism would guarantee that pions and other light mesons would have zero mass. Instead, the quark masses make these mesons into pseudo-Goldstone bosons, whose masses are proportional to the square root of the quark masses [9]. This mechanism explains why the pions and other light mesons are as light as they are compared to the baryons, as the lightness of the quarks themselves transfers over to the mesons as well.

Throughout this dissertation, we will be working in the null-plane formalism. Ordinarily when working with state vectors in a quantum field theory we define them at a specific time, then evolve the states to a different time using the Hamiltonian $H = P_0$, in what is known as the instant form. In the null-pane formalism, we instead define the states using light-cone

coordinates $x^{\pm} = \frac{1}{\sqrt{2}}(x^0 \pm x^3)$ at $x^+ = 0$ and evolve the states to a different value of x^+ with the null-pane Hamiltonian P^-. The benefit of this formalism comes from considering the full Poincaré group and the dynamical generators, which are the generators that evolve states out of the initial plane that they are defined in. The Poincaré group is the group generated by the momentum operators P^μ, which generate spacetime translations, along with the rotation and boost generators $M^{\mu\nu}$ from the Lorentz group of special relativity. In the instant form, these generators are more commonly used in the form $J^i = \frac{1}{2}\epsilon_{0ijk}M^{jk}$ for spatial rotations and $K^i = M^{0i}$ for boosts. They can also be written in terms of spacetime coordinates as $M^{\mu\nu} = x^\mu\partial^\nu - x^\nu\partial^\mu + S^{\mu\nu}$, where $S^{\mu\nu}$ is a matrix that acts upon spin degrees of freedom. The dynamical generators in the instant form are the time translation operator P^0 and the boosts K^i since they contain time derivatives.

In the null plane, the dynamical generators contain the derivative $\partial^- = \partial_+$, which include P^-, $M^{-,1}$, and $M^{-,2}$. $M^{+,-}$ would be a dynamical generator as well since it contains a term given by $x^+\partial^-$, but on the null plane $x^+ = 0$ so this term vanishes, so this generator turns out to not be dynamical after all. Thus there are only 3 dynamical generators on the null plane compared to the usual 4. This is especially useful when we repackage these generators using $\mathcal{M}^2 = 2P^-P^+ - (P^1)^2 - (P^2)^2$ instead of P^- and $\mathcal{J}^r$ instead of $M^{-,r}$ for $r = 1, 2$. With the Pauli-Lubanski operator defined by $W_\mu = \frac{1}{2}\epsilon_{\mu\nu\alpha\beta}P^\nu M^{\alpha\beta}$, the operators $\mathcal{J}^r$ are defined by $\mathcal{M}\mathcal{J}^r = W^r - \frac{P^r}{P^+}W^+$, along with $\mathcal{J}^3 = \frac{W^+}{P^+}$ which is not dynamical. The operator $\mathcal{M}^2$ commutes with all other Poincaré generators, while the operators $\mathcal{J}^i$ for $i = 1, 2, 3$ obey $[\mathcal{J}^i, \mathcal{J}^j] = i\epsilon_{ijk}\mathcal{J}^k$ among each other and commute with the remaining generators $P^+, P^r, M^{+,-}$, and $M^{+,r}$ [10]. This means that the dynamics transformations in the null plane formalism can be separated algebraically from the kinematics on the plane. Note that this would not be possible in the instant form since the 4th dynamical generator given by $\sum_{i=1}^{3} P^i K^i$ is not contained in the Pauli-Lubanski operators and therefore cannot be algebraically separated from the other Poincaré generators.

There are a number of ways to modify the theory of QCD which can maintain some aspects of the original theory while being simpler to work with. One such method is to

change the number of color charges in the theory [11–13]. For a QCD-like theory with a number of colors N_c, the corresponding action will look identical to that of QCD, except that the gauge symmetry will be $SU(N_c)$, with the quarks in its fundamental representation and the gluons in its adjoint representation. It turns out that the limit in which N_c becomes infinite, known as the large-N_c limit, is a much simpler theory to work with that still resemble real QCD in a number of ways. This is because the large-N_c limit suppresses interactions where quark-antiquark pairs are created and annihilated, leaving only the quark interactions where they absorb and emit gluons. The mesons in large-N_c are thus only composed of one quark, one antiquark, and gluons. Baryons in large-N_c are much more difficult to work with because they must contain N_c valence quarks and so some of its properties go to infinity, such as its mass, but not all of them do. The large-N_c limit will be important in the chapters to come because they only contain valence quarks, so there are no sea quarks to be entangled with, making this limit an important touchstone for defining quark entanglement.

Another useful way to modify the theory of QCD is to change the number of spatial dimensions, in particular looking at QCD in one space and one time dimension. Again, the action will look identical in terms of the field, but the fields themselves will change. In this case, the quark fields will be 2-component spinors instead of 4, losing their spin entirely but keeping chirality, while the gluons are 2-component vectors. The gauge symmetry can be used to eliminate one of the two gauge field components, and the remaining one can be integrated out within the path integral to leave a theory in terms of only quarks. This makes it particularly suitable for an analysis in the Hamiltonian formalism, which we will use extensively later on. This variation on QCD is useful because it exhibits confinement [14], so it can be a helpful toy model for understanding QCD at low energy scales.

1.2 Information Theory, Entropy, and Entanglement

This section is intended to define and explain the concepts of entropy and entanglement to the extent that they will be needed for this dissertation. For a more complete introduction on information theory, see [15]. Information theory is exactly what it sounds like: the study

of information and how it can be used. It is primarily under the domain of computer science, but it has seen some applications in physics through topics such as statistical mechanics and holography. The rising interest in quantum computing, which is by nature in the intersection between physics and computer science, also relies heavily on information theory for its development and application. This has also sparked an increase in research toward a broader application of information theory to quantum physics as the understanding of how current physical theories hold and move information would aid their simulation on a quantum computer.

Perhaps the most important quantitative measure of information is the entropy of a system. Readers may have first heard of entropy in the context of thermodynamics and its second law which states that it may never decrease in a closed system such as our universe. Entropy in information theory is deeply connected to but not quite the same as thermodynamic entropy. In this work, we refer exclusively to the concept of entropy used in information theory.

Entropy can be thought of as *potential information to be gained through measurement*. To understand this, consider a single computational bit, which can either be on or off. If we know what it is, then has an entropy of 0, and if the value it takes is completely unknown to us with an equal probability of both outcomes, then we define it to have 1 unit of entropy. If we have n unknown bits, then they have a total entropy of n units. This highlights that we want the entropy of disjoint systems to be additive. A more general formula for a system with D possible outcomes that are equally likely to is given by $S = \log_2(D)$.

Now consider the output of two completely random bits being put through an AND gate. The output bit will have a 75% chance of being off and a 25% chance of being on. We don't know exactly what the bit is, so its entropy should be greater than 0, but we do have *some* information about since we expect it to be off more than we expect it to be on, so its entropy should be less than 1. We want entropy to be additive, so that the total entropy of the two random input bits is equal to the entropy of the AND output plus the expected value of the entropy after measuring said output. If the output bit is on, then we know

that both of the input bits must be on as well, so there is no missing information left and the entropy is 0. If the output bit is off, then the input bits could be in any of the other 3 configurations of off and on, so this outcome has an entropy of $\log_2(3)$. Thus the residual entropy is $\frac{3}{4}\log_2(3)$ since there is a 75% chance of it being $\log_2(3)$ and a 25% chance of it being 0 after the measurement. Since the total entropy prior to measurement was 2, the entropy of the measurement alone must be

$$S = 2 - \frac{3}{4}\log_2(3) = -\frac{1}{4}\log_2\left(\frac{1}{4}\right) - \frac{3}{4}\log_2\left(\frac{3}{4}\right) \tag{1.8}$$

If we apply this reasoning to a general system with n outcomes, each with an associated probability p_i of the ith outcome occurring, then we obtain a formula for the Shannon entropy

$$S(p) = -\sum_i p_i \log_2(p_i) \tag{1.9}$$

We see from the end of Eq. (1.8) that the entropy of the single bit from our example does indeed match this expression. The Shannon entropy has a number of useful properties that make it a suitable candidate for quantifying information. The maximum value is given by $\log_2(n)$ for a system of n outcomes, while the minimum value is 0. This means that the entropy is largest when we know nothing about the system and is 0 when we know it exactly, which is what we intend for a measure of information. For two disjoint systems A and B where the probabilities are given by $p_{AB} = p_A * p_B$, the Shannon entropy is additive so that $S_{AB} = S_A + S_B$. The Shannon entropy is also concave, meaning that if we linearly interpolate between two probability distributions, the entropy of the interpolated distribution is greater than or equal to the linear interpolation of the two entropies of the distributions.

So far, we have been discussing entropy in the context of purely classical information theory. The quantum bit, or qubit, can not only take binary values $|0\rangle$ and $|1\rangle$, but it can also take superpositions of both. This adds an entirely new dimension to the notion of quantifying information, since we now have to worry about the basis that we measure in addition to the state. A quantum state given by $\frac{1}{\sqrt{2}}(|0\rangle + |1\rangle)$ is a completely specified state and should therefore have 0 entropy, but if we measure whether it is in the $|0\rangle$ of $|1\rangle$ state we

get a completely random result. We need a better way to define entropy that doesn't rely on measurement.

To do this, we need to introduce the notion of a density matrix. For a completely specified state $|\psi\rangle$, usually called a pure state, the corresponding density matrix is given by $\rho = |\psi\rangle \langle\psi|$. There are also mixed states, which are randomized pure states $\rho = \sum_i \alpha_i \rho_i$ for some probability distribution α. In all cases, the trace of a density matrix is equal to 1, which is just a consequence of the total probability being equal to 1. We can now define the quantum analog of Shannon entropy, known as the von Neumann entropy, to be

$$S(\rho) = -\mathrm{Tr}\left[\rho \log_2 \rho\right] = -\sum_i \lambda_i \log_2 \lambda_i, \tag{1.10}$$

where the λ_i's are the eigenvalues of the density matrix ρ. This has a lot of the same properties as the Shannon entropy, such as additivity, concavity, and being minimized for pure states and maximized for a purely random result. This can be interpreted in the following way. Since in a quantum system we can change the basis in a myriad of ways, defining the entropy as the Shannon entropy of a density matrix in a given basis will yield a range of different values, given by $-\rho_{ii} \log_2 \rho_{ii}$, where ρ_{ii} is the ith diagonal element of ρ in some basis. It can be shown that these entropies are all greater than or equal to the von Neumann entropy, where equality occurs of the basis in question is a diagonal basis of the density matrix ρ. Thus the von Neumann entropy represents the *basis-independent potential information to be gained through measurement*, as measuring the density matrix in any basis will give you this amount of information plus an additional basis-dependent contribution which may be zero.

With the distinction between pure states and mixed states defined, we can now discuss entanglement. Quantum entanglement describes the correlation between quantum states that arises from them being in superposition as part of a larger state. It is a purely quantum phenomenon, and is responsible for the potential advantages of quantum computing. It is easiest to describe using an example. Consider the two-qubit state $\frac{1}{\sqrt{2}}(|00\rangle + |11\rangle)$. It is a pure state, so it has no entropy as a complete quantum state, but if we look at the individual

qubits we see that we have no knowledge of what either one will be. Thus the one-qubit entropy is 1 while the two-qubit entropy is 0, so we say that there is 1 unit of entanglement entropy between the two quarks. This represents information that is in some sense stored *between* the two qubits. In classical information theory, the entropy of two bits can never be less than the entropy of either of the bits that compose it, but we see here that this is not true in quantum theory, and the violation of this classical rule is a telltale signature of quantum entanglement.

More generally, we can define the entanglement entropy of a pure state as follows. If the space of states that the pure state $|\psi\rangle$ exists in can be separated into two regions A and B, then we can define a reduced density matrix to be $\rho_A = \mathrm{Tr}_B\left[|\psi\rangle\langle\psi|\right]$, where we are taking the density matrix of the pure state and trace out only the states in region B. The entanglement entropy of state $|\psi\rangle$ between regions A and B is given by the von Neumann entropy of the reduced density matrix $S(\rho_A)$. Defining entanglement entropy for mixed states is much trickier. This is because the entanglement entropy needs to be separated from the rest of the entropy which is classical in origin, and there are multiple ways to define this for a mixed state. One such way is through entanglement distillation [16], where we take a large number of copies of a mixed state and transform then into as many Bell pairs as possible, which are states that have exactly 1 unit of entanglement entropy. Another method is to find the entanglement cost [17], which asks the opposite question of what is the minimum number of Bell pairs needed to form the mixed state. For pure states these are all equivalent to the von Neumann entropy, and in this work we are only considering the entanglement of pure states, so these measures will not be needed later.

The rest of this dissertation will proceed as follows. Chapter 2 details the contents of Ref. [18], where we established a connection between the entanglement of valence and non-valence spin degrees of freedom and chiral symmetry breaking in QCD. To do this, we constructed a simple model for helicity entanglement in nucleons involving only two basis states. When fit to experimental data, the entropy in this model approaches it's maximum, providing a picture of the spin decomposition of the nucleon which is not dominated by

the valence quark contribution. Chapter 3 presents further work yet to be published that extends this model to include many chiral basis states, based solely in the symmetries of QCD and general physical principles. In these models, the null-plane formalism will be used to justify representing the nucleon state with only a handful of chiral basis states defined by the helicity and isospin representations of the valence quarks. By fitting experimental data for static nuclear properties such as the axial coupling g_A to their results in the chiral basis, we will be able to obtain results that are sensitive to chiral symmetry breaking. Chapter 4 details another paper yet to be published which focuses on quark entanglement in $1+1$ dimensional QCD. Here we define a notion of valence-sea entanglement that is applicable to general states in QCD. This is used alongside discrete light-cone quantization to quantify the entanglement between quark in the hadrons of $1+1$d QCD, whose results are applicable to real QCD in the confined phase. The dissertation concludes in Chapter 5 with a discussion of how all of these results give us a sketch of the valence-sea entanglement of real nucleons as a function of scale.

Chapter 2

CHIRAL SYMMETRY BREAKING, ENTANGLEMENT, AND THE NUCLEON SPIN DECOMPOSITION

2.1 Introduction

An important goal of present-day nuclear science is the development of a qualitative and quantitative understanding of the structure of the proton directly from the underlying QCD interactions. For instance, the decomposition of the spin of the proton into components that have a well-defined interpretation in terms of the fundamental quark and gluon degrees of freedom of QCD is a primary goal [19]. QCD reveals that the proton is a complicated many-body quantum system, and therefore the breakdown of its spin content is highly complex and requires intrinsically non-perturbative methods to unravel. Recent work in lattice QCD addresses the nucleon spin decomposition in a quantitative manner with controlled uncertainties [20–22]. Lattice QCD and experimental input suggest that the valence quark spins, the gluons, and the quark sea contribute 30-40%, 20-30%, and 10% [2], respectively, to the total proton spin. However, qualitative features of this decomposition, such as the relative size of the nucleon's valence spin content, remain enigmatic, and call out for an explanation grounded in QCD.

The complex decomposition of the nucleon spin is a striking signature of strong entanglement among the nucleon's constituents. How does one characterize nucleon entanglement in a strongly-coupled quantum field theory like QCD? One way is to partition the nucleon state vector into a bipartite system, trace over one of the subspaces, and obtain an entanglement entropy. This partitioning has been done in momentum space in the context of high-energy scattering [23], and in position space in the context of deep-inelastic scattering [24]. These partitionings rely on being in a regime of large momentum transfer where non-perturbative

aspects of QCD are subsumed into parton distribution functions. Many interesting findings and potential experimental signatures are found in these studies; a common qualitative conclusion is that in high energy processes the nucleon constituents decohere, giving rise to a maximal entanglement entropy given by the logarithm of the number of gluons in the nucleon, which grows exponentially with energy in a known manner [25, 26].

In this chapter, it is argued that spin entanglement between valence and non-valence spin degrees of freedom provides valuable insight into the nucleon spin decomposition, and, more generally, into the nature of chiral symmetry breaking in QCD. As a first step toward addressing spin entanglement in the nucleon, special care must be taken to define a relativistic nucleon state vector which represents the internal degrees of freedom of the nucleon in a manner that is independent of kinematics. This is achieved through the use of light-cone coordinates; that is, using null-planes as quantization surfaces. In the Fock-space basis, which emerges naturally in light-cone coordinates, the nucleon state vector of definite helicity is built out of elements labeled by the number of fundamental QCD constituents, which we will refer to in this work as partons. The nucleon state vector can also be expressed in a chiral basis, which makes use of a fundamental property of the null-plane quark fields: states of definite helicity transform irreducibly with respect to the chiral symmetry group. The chiral basis therefore suggests a natural bipartite Hilbert space description of the nucleon state vector: the valence space is by definition the space which carries non-vanishing chiral charge, while the non-valence space, or parton sea, carries spin, but no chiral charge. The entanglement entropy between these two subspaces drives chiral symmetry breaking in the nucleon and provides both a qualitative and quantitative explanation of why the valence spin content of the nucleon is not expected to be the dominant component.

2.2 A relativistic state vector

In non-relativistic quantum mechanics, the state vector of a many-body system describes the internal degrees of freedom in a manner that is independent of the choice of reference frame. This is because the underlying kinematics is governed by the Galilean group, and

Galilean boosts do not depend on the interaction. By contrast, in a relativistic theory of quantum mechanics, the spacetime symmetry group is the Poincaré group. In general, the Poincaré boost operator depends on the interaction, unless a foliation of spacetime is chosen such that the boost operator is non-dynamical [27]. This can be realized if null-planes are chosen as initial quantization surfaces [10, 27, 28]. In this choice of light-cone coordinates, the energy and the two transverse components of spin are dynamical, while the boosts, the momenta and the longitudinal component of spin —the helicity —are kinematical. In an arbitrary reference frame, the energy and transverse spin which act on the internal degrees of freedom are described by the (Hamiltonian) operators M^2 and $M\mathcal{J}_r$ $(r = 1, 2)$, respectively, which commute with boosts and momenta, and together with $\mathcal{J}_3$, satisfy the algebra of the Poincaré group [10]. An eigenstate of momentum and helicity, describing a nucleon, N, can be expressed as

$$|N\,,\,\Lambda\,;\,p^+\,,\,\mathbf{p}_\perp\,\rangle = |N\,,\,\Lambda\,\rangle \otimes |\,p^+\,,\,\mathbf{p}_\perp\,\rangle\,, \tag{2.1}$$

where p^+ and $\mathbf{p}_\perp$ are the longitudinal and transverse components of the nucleon momenta, respectively[1], and Λ is the total helicity, the eigenvalue of $\mathcal{J}_3$. The direct product on the right indicates that the part of the state which describes the internal degrees of freedom can be separated completely from the kinematics. Achieving this separation is essential as otherwise there is no starting point for a description of the state vector of a nucleon which represents the internal degrees of freedom. In principle, specification of the operators M^2 and $M\mathcal{J}_r$, which act on the state $|N\,,\,\Lambda\,\rangle$, followed by diagonalization completely solves the dynamics. While this is intractable in QCD, the symmetry properties of these operators can be exploited to powerful effect, as will be seen below.

2.3 Fock-space expansion and the chiral basis

The separation of dynamics and kinematics described above allows the Fock-basis expansion of the nucleon state, in which the state vector is given by a (infinite) sum of contributions

[1]The conventions for the light-cone coordinates and momenta are defined and described in Ref. [29, 30].

labeled by the QCD field content [2]. The contributions involving the fewest numbers of partons have been worked out in Refs. [30, 33–35]. The dynamical light-cone quark field ψ_+ is

$$\psi_+(x) \;=\; \sum_{\lambda=\uparrow\downarrow}\int \frac{dk^+d^2\boldsymbol{k}_\perp}{2k^+(2\pi)^3}\left\{b_\lambda(k^+,\boldsymbol{k}_\perp)u_+(k,\lambda)\mathrm{e}^{-ik\cdot x}\right. \\ \left. +d^\dagger_\lambda(k^+,\boldsymbol{k}_\perp)v_+(k,\lambda)\mathrm{e}^{ik\cdot x}\right\}\;, \tag{2.2}$$

where x is the light-cone coordinate, k^+ and $\boldsymbol{k}_\perp$ are the light-cone longitudinal and transverse momenta, respectively, u_+, v_+ are Dirac wavefunctions, $b_\lambda(k^+,\boldsymbol{k}_\perp)$ destroys a quark and $d^\dagger_\lambda(k^+,\boldsymbol{k}_\perp)$ creates an antiquark, and the flavor and color indices have been suppressed. With standard normalization, the simplest Fock component in the proton state with $\Lambda=\frac{1}{2}$ is then

$$|u_\uparrow u_\downarrow d_\uparrow,\tfrac{1}{2},\mathbf{0}\rangle \;=\; \tfrac{1}{2}\int\tfrac{[dx][d^2\boldsymbol{k}_\perp]}{\sqrt{x_1x_2x_3}}\,\phi(\kappa_1,\kappa_2,\kappa_3)\tfrac{\varepsilon^{abc}}{\sqrt{6}} \\ \times u^{a\dagger}_\uparrow(x_1,\boldsymbol{k}_{1\perp})\left\{u^{b\dagger}_\downarrow(x_2,\boldsymbol{k}_{2\perp})d^{c\dagger}_\uparrow(x_3,\boldsymbol{k}_{3\perp})-(u\leftrightarrow d)\right\}|0\rangle \tag{2.3}$$

where x_i is the longitudinal momentum of the quark in units of the proton longitudinal momentum, the shorthand, $\kappa_i\equiv(x_i,\boldsymbol{k}_{i\perp})$, has been used, the integrations are over all constituent momenta, and $\phi(\kappa_1,\kappa_2,\kappa_3)$ is the (Fourier transform of the) light-cone wavefunction for this particular Fock component. Here the states are labeled by the QCD field content, the total valence quark light-cone helicity, and all other sources of helicity (including orbital components), respectively. Therefore, for instance, a Fock component of the helicity-$\frac{1}{2}$ proton with, in addition to the valence quarks, one gluon and no source of orbital angular momentum could be labeled as $|u_\uparrow u_\downarrow d_\downarrow g_\uparrow,-\frac{1}{2},\mathbf{1}\rangle$. Note that in Eq. 2.3, the proton is in the special frame with $p^+=1$ and $\boldsymbol{p}_\perp=0$. The Fock component in a boosted frame is obtained by simply re-labeling the momenta of the field creation operators, while leaving the wavefunction, which carries the internal information, unchanged, in accord with the claim made above that the internal degrees of freedom are cleanly separated from the kinematics.

[2] Clear explanations of the QCD Fock basis are found in Refs. [31, 32].

The difficulty with the Fock expansion of the nucleon state vector is that there is no small parameter in QCD to indicate which components should dominate out of the infinite space of possible contributions (the large-N_c approximation is an exception as we will argue below).

Assuming QCD with two massless flavors, and therefore $SU(2)_L \otimes SU(2)_R$ chiral symmetry, the associated light-cone charges are straightforward to construct [29]. With these charges, it is found that the light-cone quark fields of definite helicity transform irreducibly with respect to the chiral group $SU(2)_L \otimes SU(2)_R$:

$$\psi_{+R} \;=\; \psi_{\uparrow} \;\in\; (\mathbf{1},\mathbf{2}) \quad , \quad \psi_{+L} \;=\; \psi_{\downarrow} \;\in\; (\mathbf{2},\mathbf{1}) \tag{2.4}$$

where $(\mathcal{R}_{\mathbf{L}},\mathcal{R}_{\mathbf{R}})$ labels the $SU(2)_L \otimes SU(2)_R$ content and $\mathcal{R}_{\mathbf{L},\mathbf{R}}$ are $SU(2)_{L,R}$ representations.

Hence in the chiral basis, the most general helicity-$\frac{1}{2}$ nucleon state, $|\, N\,,\,\frac{\mathbf{1}}{\mathbf{2}}\rangle$, with three valence quarks will, in general, be a linear combination of the six classes [3] of states: $|(\mathbf{2},\mathbf{1})\,,\,\frac{1}{2}\,,\,\mathbf{0}\rangle$, $|(\mathbf{2},\mathbf{3})_{\mathbf{2}}\,,\,\frac{1}{2}\,,\,\mathbf{0}\rangle$, $|(\mathbf{1},\mathbf{2})\,,\,-\frac{1}{2}\,,\,\mathbf{1}\rangle$, $|(\mathbf{3},\mathbf{2})_{\mathbf{2}}\,,\,-\frac{1}{2}\,,\,\mathbf{1}\rangle$, $|(\mathbf{1},\mathbf{2})\,,\,\frac{3}{2}\,,\,-\mathbf{1}\rangle$, $|(\mathbf{2},\mathbf{1})\,,\,-\frac{3}{2}\,,\,\mathbf{2}\rangle$, where the states have been labeled as

$$|\,(\mathcal{R}_{\mathbf{L}},\mathcal{R}_{\mathbf{R}})_{\mathcal{R}}\,,\,\lambda\,,\,\mathbb{p}_3\,\rangle \;\equiv\; |\,(\mathcal{R}_{\mathbf{L}},\mathcal{R}_{\mathbf{R}})_{\mathcal{R}}\,,\,\lambda\,\rangle \otimes |\,\mathbb{p}_3\,\rangle \;, \tag{2.5}$$

where $\mathcal{R}$ is an $SU(2)$-isospin representation in the product $\mathcal{R}_{\mathbf{R}} \otimes \mathcal{R}_{\mathbf{L}}$. The total helicity operator is divided into a valence spin operator, $\hat{S}_3$, and an operator, $\hat{\mathbb{P}}_3$, that counts all other sources of spin, including the quark orbital helicity:

$$\mathcal{J}_3 = \hat{S}_3 \otimes \mathbb{1} \;+\; \mathbb{1} \otimes \hat{\mathbb{P}}_3 \;, \tag{2.6}$$

so that $\hat{S}_3|\,\lambda\,\rangle = \lambda|\,\lambda\,\rangle$, $\hat{\mathbb{P}}_3|\,\mathbb{p}_3\,\rangle = \mathbb{p}_3|\,\mathbb{p}_3\,\rangle$ and the total helicity is $\Lambda = \lambda + \mathbb{p}_3$. In QCD, the gauge-invariant operator $\hat{S}_3$ is, up to a factor of two, given by the anomalous $U(1)_A$ chiral charge [29]. This decomposition is therefore gauge invariant, but scale dependent.

Like the Fock basis, the chiral basis is *a priori* infinite dimensional, as each of the six classes of states of definite chiral charge can couple to any number of helicity states in the sea. An important advantage of the chiral basis is that the chiral transformation properties

[3] The states with $\mathcal{R}_{\mathbf{L}} \leftrightarrow \mathcal{R}_{\mathbf{R}}$ are contained in $|\,N\,,\,-\frac{\mathbf{1}}{\mathbf{2}}\rangle$.

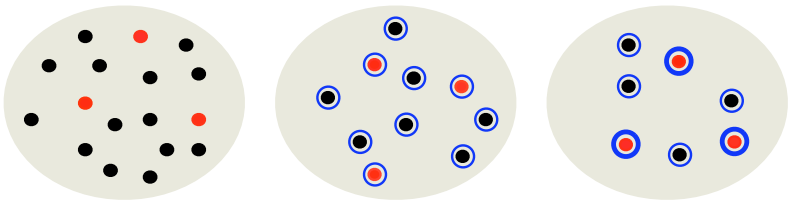

Figure 2.1: Nucleon as a collection of partons with some distribution in x (left panel). As the partons with low-x are integrated out (middle and right panels), the ground state should be described in terms of some valence degrees of freedom (red dots) and a finite number of sea partons (black dots), where the blue rings indicate that the partons and their interactions are dressed by the renormalization-group evolution.

of the energy and transverse spin are known in QCD [29, 36, 37]. In particular, both the energy M^2 and the transverse spin $M\mathcal{J}_r$ transform as linear combinations of $(\mathbf{1},\mathbf{1})$ and $(\mathbf{2},\mathbf{2})$ representations of $SU(2)_L \otimes SU(2)_R$; that is, in an obvious notation, $M^2 = M^2_{\mathbf{1}} + M^2_{\mathbf{22}}$ and likewise for the transverse spin.

A second, related, advantage of the chiral basis is that the large-N_c limit of the nucleon $\Lambda = \frac{1}{2}$ state vector is given by the single state $|(\mathbf{2},\mathbf{3})_{\mathbf{2}}\,,\,\frac{1}{2}\,,\,\mathbf{0}\rangle$, whose spin is carried entirely by the valence quarks. The nucleon is joined in this chiral representation by the Δ (resonance) whose $\Lambda = \frac{1}{2}$ state vector is given by the single state $|(\mathbf{2},\mathbf{3})_{\mathbf{4}}\,,\,\frac{1}{2}\,,\,\mathbf{0}\rangle$ (the $\Lambda = \frac{3}{2}$ component is given by $|(\mathbf{1},\mathbf{4})\,,\,\frac{3}{2}\,,\,\mathbf{0}\rangle$). These state assignments are easily shown to be equivalent to placing the degenerate nucleon and Δ in the **20**-dimensional representation of $SU(4)$ [29, 38], which is the large-N_c expectation. The success of the large-N_c expansion in describing nucleon properties [39–41] suggests that the nucleon state vector is dominated by the large-N_c component with an admixture of other components which would provide the nucleon-Δ mass splitting as well as a source of non-valence spin. It is unclear from the perspective of the large-N_c approximation how to account for subleading corrections to the large-N_c limit in the chiral basis. However, simple renormalization group (RG) arguments suggest that the nucleon state vector may be well-approximated by a small number of components [42, 43].

2.4 The renormalization group, wee partons, and the vacuum

Consider a nucleon on the initial hyperplane defined by $x^+ = 0$ and with longitudinal momentum p^+ and in a frame with vanishing transverse momentum. On the initial time slice, a nucleon is defined to be a collection of (quasi)free massless partons, each of which is labeled by i and carries a longitudinal momentum fraction $x_i \equiv k_i^+/p^+$ and a transverse momentum $\mathbf{k}_{i\perp}$ so that the nucleon energy is

$$M^2 \;=\; \sum_i \frac{\mathbf{k}_{i\perp}^2}{x_i} \;+\; \ldots \tag{2.7}$$

In null-plane quantization small x_i means high energy, and therefore integrating out high-energy physics is equivalent to integrating out low-x_i partons (so-called wee partons). Assuming, for simplicity, that interactions are local in x_i (nearest-neighbor), and integrating out shells, one first integrates out all partons with $x_i < x_{\epsilon_1}$. Integrating out these small x_i partons result in "dressed" partons that have new interactions with the "frozen partons" that are represented by effective Hamiltonians with a hierarchy of interactions governed by the small parameter x_{ϵ_1}/x_i [42, 43]. Schematically, the energy takes the form

$$M^2 \;=\; M^2_{x_i > x_{\epsilon_1}} \;+\; M^2_{x_i = x_{\epsilon_1}} \;+\; \ldots \tag{2.8}$$

where the dots represent the frozen degrees of freedom with $x_i < x_{\epsilon_1}$. The first term represents the active, dynamical partons, while the second term corresponds to the interaction of these partons with the frozen sea. As non-perturbative physics in null-plane quantization is carried by the low-x_i partons, this second term carries the chiral-symmetry breaking contribution to the energy; i.e. the part of the energy that carries non-vanishing chiral charge and transforms as $(\mathbf{2},\mathbf{2})$ with respect to the chiral group: $M^2_{\mathbf{22}}$. One can then further integrate out the partons with $x_i < x_{\epsilon_2}$, *etc.* Finally this procedure results in a description of the ground state that involves a minimal number of partons —presumably the valence partons —interacting with a few sea partons. This procedure of integrating out low-x_i partons is illustrated in Fig. 2.1. The resulting effective Hamiltonians are complicated, because, as

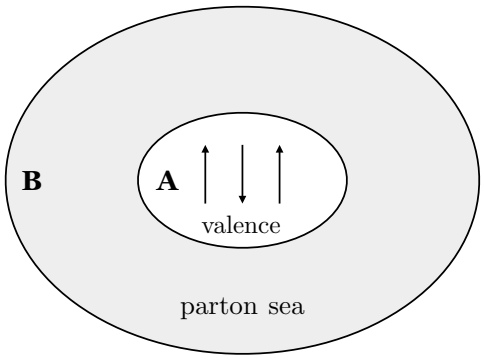

Figure 2.2: Bipartite Hilbert space $\mathcal{H}_A \otimes \mathcal{H}_B$ consisting of the valence quark helicity ($\mathcal{H}_A$) and the helicity of the parton sea ($\mathcal{H}_B$). This decomposition, as illustrated here, *does not* imply that the valence charges are in any sense localized in space.

noted above, non-perturbative physics is low-x_i physics and therefore the RG evolution necessarily accounts for the non-perturbative physics of QCD. The practical consequence of this simple RG argument is that the nucleon ground state can be described by a nucleon state vector, with a finite number of states of definite chiral charge, whose detailed form can be fit to experimental data. Crucially, the truncation of the chiral basis is scale dependent as it depends on the energy cutoff, x_ϵ.

2.5 Spin entanglement defined

In the chiral basis, the nucleon state vector decomposes into a bipartite Hilbert space $\mathcal{H}_A \otimes \mathcal{H}_B$, illustrated in Fig. 2.2, in which the valence helicity lives in $\mathcal{H}_A$, and all other sources of helicity live in $\mathcal{H}_B$. When measuring the valence helicity content of the nucleon, it is convenient to trace over the sea to give the reduced density matrix of the valence helicity,

$$\rho_A = \mathrm{tr}_B \left(|\, N\,,\, \Lambda \,\rangle\langle\, N\,,\, \Lambda\,| \right), \tag{2.9}$$

and the corresponding entanglement entropy is then

$$S_N = -\mathrm{tr}_A \left(\rho_A \log \rho_A \right). \tag{2.10}$$

The general form of the nucleon state vector is

$$|N\,,\,\Lambda\,\rangle \;=\; \sum_{i}^{n_\chi}\sum_{j}^{n_s} a_{ij}|\,(\mathcal{R}_{\mathbf{L}},\mathcal{R}_{\mathbf{R}})_{\mathcal{R}}\,,\,\lambda\,\rangle_i \otimes |\,\mathbb{p}_3\,\rangle_j \tag{2.11}$$

where n_χ (n_s) is the number of valence (non-valence) states. Generally, it is expected that $n_s \gg n_\chi$, as is the case in the Fock expansion where components with arbitrary numbers of sea partons can contribute, however, the renormalization group argument given above suggests that many of the components are high-energy degrees of freedom that can be integrated out of the ground-state state vector under consideration. In any event, the Schmidt decomposition theorem reveals that via a basis change, the state vector can be expressed in a basis of dimension given by $n = \min\{n_\chi, n_s\}$. It is convenient to view the nucleon state vector as a perturbation of the large-N_c result,

$$|N\,,\,\tfrac{\mathbf{1}}{\mathbf{2}}\,\rangle \;=\; |(\mathbf{2},\mathbf{3})_{\mathbf{2}}\,,\,\tfrac{1}{2}\,,\,\mathbf{0}\rangle \;=\; |(\mathbf{2},\mathbf{3})_{\mathbf{2}}\,,\,\tfrac{1}{2}\rangle \otimes |\,\mathbf{0}\,\rangle\;, \tag{2.12}$$

which is a product state ($n = 1$) and therefore has vanishing entanglement entropy. As the matrix element of the symmetry-breaking energy, $M^2_{\mathbf{22}}$, vanishes between these states and turns on only when the nucleon state vector ceases to be a product state, it is clear that the spin entanglement defined here is intimately related to chiral symmetry breaking and, consequently, to the nucleon spin decomposition. Evidently, chiral symmetry is broken in the nucleon if and only if $n > 1$. Therefore, some measure of entanglement is acting as an order parameter of chiral symmetry breaking. This claim is considered in generality in Ref. [44]. Here a simple two-component model which captures the essence of the idea is explored.

2.6 An illustrative model

Consider the simplest nucleon state vector that extends the large-N_c result to include chiral symmetry breaking:

$$|\,N\,,\,\tfrac{\mathbf{1}}{\mathbf{2}}\,\rangle \;\;=\;\; \sin\psi\,|(\mathbf{1},\mathbf{2}),-\tfrac{1}{2},\mathbf{1}\rangle + \cos\psi\,|(\mathbf{2},\mathbf{3})_{\mathbf{2}},\tfrac{1}{2},\mathbf{0}\rangle. \tag{2.13}$$

The state orthogonal to the nucleon in this model may be viewed as a collective of isodoublet excited states of both parities. The vector space spans the reducible chiral representation

$(\mathbf{1},\mathbf{2}) \oplus (\mathbf{2},\mathbf{3})$. The large-$N_c$ limit is recovered as $\psi \to 0$, and the matrix element of the symmetry-breaking Hamiltonian scales as

$$\langle\, N\,,\, \tfrac{\mathbf{1}}{\mathbf{2}} \,|\, M^2_{\mathbf{22}} \,|\, N\,,\, \tfrac{\mathbf{1}}{\mathbf{2}} \,\rangle \;\; \propto \;\; \sin 2\psi \;. \tag{2.14}$$

The valence or intrinsic helicity contribution is

$$\langle\, N\,,\, \tfrac{\mathbf{1}}{\mathbf{2}} \,|\, \hat{S}_3 \,|\, N\,,\, \tfrac{\mathbf{1}}{\mathbf{2}} \,\rangle \;\equiv\; \tfrac{1}{2}\Delta\Sigma^V \;=\; \tfrac{1}{2}\cos 2\psi \;. \tag{2.15}$$

Tracing over the sea gives the density matrix for the valence content

$$\rho_A \;=\; \sin^2\psi|(\mathbf{1},\mathbf{2})\rangle\langle(\mathbf{1},\mathbf{2})| + \cos^2\psi|(\mathbf{2},\mathbf{3})_{\mathbf{2}}\rangle\langle(\mathbf{2},\mathbf{3})_{\mathbf{2}}| \tag{2.16}$$

from which follows the entanglement entropy

$$S_N(\psi) = -\sin^2\psi \log\left(\sin^2\psi\right) - \cos^2\psi \log\left(\cos^2\psi\right). \tag{2.17}$$

The probability amplitude for a spin-flip interaction is

$$\sin\psi \;=\; \langle(\mathbf{1},\mathbf{2})\,,\, -\tfrac{1}{2}\,,\, \mathbf{1}|\, N\,,\, \tfrac{\mathbf{1}}{\mathbf{2}}\,\rangle\;. \tag{2.18}$$

This amplitude depends not on the parton momentum fractions, which are integrated over in the state vector, but rather on the cutoff on the parton momentum fractions, x_ϵ, as suggested by the RG arguments given above. A simple way of modeling this amplitude is to neglect sea quarks and assume that there are interactions between one of the valence quarks —which carries longitudinal momentum fraction x_ϵ, and a sea of gluons [45]. Taking $\mathcal{G}(x_\epsilon)$ to be the density of the sea of gluons relative to valence quarks and $\mathcal{P}(x_\epsilon)$ to be the probability of a spin-flip interaction between the valence quark and the sea, then $\frac{1}{2}\mathcal{P}(x_\epsilon)\mathcal{G}(x_\epsilon) + 1$ is the number of spins aligned in the initial direction of the valence quark's spin and $\frac{1}{2}\mathcal{P}(x_\epsilon)\mathcal{G}(x_\epsilon)$ is the number of spins in the opposite direction. Assuming a purely statistical distribution of the spins among interacting partons gives the probability of a spin-flip interaction

$$\sin^2\psi \;=\; \frac{\frac{1}{2}\mathcal{P}(x_\epsilon)\mathcal{G}(x_\epsilon)}{1+\mathcal{P}(x_\epsilon)\mathcal{G}(x_\epsilon)}\;. \tag{2.19}$$

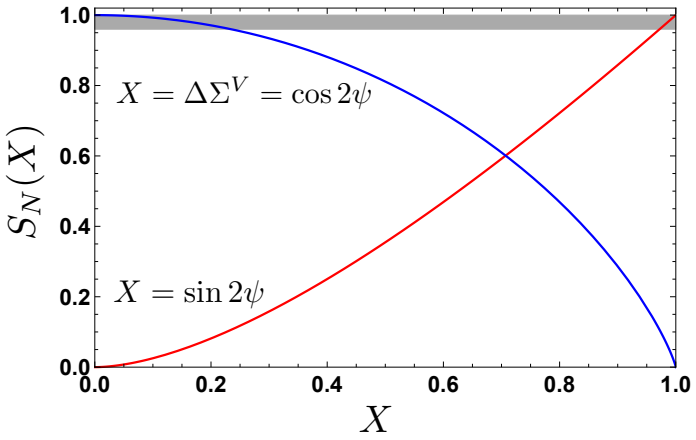

Figure 2.3: Entanglement entropy (in units of its maximum) versus the chiral order parameter (red curve) and the valence quark helicity content of the proton (blue curve) in the minimal model of chiral-symmetry breaking. The grey band is determined by experiment.

Note that if there is no spin-flip interaction, then this amplitude vanishes and the large-N_c result is recovered. In terms of the valence quark spin content of the nucleon,

$$\Delta\Sigma^V \;=\; \cos 2\psi \;=\; \frac{1}{\mathcal{P}(x_\epsilon)\mathcal{G}(x_\epsilon)+1}\;. \tag{2.20}$$

Since the density of the sea, as given by the (spin-averaged) gluon distribution function, is expected to diverge as a power law with x_ϵ, it is expected that

$$\cos 2\psi \xrightarrow[x_\epsilon \to 0]{} x_\epsilon^\delta \tag{2.21}$$

where δ is a positive number (assuming BFKL evolution for the gluon distribution function [25, 26], $\delta \sim 4\alpha_s N_c \log 2/\pi$, where α_s is the strong coupling constant and N_c is the number of QCD colors). As the cutoff is taken to zero and the density of gluons diverges, the nucleon is driven to the maximally entangled state with $\psi = 45°$, and the nucleon spin is given entirely by the spin of the sea. Of course, this divergence is expected to be cut off by some kind of saturation mechanism [46]. The behavior of the entanglement entropy as a function of chiral symmetry breaking and valence spin content is shown in Fig. 2.3. The

value of the mixing angle can be fit directly to low-energy data. In this model, it is straightforward to find the nucleon and Δ axial and vector couplings. For instance, $|\mathcal{C}_{\Delta N}| = 2\cos\psi$ and $|g_A| = \frac{1}{3}(4 + \cos 2\psi)$. Fitting $|\mathcal{C}_{\Delta N}|$ to the Δ-resonance decay width to pions gives $\psi = 41 \pm 4^\circ$ which determines, among other things [44], $g_A = 1.38 \pm 0.05$, $\Delta\Sigma^V = 0.14 \pm 0.13$ and $S_N = 0.98 \pm 0.02$ (in units of the maximum entropy of $\log 2$). The result for g_A is to be compared to the world average $g_A = 1.2723 \pm 0.0023$ [47]. This result for the valence spin content is to be compared to $\Delta\Sigma^V = 0.41 \pm 0.06$ taken from the JAM collaboration's global analysis [48], at a renormalization scale of $Q^2 = 1$ GeV^2 (Note that the JAM number is quoted with the sea contribution removed).

2.7 Realistic model-independent state vectors

In realistic models of the nucleon state vector, the number of states in the sum, Eq. 2.11, should grow as the RG scale x_ϵ is reduced, with the mass of the highest excitation in the nucleon's chiral representation setting the scale of the separation into valence and sea spin. Detailed construction of such realistic models is beyond the scope of this chapter but may be found in Ref. [44]. Many of the generic features of the two-component model persist in more realistic state vectors: for instance, the large-N_c component is always dominant due to the prominent nucleon-Δ axial transition, but not so much so that it has much of an effect on the entanglement entropy, which is always near its maximum value[4]. The valence spin content in these models is generally small and consistent with the experimental range, as expected in a system where the entanglement entropy is large.

2.8 Conclusion

Entanglement between the valence and non-valence helicity components of the nucleon state vector drives chiral symmetry breaking in the nucleon. The entanglement entropy therefore acts as an order parameter of chiral symmetry breaking in the nucleon, and provides an

[4]By contrast, recent work has found that entanglement in the nuclear force, as measured by the entanglement power, is minimized by the experimental data, and is very near large-N_c expectations [49].

explanation for why the valence spin content of the nucleon is not expected to dominate in the following sense. The interaction of the valence chiral charge with the sea, which breaks chiral symmetry, becomes stronger as the density of sea partons increases and the entanglement entropy rises. The separation between valence and non-valence spin is scale dependent, and the renormalization group implies that a state vector with a small number of components should suffice to provide a reasonably accurate description of the ground state. As the highly-energetic sea partons are integrated out, reducing the size of the vector space, the entanglement entropy decreases and the valence spin content of the nucleon increases. Conversely, as more sea partons are integrated in, increasing the size of the vector space, the entanglement entropy increases till it reaches its maximum value where presumably some kind of equilibrium or saturation state is achieved. It is interesting that this pattern of RG evolution is consistent with perturbative QCD evolution [50]. Realistic models of the nucleon state vector in the chiral basis which are fit to low-energy observables give values of the valence spin content which are consistent with experiment and with lattice QCD simulations, and possess an entanglement entropy near its maximum value. It would be interesting to access this chiral entanglement entropy in lattice QCD simulations.

In the next chapter, these ideas will be expanded upon and treated more rigorously using the null plane formalism. The null plane is useful because the dynamical generators of the Poincaré group can be cast in such a way that they commute with most of the other generators. This gives a precedent for building models of the nucleon state that captures the internal spin structure of the nucleon without needing to explicitly determine its parton dynamics. These models will further elaborate on the connection between spin entanglement and chiral symmetry breaking and provide a clearer picture as to how the spin decomposition of the nucleon come about in QCD.

Chapter 3

CHIRAL SYMMETRY BREAKING AND SPIN ENTANGLEMENT IN THE NUCLEON ON THE NULL PLANE

3.1 Introduction

The decomposition of the spin of the proton into components that have a well-defined interpretation in terms of the fundamental quark and gluon degrees of freedom of QCD is a primary goal of modern nuclear science [19]. The proton is a complicated many-body quantum-mechanical system, and therefore the breakdown of its spin content according to the fundamental QCD degrees of freedom is highly-complex and requires intrinsically non-perturbative methods. Recently, lattice QCD simulations have begun to address the issue in a quantitative manner [20–22, 51]. The current theoretical and experimental effort largely focuses on probing the proton at short distances (large Q^2) where a description in terms of various parton distribution functions is available. The theoretical basis of the parton distributions lies in null-plane quantization of QCD; that is, treating initial surfaces as lightlike hyperplanes [10, 27, 28]. This is a natural quantization surface because the generalized parton distributions are proton matrix elements of non-local operators that probe correlations along the light cone. On the other hand, the fundamental quantum mechanical object that describes the nucleon, the null-plane wavefunction is usually treated as a black box which can be accessed only via modeling[1]. This is because the wavefunction carries all the non-perturbative information about chiral symmetry breaking and confinement that is relevant to nucleon structure.

In the Fock space picture, in which the nucleon state is built out of contributions with ever increasing numbers of fundamental QCD constituents, the situation appears theoreti-

[1]See, for instance, Refs. [33–35, 52, 53]

cally intractable. While the success of the naive quark model in describing basic nucleonic observables suggests that the null-plane wavefunction is dominated by Fock components with valence degrees of freedom and that therefore a truncation of the Fock space expansion to a few terms would constitute a reasonable approximation, there is no particularly satisfying *a priori* understanding of why this is the case. The recovery of the spin-flavor symmetry of the naive quark model in the large-N_c limit of QCD [39–41] does suggest that in some sense nature is near this limit. However, the current consensus that only a fraction of the nucleon spin is accounted for by the spins of the valence quarks suggests that there are important corrections to the large-N_c limit in the null-plane wavefunction which are essential for understanding nucleon structure.

The situation appears even more complex when one considers that nucleon properties are strongly dependent on nonperturbative phenomena, like spontaneous chiral symmetry breaking, which are expected to arise from the presence of a divergent number of partonic constituents in the nucleon. In null-plane quantization, the effect of chiral symmetry breaking is communicated to the wavefunction via the interaction between the valence degrees of freedom and partons at very-low x, the wee partons, whose density is expected to grow with an inverse power of x [42, 43]. Generally, it is expected that a divergent number of constituents is required to achieve spontaneous symmetry breaking. If the wee partons are important, then how can the Fock expansion truncated to a few terms capture the essential physics of spontaneous chiral symmetry breaking? The renormalization group suggests a qualitative way of thinking about this problem. Low-x partons are high-energy degrees of freedom and therefore if one views the nucleon as a many-body system of partons, then in considering the properties of the nucleon ground state, one should successively integrate out the low-x modes until one is left with the valence degrees of freedom and possibly a few other degrees of freedom which experience effective interactions which account for the now frozen low-x modes and transmit the chiral symmetry breaking to the null-plane wavefunction. This picture suggests that a much simplified description of the nucleon with a finite number of partons may provide a useful quantitative approximation to the wavefunction. A useful

fundamental property of the null-plane formulation that will be exploited in this chapter is that the quark fields of definite helicity have definite chiral transformation properties. Therefore, assuming a particular valence content for a hadron allows a decomposition of the hadron state into a finite number of components which transform irreducibly with respect to the chiral symmetry group. Of course each of these components can contain an arbitrarily complicated amount of non-valence information.

A fundamental issue that this chapter addresses is that of the entanglement of nucleons and its relation with symmetry. How does one characterize entanglement in a complicated QFT like QCD? One way is to consider tracing over some partial volume of the system. However, this requires a hard probe. Recent work has addressed the issue of entanglement between different spatial regions probed in the nucleon wavefunction [23, 24, 54–63]. Deep Inelastic Scattering (DIS) probes a region of size $1/Q$ and $1/Mx$ where Q is the momentum transfer, M is the nucleon mass and x is Bjorken-x. This separation of the Hilbert space into product space consisting of two spatial regions is possible only because DIS is a short-distance process. One qualitative conclusion resulting from these studies is that in high energy processes the nucleon constituents decohere, which in turn gives rise to a maximal entanglement entropy which scales as the logarithm of the number of gluons in the nucleon, a quantity which grows exponentially with energy in a known manner [25, 26]. When probing chiral symmetry breaking in the nucleon wavefunction, no such spatial separation is possible since one is strictly in the long-distance, non-perturbative regime of QCD. A qualitative picture suggests that chiral symmetry breaking arises from high-energy physics of the wee partons near $x = 0$. However, it is possible to achieve a bipartite Hilbert space by considering the entanglement between the spin of the valence quarks and the spin of everything else (which we refer to as the parton sea).

3.2 Null-plane QCD constraints

3.2.1 Folliation of spacetime and QCD conventions

In the front-form of relativistic Hamiltonian dynamics [27], one chooses the initial state of the system to be on a light-like plane, or null-plane, which is a hypersurface of points x in Minkowski space such that $x \cdot n = \tau$, which serves as the time variable. Here n is chosen to be a light-like vector

$$n^\mu \equiv \tfrac{1}{\sqrt{2}}(1,0,0,-1) \quad , \quad n^{*\mu} \equiv \tfrac{1}{\sqrt{2}}(1,0,0,1)\,, \tag{3.1}$$

which satisfies $n^2 = n^{*2} = 0$ and $n \cdot n^* = 1$. Referring to a null-plane as the surface Σ_n^τ, the subgroup of the Poincaré group that maps Σ_n^τ to itself is called the stability group of the null-plane and determines the kinematics within the null-plane. The seven kinematical generators which form the stability group include the three momenta, the three boosts and the helicity operator, $\mathcal{J}_3$. The remaining three Poincaré generators map Σ_n^τ to a new surface, $\Sigma_n^{\tau'}$, and therefore describe the evolution of the system in time. It is convenient to trade the three dynamical generators which correspond to transverse spin and time evolution with the three reduced Hamiltonians, $M\mathcal{J}_r$ with $r = 1, 2$ and M^2, respectively, which encode all non-trivial dynamics of the system. Taking the initial surface to be the null-plane Σ_n^0, a coordinate system adapted to null-planes is given by

$$x^+ \equiv x \cdot n = \tfrac{1}{\sqrt{2}}(x^0 + x^3)\,, \qquad x^- \equiv x \cdot n^* = \tfrac{1}{\sqrt{2}}(x^0 - x^3) \tag{3.2}$$

which are the time variable and "longitudinal" position, respectively.

It is a straightforward matter to find that the QCD null-plane chiral charges satisfy the $SU(2)_L \otimes SU(2)_R$ algebra

$$[\,\tilde{Q}^\alpha\,,\,\tilde{Q}^\beta\,] \;=\; i\,\epsilon^{\alpha\beta\gamma}\,\tilde{Q}^\gamma\;, \tag{3.3}$$

$$[\,\tilde{Q}_5^\alpha(x^+)\,,\,\tilde{Q}^\beta\,] \;=\; i\,\epsilon^{\alpha\beta\gamma}\,\tilde{Q}_5^\gamma(x^+)\;, \tag{3.4}$$

$$[\,\tilde{Q}_5^\alpha(x^+)\,,\,\tilde{Q}_5^\beta(x^+)\,] \;=\; i\,\epsilon^{\alpha\beta\gamma}\,\tilde{Q}^\gamma\;. \tag{3.5}$$

Note that the chiral charges are functions of time. This is the fundamental feature of null-plane quantization that will be exploited in this chapter. As there are no symmetry-breaking condensates, all spontaneous chiral symmetry breaking must be present in the reduced Hamiltonians, which in turn cannot commute with the chiral charges.

The quark fields transform as

$$[\,\tilde{Q}^{\alpha}\,,\,\psi_{+}\,] \;=\; -T^{\alpha}\,\psi_{+} \quad ; \quad [\,\tilde{Q}_{5}^{\alpha}(x^{+})\,,\,\psi_{+}\,] \;=\; -\gamma_{5}\,T^{\alpha}\,\psi_{+}\;. \tag{3.6}$$

Breaking down the dynamical null-plane quark fields into left- and right-handed components,

$$\psi_{+R} \;=\; \tfrac{1}{2}(1+\gamma_{5})\psi_{+} \qquad , \qquad \psi_{+L} \;=\; \tfrac{1}{2}(1-\gamma_{5})\psi_{+}\;, \tag{3.7}$$

and noting that

$$\begin{aligned} \tilde{Q}^{\alpha} \;&=\; \tilde{Q}_{R}^{\alpha} \;+\; \tilde{Q}_{L}^{\alpha} \\ \tilde{Q}_{5}^{\alpha} \;&=\; \tilde{Q}_{R}^{\alpha} \;-\; \tilde{Q}_{L}^{\alpha}\;, \end{aligned} \tag{3.8}$$

one verifies the fermion transformation properties with respect to $SU(2)_{L}\otimes SU(2)_{R}$:

$$\psi_{+R} \;=\; \psi_{\uparrow} \;\;\in\;\; (\mathbf{1},\mathbf{2}) \qquad , \qquad \bar{\psi}_{+R} \;=\; \bar{\psi}_{\downarrow} \;\in\; (\mathbf{1},\mathbf{2})\;; \tag{3.9}$$

$$\psi_{+L} \;=\; \psi_{\downarrow} \;\;\in\;\; (\mathbf{2},\mathbf{1}) \qquad , \qquad \bar{\psi}_{+L} \;=\; \bar{\psi}_{\uparrow} \;\in\; (\mathbf{2},\mathbf{1})\;. \tag{3.10}$$

where $(\mathcal{R}_{\mathbf{L}},\mathcal{R}_{\mathbf{R}})$ labels the $SU(2)_{L}\otimes SU(2)_{R}$ content and $\mathcal{R}_{\mathbf{L,R}}$ are $SU(2)_{\mathbf{L,R}}$ representations.

3.2.2 Symmetry breaking Hamiltonians

In null-plane quantization, all dynamical information of a Poincaré invariant theory of quantum mechanics is contained in the three reduced Hamiltonians $M\mathcal{J}_{r}$ and M^{2} which encode the spin content and spectrum, respectively [10]. The reduced Hamiltonians commute with six of the kinematical generators of the Poincaré algebra and satisfy the $U(2)$ algebra together with the seventh kinematical generator $\mathcal{J}_{3}$:

$$\begin{aligned} [\,\mathcal{J}_{3}\,,\,M\mathcal{J}_{r}\,] \;&=\; i\,\epsilon_{rs}M\mathcal{J}_{s} \qquad , \qquad [\,\mathcal{J}_{3}\,,\,M^{2}\,] \;=\; 0\;; \\ [\,M\mathcal{J}_{r}\,,\,M\mathcal{J}_{s}\,] \;&=\; i\,\epsilon_{rs}M^{2}\mathcal{J}_{3} \qquad , \qquad [\,M^{2}\,,\,M\mathcal{J}_{r}\,] \;=\; 0\;, \end{aligned} \tag{3.11}$$

where r, s are transverse indices. As spin is dynamical, consequences of Lorentz invariance such as the arrangement of the spectrum of the theory into representations of the Lorentz group are evident only in the solution of the theory, as we will see explicitly in several examples below. In particular, while the spin of the system is usually given by the sum of the spins of the constituents, here that is no longer the case. The spin of the system is given by the sum of the spins of the constituents as well as by the interactions among the constituent spins.

The Lie brackets among the reduced Hamiltonians and the chiral charges are

$$\mathcal{P}^{\alpha\beta;\mu\nu}\,[\tilde{Q}_5^\mu(x^+)\,,\,[\,\tilde{Q}_5^\nu(x^+)\,,\,M^2]]\;=\;\mathcal{P}^{\alpha\beta;\mu\nu}\,[\tilde{Q}_5^\mu(x^+)\,,\,[\,\tilde{Q}_5^\nu(x^+)\,,\,M\mathcal{J}_\pm]]\;=\;0\;, \tag{3.12}$$

where $\mathcal{P}^{\alpha\beta;\mu\nu}\;\equiv\;\delta^{\alpha\nu}\delta^{\beta\mu}\;-\;\delta^{\alpha\beta}\delta^{\mu\nu}/3$ and $M\mathcal{J}^\pm \equiv M\mathcal{J}_1 \pm iM\mathcal{J}_2$. It is straightforward to show that these constraints imply that M^2 and $M\mathcal{J}_\pm$ transform as linear combinations of $(\mathbf{1},\mathbf{1})$ and $(\mathbf{2},\mathbf{2})$ representation of $SU(2)_L \otimes SU(2)_R$. That is,

$$M^2 \;=\; M_{\mathbf{1}}^2 \;+\; M_{\mathbf{22}}^2\;; \tag{3.13}$$

$$M\mathcal{J}^\pm \;=\; M\mathcal{J}_{\mathbf{1}}^\pm \;+\; M\mathcal{J}_{\mathbf{22}}^\pm\,. \tag{3.14}$$

The chiral transformation properties of the energy and transverse spin were first obtained in Refs. [36, 37, 64] by considering the asymptotic behavior of scattering amplitudes involving massless pions.

As the chiral-symmetry breaking parts of the Hamiltonians represent the effect of spontaneous symmetry breaking on the null-plane, it is imperative that these contributions not break Lorentz invariance spontaneously. In particular, a fundamental constraint on chiral symmetry breaking is

$$[\,\mathcal{J}_3\,,\,M_{\mathbf{22}}^2\,]\;=\;0\;. \tag{3.15}$$

As will be seen below, this constraint is remarkably powerful, and leads directly to the picture of the nucleon as a source of valence spin whose entanglement with the spin of the sea gives rise to chiral symmetry breaking.

3.2.3 Hadronic states and selection rules

A general hadronic null-plane momentum eigenstate may be written as

$$|h\,,\,\Lambda\rangle \equiv\ |h\,,\,\Lambda\,;\,p^+\,,\,\mathbf{p}_\perp\rangle = |h\,,\,\Lambda\rangle\otimes|\,p^+\,,\,\mathbf{p}_\perp\rangle\ . \tag{3.16}$$

A useful feature of the front form is that the dynamical and kinematical properties of a state are cleanly separated. This is related to the fact that the boost operators are purely kinematical. In the instant form the boost that takes one from one momentum state to another is dynamical. In this equation n are additional variables that may be needed to specify the state of a system at rest, and Λ is helicity, the eigenvalue of $\mathcal{J}_3$:

$$\mathcal{J}_3\,|h\,,\,\Lambda\,;\,p^+\,,\,\mathbf{p}_\perp\rangle\ =\ \Lambda\,|h\,,\,\Lambda\,;\,p^+\,,\,\mathbf{p}_\perp\rangle\ . \tag{3.17}$$

Naively the parity operation interchanges null-plane time and the longitudinal coordinate. Defining the generalized parity operator, $\mathcal{Y}\equiv P\exp\left(i\pi J_2\right)$, the product of the parity operator P and a rotation about the 2-direction gives [65]

$$\mathcal{Y}\,|h\,,\,\Lambda\,;\,p^+\,,\,\mathbf{p}_\perp\rangle\ =\ (-1)^{J-\Lambda}\eta_h\,|h\,,\,-\Lambda\,;\,p^+\,,\,(\mathbf{p}_1,-\mathbf{p}_2)\rangle\ , \tag{3.18}$$

where η_h is the intrinsic parity of h. Defining canonical angular momentum raising and lowering operators, $\hat{J}^\pm$ whose action on a state of definite spin J (at rest) is

$$\hat{J}^+\,|h\,,\,\Lambda\rangle\ =\ \sqrt{J(J+1)-\Lambda(\Lambda+1)}|h\,,\,\Lambda+1\rangle\ , \tag{3.19}$$

one then has

$$\langle h\,,\,-\Lambda-1\,|\,\mathcal{Y}\hat{J}^+\,|h\,,\,\Lambda\rangle\ =\ \sqrt{J(J+1)-\Lambda(\Lambda+1)}(-1)^{J-\Lambda}\eta_h\ . \tag{3.20}$$

Note that $\mathcal{Y}$ is an endomorphism of the chiral algebra [64], as

$$\mathcal{Y}\,\tilde{Q}^\alpha_5(x^+)\,\mathcal{Y}\ =\ -\tilde{Q}^\alpha_5(x^+)\quad,\quad\mathcal{Y}\,\tilde{Q}^\alpha\,\mathcal{Y}\ =\ \tilde{Q}^\alpha\ . \tag{3.21}$$

3.2.4 The chiral basis

Consider the hadronic matrix elements between null-plane momentum states of the following QCD operators

$$\begin{aligned}
\langle h',\Lambda';p'^{+},\mathbf{p}'_{\perp}|\tilde{Q}^5_{\alpha}(x^{+})|h,\Lambda;p^{+},\mathbf{p}_{\perp}\rangle &= (2\pi)^3 2p^{+}\delta(q^{+})\delta^2(\mathbf{q}_{\perp})\,\langle h',\Lambda'|\tilde{Q}^5_{\alpha}|h,\Lambda\rangle\,\delta_{\Lambda',\Lambda}\\
\langle h',\Lambda';p'^{+},\mathbf{p}'_{\perp}|\tilde{Q}_{\alpha}|h,\Lambda;p^{+},\mathbf{p}_{\perp}\rangle &= (2\pi)^3 2p^{+}\delta(q^{+})\delta^2(\mathbf{q}_{\perp})\,\langle h',\Lambda'|\tilde{Q}_{\alpha}|h,\Lambda\rangle\,\delta_{\Lambda',\Lambda}\delta_{h',h}\\
\langle h',\Lambda';p'^{+},\mathbf{p}'_{\perp}|M^2|h,\Lambda;p^{+},\mathbf{p}_{\perp}\rangle &= (2\pi)^3 2p^{+}\delta(q^{+})\delta^2(\mathbf{q}_{\perp})\,\langle h',\Lambda'|M^2|h,\Lambda\rangle\,\delta_{\Lambda',\Lambda}\delta_{h',h}\\
\langle h',\Lambda';p'^{+},\mathbf{p}'_{\perp}|M\mathcal{J}^{\pm}|h,\Lambda;p^{+},\mathbf{p}_{\perp}\rangle &= (2\pi)^3 2p^{+}\delta(q^{+})\delta^2(\mathbf{q}_{\perp})\,\langle h',\Lambda'|M\mathcal{J}^{\pm}|h,\Lambda\rangle\,\delta_{\Lambda',\Lambda\pm1}\delta_{h',h}\\
\langle h',\Lambda';p'^{+},\mathbf{p}'_{\perp}|\mathcal{J}_3|h,\Lambda;p^{+},\mathbf{p}_{\perp}\rangle &= (2\pi)^3 2p^{+}\delta(q^{+})\delta^2(\mathbf{q}_{\perp})\,\langle h',\Lambda'|\mathcal{J}_3|h,\Lambda\rangle\,\delta_{\Lambda',\Lambda}\delta_{h',h}\ . \qquad (3.22)
\end{aligned}$$

Our goal will be to construct a representation of the operators on the right hand side (using the same symbol for the operator) which act only on the spin degrees of freedom that label the state $|h,\Lambda\rangle$ and satisfy the algebraic constraints which enforce: 1) the correct pattern of chiral symmetry breaking, Eq. (3.5), and 2) a Poincaré invariant description, Eq. (3.11), of the hadronic system[2]. The resulting spin system provides valuable insight into the nature of chiral symmetry breaking and the structure of baryon states, and imposes powerful quantitative constraints on the spectrum.

We will label baryon states as

$$|\,(\mathcal{R}_{\mathbf{L}},\mathcal{R}_{\mathbf{R}})_{\mathcal{R}}\,,\,\lambda\,\rangle \qquad (3.23)$$

where $\mathcal{R}$ is an $SU(2)$-isospin representation in the product $\mathcal{R}_{\mathbf{R}}\otimes\mathcal{R}_{\mathbf{L}}$. For instance, a $\lambda=\frac{1}{2}$ baryon state can be in a $(\mathbf{2},\mathbf{1})$ which contains a single isodoublet, or it can be in an $(\mathbf{2},\mathbf{3})$ state which contains an isodoublet $(\mathbf{2},\mathbf{3})_{\mathbf{2}}$ and an isoquartet $(\mathbf{2},\mathbf{3})_{\mathbf{4}}$. The physical baryon states will be labelled as $^{\mathbf{2J+1}}\mathcal{R}$ where J is the spin of the state. Therefore, we have states of type $^{\mathbf{2J+1}}N$ and $^{\mathbf{2J+1}}\Delta$.

---

[2]Note that Poincaré invariance does not imply the more stringent constraint of Poincaré covariance. This paper has nothing to say about covariance as that pertains to the action of the Poincaré generators on the space and time dependence of the wavefunction and here the spatial coordinates are present only as some orbital contribution to the total spin of the state.

As the normality parity operator flips the sign of the spin,

$$\mathcal{Y}\left(\tilde{Q}^{\alpha} \pm \tilde{Q}_5^{\alpha}\right)\mathcal{Y}^{-1} \;=\; \left(\tilde{Q}^{\alpha} \mp \tilde{Q}_5^{\alpha}\right) \;, \tag{3.24}$$

the action of normality on the chiral basis states is

$$\mathcal{Y}|\,(\mathcal{R}_{\mathbf{L}},\mathcal{R}_{\mathbf{R}})_{\mathcal{R}}\,,\,\lambda\,\rangle \;=\; \phi|\,(\mathcal{R}_{\mathbf{R}},\mathcal{R}_{\mathbf{L}})_{\mathcal{R}}\,,\,-\lambda\,\rangle \;, \tag{3.25}$$

where ϕ is a phase chosen for convenience. The total angular momentum operator is given by the helicity; that is, $\mathcal{J}_3 = \hat{S}_3$, where $\hat{S}_3|\,\lambda\,\rangle = \lambda|\,\lambda\,\rangle$.

As the chiral states are states of definite helicity, it is useful to express the states in terms of their transformation properties with respect to the permutation group $\mathbf{S}_3$. The construction is similar to the states of the nonrelativistic quark model. However, the chiral states have less symmetry since they are not eigenstates of the spin operator; indeed the chiral states are linear combinations of states of definite spin; that is, they transform reducibly with respect to the Lorentz group.

3.2.5 The Casher-Susskind theorem and entanglement

It is clear that in order to break chiral symmetry without breaking Lorentz invariance, that is, simultaneously satisfy

$$[\,\mathcal{J}_3\,,\,M^2_{\mathbf{22}}\,] \;=\; 0 \quad , \quad [\,\tilde{Q}_5^{\alpha}\,,\,M^2_{\mathbf{22}}\,] \;\neq\; 0 \;, \tag{3.26}$$

there must be a non-valence source of angular momentum which is denoted $\hat{\mathbb{P}}_3$ and defined such that the total helicity is given by

$$\mathcal{J}_3 = \hat{S}_3 \otimes \mathbb{1} \;+\; \mathbb{1} \otimes \hat{\mathbb{P}}_3 \;. \tag{3.27}$$

Here, the additional angular momentum generally arises from the sum

$$\hat{\mathbb{P}}_3 \;\;=\;\; \hat{\mathbb{P}}_3^{(1)} \otimes \mathbb{1} \otimes \cdots + \mathbb{1} \otimes \hat{\mathbb{P}}_3^{(2)} \otimes \cdots + \ldots \;. \tag{3.28}$$

This well-known feature of null-plane QCD was demonstrated long ago by Casher and Susskind [42]. Assume that the total helicity, $\mathcal{J}_3$, is given entirely by the valence quark

helicity, $\hat{S}_3$. Then the first commutator in Eq. (3.26) implies that $M^2_{\mathbf{22}}$ is a function of $\hat{S}_3$, $M^2_{\mathbf{22}} = M^2_{\mathbf{22}}(\hat{S}_3)$, which is clearly inconsistent as then the second commutator must vanish. However, as soon as there is an additional source of helicity, then the first commutator can be satisfied by compensating a change in the valence helicity with the additional source; that is, $M^2_{\mathbf{22}} = M^2_{\mathbf{22}}(\hat{J}_3, \hat{S}^+\hat{\mathbb{P}}^-, \hat{S}^-\hat{\mathbb{P}}^+)$ and the second commutator need not vanish. The chiral constraints are then satisfied since

$$[\tilde{Q}^\beta_5\,,\,[\,\tilde{Q}^\alpha_5\,,\,\hat{S}^\pm]] \;=\; \delta^{\alpha\beta}\hat{S}^\pm\;, \tag{3.29}$$

which implies that $\hat{S}^\pm$ transforms in the $(\mathbf{2},\mathbf{2})$ representation of $SU(2)_L \otimes SU(2)_R$. Here the angular momentum algebra is assumed to be satisfied by the various components of spin,

$$[\,\hat{S}_i\,,\,\hat{S}_j\,] \;=\; i\,\epsilon_{ijk}\hat{S}_k \quad , \quad [\,\hat{\mathbb{P}}^{(a)}_i\,,\,\hat{\mathbb{P}}^{(a)}_j\,] \;=\; i\,\epsilon_{ijk}\hat{\mathbb{P}}^{(a)}_k\;. \tag{3.30}$$

The valence spin in this case is no longer a constant of the motion and will therefore, like the chiral charge, induce transitions between states that carry different energy [3]. We now have a bipartite Hilbert space in which the valence spin lives in $\mathcal{H}_A$, and all other sources of spin live in $\mathcal{H}_B$, which we denote $\mathcal{H}_A \otimes \mathcal{H}_B$. In QCD, the QCD operator that counts the valence helicity is gauge invariant, and therefore $\mathcal{H}_A$ and $\mathcal{H}_B$ are gauge-invariant subspaces. Our product basis states are now:

$$|\,(\mathcal{R}_{\mathbf{L}},\mathcal{R}_{\mathbf{R}})_{\mathcal{R}}\,,\,\lambda\,\rangle \otimes |\,\mathbb{p}_3\,\rangle \;\equiv\; |\,(\mathcal{R}_{\mathbf{L}},\mathcal{R}_{\mathbf{R}})_{\mathcal{R}}\,,\,\lambda\,;\,\mathbb{p}_3\,\rangle \tag{3.31}$$

where $\hat{\mathbb{P}}_3|\,\mathbb{p}_3\,\rangle = \mathbb{p}_3|\,\mathbb{p}_3\,\rangle$ and the total helicity is now $\Lambda = \lambda + \mathbb{p}_3$. As

$$[\,\hat{\mathbb{P}}_r\,,\,M^2_{\mathbf{1}}\,] \;\neq\; 0\;, \tag{3.32}$$

in general these states of definite helicity, $\mathbb{p}_3$, can be expanded in orthonormal states of definite $\mathbb{p}$:

$$|\,\mathbb{p}_3\,\rangle^{(\ell)} \;=\; \sum_{\mathbb{p}=|\mathbb{p}_3|}^{N_{\mathbb{p}}} \sum_{\mathfrak{a}=1}^{g_{\mathbb{p}}} c^{\ell\,\mathfrak{a}}_{\mathbb{p}\mathbb{p}_3}|\,\mathbb{p},\mathbb{p}_3\,\rangle^{(\mathfrak{a})}\;, \tag{3.33}$$

[3] On the null plane, the valence helicity operator coincides with the axial $U(1)$ generator which is anomalous.

where $N_{\mathbb{p}}$ is the maximum allowed integer spin and $g_{\mathbb{p}}$ is the number of states of spin $\mathbb{p}$. The number of states of definite helicity, $\mathbb{p}_3$, is

$$\chi_{\mathbb{p}_3} \;=\; \sum_{\mathbb{p}=|\mathbb{p}_3|}^{N_{\mathbb{p}}} g_{\mathbb{p}} \;. \tag{3.34}$$

The normalization condition on the expansions coefficients is:

$$\sum_{\mathbb{p}=|\mathbb{p}_3|}^{N_{\mathbb{p}}} \sum_{\mathfrak{a}=1}^{g_{\mathbb{p}}} c^{*\ell'\,\mathfrak{a}}_{\mathbb{p}\mathbb{p}_3} c^{\ell\,\mathfrak{a}}_{\mathbb{p}\mathbb{p}_3} \;=\; \delta^{\ell'\,\ell} \;. \tag{3.35}$$

A necessary condition for chiral symmetry breaking is that at least one of the following matrix elements is non-vanishing:

$${}^{(\ell')}\langle\, \mathbb{p}_3 \pm 1 \,|\hat{\mathbb{P}}^{\pm}|\, \mathbb{p}_3 \,\rangle^{(\ell)} \;=\; \sum_{\mathbb{p}=|\mathbb{p}_3|}^{N_{\mathbb{p}}} \sum_{\mathfrak{a}=1}^{g_{\mathbb{p}}} c^{*\ell'\,\mathfrak{a}}_{\mathbb{p}\mathbb{p}_3\pm 1} c^{\ell\,\mathfrak{a}}_{\mathbb{p}\mathbb{p}_3} \sqrt{\mathbb{p}(\mathbb{p}+1) - \mathbb{p}_3(\mathbb{p}_3+1)} \;. \tag{3.36}$$

A priori, in QCD, there is no reason to expect that $N_{\mathbb{p}}$ is finite as it governs the maximum spin state that can be achieved by the parton sea. However, the renormalization group suggests that many of these spin degrees of freedom are high-energy states and may therefore be integrated out to give a description in terms of a finite number of spins. Of course the minimal number will be required to describe the ground state and then more spin modes will have to be integrated in as higher energy excitations of the system are probed[4].

The general chiral decomposition of the baryon null-plane wavefunctions is then as follows for states with total helicity Λ. For $I = \frac{1}{2}$ states,

$$|\, N\,;\, \boldsymbol{\Lambda}\,\rangle : \quad \begin{cases} |(\mathbf{2},\mathbf{1})\,,\, \frac{1}{2}\,,\, \Lambda - \frac{1}{2}\rangle \;,\; |(\mathbf{2},\mathbf{3})_{\mathbf{2}}\,,\, \frac{1}{2}\,;\, \Lambda - \frac{1}{2}\rangle \;, \\ |(\mathbf{1},\mathbf{2})\,,\, -\frac{1}{2}\,,\, \Lambda + \frac{1}{2}\rangle \;,\; |(\mathbf{3},\mathbf{2})_{\mathbf{2}}\,,\, -\frac{1}{2}\,;\, \Lambda + \frac{1}{2}\rangle \;, \\ |(\mathbf{1},\mathbf{2})\,,\, \frac{3}{2}\,;\, \Lambda - \frac{3}{2}\rangle \;,\; |(\mathbf{2},\mathbf{1})\,,\, -\frac{3}{2}\,;\, \Lambda + \frac{3}{2}\rangle \;, \end{cases} \tag{3.37}$$

[4]For instance, assume that the parton sea is populated by $xG(x)$ non-interacting gluons...

and for $I = \frac{3}{2}$ states,

$$|\,\Delta\,;\,\mathbf{\Lambda}\,\rangle : \quad \begin{cases} |(\mathbf{2},\mathbf{3})_{\mathbf{4}}\,,\,\frac{1}{2}\,;\,\Lambda-\frac{1}{2}\rangle\;,\;|(\mathbf{3},\mathbf{2})_{\mathbf{4}}\,,\,-\frac{1}{2}\,;\,\Lambda+\frac{1}{2}\rangle\;, \\ \\ |(\mathbf{1},\mathbf{4})\,,\,\frac{3}{2}\,;\,\Lambda-\frac{3}{2}\rangle\;,\;|(\mathbf{4},\mathbf{1})\,,\,-\frac{3}{2}\,;\,\Lambda+\frac{3}{2}\rangle\;. \end{cases} \tag{3.38}$$

The action of normality on the chiral basis states is now

$$\mathcal{Y}|\,(\mathcal{R}_{\mathbf{L}},\mathcal{R}_{\mathbf{R}})_{\mathcal{R}}\,,\,\lambda\,;\,\mathbb{p}_3\,\rangle \;=\; \phi|\,(\mathcal{R}_{\mathbf{R}},\mathcal{R}_{\mathbf{L}})_{\mathcal{R}}\,,\,-\lambda\,;\,-\mathbb{p}_3\,\rangle\;, \tag{3.39}$$

where again ϕ is a phase which depends on the particular chiral representation, and is determined by ensuring that Eq. (3.18) is satisfied for a particular hadronic state.

Of course a fundamental assumption that we have made in formulating these basis states is that the valence content of the light baryons is given by three light quarks. If this were not the case, then baryon states with isospin greater than 3/2 would be observed in the spectrum and we would have to consider states with additional valence content. However, we have made no assumption regarding the non-valence contributions to the baryon spin.

3.3 Nucleon state in the chiral basis

3.3.1 The general case

In the chiral basis the nucleon $\Lambda = 1/2$ state can be expressed as the pure state

$$|\,N\,;\,\tfrac{\mathbf{1}}{\mathbf{2}}\,\rangle \;=\; |\,\tfrac{1}{2}\,;\,\mathbf{0}\big) \;+\; |\,-\tfrac{1}{2}\,;\,\mathbf{1}\big) \;+\; |\,\tfrac{3}{2}\,;\,-\mathbf{1}\big) \;+\; |\,-\tfrac{3}{2}\,;\,\mathbf{2}\big)\;, \tag{3.40}$$

where we have adopted the vector notation such that

$$\begin{aligned}
|\,\tfrac{1}{2}\,;\,\mathbf{0}\big) \;&\equiv\; \sum_{i=1}^{3}\sum_{\ell=1}^{\chi_0}\big(\Phi_1^{i\ell}|(\mathbf{2},\mathbf{1})\,,\,\tfrac{1}{2}\,\rangle^{(i)} + \Phi_2^{i\ell}|(\mathbf{2},\mathbf{3})_{\mathbf{2}}\,,\,\tfrac{1}{2}\,\rangle^{(i)}\big)\otimes|\,\mathbf{0}\,\rangle^{(\ell)}\;; \\
|\,-\tfrac{1}{2}\,;\,\mathbf{1}\big) \;&\equiv\; \sum_{i=1}^{3}\sum_{\ell=1}^{\chi_1}\big(\Phi_3^{i\ell}|(\mathbf{1},\mathbf{2})\,,\,-\tfrac{1}{2}\,\rangle^{(i)} + \Phi_4^{i\ell}|(\mathbf{3},\mathbf{2})_{\mathbf{2}}\,,\,-\tfrac{1}{2}\,\rangle^{(i)}\big)\otimes|\,\mathbf{1}\,\rangle^{(\ell)}\;; \\
|\,\tfrac{3}{2}\,;\,-\mathbf{1}\big) \;&\equiv\; \sum_{m=1}^{2}\sum_{\ell=1}^{\chi_1}\Phi_5^{m\ell}|(\mathbf{1},\mathbf{2})\,,\,\tfrac{3}{2}\,\rangle^{(m)}\otimes|\,-\mathbf{1}\,\rangle^{(\ell)}\;; \\
|\,-\tfrac{3}{2}\,;\,\mathbf{2}\big) \;&\equiv\; \sum_{m=1}^{2}\sum_{\ell=1}^{\chi_2}\Phi_6^{m\ell}|(\mathbf{2},\mathbf{1})\,,\,-\tfrac{3}{2}\,\rangle^{(m)}\otimes|\,\mathbf{2}\,\rangle^{(\ell)}\;,
\end{aligned} \tag{3.41}$$

with normalization

$$\sum_{\gamma=1}^{6} \mathrm{tr}\left(\hat{\Phi}_\gamma^\dagger \hat{\Phi}_\gamma\right) \;=\; 1\;. \tag{3.42}$$

In the Fock basis these six types of states with orbital angular momentum, three with $\mathbb{p} = \pm 1$, two with $\mathbb{p} = 0$ and one with $\mathbb{p} = 2$, have been written down explicitly in terms of null-plane quark fields in Ref. [33]. Note that we have taken the available valence states from the quark model wavefunctions constructed in the appendices. This form is the most general form of the nucleon state as it includes Fock-space components with arbitrary amounts of glue. Given that in general one expects that the $\mathcal{H}_L$ Hilbert space is infinite dimensional, it may seem that constraining this wavefunction is a lost cause. However, here the renormalization group comes to the rescue. The density of partons and therefore the number of spin states increases as one goes to lower and lower x. However, these low-x states are high energy states whose detailed form should be irrelevant to the ground state baryon wavefunction of the theory. Therefore, it is sensible to assume that the nucleon wavefunction may have only a few important components in which the valence sector interacts with a frozen parton sea.

3.3.2 Entanglement entropy as an order parameter

The density matrix of the valence spin is defined by

$$\rho_A = \mathrm{tr}_B\left(|\, N\,,\, \tfrac{\mathbf{1}}{\mathbf{2}}\,\rangle\langle\, N\,,\, \tfrac{\mathbf{1}}{\mathbf{2}}\,|\right), \tag{3.43}$$

which gives, in supermatrix form,

$$\rho_A = \begin{array}{c} \\ |\,(2,1)\,,\,\frac{1}{2}\,\rangle^{(j)} \\ |\,(2,3)_2\,,\,\frac{1}{2}\,\rangle^{(j)} \\ |\,(1,2)\,,\,-\frac{1}{2}\,\rangle^{(j)} \\ |\,(3,2)_2\,,\,-\frac{1}{2}\,\rangle^{(j)} \\ |\,(1,2)\,,\,\frac{3}{2}\,\rangle^{(n)} \\ |\,(2,1)\,,\,-\frac{3}{2}\,\rangle^{(n)} \end{array} \begin{array}{c} \begin{array}{cccccc} {}^{(i)}\langle\,(2,1)\,,\,\frac{1}{2}\,| & {}^{(i)}\langle\,(2,3)_2\,,\,\frac{1}{2}\,| & {}^{(i)}\langle\,(1,2)\,,\,-\frac{1}{2}\,| & {}^{(i)}\langle\,(3,2)_2\,,\,-\frac{1}{2}\,| & {}^{(m)}\langle\,(1,2)\,,\,\frac{3}{2}\,| & {}^{(m)}\langle\,(2,1)\,,\,-\frac{3}{2}\,| \end{array} \\ \left[\begin{array}{cccccc} (\hat{\Phi}_1\hat{\Phi}_1^\dagger)_{ij} & (\hat{\Phi}_1\hat{\Phi}_2^\dagger)_{ij} & 0 & 0 & 0 & 0 \\ (\hat{\Phi}_2\hat{\Phi}_1^\dagger)_{ij} & (\hat{\Phi}_2\hat{\Phi}_2^\dagger)_{ij} & 0 & 0 & 0 & 0 \\ 0 & 0 & (\hat{\Phi}_3\hat{\Phi}_3^\dagger)_{ij} & (\hat{\Phi}_3\hat{\Phi}_4^\dagger)_{ij} & 0 & 0 \\ 0 & 0 & (\hat{\Phi}_4\hat{\Phi}_3^\dagger)_{ij} & (\hat{\Phi}_4\hat{\Phi}_4^\dagger)_{ij} & 0 & 0 \\ 0 & 0 & 0 & 0 & (\hat{\Phi}_5\hat{\Phi}_5^\dagger)_{mn} & 0 \\ 0 & 0 & 0 & 0 & 0 & (\hat{\Phi}_6\hat{\Phi}_6^\dagger)_{mn} \end{array}\right] \end{array} \tag{3.44}$$

from which follows the entanglement entropy

$$S_N(\rho_A) = -\mathrm{tr}_A\left(\rho_A \log \rho_A\right). \tag{3.44}$$

The entanglement entropy is non-vanishing if the nucleon state in Eq. (3.40) contains more than one term. The mixing angles are of course determined by the Hamiltonians. They deviate from unity if and only if the M^2 Hamiltonian contains an off-diagonal component. Since all off-diagonal components break chiral symmetry, it is clear that the nucleon state contains chiral symmetry breaking if and only if $S_N > 0$. This suggests that in null-plane quantization the entanglement entropy is an order parameter for chiral symmetry breaking. The maximally entangled state occurs when ρ_A is proportional to the identity; that is, the maximal entanglement entropy is the logarithm of the total number of states:

$$S_N(\rho_A) \;\leq\; \log 2 \;+\; \log\left(3\chi_0 + 4\chi_1 + \chi_2\right) \;. \tag{3.45}$$

At the maximum value of the entanglement entropy, the valence spin content of the nucleon vanishes and the neutron does not decay. That is, one finds in this limit $\Delta\Sigma = g_A = 0$. It is not clear how this definition of entanglement entropy is useful. It is evidently non-local since in principle the spin interactions that give rise to it are non-local.

3.3.3 The large-N_c limit

The large-N_c limit leads to a tremendous simplification and indeed allows an exact solution to the problem posed by the various algebraic constraints [29, 38]. It is important to emphasize that this has nothing whatsoever to do with the non-relativistic quark model. The large-N_c constraints [40, 41] are a consequence of unitarity and, as they place powerful constraints on axial matrix elements of the nucleon, they must be reflected in the null-plane QCD chiral constraints. If we take

$$[\,\tilde{Q}_5^\alpha\,,\,M\,] \;\equiv\; \epsilon^\alpha\;, \tag{3.46}$$

and throw away terms of $\mathcal{O}(\epsilon)$. This implies that all chiral symmetry breaking must occur in the spin Hamiltonians, $M\mathcal{J}_{\pm}$. In this limit, the QCD operator algebra reduces to

$$[\,\mathcal{J}_i\,,\,\mathcal{J}_j\,] \;=\; i\,\epsilon_{ijk}\,\mathcal{J}_k \tag{3.47}$$

which generates $SU(2)$ spin, the $SU(2)_L \otimes SU(2)_L$ algebra of eq. 3.5, and the remaining non-trivial Lie bracket mixes the chiral generators and the spin Hamiltonians:

$$\mathcal{P}^{\alpha\beta;\mu\nu}\,[\tilde{Q}_5^{\mu}\,,\,[\,\tilde{Q}_5^{\nu}\,,\,\mathcal{J}_{\pm}]] \;=\; 0\;. \tag{3.48}$$

Remarkably, this simplified algebra can be put into a familiar form. Consider an operator $G_{\alpha i}$, which transforms as an adjoint of $SU(2)$ (flavor) and as a vector with respect to rotations. Identifying $G^{\alpha 3} \;\equiv\; \tilde{Q}_5^{\alpha}$. Detailed consideration of the properties of $G^{\alpha\beta}$ leads to [29, 38]

$$[\,G_{\alpha i}\,,\,G_{\beta j}\,] \;=\; i\,\delta_{ij}\,\epsilon_{\alpha\beta\gamma}\,\tilde{Q}_{\gamma} \;+\; i\,\delta_{\alpha\beta}\,\epsilon_{ijk}\,\mathcal{J}_k \tag{3.49}$$

which together with

$$[\,\tilde{Q}_{\alpha}\,,\,G_{\beta i}\,] \;=\; i\,f_{\alpha\beta\gamma}\,G_{\gamma i} \quad , \quad [\,\mathcal{J}_i\,,\,G_{\alpha j}\,] \;=\; i\,\epsilon_{ijk}\,G_{\alpha k}\;; \tag{3.50}$$

$$[\,\tilde{Q}_{\alpha}\,,\,\tilde{Q}_{\beta}\,] \;=\; i\,f_{\alpha\beta\gamma}\,\tilde{Q}_{\gamma} \quad , \quad [\,\mathcal{J}_i\,,\,\mathcal{J}_j\,] \;=\; i\,\epsilon_{ijk}\,\mathcal{J}_k \tag{3.51}$$

close to the algebra of the group $SU(4)$. It is important to stress that this $SU(4)$ symmetry is truly a dynamical symmetry; it is unrelated to the invariance of QCD in the non-interacting limit.

$(\mathbf{2},\mathbf{3}) \oplus (\mathbf{1},\mathbf{4})$: the $SU(4)$ (large-N_c) limit. We will now describe the mapping between the symmetric and antisymmetric irreducible representations of $SU(4)$ and representations of $SU(2)_R \otimes SU(2)_L$. The symmetric **20** of $SU(4)$ is reproduced by

$$\Lambda = \pm\tfrac{1}{2} \qquad \begin{cases} |(\mathbf{2},\mathbf{3})_{\mathbf{2}}\,,\,\tfrac{1}{2},\,\mathbf{0}\rangle\;,\;|(\mathbf{2},\mathbf{3})_{\mathbf{4}}\,,\,\tfrac{1}{2},\,\mathbf{0}\rangle \\ \\ |(\mathbf{3},\mathbf{2})_{\mathbf{2}}\,,\,-\tfrac{1}{2},\,\mathbf{0}\rangle\;,\;|(\mathbf{3},\mathbf{2})_{\mathbf{4}}\,,\,-\tfrac{1}{2},\,\mathbf{0}\rangle \end{cases}$$

$$\Lambda = \pm\tfrac{3}{2} \qquad \begin{cases} |(\mathbf{1},\mathbf{4})\,,\,\tfrac{3}{2},\,\mathbf{0}\rangle \\ \\ |(\mathbf{4},\mathbf{1})\,,\,-\tfrac{3}{2},\,\mathbf{0}\rangle\;, \end{cases} \tag{3.52}$$

Note that here $\mathbb{p} = \mathbb{p}_3 = 0$. The physical positive helicity eigenstates can be written as

$$\begin{aligned} |\, N\,,\, \tfrac{\mathbf{1}}{\mathbf{2}}\,\rangle &= |(\mathbf{2},\mathbf{3})_{\mathbf{2}}\,,\, \tfrac{1}{2}\,,\, \mathbf{0}\rangle \\ |\, \Delta\,,\, \tfrac{\mathbf{1}}{\mathbf{2}}\,\rangle &= |(\mathbf{2},\mathbf{3})_{\mathbf{4}}\,,\, \tfrac{1}{2}\,,\, \mathbf{0}\rangle\ , \\ |\, \Delta\,,\, \tfrac{\mathbf{3}}{\mathbf{2}}\,\rangle &= |(\mathbf{1},\mathbf{4})\,,\, \tfrac{3}{2}\,,\, \mathbf{0}\rangle\ . \end{aligned} \tag{3.53}$$

To obtain the negative helicity eigenstates one acts with the $\mathcal{Y}$ operator on these states and fixes the phases in Eq. (3.39) by requiring that Eq. (3.18) be satisfied.

$$\begin{aligned} |\, N\,,\, -\tfrac{\mathbf{1}}{\mathbf{2}}\,\rangle &= |(\mathbf{3},\mathbf{2})_{\mathbf{2}}\,,\, -\tfrac{1}{2}\,,\, \mathbf{0}\rangle\ , \\ |\, \Delta\,,\, -\tfrac{\mathbf{1}}{\mathbf{2}}\,\rangle &= |(\mathbf{3},\mathbf{2})_{\mathbf{4}}\,,\, -\tfrac{1}{2}\,,\, \mathbf{0}\rangle\ , \\ |\, \Delta\,,\, -\tfrac{\mathbf{3}}{\mathbf{2}}\,\rangle &= |(\mathbf{4},\mathbf{1})\,,\, -\tfrac{3}{2}\,,\, \mathbf{0}\rangle\ . \end{aligned} \tag{3.54}$$

Since the physical states are in irreducible representations of the chiral group, this phase dependence does not appear.

3.4 Realistic nucleon wavefunctions

3.4.1 Saturation scheme 1: N_A, N_B, Δ

Hamiltonian constraints

Here the model of the previous section will be considered in more detail. This is consistent with the nucleon being a mixture of $\mathbf{20}_S$ and $\mathbf{4}_A$ of $SU(4)$. This is the simplest non-trivial model that extends the $SU(4)$ picture of degenerate nucleon and delta. The positive helicity eigenstates can be chosen to be

$$\begin{aligned} |N_A\,,\, \tfrac{\mathbf{1}}{\mathbf{2}}\,\rangle &= \sin\psi\,|(\mathbf{1},\mathbf{2})\,,\, -\tfrac{1}{2}\,,\, \mathbf{1}\rangle + \cos\psi\,|(\mathbf{2},\mathbf{3})_{\mathbf{2}}\,,\, \tfrac{1}{2}\,,\, \mathbf{0}\rangle \\ |N_B\,,\, \tfrac{\mathbf{1}}{\mathbf{2}}\,\rangle &= -\cos\psi\,|(\mathbf{1},\mathbf{2})\,,\, -\tfrac{1}{2}\,,\, \mathbf{1}\rangle + \sin\psi\,|(\mathbf{2},\mathbf{3})_{\mathbf{2}}\,,\, \tfrac{1}{2}\,,\, \mathbf{0}\rangle \\ |\Delta\,,\, \tfrac{\mathbf{1}}{\mathbf{2}}\,\rangle &= |(\mathbf{2},\mathbf{3})_{\mathbf{4}}\,,\, \tfrac{1}{2}\,,\, \mathbf{0}\rangle\ . \end{aligned} \tag{3.55}$$

Acting with the normality operator on the physical states via Eq. (3.18) and on the basis

states via Eq. (3.39) gives the negative-helicity mixed states:

$$\begin{aligned}(-1)^{J_{N_A}-\frac{1}{2}}\eta_{N_A}|N_A\,,\,-\mathbf{\frac{1}{2}}\,\rangle &= \sin\psi\,\phi_1|(\mathbf{2},\mathbf{1})\,,\,\tfrac{1}{2}\,,\,-\mathbf{1}\rangle\;+\cos\psi\,\phi_2|(\mathbf{3},\mathbf{2})_{\mathbf{2}}\,,\,-\tfrac{1}{2}\,,\,\mathbf{0}\rangle \\ (-1)^{J_{N_B}-\frac{1}{2}}\eta_{N_B}|N_B\,,\,-\mathbf{\frac{1}{2}}\,\rangle &= -\cos\psi\,\phi_1|(\mathbf{2},\mathbf{1})\,,\,\tfrac{1}{2}\,,\,-\mathbf{1}\rangle\;+\sin\psi\,\phi_2|(\mathbf{3},\mathbf{2})_{\mathbf{2}}\,,\,-\tfrac{1}{2}\,,\,\mathbf{0}\rangle\end{aligned} \tag{3.56}$$

where $\phi_{1,2}$ are phases. It is clear that the dependence on the total spin and parity of the states cannot be completely removed by appropriate choice of phases. This is expected since spin and parity are dynamical quantities that are constrained by interaction, and the presence of mixing signals dynamical chiral symmetry breaking. Choosing $\phi_1 = \phi_2 = (-1)^{J_{N_A}-\frac{1}{2}}\eta_{N_A}$, then gives the negative helicity eigenstates:

$$\begin{aligned}|N_A\,,\,-\mathbf{\frac{1}{2}}\,\rangle &= \sin\psi\,|(\mathbf{2},\mathbf{1})\,,\,\tfrac{1}{2}\,,\,-\mathbf{1}\rangle\;+\cos\psi\,|(\mathbf{3},\mathbf{2})_{\mathbf{2}}\,,\,-\tfrac{1}{2}\,,\,\mathbf{0}\rangle \\ (-1)^{\pi_{N_BN_A}}|N_B\,,\,-\mathbf{\frac{1}{2}}\,\rangle &= -\cos\psi\,|(\mathbf{2},\mathbf{1})\,,\,\tfrac{1}{2}\,,\,-\mathbf{1}\rangle\;+\sin\psi\,|(\mathbf{3},\mathbf{2})_{\mathbf{2}}\,,\,-\tfrac{1}{2}\,,\,\mathbf{0}\rangle \\ |\Delta\;,\,-\mathbf{\frac{1}{2}}\,\rangle &= |(\mathbf{3},\mathbf{2})_{\mathbf{4}}\,,\,-\tfrac{1}{2}\,,\,\mathbf{0}\rangle\;.\end{aligned} \tag{3.57}$$

where $(-1)^{\pi_{xy}} \equiv (-1)^{J_x-J_y}\eta_x\eta_y$. The Hamiltonians take the form

$$M^2 = \begin{matrix}\\ \langle\,(1,2)\,| \\ \langle\,(2,3)\,|\end{matrix}\begin{matrix}\begin{matrix}|\,(1,2)\,\rangle & |\,(2,3)\,\rangle\end{matrix}\\ \begin{bmatrix} m^2_{\mathbf{1a}} & m^2_{\mathbf{22}} \\ m^2_{\mathbf{22}} & m^2_{\mathbf{1b}}\end{bmatrix}\end{matrix}\quad,\qquad M\mathcal{J}^+ = \begin{matrix}\\ \langle\,(1,2)\,| \\ \langle\,(2,3)\,|\end{matrix}\begin{matrix}\begin{matrix}|\,(2,1)\,\rangle & |\,(3,2)\,\rangle\end{matrix}\\ \begin{bmatrix} mj_{\mathbf{22a}} & 0 \\ 0 & mj_{\mathbf{22b}}\end{bmatrix}\end{matrix}.$$

As there are three physical squared masses with one orthogonality condition and three mass-squared matrix elements, one sum rule is expected from the mass-squared Hamiltonian. One finds

$$M^2_{N_A}\cos^2\psi \;+\; M^2_{N_B}\sin^2\psi \;=\; M^2_{\Delta}\;. \tag{3.58}$$

Only the isodoublet sector is constrained by the spin Hamiltonians and as there are two physical masses with one orthogonality condition and two spin Hamiltonian matrix elements, one sum rum is expected. Taking matrix elements of the spin Hamiltonians yields:

$$(-1)^{\pi_{N_BN_A}}\left(J_{N_A}+\tfrac{1}{2}\right)M_{N_A} \;=\; \left(J_{N_B}+\tfrac{1}{2}\right)M_{N_B}\;. \tag{3.59}$$

It is quite clear that this latter constraint is not consistent with a single nucleon as the ground state. Therefore this saturation scheme is unambiguously inconsistent with experiment.

Axial couplings

In the physical basis, the quark helicity and axial-coupling matrices take the form:

$$\mathbf{\Delta\Sigma} \;=\; \begin{pmatrix} \cos 2\psi & \sin 2\psi \\ \sin 2\psi & -\cos 2\psi \end{pmatrix} \quad , \quad \mathbf{g_A} \;=\; \tfrac{1}{3}\begin{pmatrix} (4+\cos 2\psi) & \sin 2\psi \\ \sin 2\psi & (4-\cos 2\psi) \end{pmatrix} . \tag{3.60}$$

Identifying N_A with the nucleon, the familiar nucleon axial charges are

$$g_A \;=\; (\mathbf{g_A})_{AA} \;=\; \tfrac{1}{3}\,(4+\cos 2\psi) \quad , \quad \Delta\Sigma \;=\; (\mathbf{\Delta\Sigma})_{AA} \;=\; \cos 2\psi \; . \tag{3.61}$$

Other axial couplings are

$$\mathcal{C}_{\Delta N_A} \;=\; -2\cos\psi \quad , \quad \mathcal{C}_{\Delta N_B} \;=\; -2\sin\psi \quad , \quad \mathcal{H}_{\Delta\Delta} \;=\; -3 \; . \tag{3.62}$$

The consistency of the scheme is readily checked by taking matrix elements of the chiral algebra, Eq. (3.5), between all of the states in the saturation scheme, and inserting complete sets of states. For instance, the matrix elements between nucleon states

$$\langle\, N_A\,,\, \tfrac{\mathbf{1}}{\mathbf{2}}\,|[\,\tilde{Q}_5^+\,,\,\tilde{Q}_5^-\,]|\,N_A\,,\,\tfrac{\mathbf{1}}{\mathbf{2}}\,\rangle \;=\; \langle\, N_A\,,\,\tfrac{\mathbf{1}}{\mathbf{2}}\,|2\tilde{Q}^3|\,N_A\,,\,\tfrac{\mathbf{1}}{\mathbf{2}}\,\rangle \; , \tag{3.63}$$

and using the matrix elements of definite chirality constructed in the appendices, yields

$$(\mathbf{g_A})^2_{AA} \;+\; (\mathbf{g_A})^2_{AB} \;-\; \frac{4}{9}\,\mathcal{C}^2_{\Delta N_A} \;=\; 1 \; , \tag{3.64}$$

which is of course satisfied. This is the pole-saturated form of the nucleon Adler-Weisberger (AW) sum rule and points to a fundamental property that must be satisfied by the nucleon state: it satisfies an exact chiral symmetry regardless of the size of the (reducible) representation in which it finds itself. These sum rules are all trivial unless the Hamiltonians have chiral-symmetry breaking contributions, and indeed the Hamiltonian sum rules found above are checked by taking matrix elements of the algebraic constraints of Eq. (3.12).

There are, in addition, other interesting sum rules that are particular to the choice of saturation scheme. For instance, in this scheme one finds

$$\Delta\Sigma \;=\; \frac{2}{3}\mathcal{C}^2_{\Delta N_C} \;-\; g_A \;. \tag{3.65}$$

Entanglement entropy

We can trace over the sea and get the density matrix for the valence content

$$\rho_A = \mathrm{tr}_B\left(|\,N\,,\,\tfrac{\mathbf{1}}{\mathbf{2}}\,\rangle\langle\,N\,,\,\tfrac{\mathbf{1}}{\mathbf{2}}\,|\right) = \sin^2\psi|(\mathbf{1},\mathbf{2})\rangle\langle(\mathbf{1},\mathbf{2})| + \cos^2\psi|(\mathbf{2},\mathbf{3})_{\mathbf{2}}\rangle\langle(\mathbf{2},\mathbf{3})_{\mathbf{2}}| \tag{3.66}$$

from which follows the entanglement entropy

$$S_N(\psi) = -\sin^2\psi\log\left(\sin^2\psi\right) - \cos^2\psi\log\left(\cos^2\psi\right) \;. \tag{3.67}$$

The entanglement entropy, given in Eq. (3.67), can be expressed as

$$S_N(\Delta\Sigma) \;=\; -\tfrac{1}{2}\,(1-\Delta\Sigma)\log\tfrac{1}{2}\,(1-\Delta\Sigma) - \tfrac{1}{2}\,(1+\Delta\Sigma)\log\tfrac{1}{2}\,(1+\Delta\Sigma) \tag{3.68}$$

$$S_N(g_A) \;=\; -\tfrac{3}{2}\,(\tfrac{5}{3}-g_A)\log\tfrac{3}{2}\,(\tfrac{5}{3}-g_A) - \tfrac{3}{2}\,(g_A-1)\log\tfrac{3}{2}\,(g_A-1) \;. \tag{3.69}$$

3.4.2 Saturation scheme 2: N_A, N_B, Δ_A, Δ_B

Hamiltonian constraints

Consider next the scheme consistent with the nucleon being a mixture of $\mathbf{20}_S$ and $\mathbf{20}_M$ of $SU(4)$. The $\Lambda = +\frac{1}{2}$ eigenstates can be chosen to be

$$\begin{aligned}
|N_A\,,\,\tfrac{\mathbf{1}}{\mathbf{2}}\,\rangle &= \sin\phi|(\mathbf{3},\mathbf{2})_{\mathbf{2}},-\tfrac{1}{2},\mathbf{1}\rangle \;+\; \cos\phi\,|(\mathbf{2},\mathbf{3})_{\mathbf{2}},\tfrac{1}{2},\mathbf{0}\rangle \\
|N_B\,,\,\tfrac{\mathbf{1}}{\mathbf{2}}\,\rangle &= -\cos\phi\,|(\mathbf{3},\mathbf{2})_{\mathbf{2}},-\tfrac{1}{2},\mathbf{1}\rangle \;+\; \sin\phi\,|(\mathbf{2},\mathbf{3})_{\mathbf{2}},\tfrac{1}{2},\mathbf{0}\rangle \\
|\Delta_A\,,\,\tfrac{\mathbf{1}}{\mathbf{2}}\,\rangle &= \sin\omega|(\mathbf{3},\mathbf{2})_{\mathbf{4}}\,,\,-\tfrac{1}{2}\,,\,\mathbf{1}\rangle \;+\; \cos\omega|(\mathbf{2},\mathbf{3})_{\mathbf{4}}\,,\,\tfrac{1}{2}\,,\,\mathbf{0}\rangle \\
|\Delta_B\,,\,\tfrac{\mathbf{1}}{\mathbf{2}}\,\rangle &= -\cos\omega|(\mathbf{3},\mathbf{2})_{\mathbf{4}}\,,\,-\tfrac{1}{2}\,,\,\mathbf{1}\rangle \;+\; \sin\omega|(\mathbf{2},\mathbf{3})_{\mathbf{4}}\,,\,\tfrac{1}{2}\,,\,\mathbf{0}\rangle \;,
\end{aligned} \tag{3.70}$$

The negative helicity eigenstates are then obtained with the action of $\mathcal{Y}$:

$$\begin{aligned}
|N_A\,,\,-\tfrac{\mathbf{1}}{\mathbf{2}}\rangle &= \sin\phi|(\mathbf{2},\mathbf{3})_{\mathbf{2}},\tfrac{1}{2},-\mathbf{1}\rangle \;+\; \cos\phi\,|(\mathbf{3},\mathbf{2})_{\mathbf{2}},-\tfrac{1}{2},\mathbf{0}\rangle \\
(-1)^{\pi_{N_BN_A}}|N_B\,,\,-\tfrac{\mathbf{1}}{\mathbf{2}}\rangle &= -\cos\phi\,|(\mathbf{2},\mathbf{3})_{\mathbf{2}},\tfrac{1}{2},-\mathbf{1}\rangle \;+\; \sin\phi\,|(\mathbf{3},\mathbf{2})_{\mathbf{2}},-\tfrac{1}{2},\mathbf{0}\rangle \\
|\,\Delta_A\,,\,-\tfrac{\mathbf{1}}{\mathbf{2}}\rangle &= \sin\omega|(\mathbf{2},\mathbf{3})_{\mathbf{4}}\,,\,\tfrac{1}{2}\,,\,-\mathbf{1}\rangle \;+\; \cos\omega|(\mathbf{3},\mathbf{2})_{\mathbf{4}}\,,\,-\tfrac{1}{2}\,,\,\mathbf{0}\rangle \\
(-1)^{\pi_{\Delta_B\Delta_A}}|\,\Delta_B\,,\,-\tfrac{\mathbf{1}}{\mathbf{2}}\rangle &= -\cos\omega|(\mathbf{2},\mathbf{3})_{\mathbf{4}}\,,\,\tfrac{1}{2}\,,\,-\mathbf{1}\rangle \;+\; \sin\omega|(\mathbf{3},\mathbf{2})_{\mathbf{4}}\,,\,-\tfrac{1}{2}\,,\,\mathbf{0}\rangle\;, \qquad (3.71)
\end{aligned}$$

For both the N and Δ states, the Hamiltonians take the form

$$M^2 = \begin{matrix} \\ \langle(3,2)| \\ \langle(2,3)| \end{matrix}\!\!\begin{matrix} \begin{matrix} |(3,2)\rangle & |(2,3)\rangle \end{matrix} \\ \begin{bmatrix} m^2_{\mathbf{1a}} & m^2_{\mathbf{22c}} \\ m^2_{\mathbf{22c}} & m^2_{\mathbf{1c}} \end{bmatrix} \end{matrix} \quad , \qquad M\mathcal{J}^+ = \begin{matrix} \\ \langle(3,2)| \\ \langle(2,3)| \end{matrix}\!\!\begin{matrix} \begin{matrix} |(2,3)\rangle & |(3,2)\rangle \end{matrix} \\ \begin{bmatrix} mj_{\mathbf{22e}} & mj_{\mathbf{1a}} \\ mj_{\mathbf{1a}} & mj_{\mathbf{22f}} \end{bmatrix} \end{matrix} . \qquad (3.72)$$

There are two sum rules from the mass-squared Hamiltonian:

$$\left(M^2_{N_A} - M^2_{N_B}\right)\cos 2\psi \;=\; \left(M^2_{\Delta_A} - M^2_{\Delta_B}\right)\cos 2\omega \qquad (3.73)$$

$$M^2_{N_A} + M^2_{N_B} \;=\; M^2_{\Delta_A} + M^2_{\Delta_B}\;, \qquad (3.74)$$

and one sum rule from the spin Hamiltonians:

$$\begin{aligned}
&(-1)^{\pi_{\Delta_B\Delta_A}}\left[\left(J_{\Delta_B}+\tfrac{1}{2}\right)M_{\Delta_B} \;-\; (-1)^{\pi_{N_BN_A}}\left(J_{N_A}+\tfrac{1}{2}\right)M_{N_A}\right]\sin 2\phi \\
&\quad= (-1)^{\pi_{N_BN_A}}\left[\left(J_{\Delta_B}+\tfrac{1}{2}\right)M_{\Delta_B} \;-\; (-1)^{\pi_{\Delta_B\Delta_A}}\left(J_{\Delta_A}+\tfrac{1}{2}\right)M_{\Delta_A}\right]\sin 2\omega\;. \qquad (3.75)
\end{aligned}$$

It is clear from Eq. (3.74) that this saturation scheme is not useful.

Axial couplings

In the physical basis, the quark helicity and axial-coupling matrices take the form:

$$\mathbf{\Delta\Sigma} \;=\; \begin{pmatrix} \cos 2\psi & \sin 2\psi \\ \sin 2\psi & -\cos 2\psi \end{pmatrix} \quad , \quad \mathbf{g_A} \;=\; \tfrac{5}{3}\begin{pmatrix} \cos 2\psi & -\sin 2\psi \\ -\sin 2\psi & -\cos 2\psi \end{pmatrix} . \qquad (3.76)$$

3.4.3 Saturation scheme 3: N_A, N_B, N_C, Δ

The simplest extension of saturation scheme 1 is to add a third ${}^{\mathbf{2}}N$ state. In the $SU(4)$ language, this is like adding a second $\mathbf{4}_A$ state, and since the tensor product of three quarks gives only a single $\mathbf{4}_A$ state, the expectation is that this representation will require heavier excited states. It is nevertheless interesting to explore due to its relative simplicity and basic agreement with data.

Hamiltonian constraints

The positive helicity eigenstates can be chosen to be

$$\begin{aligned}
|N_A\,,\,\tfrac{\mathbf{1}}{\mathbf{2}}\rangle &= U_{11}\,|(\mathbf{2},\mathbf{1}),\tfrac{1}{2},\mathbf{0}\rangle + U_{12}\,|(\mathbf{1},\mathbf{2}),-\tfrac{1}{2},\mathbf{1}\rangle + U_{13}\,|(\mathbf{2},\mathbf{3})_{\mathbf{2}},\tfrac{1}{2},\mathbf{0}\rangle \\
|N_B\,,\,\tfrac{\mathbf{1}}{\mathbf{2}}\rangle &= U_{21}\,|(\mathbf{2},\mathbf{1}),\tfrac{1}{2},\mathbf{0}\rangle + U_{22}\,|(\mathbf{1},\mathbf{2}),-\tfrac{1}{2},\mathbf{1}\rangle + U_{23}\,|(\mathbf{2},\mathbf{3})_{\mathbf{2}},\tfrac{1}{2},\mathbf{0}\rangle \\
|N_C\,,\,\tfrac{\mathbf{1}}{\mathbf{2}}\rangle &= U_{31}\,|(\mathbf{2},\mathbf{1}),\tfrac{1}{2},\mathbf{0}\rangle + U_{32}\,|(\mathbf{1},\mathbf{2}),-\tfrac{1}{2},\mathbf{1}\rangle + U_{33}\,|(\mathbf{2},\mathbf{3})_{\mathbf{2}},\tfrac{1}{2},\mathbf{0}\rangle \\
|\Delta\,,\,\tfrac{\mathbf{1}}{\mathbf{2}}\rangle &= |(\mathbf{2},\mathbf{3})_{\mathbf{4}}\,,\,\tfrac{1}{2}\,,\,\mathbf{0}\rangle \\
|\Delta\,,\,\tfrac{\mathbf{3}}{\mathbf{2}}\rangle &= |(\mathbf{1},\mathbf{4})\,,\,\tfrac{3}{2}\,,\,\mathbf{0}\rangle\,.
\end{aligned} \tag{3.77}$$

The negative helicity eigenstates are then

$$\begin{aligned}
(-1)^{\pi_{N_C N_A}}|N_A\,,\,-\tfrac{\mathbf{1}}{\mathbf{2}}\rangle &= U_{11}\,|(\mathbf{1},\mathbf{2}),-\tfrac{1}{2},\mathbf{0}\rangle + U_{12}\,|(\mathbf{2},\mathbf{1}),\tfrac{1}{2},-\mathbf{1}\rangle + U_{13}\,|(\mathbf{3},\mathbf{2})_{\mathbf{2}},-\tfrac{1}{2},\mathbf{0}\rangle \\
(-1)^{\pi_{N_C N_B}}|N_B\,,\,-\tfrac{\mathbf{1}}{\mathbf{2}}\rangle &= U_{21}\,|(\mathbf{1},\mathbf{2}),-\tfrac{1}{2},\mathbf{0}\rangle + U_{22}\,|(\mathbf{2},\mathbf{1}),\tfrac{1}{2},-\mathbf{1}\rangle + U_{23}\,|(\mathbf{3},\mathbf{2})_{\mathbf{2}},-\tfrac{1}{2},\mathbf{0}\rangle \\
|N_C\,,\,-\tfrac{\mathbf{1}}{\mathbf{2}}\rangle &= U_{31}\,|(\mathbf{1},\mathbf{2}),-\tfrac{1}{2},\mathbf{0}\rangle + U_{32}\,|(\mathbf{2},\mathbf{1}),\tfrac{1}{2},-\mathbf{1}\rangle + U_{33}\,|(\mathbf{3},\mathbf{2})_{\mathbf{2}},-\tfrac{1}{2},\mathbf{0}\rangle \\
|\Delta\,,\,-\tfrac{\mathbf{1}}{\mathbf{2}}\rangle &= |(\mathbf{3},\mathbf{2})_{\mathbf{4}}\,,\,-\tfrac{1}{2}\,,\,\mathbf{0}\rangle \\
|\Delta\,,\,-\tfrac{\mathbf{3}}{\mathbf{2}}\rangle &= |(\mathbf{4},\mathbf{1})\,,\,-\tfrac{3}{2}\,,\,\mathbf{0}\rangle.
\end{aligned} \tag{3.78}$$

For the mixing angles, the following choice of the Euler angles is used:

$$\hat{U} = \begin{pmatrix}
\cos\phi\cos\theta - \cos\psi\sin\theta\sin\phi & -\sin\phi\cos\theta - \cos\phi\sin\theta\cos\psi & \sin\psi\sin\theta \\
\cos\phi\sin\theta + \cos\psi\cos\theta\sin\phi & -\sin\phi\sin\theta + \cos\phi\cos\theta\cos\psi & -\sin\psi\cos\theta \\
\sin\psi\sin\phi & \cos\phi\sin\psi & \cos\psi
\end{pmatrix}. \tag{3.79}$$

The Hamiltonians take the form

$$M^2 = \begin{array}{c} \\ \langle\,(2,1)\,| \\ \langle\,(1,2)\,| \\ \langle\,(2,3)\,| \end{array} \begin{array}{c} \begin{array}{ccc} |\,(2,1)\,\rangle & |\,(1,2)\,\rangle & |\,(2,3)\,\rangle \end{array} \\ \begin{bmatrix} m^2_{\mathbf{1a}} & m^2_{\mathbf{22a}} & 0 \\ m^2_{\mathbf{22a}} & m^2_{\mathbf{1b}} & m^2_{\mathbf{22b}} \\ 0 & m^2_{\mathbf{22b}} & m^2_{\mathbf{1c}} \end{bmatrix} \end{array} \quad , \quad M\mathcal{J}^+ = \begin{array}{c} \\ \langle\,(2,1)\,| \\ \langle\,(1,2)\,| \\ \langle\,(2,3)\,| \end{array} \begin{array}{c} \begin{array}{ccc} |\,(1,2)\,\rangle & |\,(2,1)\,\rangle & |\,(3,2)\,\rangle \end{array} \\ \begin{bmatrix} mj_{\mathbf{22a}} & mj_{\mathbf{1a}} & mj_{\mathbf{22b}} \\ mj_{\mathbf{1a}} & mj_{\mathbf{22c}} & 0 \\ mj_{\mathbf{22b}} & 0 & mj_{\mathbf{22d}} \end{bmatrix} \end{array} .$$

The assumption that these matrix elements are non-vanishing implies that the sea states that enter the representation have non-vanishing matrix elements of the sea angular momentum raising and lowering operators. Here there are four physical squared masses with three orthogonality conditions and five mass-squared matrix elements, and therefore two sum rules are expected from the mass-squared Hamiltonian. One finds

$$M^2_\Delta \;-\; M^2_{N_C}\cos^2\psi \;\;=\;\; \left(\, M^2_{N_A}\cos^2\theta \;+\; M^2_{N_B}\sin^2\theta \,\right)\sin^2\psi \;; \tag{3.80}$$

$$\left(\, M^2_{N_A} \;-\; M^2_{N_B} \,\right)\sin\theta\cos\theta\cos\phi \;\;=\;\; \sin\phi\cos\psi\left(\, M^2_{N_A}\cos^2\theta \;+\; M^2_{N_B}\sin^2\theta \;-\; M^2_{N_C} \,\right). \tag{3.81}$$

Again the spin Hamiltonian act non-trivially only in the isodoublet sector. Here there are three physical masses with three orthogonality conditions and five spin Hamiltonian matrix elements and therefore one sum rum is expected. One finds

$$\begin{aligned} &(-1)^{\pi_{N_A N_C}} M_{N_C}\left(J_{N_C}+\tfrac{1}{2}\right) - M_{N_A}\left(J_{N_A}+\tfrac{1}{2}\right)\sin^2\theta - (-1)^{\pi_{N_A N_B}} M_{N_B}\left(J_{N_B}+\tfrac{1}{2}\right)\cos^2\theta \\ &\quad = \tan\phi\sin\theta\cos\theta\sec\psi\left(M_{N_A}\left(J_{N_A}+\tfrac{1}{2}\right) - (-1)^{\pi_{N_A N_B}} M_{N_B}\left(J_{N_B}+\tfrac{1}{2}\right)\right) . \end{aligned} \tag{3.82}$$

This scheme has been analyzed previously in Ref. [66].

Axial couplings

In the physical basis, the quark helicity and axial-coupling matrices $\mathbf{\Delta\Sigma}$ and $\mathbf{g_A}$, respectively are easily obtained. Identifying the nucleon with N_C one has the nucleon axial couplings

$$\begin{aligned} g_A \;&=\; (\mathbf{g_A})_{CC} \;=\; \tfrac{5}{3}\cos^2\psi \;+\; \cos 2\phi\sin^2\psi \;; \\ \Delta\Sigma \;&=\; (\mathbf{\Delta\Sigma})_{CC} \;=\; \cos^2\phi\cos 2\psi \;+\; \sin^2\phi \;, \end{aligned} \tag{3.83}$$

and the nucleon axial couplings to the excited states

$$\begin{aligned}(\mathbf{g_A})_{AC} &= -\tfrac{1}{2}\left(\cos 2\phi - \tfrac{5}{3}\right)\sin 2\psi \sin\theta \;-\; \sin\psi \sin 2\phi \cos\theta \;; \\ (\mathbf{g_A})_{BC} &= \tfrac{1}{2}\left(\cos 2\phi - \tfrac{5}{3}\right)\sin 2\psi \cos\theta \;-\; \sin\psi \sin 2\phi \sin\theta \;. \end{aligned} \tag{3.84}$$

Identifying the delta with Δ, the axial couplings are

$$\mathcal{C}_{\Delta N_C} \;=\; -2\cos\psi \;,\; \mathcal{C}_{\Delta N_B} \;=\; 2\sin\psi\cos\theta \;,\; \mathcal{C}_{\Delta N_A} \;=\; -2\sin\psi\sin\theta \;,\; \mathcal{H}_{\Delta\Delta} \;=\; -3\,. \tag{3.85}$$

Taking matrix elements of the chiral algebra between nucleon states gives the nucleon AW sum rule

$$(\mathbf{g_A})^2_{CC} \;+\; (\mathbf{g_A})^2_{AC} \;+\; (\mathbf{g_A})^2_{BC} \;-\; \frac{4}{9}\mathcal{C}^2_{\Delta N_C} \;=\; 1 \;, \tag{3.86}$$

which is seen to be satisfied by Eqs. (3.83), (3.84) and (3.85).

In this scheme, there is a solution that is consistent with experiment. The angles $\psi = 40 \pm 5^o$ and $\phi = 23 \pm 11^o$ are determined from the experimental values of g_A and $\mathcal{C}_{\Delta N_C}$. With the nucleon mass, spin and parity and the delta mass as additional input, simultaneous solutions to the three Hamiltonian sum rules of Eqs. (3.80), (3.81), and (3.82) are searched for to give the angle $\theta = 39 \pm 33^o$, and the masses, spins and parities of N_A and N_B as tabulated in Table 3.2. This solution is not unique, however other solutions predict states that are not within one sigma of PDG [47] states. As in scheme 1, the spin content of the proton can be expressed as

$$\Delta\Sigma \;=\; \frac{2}{3}\mathcal{C}^2_{\Delta N_C} \;-\; g_A \;. \tag{3.87}$$

As both of these axial couplings are input from experiment, in this scheme, the proton valence spin content is determined directly from experimental data (see Table 3.2). In QCD, this quantity is scheme and scale dependent.

Entanglement entropy

The nucleon state in this scheme is determined entirely by the nucleon axial charge and the delta decay rate. It is instructive to write the nucleon state, with its experimentally

determined mixing angles, in a manner that exhibits the bipartite nature of the state:

$$|N\,,\,\tfrac{\mathbf{1}}{\mathbf{2}}\rangle \;=\; U_{31}\,|(\mathbf{2},\mathbf{1}),\tfrac{1}{2}\rangle\otimes|\mathbf{0}\rangle^{(m)} \;+\; U_{32}\,|(\mathbf{1},\mathbf{2}),-\tfrac{1}{2}\rangle\otimes|\mathbf{1}\rangle \;+\; U_{33}\,|(\mathbf{2},\mathbf{3})_{\mathbf{2}},\tfrac{1}{2}\rangle\otimes|\mathbf{0}\rangle^{(n)}, \tag{3.88}$$

with ${}^{(m)}\langle\mathbf{0}|\mathbf{0}\rangle^{(n)} = \delta^{mn}$ to allow for the possibility that there is/are one or two helicity-zero states. The chiral states are clearly orthogonal. The mixing angles are $U_{31} = 0.24 \pm 0.08$, $U_{32} = 0.60 \pm 0.07$ and $U_{33} = -0.76 \pm 0.05$. With $m \neq n$, the entanglement entropy is (in units of the maximal entanglement entropy)

$$S_N \;=\; -U_{31}^2 \log U_{31}^2 \;-\; U_{32}^2 \log U_{32}^2 \;-\; U_{33}^2 \log U_{33}^2 \;=\; (0.81 \pm 0.18)\log 3 \tag{3.89}$$

and with $m = n$,

$$S_N \;=\; -\left(U_{31}^2 \;+\; U_{33}^2\right)\log\left(U_{31}^2 \;+\; U_{33}^2\right) \;-\; U_{32}^2 \log U_{32}^2 \;=\; (0.96 \pm 0.23)\log 2\;. \tag{3.90}$$

It is interesting that in nucleon chiral representations that are consistent with data, the entanglement entropy is near its maximum value.

Summary

While this saturation scheme is consistent with experimental data, it involves the coupling of the nucleon to higher excited states in a rather unnatural way as it "skips" low-lying states that have significant axial couplings to the nucleon and which one would expect should be present in the nucleon's chiral representation.

3.4.4 Saturation scheme 4: N_A, N_B, N_C, Δ_A , Δ_B

Hamiltonian constraints

Consider next the scheme consistent with the nucleon being a mixture of $\mathbf{20}_S$ and $\mathbf{20}_M$ of

$SU(4)$. The $\Lambda = +\frac{1}{2}$ eigenstates can be chosen to be

$$\begin{aligned}
|N_A\,,\,\mathbf{\tfrac{1}{2}}\rangle &= U_{11}\,|(\mathbf{3},\mathbf{2})_{\mathbf{2}},-\tfrac{1}{2},\mathbf{1}\rangle + U_{12}\,|(\mathbf{1},\mathbf{2}),-\tfrac{1}{2},\mathbf{1}\rangle + U_{13}\,|(\mathbf{2},\mathbf{3})_{\mathbf{2}},\tfrac{1}{2},\mathbf{0}\rangle \\
|N_B\,,\,\mathbf{\tfrac{1}{2}}\rangle &= U_{21}\,|(\mathbf{3},\mathbf{2})_{\mathbf{2}},-\tfrac{1}{2},\mathbf{1}\rangle + U_{22}\,|(\mathbf{1},\mathbf{2}),-\tfrac{1}{2},\mathbf{1}\rangle + U_{23}\,|(\mathbf{2},\mathbf{3})_{\mathbf{2}},\tfrac{1}{2},\mathbf{0}\rangle \\
|N_C\,,\,\mathbf{\tfrac{1}{2}}\rangle &= U_{31}\,|(\mathbf{3},\mathbf{2})_{\mathbf{2}},-\tfrac{1}{2},\mathbf{1}\rangle + U_{32}\,|(\mathbf{1},\mathbf{2}),-\tfrac{1}{2},\mathbf{1}\rangle + U_{33}\,|(\mathbf{2},\mathbf{3})_{\mathbf{2}},\tfrac{1}{2},\mathbf{0}\rangle \\
|\,\Delta_A\,,\,\mathbf{\tfrac{1}{2}}\rangle &= \sin\omega|(\mathbf{3},\mathbf{2})_{\mathbf{4}}\,,\,-\tfrac{1}{2}\,,\,\mathbf{1}\rangle + \cos\omega|(\mathbf{2},\mathbf{3})_{\mathbf{4}}\,,\,\tfrac{1}{2}\,,\,\mathbf{0}\rangle \\
|\,\Delta_B\,,\,\mathbf{\tfrac{1}{2}}\rangle &= -\cos\omega|(\mathbf{3},\mathbf{2})_{\mathbf{4}}\,,\,-\tfrac{1}{2}\,,\,\mathbf{1}\rangle + \sin\omega|(\mathbf{2},\mathbf{3})_{\mathbf{4}}\,,\,\tfrac{1}{2}\,,\,\mathbf{0}\rangle\,,
\end{aligned} \tag{3.91}$$

where same choice of the Euler angles written down above is used. The negative helicity eigenstates are then obtained with the action of $\mathcal{Y}$:

$$\begin{aligned}
(-1)^{\pi_{N_C N_A}}|N_A\,,\,-\mathbf{\tfrac{1}{2}}\rangle &= U_{11}\,|(\mathbf{2},\mathbf{3})_{\mathbf{2}},\tfrac{1}{2},-\mathbf{1}\rangle + U_{12}\,|(\mathbf{2},\mathbf{1}),\tfrac{1}{2},-\mathbf{1}\rangle + U_{13}\,|(\mathbf{3},\mathbf{2})_{\mathbf{2}},-\tfrac{1}{2},\mathbf{0}\rangle \\
(-1)^{\pi_{N_C N_B}}|N_B\,,\,-\mathbf{\tfrac{1}{2}}\rangle &= U_{21}\,|(\mathbf{2},\mathbf{3})_{\mathbf{2}},\tfrac{1}{2},-\mathbf{1}\rangle + U_{22}\,|(\mathbf{2},\mathbf{1}),\tfrac{1}{2},-\mathbf{1}\rangle + U_{23}\,|(\mathbf{3},\mathbf{2})_{\mathbf{2}},-\tfrac{1}{2},\mathbf{0}\rangle \\
|N_C\,,\,-\mathbf{\tfrac{1}{2}}\rangle &= U_{31}\,|(\mathbf{2},\mathbf{3})_{\mathbf{2}},\tfrac{1}{2},-\mathbf{1}\rangle + U_{32}\,|(\mathbf{2},\mathbf{1}),\tfrac{1}{2},-\mathbf{1}\rangle + U_{33}\,|(\mathbf{3},\mathbf{2})_{\mathbf{2}},-\tfrac{1}{2},\mathbf{0}\rangle \\
|\,\Delta_A\,,\,-\mathbf{\tfrac{1}{2}}\rangle &= \sin\omega|(\mathbf{2},\mathbf{3})_{\mathbf{4}}\,,\,\tfrac{1}{2}\,,\,-\mathbf{1}\rangle + \cos\omega|(\mathbf{3},\mathbf{2})_{\mathbf{4}}\,,\,-\tfrac{1}{2}\,,\,\mathbf{0}\rangle \\
(-1)^{\pi_{\Delta_B \Delta_A}}|\,\Delta_B\,,\,-\mathbf{\tfrac{1}{2}}\rangle &= -\cos\omega|(\mathbf{2},\mathbf{3})_{\mathbf{4}}\,,\,\tfrac{1}{2}\,,\,-\mathbf{1}\rangle + \sin\omega|(\mathbf{3},\mathbf{2})_{\mathbf{4}}\,,\,-\tfrac{1}{2}\,,\,\mathbf{0}\rangle\,,
\end{aligned} \tag{3.92}$$

The mass-squared Hamiltonians are

$$M^2 = \begin{array}{c} \\ \langle\,(3,2)\,| \\ \langle\,(1,2)\,| \\ \langle\,(2,3)\,| \end{array} \begin{array}{c} \begin{array}{ccc} |\,(3,2)\,\rangle & |\,(1,2)\,\rangle & |\,(2,3)\,\rangle \end{array} \\ \begin{bmatrix} m^2_{\mathbf{1a}} & 0 & m^2_{\mathbf{22a}} \\ 0 & m^2_{\mathbf{1b}} & m^2_{\mathbf{22b}} \\ m^2_{\mathbf{22a}} & m^2_{\mathbf{22b}} & m^2_{\mathbf{1c}} \end{bmatrix} \end{array} \quad , \qquad M^2 = \begin{array}{c} \\ \langle\,(3,2)\,| \\ \langle\,(2,3)\,| \end{array} \begin{array}{c} \begin{array}{cc} |\,(3,2)\,\rangle & |\,(2,3)\,\rangle \end{array} \\ \begin{bmatrix} m^2_{\mathbf{1a}} & m^2_{\mathbf{22c}} \\ m^2_{\mathbf{22c}} & m^2_{\mathbf{1c}} \end{bmatrix} \end{array} \tag{3.93}$$

and the spin Hamiltonians are

$$M\mathcal{J}^+ = \begin{array}{c} \\ \langle\,(3,2)\,| \\ \langle\,(1,2)\,| \\ \langle\,(2,3)\,| \end{array} \begin{array}{c} \begin{array}{ccc} |\,(2,3)\,\rangle & |\,(2,1)\,\rangle & |\,(3,2)\,\rangle \end{array} \\ \begin{bmatrix} mj_{\mathbf{22a}} & mj_{\mathbf{22b}} & mj_{\mathbf{1a}} \\ mj_{\mathbf{22b}} & mj_{\mathbf{22c}} & 0 \\ mj_{\mathbf{1a}} & 0 & mj_{\mathbf{22d}} \end{bmatrix} \end{array} \quad , \qquad M\mathcal{J}^+ = \begin{array}{c} \\ \langle\,(3,2)\,| \\ \langle\,(2,3)\,| \end{array} \begin{array}{c} \begin{array}{cc} |\,(2,3)\,\rangle & |\,(3,2)\,\rangle \end{array} \\ \begin{bmatrix} mj_{\mathbf{22e}} & mj_{\mathbf{1a}} \\ mj_{\mathbf{1a}} & mj_{\mathbf{22f}} \end{bmatrix} \end{array} \tag{3.94}$$

for the N and Δ states, respectively.

There are three sum rules from the mass-squared Hamiltonian:

$$\begin{aligned} &4\sin 2\phi\big[\left(M^2_{\Delta_A}-M^2_{\Delta_B}\right)\cos 2\omega\sin^2\psi+\left(M^2_{N_B}-M^2_{N_A}\right)\cos 2\psi\cos 2\theta\big] \\ &\quad=\left(M^2_{N_A}-M^2_{N_B}\right)\cos\psi\sin 2\theta[(3\cos 2\phi-1)\cos 2\psi+2\cos^2\phi]\ ; \end{aligned} \tag{3.95}$$

$$\begin{aligned} &\left(M^2_{\Delta_A}+M^2_{\Delta_B}-M^2_{N_B}-M^2_{N_C}\right) \\ &\times\big[\cos\psi\sin 2\theta\left(\cos 2\phi(3\cos 2\psi+1)+2\sin^2\psi\right)+4\sin 2\phi\cos 2\psi\cos 2\theta\big] \\ &=-4\left(M^2_{\Delta_A}-M^2_{\Delta_B}\right)\cos 2\omega\cos\phi\sin^2\psi\left(\cos\phi\cos\psi\sin 2\theta-2\sin\phi\sin^2\theta\right)\ ; \end{aligned} \tag{3.96}$$

$$\begin{aligned} &\sin 2\phi\big[2\sin^2\psi\left(M^2_{N_A}+M^2_{N_B}-2M^2_{N_C}\right)+\left(M^2_{N_A}-M^2_{N_B}\right)(\cos 2\psi+3)\cos 2\theta\big] \\ &\quad=-4\left(M^2_{N_A}-M^2_{N_B}\right)\cos 2\phi\cos\psi\sin 2\theta\ , \end{aligned} \tag{3.97}$$

and there are two sum rules from the spin Hamiltonians:

$$\begin{aligned} &\big[\left(J_{N_C}+\tfrac{1}{2}\right)M_{N_C}-\left(J_{N_B}+\tfrac{1}{2}\right)M_{N_B}(-1)^{\pi_{N_CN_B}}\big]\sin 2\psi= \\ &\big[\left(J_{\Delta_A}+\tfrac{1}{2}\right)M_{\Delta_A}-\left(J_{\Delta_B}+\tfrac{1}{2}\right)M_{\Delta_B}(-1)^{\pi_{\Delta_B\Delta_A}}\big]\sin 2\omega\left(\sin\phi+\cos\phi\tan\theta\cos\psi\right)\ ; \end{aligned} \tag{3.98}$$

$$\begin{aligned} &\big[\left(J_{N_B}+\tfrac{1}{2}\right)M_{N_B}-\left(J_{N_A}+\tfrac{1}{2}\right)M_{N_A}(-1)^{\pi_{N_AN_B}}\big](2\sec\psi\sin\phi\sin\theta\cos\theta-\cos\phi\cos 2\theta) \\ &=\big[\left(J_{N_B}+\tfrac{1}{2}\right)M_{N_B}+\left(J_{N_A}+\tfrac{1}{2}\right)M_{N_A}(-1)^{\pi_{N_AN_B}}-2\left(J_{N_C}+\tfrac{1}{2}\right)M_{N_C}(-1)^{\pi_{N_CN_B}}\big]\cos\phi \end{aligned} \tag{3.99}$$

Axial couplings

In the physical basis, the quark helicity and axial-coupling matrices $\mathbf{\Delta\Sigma}$ and $\mathbf{g_A}$, respectively are easily obtained. Identifying the nucleon with N_C one has the nucleon axial couplings

$$\begin{aligned} g_A &= \left(\mathbf{g_A}\right)_{CC} = \tfrac{1}{3}[4\cos^2\phi+(3-2\cos 2\phi)\cos 2\psi] \\ \Delta\Sigma &= \left(\mathbf{\Delta\Sigma}\right)_{CC} = \cos 2\psi\ , \end{aligned} \tag{3.100}$$

and the nucleon axial couplings to the excited states

$$\begin{aligned} \left(\mathbf{g_A}\right)_{AC} &= \tfrac{1}{3}\big[(3-2\cos 2\phi)\sin 2\psi\sin\theta\ -\ 4\cos\theta\sin 2\phi\sin\psi\big] \\ \left(\mathbf{g_A}\right)_{BC} &= \tfrac{2}{3}\sin\psi\big[(2\cos 2\phi-3)\cos\psi\cos\theta\ -\ 4\cos\phi\sin\phi\sin\theta\big] \end{aligned} \tag{3.101}$$

The delta axial couplings are

$$\begin{aligned} \mathcal{C}_{\Delta_A N_C} &= -2\left(\cos\omega\cos\phi + \sin\omega\sin\phi\sin\psi\right) \ ; \\ \mathcal{C}_{\Delta_B N_C} &= -2\left(\sin\omega\cos\phi - \cos\omega\sin\phi\sin\psi\right) \ , \end{aligned} \tag{3.102}$$

and

$$\mathcal{H}_{\Delta_A\Delta_A} = -3\cos 2\omega \ . \tag{3.103}$$

Taking matrix elements of the chiral algebra between nucleon states gives the nucleon AW sum rule

$$(\mathbf{g_A})^2_{CC} + (\mathbf{g_A})^2_{AC} + (\mathbf{g_A})^2_{BC} - \frac{4}{9}\mathcal{C}^2_{\Delta_A N_C} - \frac{4}{9}\mathcal{C}^2_{\Delta_B N_C} = 1 \ , \tag{3.104}$$

which is seen to be satisfied by Eqs. (3.100), (3.101) and (3.102).

This scheme is very constrained and quite consistent with experiment. Table 3.3 gives the input parameters and some of the predictions. The predicted angles are $\phi = -0.274$, $\psi = 0.749$, $\theta = 0.632$ and $\omega = 2.868$.

Table 3.1: Saturation scheme 1, axial charges. The asterisk indicates an input parameter.

Axial charge	Theory	Expt [47]
$\lvert g_A \rvert$	$*$	1.267
$\lvert \mathcal{C}_{\Delta N} \rvert$	1.27	1.51 ± 0.10
$\lvert \mathcal{H}_{\Delta\Delta} \rvert$	3	2.2 ± 0.6
$\Delta\Sigma$	-0.2	–
S_N	$(0.97)\log 2$	–

Table 3.2: Axial charges and masses in saturation scheme 3. The asterisk indicates an input parameter and masses are given in MeV. The value of $\Delta\Sigma$ is taken from the COMPASS collaboration's analysis in Ref. [67] at a renormalization scale $Q^2 = 3$ GeV^2.

Charge	Theory	Expt [47, 67]	Mass	Theory (J^η)	Expt (J^η) [47]
$\lvert g_A \rvert$	$*$	1.267	M_{N_C}	$*$	940 $(\frac{1}{2}^+)$
$\lvert \mathcal{C}_{\Delta N} \rvert$	$*$	1.51 ± 0.10	M_Δ	$*$	1232 $(\frac{3}{2}^+)$
$\lvert \mathcal{H}_{\Delta\Delta} \rvert$	3	2.2 ± 0.6	M_{N_A}	1667 ± 102 $(\frac{1}{2}^+)$	1710 ± 30 $(\frac{1}{2}^+)$
$\Delta\Sigma$	0.27 ± 0.20	0.31 ± 0.05	M_{N_B}	1363 ± 129 $(\frac{1}{2}^-)$	1535 ± 10 $(\frac{1}{2}^-)$
$\lvert (\mathbf{g_A})_{AC} \rvert$	0.55 ± 0.19	0.07 ± 0.18	–	–	–
$\lvert (\mathbf{g_A})_{BC} \rvert$	0.56 ± 0.19	0.21 ± 0.11	–	–	–

Table 3.3: Axial charges and masses in saturation scheme 4. The asterisk indicates an input parameter and masses are given in MeV. The value of $\Delta\Sigma$ is taken from the COMPASS collaboration's analysis in Ref. [67] at a renormalization scale $Q^2 = 3$ GeV^2.

Charge	Theory	Expt [47, 67]	Mass	Theory (J^η)	Expt (J^η) [47]
$\lvert g_A \rvert$	$*$	1.267	M_{N_C}	$*$	940 ($\frac{1}{2}^+$)
$\lvert \mathcal{C}_{\Delta_A N_C} \rvert$	$*$	1.51 ± 0.10	M_{Δ_A}	$*$	1232 ($\frac{3}{2}^+$)
$\lvert \mathcal{H}_{\Delta_A \Delta_A} \rvert$	2.80 ± 0.01	2.2 ± 0.6	M_{N_A}	1700 ± 84 ($\frac{1}{2}^-$)	1530 ± 15 ($\frac{1}{2}^-$)
$\Delta\Sigma$	0.07 ± 0.11	0.31 ± 0.05	M_{N_B}	1442 ± 35 ($\frac{1}{2}^+$)	1440 ± 30 ($\frac{1}{2}^+$)
$\lvert (\mathbf{g_A})_{AC} \rvert$	0.63 ± 0.14	0.07 ± 0.18	M_{Δ_B}	1654 ± 71 ($\frac{3}{2}^-$)	1710 ± 20 ($\frac{3}{2}^-$)
$\lvert (\mathbf{g_A})_{BC} \rvert$	0.07 ± 0.05	0.21 ± 0.11	–	–	–

3.5 Conclusion

In null-plane QCD chiral symmetry and its breaking are properties of the valence quarks which carry a definite helicity. As symmetry-breaking condensates are absent when null-planes are chosen as initial quantization surfaces, the effects of spontaneous symmetry breaking are necessarily properties of hadronic null-plane states which arise from symmetry-breaking QCD operators which act as reduced Hamiltonians. The null-plane foliation of spacetime is therefore convenient for studying nonperturbative aspects of QCD because these symmetry-breaking operators or Hamiltonians in null-plane QCD satisfy algebraic constraints due to chiral symmetry and Poincaré invariance which must be replicated in the low-energy theory. This study has constructed simple nucleon state vectors that are consistent with experimental data.

The models developed present a compelling physical picture of the structure of the nucleon. In the limit that the mixing between the nucleon and its chiral partners is turned off, the nucleon reverts to its standard quark model interpretation as being in a representation of $SU(4)$ (the large-N_c limit) and having all its angular momentum given by the valence partonic constituents. Therefore, one sees explicitly that the non-trivial spin content of the nucleon, including the particular value of the axial charge, find their origin in the leakage of the chiral charge among the various states in the nucleon chiral multiplet. One might ask how this pictures from the non-relativistic quark model. In that case, as in the large-N_c limit, the gluonic excitations are assumed to be suppressed in the ground state. In constructing the first excited towers in the quark model, orbital angular momentum is added to the mixed-symmetry $SU(4)$ representations to obtain completely symmetric spin-flavor wavefunctions. By contrast, in the null-plane description, the gluons clearly must play a critical role in the ground state itself.

The main conclusions of this chapter are:

• In null-plane QCD chiral symmetry breaking is a property of the hadronic wavefunctions.

However, in the Fock basis with truncation to a few terms, the presence of chiral symmetry breaking is not manifest. Here it has been shown that chiral symmetry breaking is indeed a property of the hadronic wavefunction: it is driven by the entanglement between the valence quark spins and the parton sea, which is encoded in the bipartite nature of the hadronic state.

• The large-N_c limit corresponds to vanishing entanglement entropy. This suggests that it may be fruitful to view the large-N_c expansion for baryons as an expansion in entanglement entropy.

• The gluon sea is essential in determining the ground state null-plane wavefunctions of the nucleon and its chiral partners.

• Chiral symmetry breaking arises from the interactions between valence spins and spins in the gluon sea, and therefore the entanglement entropy between these two systems serves as a kind of order parameter for chiral symmetry breaking in the null-plane description.

• Results found here demonstrate the futility of thinking about the nucleon as a state with physical properties which in some way are separate from those of other baryon excited states. A holistic approach to the low-lying baryons is required.

• Lattice QCD methods are not making striking progress in determining parton distribution functions which will ultimately give a highly-accurate systematic determination of these quantities. What we have attempted to do here is give an understanding based solely in the symmetries of QCD and general physical principles of why the proton spin content should be expected to decompose as it does.

We would naturally like to extend this kind of analysis of entanglement to the full nucleon wavefunction in QCD. This would be an exceedingly difficult task on its own, as the Fock state representation of the nucleon contains a formally infinite number of terms, and we have

just seen that the physical properties of the nucleon state require knowledge of other states in the spectrum as well. Instead, we will compromise in the next chapter by analyzing QCD in $1+1$ dimensions. This is a sensible choice of theory for investigating quark entanglement as the large-N_c limit of $1+1$d QCD is exactly solvable, so the connection between the large-N_c expansion and valence quark entanglement will be readily apparent. The chiral properties of $1+1$d QCD are very different from those of real QCD, and there will be no gluon sea in the light-cone, so the results in the next chapter will describe a very different aspect of QCD than we've seen so far. In particular, $1+1$ QCD is confined at all energy scales, so the results of the next chapter will pertain to the confined phase of QCD only, as opposed to the chiral symmetry breaking scale.

In the next chapter, we will define a notion of valence-sea entanglement for any QCD bound state and use this to examine the quark entanglement of hadrons in $1+1$d QCD. The new definition is necessary because there is no unambiguous distinction between valence and sea quarks outside of flavor in QCD. We find that for this theory the valence quark entanglement is exceedingly small for ground state hadrons, and gets incrementally larger for the next few excited states. For mesons, this a direct consequence of the low energy states' resemblances to their large-N_c counterparts, which is presumably true in some sense for the baryons as well. This provides more evidence for a connection between the large-N_c expansion and quark entanglement and suggests that the valence-sea entanglement of nucleons in real QCD is likely small at low energy scales where confinement occurs.

Chapter 4

ENTANGLEMENT BETWEEN VALENCE AND SEA QUARKS IN HADRONS OF 1+1 DIMENSIONAL QCD

4.1 Introduction

It has been well established for decades now that QCD is the theory of the strong interactions. Though it is described in quantum field theory with just an $SU(3)$ gauge field coupled to fermionic matter, it exhibits the rich tapestry of phenomena that we observe in nuclear processes. In particular, quarks in QCD behave as nearly free particles at large energy scales beyond 1 GeV (dubbed "asymptotic freedom") [4, 5], but for lower energies the interaction is strong enough that quarks become confined and are only observed within bound states known as hadrons [68]. Despite having the theory of the strong interactions on hand, it has never been solved analytically, even when no matter fields are present. A multitude of techniques have been developed over the decades to tackle the strong interactions which approximated QCD, some of which have existed prior to the development of it.

Given that there are still difficulties in getting complete results in hadronic physics, it may prove useful to approach problems in nuclear physics from a different perspective. There has been a lot of recent interest in quantum information theory and its application to other areas of physics [6], instigated by a surge of interest and developments in quantum computing [69–115]. A key concept in quantum information science is the notion of quantum entanglement and the corresponding numerical quantity of entanglement entropy. Entanglement is very important to quantum computing as it allows for these computers to potentially exceed the capabilities of classical computing, and the entanglement entropy serves as a resource for these computers. Understanding the entanglement structure of physical theories can make them more tenable to efficient simulation on quantum computers. There have been

a number of important results on entropy in field theory [116–123], but these have been primarily focused on the subjects of black holes, conformal field theories and holography.

In nuclear physics, a quantum information approach has seen relatively little application, but this is changing. A paper by Kharzeev and Levin [24] obtained some results for the entanglement entropy of deep inelastic scattering for the purpose of better understanding the parton model description of the proton. Deep inelastic scattering only probes part of the internal structure of the proton, so the unknown remainder of the proton structure which goes into the ensuing hadron shower that is not measured in these experiments is handled statistically, resulting in a determinable entropy. Prior to this paper, the investigation of entanglement in nuclear physics had been rather sparse [23, 54, 124–135], but many papers have been written on the subject since then [18, 49, 55–60, 62, 63, 136–173]. Many of these papers focus on entanglement in field theories between two non-overlapping regions of space, with only a few looking into entanglement between other degrees of freedom [133]. Part of the goal of this project is to introduce a more general notion of entanglement to go beyond the usual focus on bipartite spatial entanglement, which we will use to define and investigate the quantum entanglement between the quarks that compose the hadrons in QCD. This would not be the first attempt to generalize entanglement; the entwinement [174–176] is an example of such a case.

The parton model, a major predecessor of QCD [177–179], was a major step toward developing the theory of strong interactions and in many ways still informs our intuitive understanding of it. One such way is through the picture of a hadron as being made up of a small handful of "valence" quarks, corresponding to the flavor quantum numbers of the hadron, that are embedded inside of a bubbling soup of "sea" quarks and gluons. However, a more accurate picture originating from QCD more directly would suggest that the hadronic state is a much more ambiguous superposition of states with many possible numbers of partons, with the only clear pattern being that the total flavor numbers for these quark ensemble states are fixed. Thus the notions of valence and sea quarks seem to have almost entirely vanished from the more accurate theory, despite being a useful picture in the past.

What this may be indicating is that there can be a high degree of entanglement between the valence and sea quarks that is being captured by QCD but is largely omitted by the parton model. QCD is in some sense more quantum mechanical than the parton model, so it stands to reason that one of the major differences between them would be rooted in a purely quantum mechanical concept such as entanglement. Through some notion of valence-sea (VS) entanglement, one may be able to quantify the degree to which the parton model picture makes sense for a given hadronic state in QCD.

By "parton model," we are referring to a model where hadrons are approximated as pointlike constituent particles, with valence partons embedded in a bath of sea partons. For example, in deep inelastic scattering of an electron off of a proton, the process can be approximated by the scattering of the electron off of an individual parton inside the proton that is then integrated over what is known as a parton distribution function (PDF) [180, 181] or its generalizations [182–184]. The PDF essentially tells us the probability of finding a specific parton within the proton that has a fraction x of its total momentum. This turns out to be the first order approximation in what is known as the twist expansion [181]. On top of this, the model also assumes that the distribution of quarks can be separated into valence and sea contribution, and that the sea contributions between quarks and antiquarks should match. For example, the up quark PDF $f_u(x)$ in a proton should be able to split into valence and sea contributions $f_u(x) = f_{u,V}(x) + f_{u,S}(x)$ with $f_{u,S}(x) = f_{\bar{u}}(x)$ under the parton model. The quark-antiquark symmetry assumes that the parton sea can be divided neatly into quark-antiquark pairs, which can presumably be used to identify which quarks are part of the sea and which ones are valence quarks. This all implies that the wavefunction for the proton is roughly factorizes into valence and sea parts $\psi(x) \sim \psi_V(x)\psi_S(x)$. If this was accurate, then the entanglement between valence and sea partons would be zero. This is the sense in which valence-sea entanglement can measure the applicability of the parton model, as a large degree of entanglement would indicate a strong violation the assumptions of the parton model as described here.

Additionally, there is no reason to assume that entanglement is accessible through per-

turbative methods, so an entanglement-based investigative approach to QCD could provide new insights into hadron structure. For VS entanglement in particular, it is known that in large-N_c QCD where diagrams with quark-antiquark pairs are suppressed [11–13, 41, 185–188], the hadrons in the spectrum have only gluons in their parton seas. Thus there can be no VS entanglement between quarks at large N_c, which shows that not even the large-N_c expansion will capture such a property of the hadrons. This further motivates an investigation into VS entanglement as a means of gaining more nonperturbative information about the makeup of hadrons.

The results of this work are obtained using QCD in 1 space and 1 time dimension, which was extensively analyzed in [189–192]. While QCD in lower dimensions lacks some of the features of full QCD, such as fermion spin and dynamical gauge field components, confinement still occurs here, and it's spectrum has been essentially solved in the large-N_c limit [12]. The relative simplicity of the lower dimensional theory combined with the presence of confinement makes it a useful model for the low energy spectrum of QCD. From our work, we find that the VS entanglement that we have defined converges to a finite value fairly quickly for the lowest energy hadrons, and the values they approach tend to be rather small. For mesons, this is a result of their wavefunctions strongly resembling their large-N_c counterparts, with this connection diminishing as we go further along the excited meson spectrum. For baryons, we cannot draw a resemblance to the large-N_c wavefunction specifically, but a similar connection to large-N_c physics more broadly is likely behind the small values as well. For ground state mesons, the N_c dependence of the VS entropy also fits nicely to a $1/N_c$ curve, which suggests that a large-N_c expansion of the VS entropy should converge rapidly. If this convergence holds in real QCD, it would open the possibility of calculating it perturbatively with the large-N_c expansion. The VS entanglement of real QCD would almost certainly be scale dependent, and so it may serve as an order parameter for the transition between quark and hadron degrees of freedom, which would show that entanglement between quarks is an important aspect in the process of hadronization.

This paper will proceed as follows. In the first section, we will define two notions of

quark entanglement: single quark (SQ) entanglement, which we will show is related to parton distribution functions, and valence-sea (VS) entanglement, which will be the primary interest of the rest of the paper. The following section will define 1+1d QCD in the Hamiltonian formalism as well as the 't Hooft model, which is the large-N_c limit of this theory. The third section will discuss discrete light-cone quantization (DLCQ) as it applies to this work, which is the main tool used to get our entanglement results from 1+1d QCD. More details about our calculational methods can be found in the appendices. The next section will show how the VS entanglement entropy relates to matrix elements that can be calculated in DLCQ. The final section will contain all of our numerical data and calculational results, which is followed by our conclusions about the work.

4.2 Extension of Entanglement

4.2.1 Definition

We can quantify valence-sea entanglement by defining an associated entropy stemming from a bipartition of the valence and sea quark degrees of freedom. However, in QCD, there is no way to make a distinction between the valence and the sea degrees of freedom outside of the specific flavors of the valence quarks. A general Fock state that is a component of a hadronic state can have multiple quarks that have the same flavor as a valence quark in the hadron, so we will need a prescription to determine which quarks count as valence quarks and which ones are part of the sea. Our approach is to duplicate the Hilbert space, apply some operators to the density matrix that pull quarks of the proper flavors that match the valence flavor structure, and then trace out the original Hilbert space to obtain a density matrix that acts in the valence quark Fock state basis. This effectively adds a contribution to the valence density matrix for every possible selection of which quarks count as valence quarks within the Fock state expansion of the hadronic state. This means that our definition of the valence density matrix is agnostic towards the properties of the valence quarks other than their flavors, and that Fock states with a higher number of quarks will be weighted

more heavily than those with fewer quarks because our procedure sums over possible valence quark assignments rather than averaging over them.

To illustrate how this formalism works, we will begin with a simple example. Consider a quantum system where particles can occupy two sites labeled A and B. Each site can either be in an occupied state $|1\rangle$ or an unoccupied state $|0\rangle$. The most general state one can make in this system is

$$|\psi\rangle = \alpha\,|00\rangle + \beta\,|01\rangle + \gamma\,|10\rangle + \delta\,|11\rangle\,, \quad \alpha^*\alpha + \beta^*\beta + \gamma^*\gamma + \delta^*\delta = 1 \tag{4.1}$$

with amplitudes $\alpha, \beta, \gamma, \delta$, where the left digit in the basis states correspond to site A while the right digit corresponds to site B. The general reduced density matrix for site A is given by

$$\rho_A = \mathrm{Tr}_B[|\psi\rangle\langle\psi|] = (\alpha\,|0\rangle + \gamma\,|1\rangle)(\alpha^*\langle 0| + \gamma^*\langle 1|) + (\beta\,|0\rangle + \delta\,|1\rangle)(\beta^*\langle 0| + \delta^*\langle 1|) \tag{4.2}$$

As we will see later, the usual notion of bipartite entanglement can always be obtained using the extended formalism. We can define another reduced density matrix given by

$$\rho_{2A} = \mathrm{Tr}_1[X_A\,|\psi\rangle_1\,|00\rangle_2\,\langle 00|_2\,\langle\psi|_1\,X_A], \tag{4.3}$$

where we have duplicated the system with our general state $|\psi\rangle$ in the original space 1 and we have chosen our starting vector in the auxiliary space to be the state $|00\rangle$. The operator X_A swaps the state in site $A1$ with the state in site $A2$, so that

$$X_A\,|\psi\rangle_1\,|00\rangle_2 = \alpha\,|00\rangle_1\,|00\rangle_2 + \beta\,|01\rangle_1\,|00\rangle_2 + \gamma\,|00\rangle_1\,|10\rangle_2 + \delta\,|01\rangle_1\,|10\rangle_2\,. \tag{4.4}$$

Putting this into the expression for ρ_{2A} and tracing out region 1 (and dropping the 2 subscripts on the remaining state vectors), we get

$$\rho_{2A} = (\alpha\,|00\rangle + \gamma\,|10\rangle)(\alpha^*\langle 00| + \gamma^*\langle 10|) + (\beta\,|00\rangle + \delta\,|10\rangle)(\beta^*\langle 00| + \delta^*\langle 10|) = \rho_A \otimes (|0\rangle\langle 0|)_B, \tag{4.5}$$

which will give the same results for any measure of entanglement as ρ_A does by itself. Note that instead of choosing $|00\rangle$ for our initial auxiliary vector we could have chosen any separable state $|\phi_A\rangle\,|\phi_B\rangle$ and achieved mostly the same result with $\rho_{2A} = \rho_A \otimes |\phi_B\rangle\langle\phi_B|$.

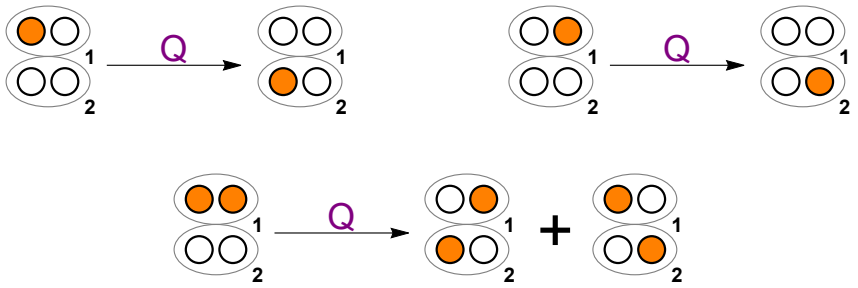

Figure 4.1: Illustration of how the operator Q acts upon states in the two-site example. When only one site is occupied Q moves it into the duplicate Hilbert space. When both are occupied, Q adds two contributions, one where the first particle is treated as the valence particle along with another where the second is treated as the valence particle

This system can also help illustrate what is meant by quark entanglement in this chapter. Instead of the operator X_A, which probes entanglement between sites A and B, we use the Hermitian operator Q given by

$$Q = \sigma^+_{A,1}\otimes\mathbb{1}_{B,1}\otimes\sigma^-_{A,2}\otimes\mathbb{1}_{B,2}+\mathbb{1}_{A,1}\otimes\sigma^+_{B,1}\otimes\mathbb{1}_{A,2}\otimes\sigma^-_{B,2}+\sigma^-_{A,1}\otimes\mathbb{1}_{B,1}\otimes\sigma^+_{A,2}\otimes\mathbb{1}_{B,2}+\mathbb{1}_{A,1}\otimes\sigma^-_{B,1}\otimes\mathbb{1}_{A,2}\otimes\sigma^+_{B,2}, \tag{4.6}$$

where $\sigma^- = \begin{pmatrix} 0 & 1 \\ 0 & 0 \end{pmatrix}$ removes a particle from an occupied state and $\sigma^+ = \begin{pmatrix} 0 & 0 \\ 1 & 0 \end{pmatrix}$ adds particles to an unoccupied state. We strategically choose $|00\rangle$ for our initial auxiliary vector here because it is fully unoccupied, so that

$$\begin{aligned} Q\,|\psi\rangle_1\,|00\rangle_2 &= (\sigma^-_{A,1}\otimes\mathbb{1}_{B,1}\otimes\sigma^+_{A,2}\otimes\mathbb{1}_{B,2}+\mathbb{1}_{A,1}\otimes\sigma^-_{B,1}\otimes\mathbb{1}_{A,2}\otimes\sigma^+_{B,2})\,|\psi\rangle_1\,|00\rangle_2 \\ &= \beta\,|00\rangle_1\,|01\rangle_2+\gamma\,|00\rangle_1\,|10\rangle_2+\delta(|01\rangle_1\,|10\rangle_2+|10\rangle_1\,|01\rangle_2). \end{aligned} \tag{4.7}$$

This makes it so that our procedure isn't generating completely artificial entanglement, guaranteeing that the entanglement we are measuring strictly originates from the original state and not the auxiliary one. The reduced density matrix for quark entanglement can

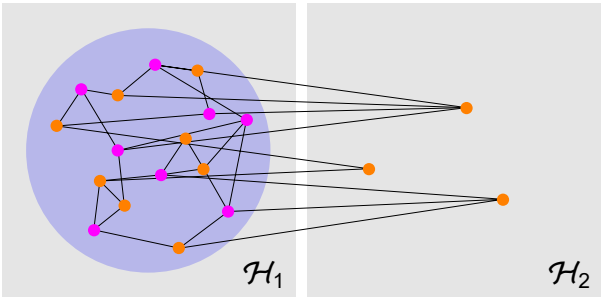

Figure 4.2: Illustration of the procedure for obtaining the valence-sea entanglement for a baryon in QCD. Our procedure pulls three quarks with appropriate flavors out of the baryon state in $\mathcal{H}_1$ and moves them into the vacuum state in $\mathcal{H}_2$. The entanglement between the valence quarks and the parton sea becomes the entanglement between $\mathcal{H}_1$ and $\mathcal{H}_2$, which can then be analyzed using standard methods for bipartite entanglement.

then be written as

$$\begin{aligned}\rho_Q &= \mathcal{N}\mathrm{Tr}_1[Q\,|\psi\rangle_1\,|00\rangle_2\,\langle 00|_2\,\langle\psi|_1\,Q] \\ &= \mathcal{N}\left((\beta\,|01\rangle + \gamma\,|10\rangle)(\beta^*\,\langle 01| + \gamma^*\,\langle 10|) + \delta^*\delta(|01\rangle\,\langle 01| + |10\rangle\,\langle 10|)\right), \qquad (4.8)\end{aligned}$$

$$\mathcal{N}^{-1} = \beta^*\beta + \gamma^*\gamma + 2\delta^*\delta = 1 + \delta^*\delta - \alpha^*\alpha. \qquad (4.9)$$

Note that the one particle states in $|\psi\rangle$ show up as a pure state contribution to the density matrix and are only counted once, while the two particle state $|11\rangle$ contributes twice in the form of an identity matrix. This is a general pattern that will hold for valence-sea entanglement as well; Fock states that only contain valence quarks do not contribute to the entropy, and Fock states with many sea quarks generally contribute more to the entropy than those with fewer sea quarks. This is because every possible assignment of which quarks count as valence quarks is summed over in the density matrix, so our measure of valence-sea entanglement is very sensitive to the presence of many sea quarks.

The procedure for obtaining the reduced density matrix in a general setting is as follows.

Given an initial pure state $|\psi\rangle$, the definition of the reduced density matrix is given by

$$\rho = \mathcal{N}\ \mathrm{Tr}_1 \left[\mathcal{O}_{12} \left|\psi\right\rangle_1 \left|0\right\rangle_2 \left\langle 0\right|_2 \left\langle \psi\right|_1 \mathcal{O}_{12}^\dagger \right]. \tag{4.10}$$

This requires the duplication of the Hilbert space so that $\mathcal{H} \to \mathcal{H}_1 \otimes \mathcal{H}_2$. This duplication serves the purpose of creating an artificial bipartition of the Hilbert space so that notions of entanglement can be rigorously defined even when no bipartition exists in the original Hilbert space. The operator $\mathcal{O}_{12}$ acts on both Hilbert spaces so that the initial states $|\psi\rangle$ and $|0\rangle$ are transformed into an entangled state and the density matrix is non-trivial. The specific choice of operator and initial state $|0\rangle_2$ defines the type of entanglement being represented by ρ. Additionally, there may be a normalization factor $\mathcal{N}$ necessary to ensure that the trace of ρ is fixed appropriately.

There are two main reasons why this definition seems appropriate. First, this formalism can be used to replicate the entanglement measures of any system that is already bipartite, including spatial entanglement. To see this, consider a state $|\psi_{AB}\rangle$ in a Hilbert space $\mathcal{H} = \mathcal{H}_A \otimes \mathcal{H}_B$, such as the two-state example we walked through previously. We can define the density matrix in this formalism by choosing an operator $X_{12}(A)$ that swaps components of the state within A so that

$$X_{12}(A) \left|\psi_A \psi'_B\right\rangle_1 \left|\phi_A \phi'_B\right\rangle_2 = \left|\phi_A \psi'_B\right\rangle_1 \left|\psi_A \phi'_B\right\rangle_2. \tag{4.11}$$

along with a separable initial state $|0\rangle = |0_A 0'_B\rangle$. In the example, this is just the operator that swaps sites $A1$ and $A2$. It is straightforward to show that $X_{12}(A)$ is both a Hermitian and unitary operator. Using a set of separable basis states $\left|\phi_{i,A}\phi'_{j,B}\right\rangle$, we can write $|\psi\rangle =$

$\sum_{i,j} \alpha_{ij} \left|\phi_{i,A}\phi'_{j,B}\right\rangle$. The density matrix is then defined by

$$\begin{aligned}
\rho &= \mathcal{N}\ \mathrm{Tr}_1 \left[X_{12}(A) \left|\psi_{AB}\right\rangle_1 \left|0\right\rangle_2 \left\langle 0\right|_2 \left\langle\psi_{AB}\right|_1 X^\dagger_{12}(A)\right] \\
&= \sum_{i,j} \alpha_{ij} \sum_{k,l} \alpha^*_{kl} \mathrm{Tr}_1 \left[\left|0_A\phi'_{j,B}\right\rangle_1 \left|\phi_{i,A}0'_B\right\rangle_2 \left\langle\phi_{k,A}0'_B\right|_2 \left\langle 0_A\phi'_{l,B}\right|_1\right] \\
&= \sum_{i,k} \left(\sum_j \alpha_{ij}\alpha^*_{kj}\right) \left|\phi_{i,A}0'_B\right\rangle_2 \left\langle\phi_{k,A}0'_B\right|_2 \\
&= \rho_{AB} \otimes \left|0'_B\right\rangle \left\langle 0'_B\right| , \qquad (4.12)
\end{aligned}$$

where $\rho_{AB} = \mathrm{Tr}_B \left[\left|\psi_{AB}\right\rangle \left\langle\psi_{AB}\right|\right]$ is the usual notion of bipartite entanglement between subspaces A and B. Since ρ_{AB} is equal to a tensor product of ρ_{AB} with a pure state density matrix $\left|0'_B\right\rangle \left\langle 0'_B\right|$, the entanglement entropy of ρ is equal to the entanglement entropy of ρ_{AB}, so our formalism reduces to the usual notion of entanglement when the original Hilbert space is already bipartite.

Second, this construction allows for the VS entanglement of the 't Hooft model mesons to be zero. The operator corresponding to VS entanglement will take a quark operator, similar to the operator Q from the example, for each valence quark from $\mathcal{H}_1$ and move them into $\mathcal{H}_2$ before tracing out $\mathcal{H}_1$. The initial state $\left|0\right\rangle$ is taken to be the free quark vacuum state so that there are no particles in the duplicate space to move into the original space and create entirely artificial entanglement, which was also a consideration in the example. For 't Hooft model mesons, the operator effectively dumps the entire meson state into $\mathcal{H}_2$, making ρ a pure state density matrix with zero entropy, which must be the case if this is to be a sensible measure of entanglement between valence and sea quarks. This also applies to the parton model state outlined in the introduction where the state $\psi(x) \sim \psi_V(x)\psi_S(x)$ would have $\psi_V(x)$ moved to $\mathcal{H}_2$ while $\psi_S(x)$ is left in $\mathcal{H}_1$ and traced out, leaving a pure state density matrix defined only by $\psi_V(x)$. Details about how VS entanglement is defined using this formalism will be given in a later section.

4.2.2 Single-Quark Entanglement

As an aside, we can also look at how an individual quark is entangled with the rest of a hadron. A single quark operator of flavor i in the light-cone formalism is given by

$$\begin{aligned} Q_i &= \int dx^- dx_\perp^{d-2}\ \bar{q}_{i,2}(x^-, \vec{x}_\perp)\gamma^+ q_{i,1}(x^-, \vec{x}_\perp) \\ \bar{Q}_i &= -\int dx^- dx_\perp^{d-2}\ \bar{q}_{i,1}(x^-, \vec{x}_\perp)\gamma^+ q_{i,2}(x^-, \vec{x}_\perp), \end{aligned} \tag{4.13}$$

where d is the spacetime dimension. In these equations and the work going forward, we use the conventions $x^\pm = \frac{x^0 \pm x^{d-1}}{\sqrt{2}}$ for the light-cone coordinates and $\gamma^\pm = \frac{\gamma^0 \pm \gamma^{d-1}}{\sqrt{2}}$. The quark fields in these expressions are full, unprojected Dirac spinors, though the γ^+ in between them will eliminate parts of these spinors in any practical calculation. Using this as our entanglement operator and applying several conservation laws, it can be shown that the resulting density matrix is given by (in light-cone gauge)

$$\begin{aligned} \rho_i &= \mathcal{N} \sum_\lambda \int_0^1 dx \int_{-\infty}^{\infty} dk_\perp^{d-2}\ f_{i,\lambda}(x, \vec{k}_\perp) \left| q_{i,\lambda}(xP^+, \vec{k}_\perp) \right\rangle \left\langle q_{i,\lambda}(xP^+, \vec{k}_\perp) \right| \\ f_{i,\lambda}(x, \vec{k}_\perp) &= \int \frac{dz^- dz_\perp^{d-2}}{2(2\pi)^{d-1}} e^{-ixP^+z^-} e^{i\vec{k}_\perp \cdot \vec{z}_\perp} \left\langle \Psi(P^+, \vec{P}_\perp) \right| \bar{q}_i(z) \Pi_\lambda \gamma^+ q_i(0) \left| \Psi(P^+, \vec{P}_\perp) \right\rangle, \end{aligned} \tag{4.14}$$

where $\left| q_{i,\lambda}(k^+, \vec{k}_\perp) \right\rangle = b_{i,\lambda}^\dagger(k^+, \vec{k}_\perp) \left| 0 \right\rangle$ represents a single quark state in $d = 2$ or 4 spacetime dimensions with momentum k, flavor i, and helicity λ, while $\left| \Psi(P^+, \vec{P}_\perp) \right\rangle$ represents a hadron with total momentum P, x is the fractional momentum k^+/P^+, and Π_λ is a helicity projection operator, given by $\Pi_\lambda = \frac{1}{2}(\mathbf{I} + \lambda\gamma^5)$. As with our position coordinates, the light-cone momenta are defined with the convention $p^\pm = \frac{p^0 \pm p^{d-1}}{\sqrt{2}}$. With $d = 4$, the expression for $f_{i,\lambda}(x, \vec{k}_\perp)$ turns out to be the expression for a parton distribution function (PDF) in QCD, including the dependence on helicity and transverse momentum. This provides an interpretation of PDFs as a measure of quark entanglement within a hadron.

The expression for the SQ density matrix above was specific to light-cone gauge. In general, a Wilson line is necessary to maintain gauge invariance in both the PDF and another line for the SQ state vectors in the duplicate space. This work is entirely in light-cone gauge as it is the natural choice for both PDFs and 1+1d QCD.

4.2.3 Other Definitions of Reduced Density Matrices

So far, we have defined our reduced density matrix by using a partial trace over the original Hilbert space. In the literature, given a Hilbert space that can be partitioned into two regions $\mathcal{H} = \mathcal{H}_A \otimes \mathcal{H}_B$, there are three equivalent ways to define reduced density matrices in a field theory [174]:

1 The standard method of doing a partial trace over the pure state density matrix $\rho = |\psi\rangle \langle\psi|$ to get a reduced density matrix $\rho_A = \mathrm{Tr}_B[\rho]$. In theories with gauge symmetry, this may become more complicated as extra physical degrees of freedom may need to be temporarily added to the Hilbert space to perform the partial trace, as in [193].

2 One can also find the density matrix by searching for the matrix $\rho_A \in \mathcal{H}_A$ that has expectation values with other operators in $\mathcal{H}_A$ equal to those of the original pure state $|\psi\rangle$. In other words, ρ_A must satisfy

$$\mathrm{Tr}_A[\rho_A \mathcal{O}_A] = \langle\psi| (\mathcal{O}_A \otimes \mathbf{I}_B) |\psi\rangle , \quad \forall \mathcal{O}_A \in \mathcal{H}_A. \tag{4.15}$$

The space of operators in $\mathcal{H}_A$ can be defined as the subset of operators in $\mathcal{H}$ that have the form $\mathcal{O}_A \otimes \mathbf{I}_B$.

3 The last definition is to write the density matrix as a path integral, and is primarily used when applying the replica trick to calculate the entanglement entropy of a low energy state. One starts with the pure state density matrix

$$\rho = \int \mathcal{D}\phi \mathcal{D}\phi' Z_\psi(\phi, \phi') |\phi\rangle \langle\phi'| , \tag{4.16}$$

where $|\phi\rangle$ is some state that diagonalizes the constituent field operators that make up ψ, and $Z_\psi(\phi, \phi') = \langle\phi'|\psi\rangle \langle\psi|\phi\rangle$ will be our path integral. Assuming that $|\phi\rangle$ represents a minimum energy state for a given set of conserved quantum numbers, $Z_\psi(\phi, \phi')$ can be written as a Euclidean path integral with an insertion of some simple operators with the appropriate quantum numbers, whose upper and lower functional bounds are given

by ϕ' and ϕ, respectively. Assuming that this functional basis can be partitioned so that $|\phi\rangle = |\phi_A\rangle |\phi_B\rangle$, the reduced density matrix is obtained by setting $\phi'_B = \phi_B$ and integrating, so that

$$\rho_A = \int \mathcal{D}\phi_A \mathcal{D}\phi'_A \left(\int \mathcal{D}\phi_B Z_\psi(\phi_A, \phi_B; \phi'_A, \phi_B) \right) |\phi_A\rangle \langle \phi'_A| \,. \tag{4.17}$$

The discussion of a broadened definition of entanglement in the previous section was entirely in terms of definition 1 above. For SQ entanglement, the density matrix can be obtained from definition 2 by matching to matrix elements of the form $\langle\psi| \bar{q}_i(x)\Gamma\gamma^+ q_i(y) |\psi\rangle$ for some arbitrary spinor matrix Γ. A similar operator definition likely exists for VS entanglement, but some subtleties discussed below may require a slight modification to either this approach or the partial trace approach to get a more sensible definition of VS entanglement. Since definition 3 makes some assumptions about the hadron, it cannot be discussed in general terms here.

4.3 1+1d QCD and the 't Hooft model

This section will give details on the 1+1d QCD null plane Hamiltonian that will serve as the mathematical foundation for everything that follows. We will also reproduce the 't Hooft model in this formalism, which serves as a useful starting point for defining valence-sea (VS) entanglement as the mesons in this model have no sea and therefore no VS entanglement. It was first worked out in a paper by 't Hooft in 1974 [12] (see also section 3.2 of [194] for a discussion of these results using this chapter's conventions), and it's Hamiltonian form has been known since the '90s [195, 196]. One appealing aspect of the 't Hooft paper at the time was that it gave us a simple model that exhibited a Regge trajectory in its meson spectrum. The paper's method was to find the meson's wavefunction using the Bethe-Salpeter equation for the large-N_c interactions in $d = 1 + 1$ QCD. The large-N_c limit made it tractable to sum up all of the relevant diagrams and get a non-perturbative result for the wavefunction. It is also an example where light-cone coordinates were of more use than conventional space-time coordinates.

4.3.1 QCD in 1+1 Dimensions

Null Plane Hamiltonian

The QCD action in $d = 2$ dimensions reads

$$S = \int d^2x \left(\bar{q}(i\gamma^\mu D_\mu - m_q)q - \frac{1}{2}\mathrm{Tr}[F^{\mu\nu}F_{\mu\nu}] \right), \tag{4.18}$$

where $D_\mu = \partial_\mu - igA_\mu$ is the covariant derivative and m_q can in principle be a diagonal matrix in flavor space for N_f flavors of fermions. To go into the null plane, we will need to separate the fermion fields into two parts using the projection operators $\Pi^\pm = \frac{1}{2}\gamma^\mp\gamma^\pm$. With $q_\pm = \Pi^\pm q$ and choosing light-cone gauge $A^+ = 0$, the action becomes

$$S = \int d^2x \left(\sqrt{2}iq_+^\dagger \partial^- q_+ + \sqrt{2}iq_-^\dagger \partial^+ q_- - \frac{1}{\sqrt{2}}(q_+^\dagger m_q \gamma^- q_- + q_-^\dagger m_q \gamma^+ q_+) + \sqrt{2}gq_+^\dagger A^- q_+ + \frac{1}{2}(\partial^+ A^{-,a})^2 \right), \tag{4.19}$$

where the index a is the adjoint index for the $SU(N_c)$ gauge field. From this expression, we can see that both q_- and A^- are non-dynamical and should be integrated out. The resulting terms from the integration will be nonlocal in x^-, and at this stage we will take care to define our quantities rigorously.

Define the inverse derivative to be

$$\frac{1}{\partial^+}\phi(x^+, x^-) = \frac{1}{2}\int_{-\infty}^{\infty} dy^- \epsilon(x^- - y^-)\phi(x^+, y^-), \tag{4.20}$$

where $\epsilon(x)$ is the sign function, whose derivative is twice the delta function. The advantage of this definition is that the inverse derivative obeys integration by parts; that is,

$$\int_{-\infty}^{\infty} dx^- \left(\frac{1}{\partial^+}\phi(x)\right)\pi(x) = -\int_{-\infty}^{\infty} dx^- \phi(x)\left(\frac{1}{\partial^+}\pi(x)\right). \tag{4.21}$$

Now we can define the fields to be

$$\phi(x^+, x^-) = \frac{1}{\partial^+}(\partial^+\phi(x^+, x^-)) + C_\phi(x^+). \tag{4.22}$$

The function C_ϕ is necessary to allow ϕ to be a completely arbitrary field under a path integral.

Returning to the QCD action, we can use the above conventions to integrate out the non-dynamical fields and obtain

$$S = \int dx^- dx^+ \left((\sqrt{2} i q_+^\dagger) \partial^- q_+ - q_+^\dagger \frac{m_q^2}{\sqrt{2} i \partial^+} q_+ - \frac{1}{2} \left(\sqrt{2} g \frac{1}{\partial^+} (q_+^\dagger T^a q_+) \right)^2 \right). \tag{4.23}$$

We also get a couple of constraints

$$\int_{-\infty}^{\infty} dx^- q_+^\dagger (x^+, x^-) = 0, \qquad \int_{-\infty}^{\infty} dx^- \left(q_+^\dagger T^a q_+ \right) (x^+, x^-) = 0. \tag{4.24}$$

from integrating out $C_{q_-}(x^+)$ and $C_A^{-,a}(x^+)$, respectively. Note that through integration by parts we could have had to integrate out $C_{q_+}(x^+)$ as well to get the complex conjugate of the first constraint. This seems to imply that states with $p^+ = 0$ are not allowed in the Hilbert space. The second constraint implies that states in the Hilbert space must be invariant under *global* $SU(N_c)$ transformations in the null plane.

From the above expression for the Lagrangian, we can identify that the fundamental commutation relation and the null plane Hamiltonian to be

$$\{ (q_+)_{a,m}(x^-), (q_+^\dagger)_{b,n}(y^-) \} = \frac{1}{\sqrt{2}} \delta_{ab} \delta_{mn} \delta(x^- - y^-) \tag{4.25}$$

$$P^- = \int_{-\infty}^{\infty} dx^- \left(q_+^\dagger \frac{m_q^2}{\sqrt{2} i \partial^+} q_+ + g^2 \left(\frac{1}{\partial^+} (q_+^\dagger T^a q_+) \right)^2 \right), \tag{4.26}$$

where the subscripts a, b represent fundamental $SU(N_c)$ color indices and m, n represent flavor indices for N_f flavors. It is clear from this expression that the Hamiltonian is composed of a kinetic term P_0^- and a potential term V proportional to g^2. If we write out the inverse derivatives in the potential, we get

$$\begin{aligned} V &= \frac{g^2}{4} \int_{-\infty}^{\infty} dx^- dy^- dz^- \epsilon(x^- - y^-) \epsilon(x^- - z^-) (q_+^\dagger T^a q_+)(y^-) (q_+^\dagger T^a q_+)(z^-) \\ &= \frac{g^2}{2} \int_{-\infty}^{\infty} dy^- dz^- (\pi \delta(0) - |y^- - z^-|) (q_+^\dagger T^a q_+)(y^-) (q_+^\dagger T^a q_+)(z^-). \end{aligned} \tag{4.27}$$

The divergent $\delta(0)$ term seems like it will be a problem at first glance, but upon closer inspection it is proportional to two factors of the global $SU(N_c)$ generator $\int dx^- q_+^\dagger T^a q_+$,

which by the second constraint above must vanish for any state in our Hilbert space. In fact, this is the same infrared divergence that 't Hooft encountered in his derivation of the self-energy that eventually disappeared in the final result. Thus we can neglect the divergent term to write the potential as

$$V = -\frac{g^2}{2}\int_{-\infty}^{\infty} dx^- dy^- |x^- - y^-| (q_+^\dagger T^a q_+)(x^-)(q_+^\dagger T^a q_+)(y^-). \tag{4.28}$$

This explicitly shows the linear confining potential of $d = 2$ QCD. One would get a similar result for $d = 2$ QED in the null plane.

Momentum Space Potentials

While this form of the Hamiltonian looks fairly simple, it is not particularly useful for analyzing the lowest lying energy states. To do this, we need to convert the Hamiltonian into a momentum space representation. The quark fields can be written as

$$q_+(x) = \int_0^\infty \frac{dk^+}{4\pi k^+}\sqrt{\sqrt{2}k^+}\left(b(k)e^{-ik^+x^-} + d^\dagger(k)e^{ik^+x^-}\right), \tag{4.29}$$

where $b(k)$ and $d(k)$ are the annihilation operators for the quark and antiquark, respectively. Note that these operators do not have a spin index because in $d = 2$ spacetime dimensions there are only 2 components to a Dirac spinor, and one of them was integrated out in the process of getting to the null plane Hamiltonian. The factor of $\sqrt{\sqrt{2}k^+}$ is a leftover remnant of the plane wave spinors that act as solutions to the Dirac equation. The fundamental anticommutation relations between the creation and annihilation operators are given by

$$\{b_{a,m}(k), b_{b,n}^\dagger(q)\} = \{d_{a,m}(k), d_{b,n}^\dagger(q)\} = 4\pi k^+ \delta_{ab}\delta_{mn}\delta(k^+ - q^+), \tag{4.30}$$

where a, b and m, n continue to represent color and flavor indices, respectively.

We will not go through the derivation of how to get the expression for P^- in terms of the $b(k)$ and $d(k)$ operators. Rather, we will categorize the different terms that appear in this expression and briefly discuss each one. In momentum space, we organize the Hamiltonian into the following terms:

$$P^- = K + V_M + V_B + V_g + V_s + V_2 - \Omega. \tag{4.31}$$

K is the free particle kinetic term, given by

$$K = \int_0^\infty \frac{dk}{4\pi k} \left(b^\dagger(k) \frac{m_q^2}{2k} b(k) + d^\dagger(k) \frac{m_q^2}{2k} d(k) \right). \tag{4.32}$$

Note that in this expression and in all of the ones to follow we are suppressing the superscript + on the momenta. Unless otherwise stated, all momenta without a superscript now refers to the + component. Also recall that m_q can in principle be a real, diagonal matrix in flavor space. This term simply adds a factor of $\frac{m_q^2}{2k}$ to the energy for each particle and antiparticle in a given state vector.

The constant Ω is the formally divergent vacuum state energy, with contributions from both the free particle Hamiltonian and the potential. Since it is a constant and only contributes to the overall phase of a given state, we will neglect it going forward.

The first term in the potential, V_M, is given by

$$\begin{aligned} V_M = -\frac{g^2}{2} \left(\prod_{i=1}^{4} \int_0^\infty \frac{dk_i}{2\pi\sqrt{2k_i}} \right) \mathscr{P} \left[\frac{1}{(k_2 - k_3)^2} \right] (2\pi)\delta(k_1 + k_2 - k_3 - k_4) \\ * \left(b^\dagger_{a,m}(k_1) d^\dagger_{a,n}(k_2) d_{b,n}(k_3) b_{b,m}(k_4) - \frac{1}{N_c} b^\dagger_{a,m}(k_1) d^\dagger_{b,n}(k_2) d_{b,n}(k_3) b_{a,m}(k_4) \right), \end{aligned} \tag{4.33}$$

where $\mathscr{P}$ refers to the principle value of quantity in brackets. This term is labeled V_M because, as we will discuss below, in the large-N_c limit it is the only part of the potential (besides V_2) that contributes in the meson sector. We can see that the leading piece corresponds to a quark-antiquark pair in a color singlet being annihilated and recreated. If we suppose that this term represents some intermediate state that forms and decays during this process, then it would be a color singlet that has two flavor indices, just like a meson. This is a further indication that this term is specifically important for the description of mesons.

The term V_B is given by

$$\begin{aligned} V_B = \frac{g^2}{4} \left(\prod_{i=1}^{4} \int_0^\infty \frac{dk_i}{2\pi\sqrt{2k_i}} \right) \mathscr{P} \left[\frac{1}{(k_2 - k_3)^2} \right] (2\pi)\delta(k_1 + k_2 - k_3 - k_4) \\ * \left(b^\dagger_{a,m}(k_1) b^\dagger_{b,n}(k_2) b_{a,n}(k_3) b_{b,m}(k_4) - \frac{1}{N_c} b^\dagger_{a,m}(k_1) b^\dagger_{b,n}(k_2) b_{b,n}(k_3) b_{a,m}(k_4) + (b \to d) \right). \end{aligned} \tag{4.34}$$

This term is labeled V_B because in the large-N_c limit it is the only part of the potential (besides V_2) that contributes in the baryon (or antibaryon) sector. This is also the only term that counts either quarks or antiquarks exclusively; that is, these are the only 4-operator terms that do not have both b's and d's in them. For mesons, however, this term is subleading in the $\frac{1}{N_c}$ expansion. In terms of diagrams, this seems to correspond to two (anti)quarks exchanging a gluon and swapping color charge in the process.

The term V_g is given by

$$V_g = \frac{g^2}{2}\left(\prod_{i=1}^{4}\int_0^\infty \frac{dk_i}{2\pi\sqrt{2k_i}}\right)\frac{1}{(k_1+k_2)^2}(2\pi)\delta(k_1+k_2-k_3-k_4)$$
$$* \left(b^\dagger_{a,m}(k_1)d^\dagger_{b,m}(k_2)d_{b,n}(k_3)b_{a,n}(k_4) - \frac{1}{N_c}b^\dagger_{a,m}(k_1)d^\dagger_{a,m}(k_2)d_{b,n}(k_3)b_{b,n}(k_4)\right). \quad (4.35)$$

This term is labeled V_g because it corresponds to a quark-antiquark pair in a *flavor* singlet but a color adjoint being annihilated and recreated. This suggests that the term represents some intermediate state with the same quantum numbers as a gluon, and the kinematical factor of $\frac{1}{(k_1+k_2)^2}$ appears to be the gluon propagator in light-cone gauge. It is subleading in the $\frac{1}{N_c}$ expansion.

The term V_s is given by

$$V_s = \frac{g^2}{2}\left(\prod_{i=1}^{4}\int_0^\infty \frac{dk_i}{2\pi\sqrt{2k_i}}\right)\frac{1}{(k_1+k_2)^2}(2\pi)\delta(k_1+k_2+k_3-k_4)\left(\delta_{ad}\delta_{bc} - \frac{1}{N_c}\delta_{ab}\delta_{cd}\right)$$
$$* \left(b^\dagger_{a,n}(k_1)d^\dagger_{b,n}(k_2)(b^\dagger_{c,m}(k_3)b_{d,m}(k_4) - d^\dagger_{d,m}(k_3)d_{c,m}(k_4)) + (h.c.)\right). \quad (4.36)$$

This term is labeled V_s because these are the only factors that have an unequal number of creation and annihilation operators, breaking the quark+antiquark number symmetry and allowing for the existence of sea quarks distinct from valence quarks. This part of the potential contributes to diagrams with virtual quark-antiquark loops in them. It is subleading in the $\frac{1}{N_c}$ expansion, as is known from the counting of N_c factors in the diagrammatic expansion.

Finally, the term V_2 is given by

$$V_2 = -g^2\frac{N_c^2-1}{2\pi N_c}\int_0^\infty \frac{dk}{4\pi k}\left(b^\dagger(k)\frac{1}{2k}b(k) + d^\dagger(k)\frac{1}{2k}d(k)\right). \quad (4.37)$$

This term is labeled V_2 since it has the only 2-operator terms in the potential. It corresponds to the self-energy of a quark, and its only effect is to shift the squared quark masses by a factor of $-g^2\frac{N_c^2-1}{2\pi N_c}$. It survives in the large-N_c limit.

4.3.2 Large-N_c Limit

Taking the large-N_c limit in the Hamiltonian formalism corresponds to the vanishing of some of the (anti)commutators between field operators. This is because the anticommutator between two field operators includes a Kronecker delta for the color indices. The sum over a Kronecker delta is given by $\sum_a \delta_{ab} = 1$, while the sum itself goes as N_c, so the delta function can be thought of as going as $\frac{1}{N_c}$. Thus the fundamental anticommutator between quark fields would seem to vanish in the large-N_c limit, but this is not strictly true, such as in cases where the quark fields are guaranteed to have the same color index. To clearly see which commutators survive the large-N_c limit, we need to work strictly with color singlet operators.

For the meson sector, the most basic color singlet operators we will need are of the form $b^\dagger b$, $d^\dagger d$, $b^\dagger d^\dagger$, and db. For the first two operators, the commutators with a single field operator all have the form

$$[b^\dagger_{b,\ell}(k) b_{b,m}(q), b^\dagger_{a,n}(p)] = (4\pi p \delta_{mn}\delta(q-p)) b^\dagger_{a,\ell}(k), \tag{4.38}$$

which is order 1 in the large-N_c expansion. Thus all of their commutators will be order 1 and we can consider these operators to be of order 1 as well. The latter two operators, $b^\dagger d^\dagger$ and db, are a bit more complicated. Between the two of them, we have

$$\begin{aligned}[d_{b,m_2}(q_2) b_{b,m_1}(q_1), b^\dagger_{a,n_1}(k_1) d^\dagger_{a,n_2}(k_2)] &= N_c(4\pi k_1 \delta_{m_1 n_1}\delta(k_1-q_1))(4\pi k_2 \delta_{m_2 n_2}\delta(k_2-q_2)) \\ &\quad - (4\pi k_2 \delta_{m_2 n_2}\delta(k_2-q_2)) b^\dagger_{a,m_1}(k_1) b_{a,n_1}(q_1) \\ &\quad - (4\pi k_1 \delta_{m_1 n_1}\delta(k_1-q_1)) d^\dagger_{a,m_2}(k_2) d_{a,n_2}(q_2), \end{aligned} \tag{4.39}$$

whose leading term is of order N_c. However, the commutators with the former two operators

is of order 1. For what follows, we will define the operator

$$L_{mn}(p,x) = \frac{1}{\sqrt{4\pi N_c x(1-x)}} d_{a,n}(p(1-x)) b_{a,m}(px)$$
$$[L_{m_1m_2}(q,y), L^\dagger_{n_1n_2}(k,x)] = 4\pi k \delta_{m_1n_1}\delta_{m_2n_2}\delta(k-q)\delta(x-y) - \mathscr{O}(\frac{1}{N_c}). \tag{4.40}$$

The letter L is chosen because this operator can be thought of as a generator (or annihilator) of a quark-antiquark loop in a color singlet configuration. With this definition, we now have all of the color singlet field operators needed for the meson sector ($b^\dagger b$, $d^\dagger d$, L, and $L^\dagger$) which scale as $\mathscr{O}(1)$ operators to leading order in the large-N_c expansion.

The 't Hooft model is $d = 2$ QCD in the large-N_c limit such that the coupling constant $g \sim \frac{1}{\sqrt{N_c}}$. The potential is proportional to g^2, so the operators must go as N_c or better to survive the large-N_c limit. The only way to achieve this with a four-operator color singlet term is with something like $(b^\dagger d^\dagger)(db) \sim N_c L^\dagger L$, which exists only in the V_M term. The V_2 is also proportional to $g^2 N_c$ as is evident from its definition above. Thus the null plane Hamiltonian for the 't Hooft model can be written as

$$\begin{aligned}
\lim_{N_c\to\infty} P^- &= \lim_{N_c\to\infty}(K^* + V_M) \\
\lim_{N_c\to\infty} K^* &= K + V_2 = \int_0^\infty \frac{dk}{4\pi k}\left(b^\dagger(k)\frac{M_q^2}{2k}b(k) + d^\dagger(k)\frac{M_q^2}{2k}d(k)\right) \\
\lim_{N_c\to\infty} V_M &= -\xi^2\frac{\pi}{N_c}\left(\prod_{i=1}^4\int_0^\infty\frac{dk_i}{2\pi\sqrt{2k_i}}\right)\mathscr{P}\left[\frac{1}{(k_2-k_3)^2}\right](2\pi)\delta(k_1+k_2-k_3-k_4) \\
&\quad * \left(b^\dagger_{a,m}(k_1)d^\dagger_{a,n}(k_2)d_{b,n}(k_3)b_{b,m}(k_4)\right) \\
&= -\xi^2\int_0^\infty\frac{dk}{4\pi k}\int_0^1 dx\int_0^1 dy\ \mathscr{P}\left[\frac{1}{(x-y)^2}\right]\frac{1}{2k}L^\dagger_{mn}(k,x)L_{mn}(k,y).
\end{aligned} \tag{4.41}$$

where $\xi^2 = \frac{g^2N_c}{2\pi}$, which remains finite in the large-N_c limit, and $M_q^2 = m_q^2 - \xi^2$. From this Hamiltonian, we can recover 't Hooft's original results and obtain an equation for the meson wavefunction that is important for finding their mass spectrum.

4.3.3 The Meson Wavefunction

The meson state vector is given by

$$|\psi, p\rangle = \int_0^\infty \frac{dk_1}{4\pi k_1} \int_0^\infty \frac{dk_2}{4\pi k_2} \Psi_{mn}(k_1, k_2; p) \frac{1}{\sqrt{N_c}} b^\dagger_{a,m}(k_1) d^\dagger_{a,n}(k_2) |0\rangle$$
$$= \int_0^1 dx\ \psi_{mn}(x) L^\dagger_{mn}(p, x) |0\rangle , \tag{4.42}$$

$$\Psi_{mn}(k_1, k_2; p) = 4\pi k \delta(k - p) \sqrt{4\pi x(1-x)} \psi_{mn}(x) \tag{4.43}$$

where $\Psi_{mn}(k_1, k_2; p)$ is the total meson wavefunction, $k = k_1 + k_2$ is the total meson momentum, $x = k_1/k$ is the fractional momentum of the quark ($1 - x$ for the antiquark), and $|0\rangle$ is the vacuum state. Since the Hamiltonian commutes with the momentum operator, this state is an eigenstate of P^+ with eigenvalue p. The state is normalized to $\langle \psi, q | \psi, p \rangle = 4\pi p \delta(p - q)$, so the wavefunction must have a normalization of

$$\int_0^1 dx\ \psi^\dagger_{mn}(x) \psi_{mn}(x) = 1 \tag{4.44}$$

This state is a bound state of the null plane Hamiltonian, which means it must satisfy the equation

$$\lim_{N_c \to \infty} P^- |\psi, p\rangle = \lim_{N_c \to \infty} (K^* + V_M) |\psi, p\rangle = \frac{\mu^2}{2p} |\psi, p\rangle , \tag{4.45}$$

where μ is the mass of the meson. Using the definitions and commutation relations above, we can apply the Hamiltonian to the state to get

$$\lim_{N_c \to \infty} K^* |\psi, p\rangle = \frac{1}{2p} \int_0^1 dx\ \left(\frac{M_m^2}{x} + \frac{M_n^2}{1-x} \right) \psi_{mn}(x) L^\dagger_{mn}(p, x) |0\rangle \tag{4.46}$$

$$\lim_{N_c \to \infty} V_M |\psi, p\rangle = \frac{1}{2p} \int_0^1 dx \left(-\xi^2 \int_0^1 dy\ \mathscr{P} \left[\frac{1}{(x-y)^2} \right] \psi_{mn}(y) \right) L^\dagger_{mn}(p, x) |0\rangle , \tag{4.47}$$

where M_n^2 is the shifted mass squared for a quark of flavor n. Putting these two equations together, we get an equation for the meson mass of

$$\left(\frac{M_m^2}{x} + \frac{M_n^2}{1-x} \right) \psi_{mn}(x) - \xi^2 \int_0^1 dy\ \mathscr{P} \left[\frac{1}{(x-y)^2} \right] \psi_{mn}(y) = \mu^2 \psi_{mn}(x). \tag{4.48}$$

This is precisely the result that 't Hooft obtained in his 1974 paper. From here, we can numerically solve this equation to find both the wavefunctions and their corresponding mass values in the meson spectrum.

4.4 Discrete Light-Cone Quantized Hamiltonian

4.4.1 Overview of DLCQ

While 1+1d QCD in the large-N_c limit is exactly solvable, the same cannot necessarily be said of QCD with a finite number of colors. Thus we will need a way to approximate the theory in a way that makes it computationally tractable. Since there is no clear perturbative expansion that can be done to obtain entanglement entropy results, we will instead discretize the theory to render the Hilbert space finite. The bulk of the investigation into VS and SQ entanglement will be done using discrete light-cone quantization (DLCQ), using the same null plane Hamiltonian $\hat{P}^-$ defined in the previous section. DLCQ is discussed in detail in [190, 197, 198], with specific applications to 1+1 QCD given in [191, 192, 199]. In DLCQ, we discretize momentum space of quarks to half-integers with spacing δp. The Hamiltonian $\hat{P}^-$ can be separated into smaller terms based on eigenstates of total momentum $\hat{P}^+$. Since this momentum is strictly positive, the total momentum $P^+ = K\ \delta p$ provides a natural cutoff for the constituent particles, so no separate large momentum cutoff is necessary. In addition, $\mathcal{M}^2 = 2\hat{P}^+\hat{P}^-$ has no explicit dependence on δp, but it does enter implicitly through K, so the continuum limit is approached as K increases toward infinity. Notes about the specifics of the simulation architecture can be found in Appendix A.

4.4.2 The Hamiltonian

Instead of working with the Hamiltonian directly, we will use the Poincaré invariant mass squared operator given by

$$\mathcal{M}^2 = 2P^+P^- = \mathcal{K} + \mathcal{V}_M + \mathcal{V}_B + \mathcal{V}_g + \mathcal{V}_s - \Omega. \tag{4.49}$$

All of these terms are directly analogous to the terms of the continuum null plane Hamiltonian defined in the previous section. $\mathcal{K}$ is the free particle kinetic term, given by

$$\mathcal{K} = n_p \sum_n \left(b^\dagger_{a,f,n} \frac{m_q^2}{n} b_{a,f,n} + d^\dagger_{a,f,n} \frac{m_q^2}{n} d_{a,f,n} \right). \tag{4.50}$$

With $\xi^2 = \frac{g^2 N_c}{2\pi}$, the discretized potentials are

$$\mathcal{V}_M = -\frac{\xi^2 n_p}{N_c} \sum_{n_1,n_2,n_3,n_4} \mathscr{P}\left[\frac{1}{(n_2-n_3)^2}\right] \delta_{n_1+n_2,n_3+n_4} \\ * \left(b^\dagger_{a,f,n_1} d^\dagger_{a,g,n_2} d_{b,g,n_3} b_{b,f,n_4} - \frac{1}{N_c} b^\dagger_{a,f,n_1} d^\dagger_{b,g,n_2} d_{b,g,n_3} b_{a,f,n_4} \right). \tag{4.51}$$

$$\mathcal{V}_B = \frac{\xi^2 n_p}{2N_c} \sum_{n_1,n_2,n_3,n_4} \mathscr{P}\left[\frac{1}{(n_2-n_3)^2}\right] \delta_{n_1+n_2,n_3+n_4} \\ * \left(b^\dagger_{a,f,n_1} b^\dagger_{b,g,n_2} b_{a,g,n_3} b_{b,f,n_4} - \frac{1}{N_c} b^\dagger_{a,f,n_1} b^\dagger_{b,g,n_2} b_{b,g,n_3} b_{a,f,n_4} + (b \to d) \right), \tag{4.52}$$

$$\mathcal{V}_g = \frac{\xi^2 n_p}{N_c} \sum_{n_1,n_2,n_3,n_4} \frac{1}{(n_1+n_2)^2} \delta_{n_1+n_2,n_3+n_4} \\ * \left(b^\dagger_{a,f,n_1} d^\dagger_{b,f,n_2} d_{b,g,n_3} b_{a,g,n_4} - \frac{1}{N_c} b^\dagger_{a,f,n_1} d^\dagger_{a,f,n_2} d_{b,g,n_3} b_{b,g,n_4} \right). \tag{4.53}$$

$$\mathcal{V}_s = \frac{\xi^2 n_p}{N_c} \sum_{n_1,n_2,n_3,n_4} \frac{1}{(n_1+n_2)^2} \delta_{n_1+n_2+n_3,n_4} \left(\delta_{ad}\delta_{bc} - \frac{1}{N_c}\delta_{ab}\delta_{cd} \right) \\ * \left(b^\dagger_{a,f,n_1} d^\dagger_{b,f,n_2} (b^\dagger_{c,g,k_3} b_{d,g,n_4} - d^\dagger_{d,g,k_3} d_{c,g,n_4}) + (h.c.) \right). \tag{4.54}$$

Since in our numerical work we are always using vector spaces that share the same total +-momentum, there is no practical difference between working with the Hamiltonian or working with $\mathcal{M}^2$. However, the single particle energy levels in the $\mathcal{M}^2$ stay discrete when extrapolated to the continuum, so it is much easier to identify these states in $\mathcal{M}^2$ when varying the total number of momentum units K.

There is no term analogous to V_2 is our discrete version of the theory. This is because we choose to define the principle value for the discrete potential to give the same answer as it would in the continuum, specifically so that

$$\sum_{n_3,n_4=1/2}^{\infty} \mathscr{P}\left[\frac{-1}{(n_2-n_3)^2}\right] \delta_{n_1+n_2,n_3+n_4} = \frac{1}{n_1} + \frac{1}{n_2}. \tag{4.55}$$

for positive half-integers n_1 and n_2. This leads to a value of f_n as defined in Appendix D of

$$f_n = \sum_{k=1}^{n-1/2} \frac{1}{k^2} + \frac{1}{n} \tag{4.56}$$

The extra factor of $\frac{1}{n_1} + \frac{1}{n_2}$ coming from this principle value cancels out the V_2 term in the Hamiltonian. This prescription was necessary in order to get a more accurate mass spectrum as the mass becomes small compared to the coupling strength g. With the more conventional choice of $\frac{\pi^2}{6}$ for the principle value, we would see some negative m^2 values emerge as the potential became stronger, which is a result of the zero modes that appear when the quarks are massless becoming states with negative m^2 values upon discretization. Our prescription for the principal value guarantees that the zero modes in the theory with massless quarks will continue to be zero modes in DLCQ, and all of the eigenstates of $\mathcal{M}^2$ do appear to have physically sound masses with this choice. Details about this choice of principle value are given in Appendix D.

The diagonal parts of the Hamiltonian applied to a color singlet vector are given by

$$\begin{aligned}
\mathcal{V}_0 \left|\psi, \alpha\right\rangle = & \frac{\xi^2 n_p}{N_c} \sum_{I,J} \frac{\delta_{f_I f_J}}{(n_I + n_J)^2} \left(\left|\psi, \alpha\right\rangle - \left|\psi, \Delta_{IJ}(\alpha)\right\rangle\right) \\
& - \frac{\xi^2 n_p}{N_c} \sum_{I,I'} \frac{\theta_\times(n_{I'} - n_I)\delta_{f_I f_{I'}}}{(n_{I'} - n_I)^2} \left(\left|\psi, \alpha\right\rangle - \frac{1}{N_c}\left|\psi, X^b_{II'}(\alpha)\right\rangle\right) \\
& - \frac{\xi^2 n_p}{N_c} \sum_{J,J'} \frac{\theta_\times(n_{J'} - n_J)\delta_{f_J f_{J'}}}{(n_{J'} - n_J)^2} \left(\left|\psi, \alpha\right\rangle - \frac{1}{N_c}\left|\psi, X^d_{JJ'}(\alpha)\right\rangle\right) \\
& + \xi^2 n_p \left(1 - \frac{1}{N_c^2}\right) (F_q + F_{\bar{q}}) \left|\psi, \alpha\right\rangle .
\end{aligned} \tag{4.57}$$

with F_q and $F_{\bar{q}}$ defined in Appendix D with the f_n discussed above.

4.5 Valence-Sea Entanglement

This section details the construction of the valence-sea entanglement for various hadrons. The initial state $|0\rangle$ is taken to be the light-cone vacuum, while the VS entanglement operator is a product of multiple Q_i operators from single-quark entanglement, one for each valence

quark. All of our results are obtained using DLCQ, so all of our expressions listed here are given using operators in discretized 1+1d momentum space. The continuum analog can be obtained fairly straightforwardly by starting with the basic expression for the density matrix using the definitions for Q_i and $\bar{Q}_i$ in Eq. (4.13). Many of the analytic results derived in this section carry over to the continuum theory.

4.5.1 VS Entanglement for Mesons

The simplest example of a valence-sea density matrix is that of a meson where the quark and antiquark have different flavors. This serves as the 1+1d analog of the π^+ meson, where the valence particles have flavors u for the quark and d for the antiquark. The VS density matrix for the π^+ analog state with total momentum K is given by

$$\begin{aligned}\rho_{\pi^+} &= \mathcal{N}\ \mathrm{Tr}_1\left[Q_u\bar{Q}_d\left|\pi^+,K\right\rangle_1|0\rangle_2\langle 0|_2\left\langle\pi^+,K\right|_1 Q_d\bar{Q}_u\right] \\ &= \mathcal{N}\sum_{a,b,c,d}\sum_{k_i} f_{k_1k_2k_3k_4,abcd}\left(b^\dagger_{k_1,u,a}d^\dagger_{k_2,d,b}|0\rangle\langle 0|\, d_{k_3,d,c}b_{k_4,u,d}\right), \end{aligned} \tag{4.58}$$

with discrete momenta k_i, color indices a,b,c,d for $SU(N_c)$ ranging from 1 to N_c, and a normalization constant $\mathcal{N}$. The Q operators in discrete momentum space are defined by

$$\begin{aligned} Q_i &= \sum_{k,c}(b^\dagger_{k,i,c,2}b_{k,i,c,1} + d_{k,i,c,2}d^\dagger_{k,i,c,1}) \\ \bar{Q}_i &= \sum_{k,c}(b_{k,i,c,2}b^\dagger_{k,i,c,1} + d^\dagger_{k,i,c,2}d_{k,i,c,1}), \end{aligned} \tag{4.59}$$

f above is defined to be

$$f_{k_1k_2k_3k_4,abcd} = \left\langle\pi^+,K\right| b^\dagger_{k_4,u,d}d^\dagger_{k_3,d,c}d_{k_2,d,a}b_{k_1,u,a}\left|\pi^+,K\right\rangle. \tag{4.60}$$

Since the meson state is a color singlet, only color singlet configurations of the creation and annihilation operators in f will give nonzero contributions. The easiest way to get the color singlet configurations is to get the irreducible representations (irreps) of the creation operators and the annihilation operators separately, and then join the matching irreps in as many ways as possible to get the number of singlets. In the case of the π^+ meson, we

have two pairs of operators of the forms db and $b^\dagger d^\dagger$, which both form into a singlet and an adjoint representation. This originates from the group theory of $SU(N_c)$, where the quark in the fundamental representation and the antiquark in the antifundamental representation combine so that $N_c \otimes \bar{N}_c = 1 \oplus (N_c^2 - 1)$, where the 1 on the right-hand side is the singlet and the $N_c^2 - 1$ is the adjoint representation. For $N_c = 3$, this reduces to the more familiar form $3 \otimes \bar{3} = 1 \oplus 8$. The singlet is formed by matching the two color indices of the operators together and summing over them, while the adjoint is formed from every configuration of the color indices such that it commutes with the conjugate of the singlet operator. This gives us two singlets overall, one for the combination of the two singlet representations from the pairs of operators, and one for the singlet combination of the two adjoint representations. The matrix element f can be decomposed into two terms corresponding to the singlet and adjoint unification terms

$$\Pi^S_{abcd} = \frac{\delta_{ab}\delta_{cd}}{N_c} \tag{4.61}$$

$$\Pi^A_{abcd} = \left(\delta_{ad}\delta_{bc} - \frac{1}{N_c}\delta_{ab}\delta_{cd}\right) \tag{4.62}$$

$$f^{S,A}_{k_1k_2k_3k_4} = \Pi^{S,A}_{abcd} f_{k_1k_2k_3k_4,abcd}, \tag{4.63}$$

with an implicit sum over all color indices in the last equation. This means that f can be written as

$$f_{k_1k_2k_3k_4,abcd} = \Pi^S_{abcd} f^S_{k_1k_2k_3k_4} + \frac{1}{N_c^2 - 1}\Pi^A_{abcd} f^A_{k_1k_2k_3k_4}. \tag{4.64}$$

This implies that the VS density matrix can be separated into an average of two density matrices

$$\rho_{\pi^+} = \omega^S(\Pi^S \otimes \rho_S) + \frac{1}{N_c^2 - 1}\omega^A(\Pi^A \otimes \rho_A), \tag{4.65}$$

where $\rho_{S,A}$ are density matrices in momentum space, while ω^S and $\omega^A = 1 - \omega^S$ form a Bernoulli distribution, representing the chances of measuring the valence quarks to be in either a singlet or an adjoint representation.

In order to get the Von Neumann entropy of the VS density matrix in terms of f^S and f^A, we need to know what matrix multiplication looks like in terms of the color and momentum

tensor f. If we have two density matrices of the same form as that of the VS density matrix in Eq. ((4.58)), then $\rho_1.\rho_2$ becomes

$$(f_1.f_2)_{k_1k_2k_3k_4,abcd} = \sum_{A,B}\sum_{q_1,q_2}(f_1)_{k_1k_2q_2q_1,abBA}(f_2)_{q_1q_2k_3k_4,ABcd} \tag{4.66}$$

at the level of the tensors f_1, f_2. According to this definition of the product of tensors, the two color tensors Π^S and Π^A have the properties $\Pi^{S,A}.\Pi^{S,A} = \Pi^{S,A}$ and $\Pi^S.\Pi^A = 0$, which makes then projection operators for two distinct vector subspaces in color space. For the remaining degrees of freedom in momentum space, we can define matrix multiplication and the trace for these distributions as

$$(A.B)_{k_1k_2k_3k_4} = \sum_{q_1,q_2} A_{k_1k_2q_2q_1}B_{q_1q_2k_3k_4} \tag{4.67}$$

$$\mathrm{Tr}[A] = \sum_{k_1,k_2} A_{k_1k_2k_2k_1}. \tag{4.68}$$

With these definitions, we can define the matrix logarithm for $f^{S,A}$ and therefore the Von Neumann entropy of the density matrix in Eq. ((4.58)). The VS entanglement entropy for the π^+ meson can be written as

$$S_{\pi^+} = \mathcal{N}\left(-\mathrm{Tr}\left[f^S.\log f^S\right] - \mathrm{Tr}\left[f^A.\log f^A\right] + \mathrm{Tr}\left[f^A\right]\log(N_c^2-1)\right) + \log(\mathcal{N}^{-1}) \tag{4.69}$$

$$\mathcal{N}^{-1} = \mathrm{Tr}\left[f^S\right] + \mathrm{Tr}\left[f^A\right]. \tag{4.70}$$

This can also be cast in the more illustrative form

$$\omega^{S,A} = \mathcal{N}\ \mathrm{Tr}\left[f^{S,A}\right] \tag{4.71}$$

$$S_{S,A} = \frac{1}{\mathrm{Tr}\left[f^{S,A}\right]}\left(-\mathrm{Tr}\left[f^{S,A}.\log f^{S,A}\right]\right) + \log\left(\mathrm{Tr}\left[f^{S,A}\right]\right) \tag{4.72}$$

$$S_{\pi^+} = \omega^S S_S + \omega^A S_A + \omega^A\log(N_c^2-1) - \omega^S\log\omega^S - \omega^A\log\omega^A. \tag{4.73}$$

From this form we can see that the VS entanglement entropy of the π^+ meson can be separated into three contributions, stemming from the fact that our density matrix can be decomposed into

$$\rho_{\pi^+} = \omega^S(\Pi^S\otimes\rho_S) + \frac{1}{N_c^2-1}\omega^A(\Pi^A\otimes\rho_A) \tag{4.74}$$

with $\Pi_S.\Pi_A = 0$. The first contribution is the average of the entropies $S_{S,A}$ of $\rho_{S,A}$, corresponding to the momentum space degrees of freedom. The second part is the average of the entropies of Π_S and $\frac{1}{N_c^2-1}\Pi^A$, which serve as the density matrices in color space. The entropy of Π_S is zero since it only projects one state, while the entropy of $\frac{1}{N_c^2-1}\Pi^A$ is the $\log(N_c^2-1)$ we see in the full entropy expression. Finally, the last term is the entropy of the distribution formed by ω^S and ω^A. This decomposition of entropy contributions also holds for a continuous momentum variable.

Thus far, we have found expressions for the VS density matrix and entanglement entropy in terms of a set of expectation values f for a meson state vector under the assumption that the valence quarks in our meson had to have different flavors. If the valence quark and antiquark share the same flavor, we can define an entanglement entropy S_{sing} in terms of the corresponding f_S and f_A tensors in much the same way as we did above for the π^+. However, the singlet density matrix ρ_{sing} has an extra vacuum state contribution given by

$$\begin{aligned}\rho_{sing} &= \mathcal{N}_{sing}\ \mathrm{Tr}_1\left[Q_f\bar{Q}_f\left|sing,K\right\rangle_1\left|0\right\rangle_2\left\langle 0\right|_2\left\langle sing,K\right|_1 Q_f\bar{Q}_f\right] &(4.75)\\ &= \mathcal{N}_{sing}\sum_{a,b,c,d}\sum_{k_i} f_{k_1k_2k_3k_4,abcd}\left(b^\dagger_{k_1,f,a}d^\dagger_{k_2,f,b}\left|0\right\rangle\left\langle 0\right| d_{k_3,f,c}b_{k_4,f,d}\right)\\ &\quad+\mathcal{N}_{sing}\ f_{vac}\left|0\right\rangle\left\langle 0\right| . &(4.76)\\ f_{vac} &= \sum_{a,b}\sum_{k_1,k_2}\left\langle sing,K\right| d^\dagger_{k_2,f,b}d_{k_2,f,b}d^\dagger_{k_1,f,a}d_{k_1,f,a}\left|sing,K\right\rangle . &(4.77)\end{aligned}$$

Thus the von Neumann entropy of this density matrix is somewhat different from S_{sing}. They are related by

$$-\mathrm{Tr}\left[\rho_{sing}\log(\rho_{sing})\right] = \mathcal{N}_{sing}\left(\mathcal{N}^{-1}\left(S_{sing}-\log(\mathcal{N}^{-1})\right)-f_{vac}\log(f_{vac})\right)+\log(\mathcal{N}_{sing}^{-1}), \quad (4.78)$$

where $\mathcal{N}_{sing} = (\mathcal{N}^{-1}+f_{vac})^{-1}$ is the normalization constant including the vacuum contribution, while $\mathcal{N}$ is the normalization without this contribution. In our work, we will define S_{sing} without the vacuum contribution, as it does not correspond to a valence quark configuration and it will only serve to obscure the conclusions we are able to draw from our data. In principle the vacuum contribution can be important to have to establish the gauge invariance of

the density matrix. However, since writing down the light-cone Hamiltonian we have been working in light-cone gauge exclusively, and the vast majority of our expressions would pick up Wilson lines in any other choice of gauge, complicating the interpretation of the entropy as a measure of quark entanglement. Thus the gauge invariance consideration is of lesser importance in this work, though it could become more important in a $3+1$ dimensional QCD calculation.

4.5.2 VS Entanglement for Baryons

The process of calculating the valence-sea entanglement for baryons is largely the same as it is for mesons. The main difference is that baryons have a number of valence quarks equal to the number of colors. This means that the density matrix becomes much more complicated as the number of colors increases. It is for this reason that we will only consider 2 and 3 color baryons in this work.

In $SU(2)$, the antifundamental representation is the same as the fundamental, so the VS density matrix for $SU(2)$ baryons will look very similar to the matrix for $SU(2)$ mesons. We have for some flavors m and n

$$\begin{aligned}\rho_{B_{mn}} &= \mathcal{N}\ \mathrm{Tr}_1\left[Q_m Q_n \left|B_{mn}, K\right\rangle_1 \left|0\right\rangle_2 \left\langle 0\right|_2 \left\langle B_{mn}, K\right|_1 \bar{Q}_n \bar{Q}_m\right] \\ &= \mathcal{N} \sum_{a,b,c,d} \sum_{k_i} f_{k_1 k_2 k_3 k_4, abcd} \left(b^\dagger_{k_1,m,a} b^\dagger_{k_2,n,b} \left|0\right\rangle \left\langle 0\right| b_{k_3,n,c} b_{k_4,m,d}\right). \end{aligned} \tag{4.79}$$

for a baryon B_{mn} with valence flavors m, n and total momentum K. All of the operators and indices are defined as they were in the previous section. f above for baryons is defined to be.

$$f_{k_1 k_2 k_3 k_4, abcd} = \left\langle B_{mn}, K\right| b^\dagger_{k_4,m,d} b^\dagger_{k_3,n,c} b_{k_2,n,a} b_{k_1,m,a} \left|B_{mn}, K\right\rangle \tag{4.80}$$

We can use the fact that the baryon states are color singlets to constrain the color structure of f, just as we did for mesons. In fact, since the fundamental and antifundamental representations of $SU(2)$ are the same, the representation breakdown of the operators also gives us two singlet configurations of the four-quark operator. The group theory of $SU(2)$

for combining two fundamental representations tells us that $2 \otimes 2 = 1 \oplus 3$, where the 1 on the right-hand side is the singlet and the $N_c^2 - 1$ is the triplet. Thus the bb and $b^\dagger b^\dagger$ operators pairs each form a singlet and a triplet, where the triplet is analogous to the adjoint representation in the meson case. The two singlets and triplets each form one overall color singlet. These two components of f are given by

$$\Pi^S_{abcd} = \frac{\delta_{ad}\delta_{bc} - \delta_{ac}\delta_{bd}}{2} \tag{4.81}$$

$$\Pi^T_{abcd} = \frac{\delta_{ad}\delta_{bc} + \delta_{ac}\delta_{bd}}{2} \tag{4.82}$$

$$f^{S,T}_{k_1k_2k_3k_4} = \Pi^{S,T}_{abcd} f_{k_1k_2k_3k_4,abcd}, \tag{4.83}$$

with an implicit sum over all color indices in the last equation. This means that f can be written as

$$f_{k_1k_2k_3k_4,abcd} = \Pi^S_{abcd} f^S_{k_1k_2k_3k_4} + \frac{1}{3}\Pi^T_{abcd} f^A_{k_1k_2k_3k_4}. \tag{4.84}$$

Once again, we see that the VS density matrix can be separated into an average of two density matrices

$$\rho_{B_{mn}} = \omega^S(\Pi^S \otimes \rho_S) + \frac{1}{3}\omega^T(\Pi^T \otimes \rho_T), \tag{4.85}$$

where $\rho_{S,T}$ are density matrices in momentum space, while ω^S and $\omega^T = 1 - \omega^S$ form a Bernoulli distribution, representing the chances of measuring the valence quarks to be in either a singlet or a triplet representation.

The multiplication of density matrices leads to a tensor product that is exactly the same as we found in the meson case. If we have two density matrices of the same form as that of the VS density matrix in Eq. ((4.79)), then $\rho_1.\rho_2$ becomes

$$(f_1.f_2)_{k_1k_2k_3k_4,abcd} = \sum_{A,B}\sum_{q_1,q_2}(f_1)_{k_1k_2q_2q_1,abBA}(f_2)_{q_1q_2k_3k_4,ABcd} \tag{4.86}$$

at the level of the tensors f_1, f_2. According to this definition of the product of tensors, the two color tensors Π^S and Π^T have the properties $\Pi^{S,T}.\Pi^{S,T} = \Pi^{S,T}$ and $\Pi^S.\Pi^T = 0$, which makes then projection operators for two distinct vector subspaces in color space. For the

remaining degrees of freedom in momentum space, we can define matrix multiplication and the trace for these distributions as

$$(A.B)_{k_1k_2k_3k_4} = \sum_{q_1,q_2} A_{k_1k_2q_2q_1} B_{q_1q_2k_3k_4} \tag{4.87}$$

$$\mathrm{Tr}[A] = \sum_{k_1,k_2} A_{k_1k_2k_2k_1}. \tag{4.88}$$

With this definition, the VS entanglement entropy for an $N_c = 2$ baryon can be written as

$$\begin{aligned} S_{B_{mn}} = \mathcal{N} \big(&-\mathrm{Tr}\left[f^S.\log f^S\right] - \mathrm{Tr}\left[f^T.\log f^T\right] \\ &+ \mathrm{Tr}\left[f^T\right]\log(3)\big) + \log(\mathcal{N}^{-1}) \end{aligned} \tag{4.89}$$

$$\mathcal{N}^{-1} = \mathrm{Tr}\left[f^S\right] + \mathrm{Tr}\left[f^T\right]. \tag{4.90}$$

This can also be cast in the more illustrative form

$$\omega^{S,T} = \mathcal{N}\ \mathrm{Tr}\left[f^{S,T}\right] \tag{4.91}$$

$$S_{S,T} = \frac{1}{\mathrm{Tr}\left[f^{S,T}\right]}\left(-\mathrm{Tr}\left[f^{S,T}.\log f^{S,T}\right]\right) + \log\left(\mathrm{Tr}\left[f^{S,T}\right]\right) \tag{4.92}$$

$$S_{B_{mn}} = \omega^S S_S + \omega^T S_T + \omega^T \log(3) - \omega^S \log\omega^S - \omega^T \log\omega^T. \tag{4.93}$$

This form, just as in the meson case, can be separated into three contributions, stemming from the fact that our density matrix can be decomposed into

$$\rho_{B_{mn}} = \omega^S(\Pi^S \otimes \rho_S) + \frac{1}{3}\omega^T(\Pi^T \otimes \rho_T) \tag{4.94}$$

with $\Pi_S.\Pi_T = 0$. The first contribution is the average of the entropies $S_{S,T}$ of $\rho_{S,T}$, corresponding to the momentum space degrees of freedom. The second part is the average of the entropies of the color space representations, with factors of $\log(1) = 0$ from the singlet and $\log(3)$ from the triplet. Finally, the last term is the entropy of the distribution formed by ω^S and ω^T. This decomposition of entropy contributions also holds for a continuous momentum variable.

The case of $SU(3)$ baryons becomes more complicated as there is a third valence quark which will combine to form more than two irreducible representations. We have for some

baryon B with flavors l, m, n and total momentum K

$$\begin{aligned}\rho_{B_{lmn}} &= \mathcal{N}\ \mathrm{Tr}_1\left[Q_l Q_m Q_n \left|B_{lmn}, K\right\rangle_1 \left|0\right\rangle_2 \left\langle 0\right|_2 \left\langle B_{lmn}, K\right|_1 \bar{Q}_n \bar{Q}_m \bar{Q}_l\right] \\ &= \mathcal{N} \sum_{a,b,c,d,e,f} \sum_{k_i} f_{k_1 k_2 k_3 k_4 k_5 k_6, abcdef} \left(b^\dagger_{k_1,l,a} b^\dagger_{k_2,m,b} b^\dagger_{k_3,n,c} \left|0\right\rangle \left\langle 0\right| b_{k_4,n,d} b_{k_5,m,e} b_{k_6,l,f}\right). \quad (4.95)\end{aligned}$$

Again, the operators and indices are defined as they have been previously. f above is defined to be.

$$f_{k_1 k_2 k_3 k_4 k_5 k_6, abcdef} = \left\langle B_{lmn}, K\right| b^\dagger_{k_6,l,f} b^\dagger_{k_5,m,e} b^\dagger_{k_4,n,d} b_{k_3,n,c} b_{k_2,m,b} b_{k_1,l,a} \left|B_{lmn}, K\right\rangle \quad (4.96)$$

Following the procedure we have outlined previously, the group theory of $SU(3)$ for combining three fundamental representations tells us that $3 \otimes 3 \otimes 3 = 1 \oplus 8 \oplus 8 \oplus 10$. Thus we find that the operator groupings bbb and $b^\dagger b^\dagger b^\dagger$ form four different irreps of $SU(3)$: one antisymmetric singlet, two different 8-dimensional adjoint representations of mixed symmetry, and a 10-dimensional fully symmetric representation. Either of the two adjoints from the bbb operator can form a color singlet with any of the two adjoints from the $b^\dagger b^\dagger b^\dagger$, giving us a total of four singlets that can be made from the mixed symmetry irreps. This gives us a total of six color singlets when the symmetric and antisymmetric irreps are included. The color tensors needed for these terms are given by

$$\mathcal{S}_{abcdef} = \frac{1}{6}(\delta_{af}(\delta_{be}\delta_{cd} + \delta_{bd}\delta_{ce}) + \delta_{ae}(\delta_{bf}\delta_{cd} + \delta_{bd}\delta_{cf}) + \delta_{ad}(\delta_{be}\delta_{cf} + \delta_{bf}\delta_{ce})) \quad (4.97)$$

$$\mathcal{A}_{abcdef} = \frac{1}{6}(\delta_{af}(\delta_{be}\delta_{cd} - \delta_{bd}\delta_{ce}) - \delta_{ae}(\delta_{bf}\delta_{cd} - \delta_{bd}\delta_{cf}) - \delta_{ad}(\delta_{be}\delta_{cf} - \delta_{bf}\delta_{ce})) \quad (4.98)$$

$$M_{++,abcdef} = \frac{1}{2}(\delta_{af}\delta_{be} + \delta_{ae}\delta_{bf})\delta_{cd} - \mathcal{S}_{abcdef} \quad (4.99)$$

$$M_{+-,abcdef} = \frac{1}{2\sqrt{3}}((\delta_{bf}\delta_{ce} - \delta_{be}\delta_{cf})\delta_{ad} + (\delta_{af}\delta_{ce} - \delta_{ae}\delta_{cf})\delta_{bd}) \quad (4.100)$$

$$M_{-+,abcdef} = \frac{1}{2\sqrt{3}}((\delta_{ae}\delta_{bd} - \delta_{ad}\delta_{be})\delta_{cf} + (\delta_{af}\delta_{bd} - \delta_{ad}\delta_{bf})\delta_{ce}) \quad (4.101)$$

$$M_{--,abcdef} = \frac{1}{2}(\delta_{af}\delta_{be} - \delta_{ae}\delta_{bf})\delta_{cd} - \mathcal{A}_{abcdef}. \quad (4.102)$$

These tensors are analogous to the Π color tensors form before. The $+$ and $-$ subscripts on the mixed symmetry tensors denote whether it is symmetric or antisymmetric in the first

two color indices (for the first subscript) or the last two indices (for the second subscript). The six components of f are then given by

$$f^A_{k_1k_2k_3k_4k_5k_6} = \mathcal{A}_{abcdef} f_{k_1k_2k_3k_4k_5k_6,abcdef} \tag{4.103}$$

$$f^S_{k_1k_2k_3k_4k_5k_6} = \mathcal{S}_{abcdef} f_{k_1k_2k_3k_4k_5k_6,abcdef} \tag{4.104}$$

$$f^{st}_{k_1k_2k_3k_4k_5k_6} = M_{st,abcdef} f_{k_1k_2k_3k_4k_5k_6,abcdef} \tag{4.105}$$

for all $s, t = \pm$ and with implicit sums over the color indices. f can then be written as

$$f_{k_1k_2k_3k_4k_5k_6,abcdef} = \mathcal{A}_{abcdef} f^A_{k_1k_2k_3k_4k_5k_6} + \frac{1}{8}\sum_{s,t=\pm} M_{st,abcdef} f^{st}_{k_1k_2k_3k_4k_5k_6} + \frac{1}{10}\mathcal{S}_{abcdef} f^S_{k_1k_2k_3k_4k_5k_6}. \tag{4.106}$$

Unlike in previous cases, these six tensors will not split the entanglement entropy into six disconnected contributions. To see this, we can look at how these color tensors stitch together when the density matrix is multiplied to itself, which we need to know in order to apply the replica trick to derive the entanglement entropy. Matrix multiplication of baryon density matrices translates to a product of f's that is defined by

$$(f_1.f_2)_{k_1k_2k_3k_4k_5k_6,abcdef} = \sum_{A,B,C}\sum_{q_1,q_2,q_3} (f_1)_{k_1k_2k_3q_3q_2q_1,abcCBA}(f_2)_{q_1q_2q_3k_4k_5k_6,ABCdef}. \tag{4.107}$$

The relevant nonzero products of color tensors for density matrix multiplication are

$$\mathcal{A}_{abcCBA}\mathcal{A}_{ABCdef} = \mathcal{A}_{abcdef} \tag{4.108}$$

$$\mathcal{S}_{abcCBA}\mathcal{S}_{ABCdef} = \mathcal{S}_{abcdef} \tag{4.109}$$

$$M_{st,abcCBA}M_{tu,ABCdef} = M_{su,abcdef}. \tag{4.110}$$

for all $s, t, u = \pm$. These tensors split the density matrix into three contributions corresponding to the 3 irreducible representations of S_3. The density matrix thus splits into three parts given by

$$\rho_{B_{lmn}} = \omega^{\mathcal{A}}(\mathcal{A} \otimes \rho_{\mathcal{A}}) + \frac{1}{8}\omega^{M}(M \otimes \rho_M) + \frac{1}{10}\omega^{\mathcal{S}}(\mathcal{S} \otimes \rho_{\mathcal{S}}). \tag{4.111}$$

Note also the four mixed symmetry tensors $M_{st,abcdef}$ combine in a way that resembles matrix multiplication of a 2×2 matrix. Thus for the fully symmetric and antisymmetric contributions we can define matrix multiplication and the trace in momentum space much like

before, where

$$(A.B)_{k_1k_2k_3k_4k_5k_6} = \sum_{q_1,q_2} A_{k_1k_2k_3q_3q_2q_1} B_{q_1q_2q_3k_4k_3k_4} \tag{4.112}$$

$$\mathrm{Tr}[A] = \sum_{k_1,k_2,k_3} A_{k_1k_2k_3k_3k_2k_1}. \tag{4.113}$$

However, for the mixed symmetry contributions there is an extra step where they must be organized into a 2×2 matrix matrix such that

$$f^M_{k_1k_2k_3k_4k_5k_6} = \begin{pmatrix} f^{--}_{k_1k_2k_3k_4k_5k_6} & f^{-+}_{k_1k_2k_3k_4k_5k_6} \\ f^{+-}_{k_1k_2k_3k_4k_5k_6} & f^{++}_{k_1k_2k_3k_4k_5k_6} \end{pmatrix}, \tag{4.114}$$

and from here matrix multiplication and tracing is defined by both uniting the momentum indices as in the previous equation along with the standard multiplication and trace of the 2×2 array shown here. With these definitions, the VS entanglement entropy for an $N_c = 3$ baryon can be written as

$$\begin{aligned} S_{B_{lmn}} = \mathcal{N} \big(&-\mathrm{Tr}\left[f^{\mathcal{A}}.\log f^{\mathcal{A}}\right] - \mathrm{Tr}\left[f^{M}.\log f^{M}\right] - \mathrm{Tr}\left[f^{\mathcal{S}}.\log f^{\mathcal{S}}\right] \\ &+ \mathrm{Tr}\left[f^{M}\right]\log(8) + \mathrm{Tr}\left[f^{\mathcal{S}}\right]\log(10)\big) + \log(\mathcal{N}^{-1}) \end{aligned} \tag{4.115}$$

$$\mathcal{N}^{-1} = \mathrm{Tr}\left[f^{\mathcal{A}}\right] + \mathrm{Tr}\left[f^{M}\right] + \mathrm{Tr}\left[f^{\mathcal{S}}\right]. \tag{4.116}$$

This can also be cast in the more illustrative form

$$\omega^{\mathcal{A},M,\mathcal{S}} = \mathcal{N}\ \mathrm{Tr}\left[f^{\mathcal{A},M,\mathcal{S}}\right] \tag{4.117}$$

$$S_{\mathcal{A},M,\mathcal{S}} = \frac{1}{\mathrm{Tr}\left[f^{\mathcal{A},M,\mathcal{S}}\right]}\left(-\mathrm{Tr}\left[f^{\mathcal{A},M,\mathcal{S}}.\log f^{\mathcal{A},M,\mathcal{S}}\right]\right) + \log\left(\mathrm{Tr}\left[f^{\mathcal{A},M,\mathcal{S}}\right]\right) \tag{4.118}$$

$$S_{B_{lmn}} = \omega^{\mathcal{A}} S_{\mathcal{A}} + \omega^{M} S_{M} + \omega^{\mathcal{S}} S_{\mathcal{S}} + \omega^{M}\log(8) + \omega^{\mathcal{S}}\log(10) - \omega^{\mathcal{A}}\log\omega^{\mathcal{A}} - \omega^{M}\log\omega^{M} - \omega^{\mathcal{S}}\log\omega^{\mathcal{S}}. \tag{4.119}$$

Once again, we see that the VS entanglement entropy splits into averages over momentum space entropies, color space entropies, and the entropy of the ω distribution, which also holds in the continuum.

4.6 Data & Results

In this work we calculate the valence-sea entanglement of an assortment of hadrons given a variety of parameters such as total momentum, number of colors, and the coupling constant. To do this, we begin by constructing the discrete light-cone quantized Hamiltonian for $1+1$d QCD and finding the eigenstates with the lowest energies. Then we form the appropriate f tensors described in the previous section by applying the eigenstates we obtained to a set of state-independent four- or six-quark operators. Finally, we arrange the f tensors into matrices in momentum space, diagonalize them, and calculate $\mathrm{Tr}[f]$ and $-\mathrm{Tr}[f.\log f]$ for each color singlet. For the figures in this section, we plot the entropy against either number of colors, total hadron momentum, or the coupling strength. The quark masses are degenerate unless otherwise specified. For the coupling strength, since the Hamiltonian separates like $2P^+H = m^2\mathcal{O}_{kin} + g^2\mathcal{O}_{pot}$ and both m and g have units of mass, the eigenstates only depend upon the ratio g/m. It is more convenient to define the variables $\xi^2 = \frac{g^2 N_c}{2\pi}$ and $\lambda = \frac{\xi^2}{m^2+\xi^2}$. We use ξ^2 because it remains constant in the large-N_c limit and it removes a recurring factor of $1/2\pi$ in the calculations. The variable λ is preferable as it ranges from 0 to 1, where $\lambda = 0$ corresponds to a theory of free quarks while $\lambda = 1$ gives us massless QCD, making it more amenable to plotting than g/m which ranges from 0 to ∞.

The following results show some general patterns in the VS entanglement entropy of low energy states that seem to hold for mesons and baryons simultaneously. First, we see that in Figs. 4.4, 4.6, and 4.9 these lower lying energy states tend to a specific value even at fairly modest values of the total momentum. This convergence becomes weaker as we increase the relative strength of the potential λ. In the plots against the relative coupling strength in Figs. 4.5, 4.6, and 4.10, we see that the ground state hadron always has low entropy, while the next few states steadily increase with λ, with some of them seeming to plateau near a particular middling value of S. The low entropy of the ground state is due to the state being dominated by the minimum particle state that has no quark sea at all, which persists even for very small quark masses [190]. This is true to a lesser extent for the first few excited

states, though they seem to have much larger contributions from Fock states with sea quarks as λ increases. If the contributions get too large, there will be a level crossing with a multi-hadron state at some specific value of λ, which causes the behavior of S as a function of λ to suddenly change. This level crossing behavior is what causes the plateauing effect in our plots. These level crossings also make it difficult for comparisons to large-N_c hadrons to be made, since that requires a clean method for distinguishing single and multi-hadron states from each other.

4.6.1 Meson Results

This section has plots of the VS entropy of the π^+ meson analog against number of colors in Fig. 4.3, total momentum in Fig. 4.4, and the relative coupling strength in Fig. 4.5. The results for the π^0 analog are similar, as are the results when a third degenerate quark flavor is added. In Fig. 4.3, the first three states look like they may eventually taper off to zero at large N_c, but the other two are increasing with N_c. This is because large-N_c states with multiple mesons can have nonzero VS entropy due to entanglement. In fact, using the expression for the entropy in terms of f_S and f_A above, we can see that there is a term proportional to $\mathrm{Tr}\left[f^A\right]\log(N_c^2-1)$. The Fermi degeneracy creates entanglement between the mesons that feeds into f_A, so the VS entropy for multi-meson states at large N_c will actually tend to infinity. However, f_S remains zero for all large N_c states, and seems to decrease asymptotically as N_c increases for all 5 states.

In general, the meson spectra seem to fall into two regimes depending on the size of g/m. If g/m is small (roughly less than 2), then the theory is in the large mass regime which contains both the free theory and the 't Hooft model. This regime is characterized by single meson states that are dominated by two-particle Fock states in momentum space. This makes it easy to distinguish the single meson states from the multiple meson states in DLCQ. When g/m is large, the theory is in the strong potential regime which contains the Schwinger model when we have a $U(1)$ gauge field. In this regime, the meson states are localized in position space and tend to have local color currents that are small. In addition,

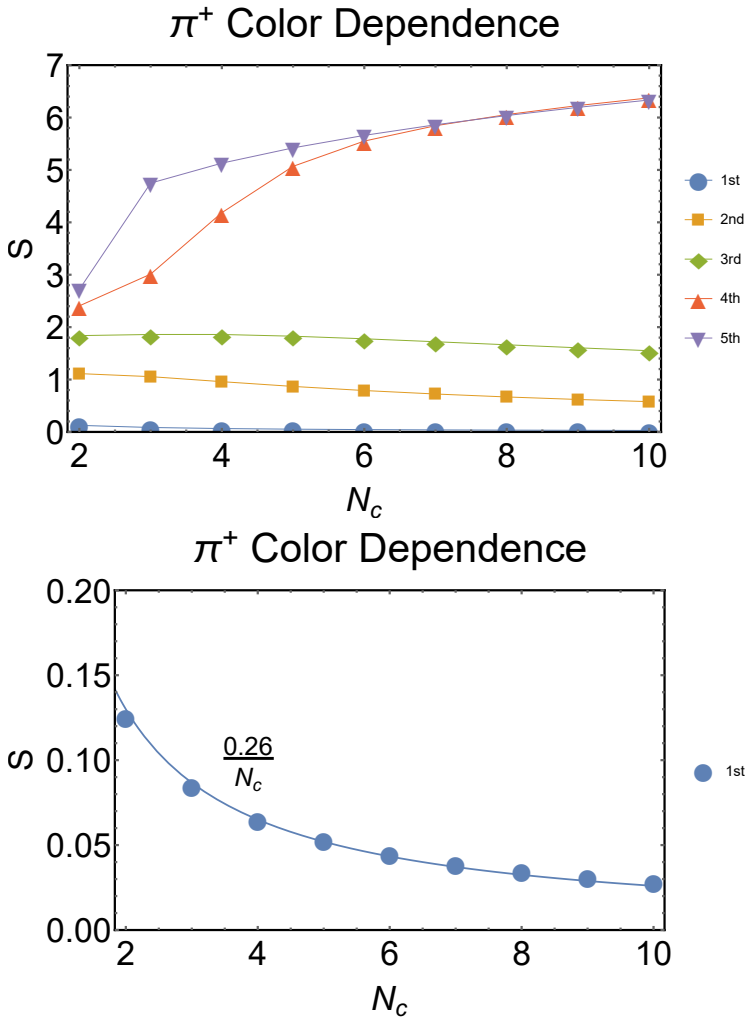

Figure 4.3: Entanglement entropy for the 5 lowest energy π^+ states with $N_f = 2$ that have $K_{tot} = 8$ units of momentum, with $m^2 = \frac{g^2 N_c}{2\pi}$ and $g^2 \sim \frac{1}{N_c}$. The lines connecting data points in the first plot are merely for visual effect and do not communicate additional data. The second plot shows the entanglement entropy of the ground state meson with a $1/N_c$ fit. The theoretical maximum entropy is $S_{max} = 2\ \mathrm{Log}_2(6N_c)$.

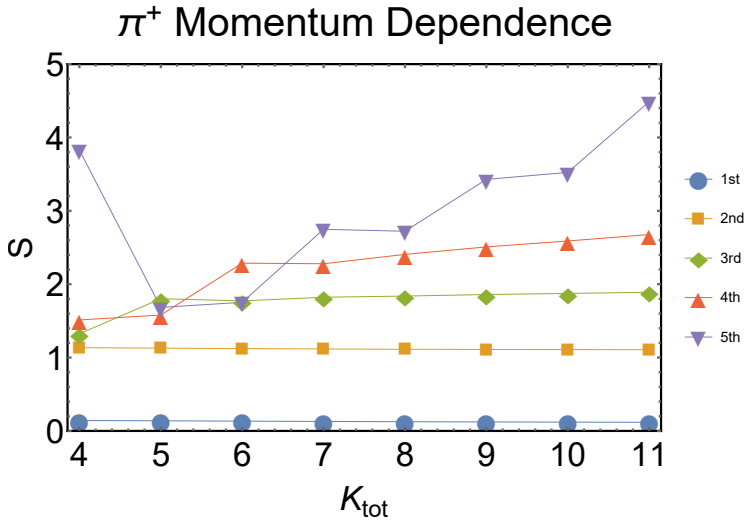

Figure 4.4: Entanglement entropy for the 5 lowest energy π^+ states with $N_f = 2$, $N_c = 2$, and $m^2 = \frac{g^2}{\pi}$. The theoretical maximum entropy is $S_{max} = \text{Log}_2(2K_{tot}(K_{tot}+1))$. The lines connecting these data are merely for visual effect and do not communicate additional data.

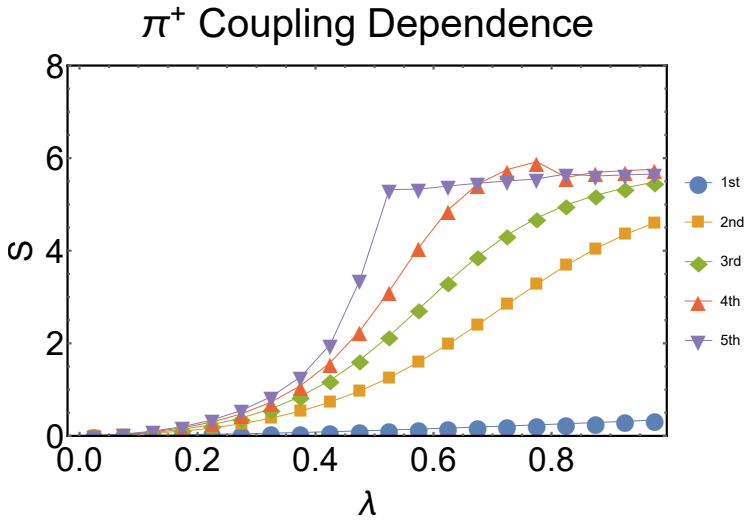

Figure 4.5: Entanglement entropy for the 5 lowest energy π^+ states with $N_f = 2$, $N_c = 2$, $K_{tot} = 11$, and $\lambda = \frac{g^2}{\pi m^2 + g^2}$. The theoretical maximum entropy is $S_{max} = \text{Log}_2(2 * 11 * 12) \approx 8.04$. The lines connecting these data points are merely for visual effect and do not communicate additional data.

the presence of massless fermions leads to zero modes in the spectrum, meaning the quark-antiquark pairs can be generated fairly easily, so particle number in momentum space cannot be used to identify bound states in this regime. The transition between these two regimes can be seen in the plots of the VS entropy against coupling λ where the excited state entropies seem to stop increasing beyond certain large values of λ.

The ground state mesons have a particularly low VS entropy compared to all other states. This is because it bears a close resemblance to its large-N_c counterpart, and this resemblance fades for higher excited states. The large-N_c connection is also what causes the Fock states with no sea contribution to dominate the Fock state expansion of the ground state. The resemblance to the large-N_c counterpart also suggests that its VS entropy could be captured by a $1/N_c$ expansion, and indeed we see in Fig. 4.4 that it has a good fit to a $1/N_c$ curve. The value of 0.26 for the fit was chosen because it minimizes the sum of the squares of the differences between the data points and the fit curve. If this perturbative behavior persists into $3+1$ dimensions, this could open the door for a perturbative calculation of VS entropy for ground state hadrons in real QCD.

4.6.2 Baryon Results

The first figure in this section, Fig. 4.6, has plots of the VS entropy of the 2-color N^0 baryon analog against total momentum and the relative coupling strength. A surprising result is that these plots are identical to Figures 4.4 and 4.5 for the pion. It turns out that when $N_c = 2$, the Hamiltonians for the baryon and meson channels where the valence particles have different flavors are not only of identical size, but have an identical eigenvalue spectrum. In other words, these Hamiltonians differ only by a unitary transformation, one that the VS entropy is apparently insensitive to. In the case that the flavors of the two particles are the same (as in Figures 4.7 and 4.8), the meson Hamiltonian is over twice as large as the baryon Hamiltonian, but there is a subsection of the meson's mass spectrum that matches the full spectrum of the baryon. A comparison of states with matching eigenvalues is given in Fig. 4.8.

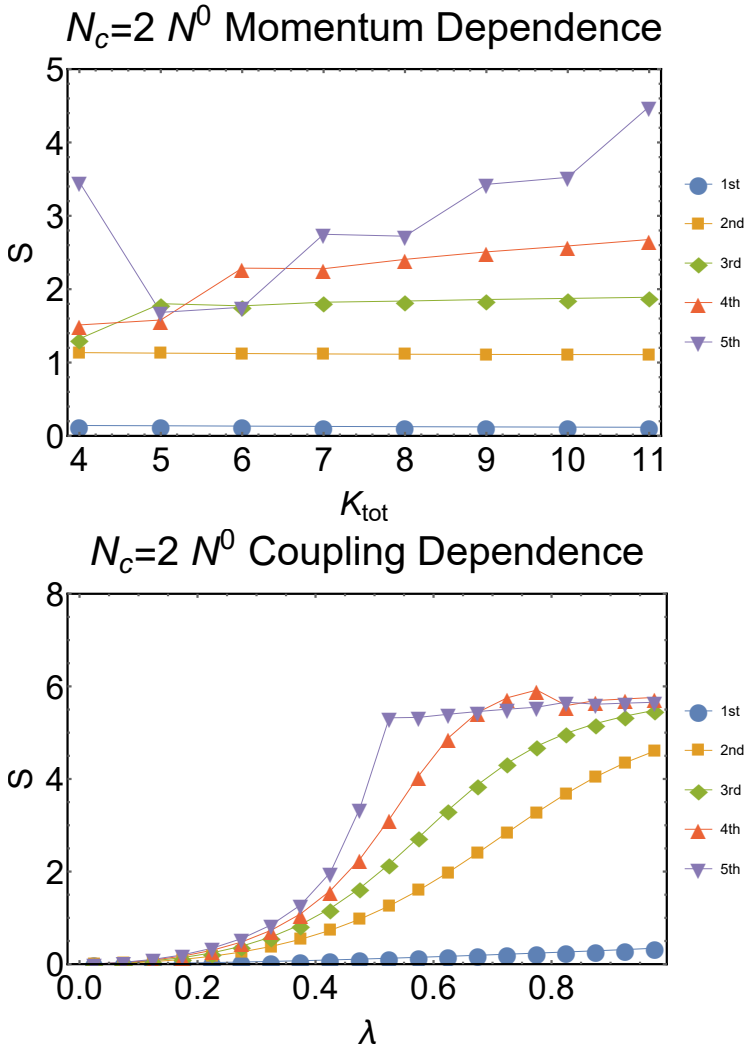

Figure 4.6: Entanglement entropy for the 5 lowest energy 2-color baryon states with $N_f = 2$ where the constituent quarks have different flavors, somewhat analogous to the neutron N^0. In the first plot, $m^2 = \frac{g^2}{\pi}$. In the second plot, $K_{tot} = 11$ and $\lambda = \frac{g^2}{\pi m^2 + g^2}$. Note the extreme similarity to the results for the π^+ above. The lines connecting these data points are merely for visual effect and do not communicate additional data.

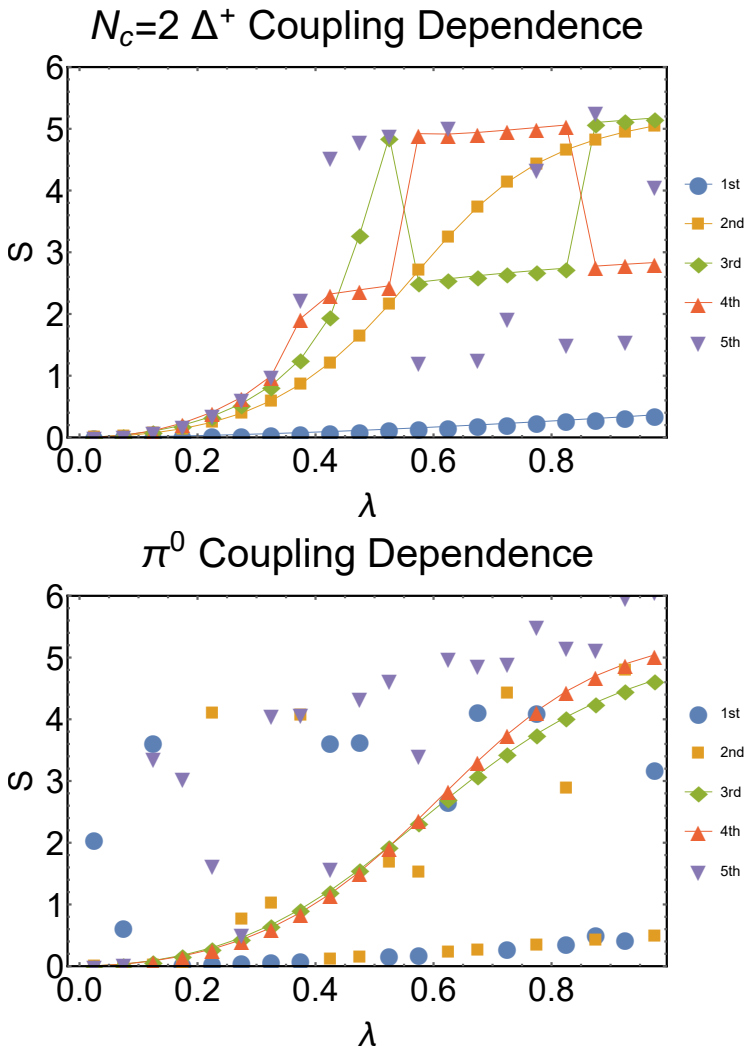

Figure 4.7: The first plot shows the entanglement entropy for the 5 lowest energy 2-color baryon states where the constituent quarks have the same flavor, somewhat analogous to the delta Δ^+. The second plot shows the entanglement entropy for the 5 lowest energy π^0 states. In both plots, $N_f = N_c = 2$, $K_{tot} = 11$, and $\lambda = \frac{g^2}{\pi m^2 + g^2}$. The theoretical maximum entropy for the Δ^+ is $S_{max} \approx 6.98$, while for π^0 it is $S_{max} \approx 8.04$. The lines connecting these data points are merely for visual effect and do not communicate additional data.

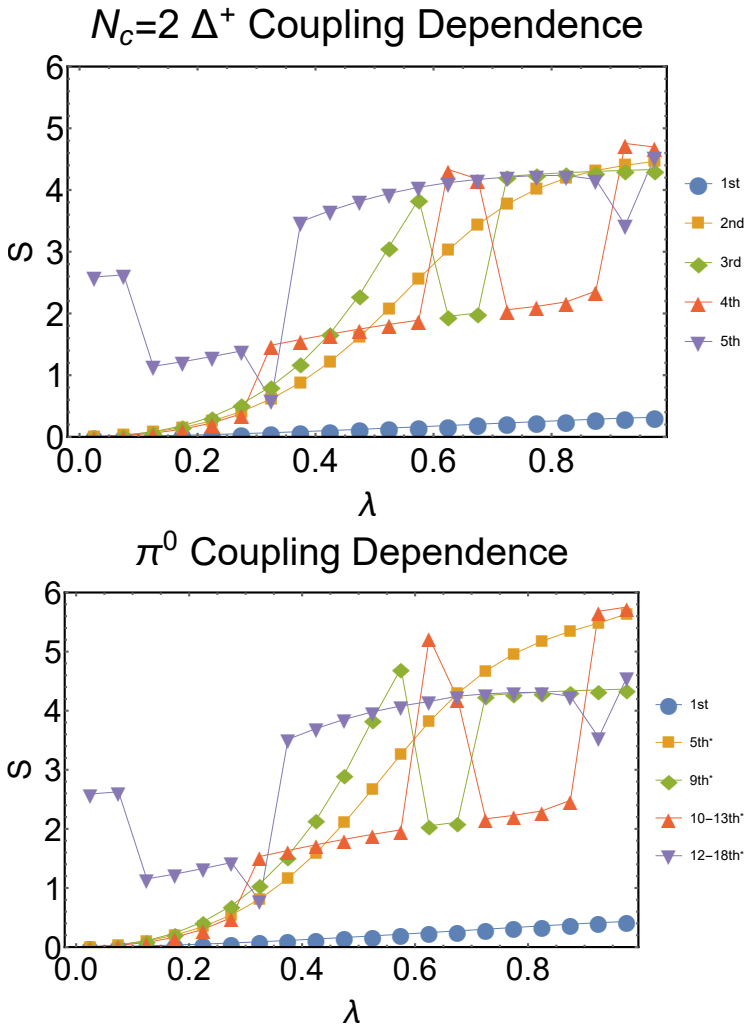

Figure 4.8: In these plots, there is a small difference in the quark masses given by $m_2^2 - m_1^2 = 0.01(\bar{m}^2 + g^2/\pi)$, where $\bar{m}^2 = (m_1^2 + m_2^2)/2$. The first plot shows the entanglement entropy for the 5 lowest energy 2-color Δ^+-analogue states. The second plot shows the entanglement entropy for the 5 π^0 states whose eigenvalues match those of the Δ^+ shown above. The asterisk indicates states whose relative ordering in the full eigenvalue spectrum changes depending on the coupling; the number or range of numbers listed indicates the usual position of the state over most of the given values of λ. In both plots, $N_f = N_c = 2$, $K_{tot} = 8$, and $\lambda = \frac{g^2}{\pi\bar{m}^2+g^2}$. The theoretical maximum entropy for the Δ^+ is $S_{max} \approx 6.09$, while for π^0 it is $S_{max} \approx 7.17$. The lines connecting these data points are merely for visual effect and do not communicate additional data.

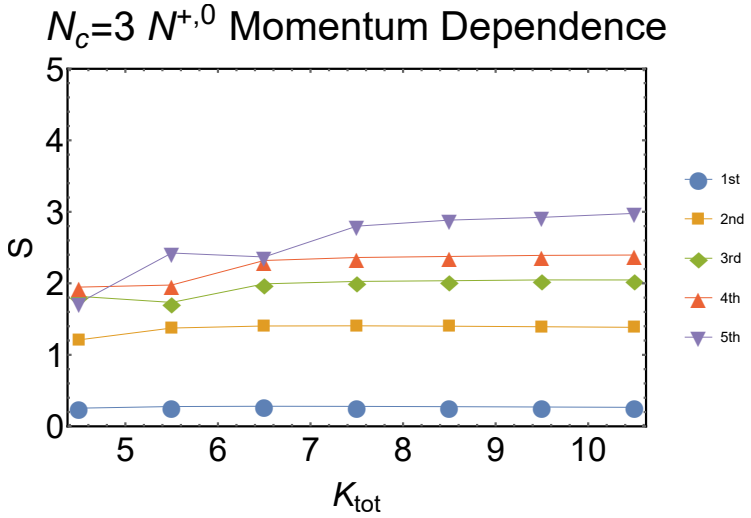

Figure 4.9: Entanglement entropy for the 5 lowest energy 3-color baryon states with $N_f = 2$ where one constituent quark has a different flavor from the other two, analogous to the nucleon $N^{+,0}$ in QCD. The quark masses are degenerate, and $m^2 = \frac{3g^2}{2\pi}$. The lines connecting these data points are merely for visual effect and do not communicate additional data.

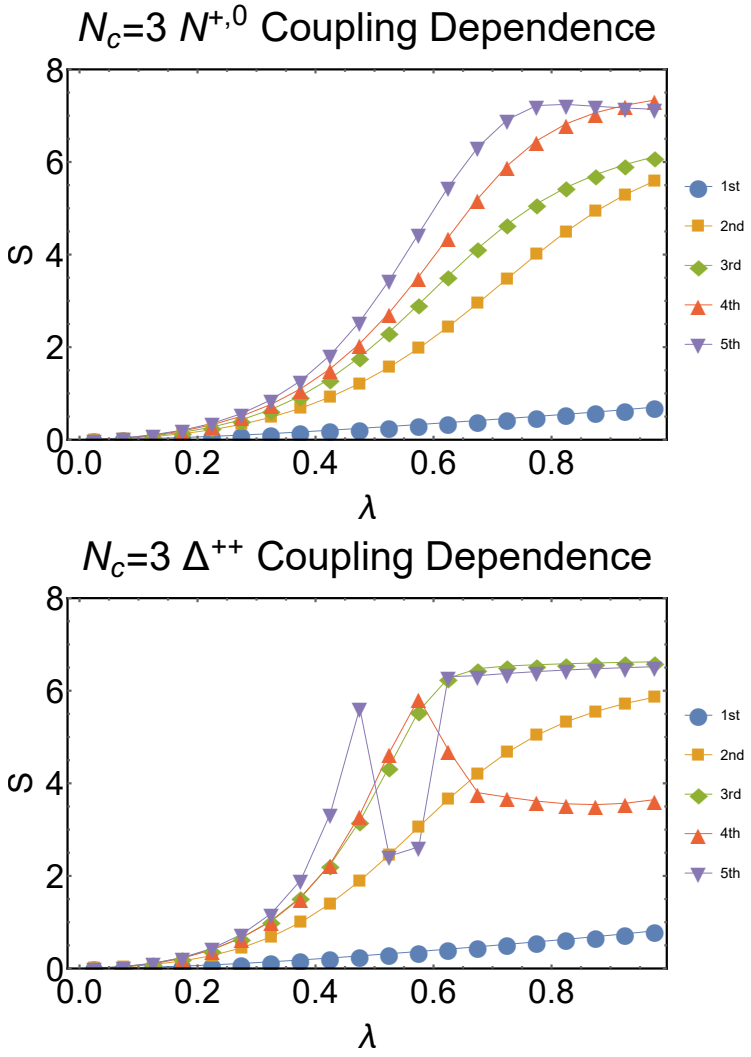

Figure 4.10: These plots show the entanglement entropy for the 5 lowest energy 3-color baryon states where $N_f = 2$, $N_c = 3$, $K_{tot} = \frac{21}{2}$, the quark masses are degenerate, and $\lambda = \frac{3g^2}{2\pi m^2 + 3g^2}$. The first plot shows the entanglement entropy for states where one constituent quark has a different flavor from the other two, analogous to the nucleon $N^{+,0}$ in QCD. The second plot shows states where the constituent quarks all have the same flavor, analogous to the delta Δ^{++} in QCD. The theoretical maximum entropy for the Δ^{++} is $S_{max} \approx 9.75$, while for $N^{+,0}$ it is $S_{max} \approx 11.47$. The lines connecting these data points are merely for visual effect and do not communicate additional data.

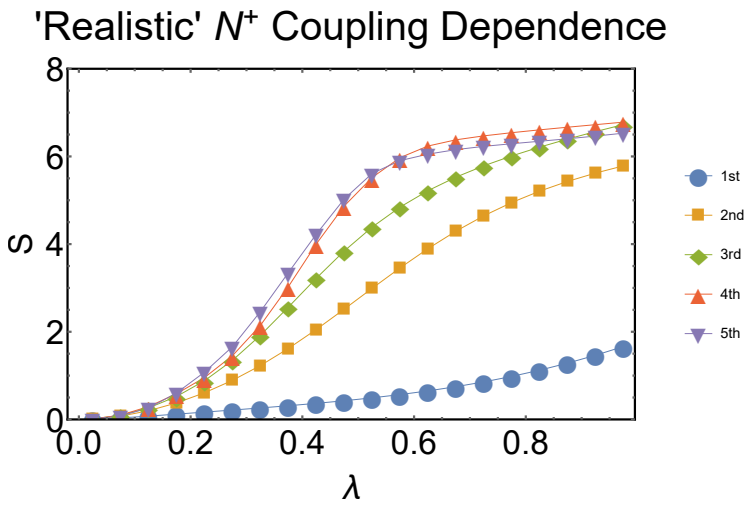

Figure 4.11: This plot shows the entanglement entropy for the 5 lowest energy 3-color baryon states analogous to the proton N^+ in QCD, where $N_f = 3$, $N_c = 3$, and $K_{tot} = \frac{17}{2}$. It is "realistic" in the sense that the quark masses are defined using approximately physical values relative to the average of the squares of the valence quark masses $\bar{m}^2 = \frac{2m_u^2+m_d^2}{3}$. The values used for the masses are $\frac{m_u^2}{\bar{m}^2} = 0.45$, $\frac{m_d^2}{\bar{m}^2} = 2.1$, $\frac{m_s^2}{\bar{m}^2} = 834$, and $\lambda = \frac{3g^2}{2\pi\bar{m}^2+3g^2}$. The theoretical maximum entropy is $S_{max} \approx 10.58$. The lines connecting these data points are merely for visual effect and do not communicate additional data.

Fig. 4.9 shows a plot of the VS entropy of the nucleon analog against total momentum, while Fig. 4.10 shows coupling dependence of both the nucleon analog and the Δ^{++} analog. The results for other baryons are similar, as are the results when a third degenerate quark flavor is added. Fig. 4.11 shows the coupling dependence of the nucleon analog for realistic quark masses. Removing the heavy strange quarks from the system barely affects the VS entropy. All of these 3-color baryon entropy plots exhibit similar qualitative features to those of the mesons and 2-color baryons, such as the very low VS entropy of the ground state, the dominance of the singlet contribution f_S for these low lying energy states, and the separation of theories into two broad regimes of large mass and strong coupling. These similarities persist despite these being fermions with 3 valence quarks instead of bosons with only two, and there is no symmetry that can relate them to the mesonic states like with the 2-color case. There is also an additional $SU(N_c)$ singlet contribution with these baryons corresponding to the mixed symmetry irrep of S_3, but this addition doesn't seem to greatly affect the general patterns of the VS entropy of low energy states. This suggests that these states also maintain features of their large-N_c counterparts, despite the large-N_c baryon wavefunction being largely inaccessible without making a sweeping assumption about its general form. Since the connection to large-N_c physics seems to hold in $3+1$ dimensions for $N_c = 3$, it may even be possible to calculate the VS entropy of real nucleons using a large-N_c expansion, assuming that the approximate $1/N_c$ behavior of the meson ground state entropy also holds for baryons.

4.7 Conclusion

In this chapter, we've defined a notion of valence-sea entanglement in QCD, despite the lack of a clear distinction between valence quarks and sea quarks, and analyzed the VS entanglement entropy in 1+1d QCD. The framework used to define VS entanglement can potentially be used to define other types of entanglement in situations when a clear bipartition of the Hilbert space does not exist. It would most likely be useful for defining entanglement between constituent fields in the bound states of other QFTs, but there could in principle

be more clever applications of the method. This also naturally leads to a definition of single quark (or antiquark) entanglement in a hadron using the same framework, in which the elements of the corresponding density matrix turn out to be parton distribution functions. This provides an interpretation of PDFs as measures of quark entanglement, which may highlight some connection between quark entanglement and the operator product expansion of the DIS cross section.

To get the VS entanglement, we also described much of the framework needed to do the calculation of the entanglement entropy in 1+1d QCD. We've gone over the terms in the Hamiltonian formalism of 1+1d light front QCD, recovered the spectrum of the 't Hooft model by taking the large-N_c limit in said formalism, and applied discrete light-cone quantization to render the Hamiltonian as a finite matrix. The expression for the VS entanglement in these hadrons was found to separate into different contributions coming from the different $SU(N_c)$ irreps of the valence quarks, as well as separating additively into momentum space and color space terms. Appendix A also details a method for deriving DLCQ operators in a basis of color singlet states that is manifestly orthonormal and complete from the beginning. To our knowledge, this has not been done in the literature as of yet, since the papers that have done explicit QCD calculations in 1+1 dimensions mention rendering the Hamiltonian in an incomplete basis as an intermediate step [191, 192, 199].

Our numerical results show that the VS entanglement is unusually low for low energy eigenstates of the QCD Hamiltonian. For mesons, this results from the fact that these states at finite N_c have almost no sea quarks and closely resemble the corresponding eigenstates in the large-N_c limit. For baryons, the connection to large-N_c cannot be made easily, but the states seem to have next to no sea quarks as well. If we treat VS entanglement as a measure of the applicability of the parton model as discussed in the introduction, then this would imply that the parton model is only applicable to the lowest mass hadrons in 1+1d QCD. This is of course consistent with our observations in real QCD, but it remains to be seen if the model breaks down for highly excited hadrons. The low values of the VS entropy also suggest that the large-N_c expansion may fail for higher excited states, perhaps

even suggesting a connection between the applicability of the parton model and the large-N_c expansion. This may not be the case in real QCD, as several papers have shown that large-N_c results in 3+1 dimensions generally agree with experiment for $N_c = 3$ [200–202].

We also found for mesons in their ground states that the VS entanglement entropy approximately follows a $1/N_c$ curve, indicating that the entropy for these specific states can be calculated perturbatively in a next to leading order $1/N_c$ expansion. Given that the ground state baryons also have very low VS entropy, it may also be perturbative in the same way. Given that the large-N_c expansion works surprisingly well in real QCD for ground state hadrons, it may be reasonable to expect the VS entropy in real QCD to be calculable in a $1/N_c$ expansion as well. The elements of the VS density matrix resemble parton distribution functions, which are scale dependent in real QCD, so the corresponding VS entanglement entropy ought to as well. Also, it would likely be small at both large scales where the coupling is weak and small scales where the hadrons resemble large-N_c states, but this may not hold true in between. Having access to this quantity could therefore lead to some very interesting insights into the transition between quark and hadron degrees of freedom, as it would likely be scale dependent and function as an order parameter for this transition. However, the presence of extra spin degree of freedom and transverse gauge fields compared to 1+1d QCD makes it difficult to make solid claims about what VS entanglement would look like in reality.

Chapter 5

CONCLUSION

In Chapter 2 and in [18], we designed a simple model for helicity entanglement in nucleons involving only two chiral basis states. It was found that this entropy quickly shot up to near its maximum value when fit to data even with only two states. This suggests that entanglement between the valence and non-valence helicity components of the nucleon state vector drives chiral symmetry breaking in the nucleon. The entanglement entropy therefore acts as an order parameter of chiral symmetry breaking in the nucleon, and provides an explanation for why the valence spin content of the nucleon is not expected to dominate. This work provides a qualitative picture for how entanglement between valence and sea partons behaves in QCD, which is further developed what follows.

In Chapter 3, The model for helicity entanglement in nucleons was extended to include many chiral basis states, based solely in the symmetries of QCD and general physical principles. In these models, the null-plane formalism was used to separate the dynamical, spin-based generators of Poincaré symmetry from the kinematical, momentum-based generators. It was argued that it may be sensible to represent a nucleon and its first few excitations through a handful of chiral basis states defined by the helicity and isospin representations of the valence quarks. Fitting experimental data for static nuclear properties such as the axial coupling g_A to their results in the chiral basis, one could find a change of basis matrix between nuclear and chiral states, and from there the entanglement entropy between the different valence representations could be calculated for the nucleon. It was found that this entropy quickly shot up to near its maximum value as before in all models analyzed. The results show that chiral symmetry breaking in the null plane formalism originates from the hadronic wavefunction, and that the gluon sea is essential in determining the ground

state null-plane wavefunctions of the nucleon and its chiral partners. It was also found that the large-N_c limit corresponds to vanishing entanglement entropy, suggesting a connection between the large-N_c expansion for baryons and the presence of entanglement entropy.

In chapter 4, we defined a notion of valence-sea entanglement in QCD, despite the lack of a clear distinction between valence quarks and sea quarks, and analyzed the VS entanglement entropy in 1+1d QCD. This naturally leads to a definition of single quark entanglement in a hadron in which the elements of the corresponding density matrix turn out to be parton distribution functions, providing an interpretation of PDFs as measures of single-quark entanglement. The expression for the VS entanglement in these hadrons was found to separate into different contributions coming from the different $SU(N_c)$ irreps of the valence quarks, as well as separating additively into momentum space and color space terms. Appendix A also details a method for deriving DLCQ operators in a basis of color singlet states that is manifestly orthonormal and complete from the beginning.

Our numerical results from this chapter show that the VS entanglement is unusually low for low energy eigenstates of the QCD Hamiltonian. For mesons, this results from the fact that these states at finite N_c have almost no sea quarks and closely resemble the corresponding eigenstates in the large-N_c limit. For baryons, the connection to large-N_c cannot be made easily, but the states seem to have next to no sea quarks as well. We also found for mesons in their ground states that the VS entanglement entropy approximately follows a $1/N_c$ curve, indicating that the entropy for these specific states can be calculated perturbatively in a next to leading order $1/N_c$ expansion. Given that the large-N_c expansion works surprisingly well in real QCD for ground state hadrons, it may be reasonable to expect the VS entropy in real QCD to be calculable in a $1/N_c$ expansion as well. The VS entropy in real QCD would likely be scale dependent and function as an order parameter for this transition, as it does for chiral symmetry breaking in the chiral basis models from Chapter 3.

While it may seem like the results from chapters 2 and 3 contradict the claim in chapter 4 that the VS entropy of real hadrons will be small, this is not the case as the models of

entanglement between the valence and sea quarks in each chapter are probing very different aspects of real QCD. In chapters 2 and 3, the models devised for the baryon state vectors are sensitive to chiral symmetry breaking and are constrained entirely by static nuclear properties. The only information about the interior dynamics of the bound quarks comes implicitly through the experimental data for the masses and charges used as input, which only provides information about the average entanglement over multiple energy scales. In chapter 4, we focused on QCD in $1+1$ dimensions, which does not have chiral symmetry breaking, but was found to be simple enough to be investigated numerically at the quark level. Since $1+1$d QCD is always in the confining phase, our results for this theory apply only to real QCD at low energy scales where confinement occurs.

This gives us a picture for how VS entanglement in real QCD may behave, sketched out in Fig. 5.1. Due to asymptotic freedom, the quark interactions are weak at very high energy scales, so we can expect low VS entanglement at scales well beyond Λ_{QCD}. From our work in chapter 4, we can also expect that VS entanglement is low for ground state hadrons at scales below Λ_{QCD}. The question remains as to how entangled the quarks are near Λ_{QCD}, but the results of chapters 2 and 3 suggest that the average VS entropy is large. The only possible source for that entanglement must therefore be at scales near Λ_{QCD}, which also tracks with chiral symmetry breaking being the source of entanglement in those models. Thus we expect that the VS entropy in real QCD should act as an order parameter for the transition between quark and hadron degrees of freedom, as it should remain low except near the scale at which hadrons begin to form and chiral symmetry is spontaneously broken.

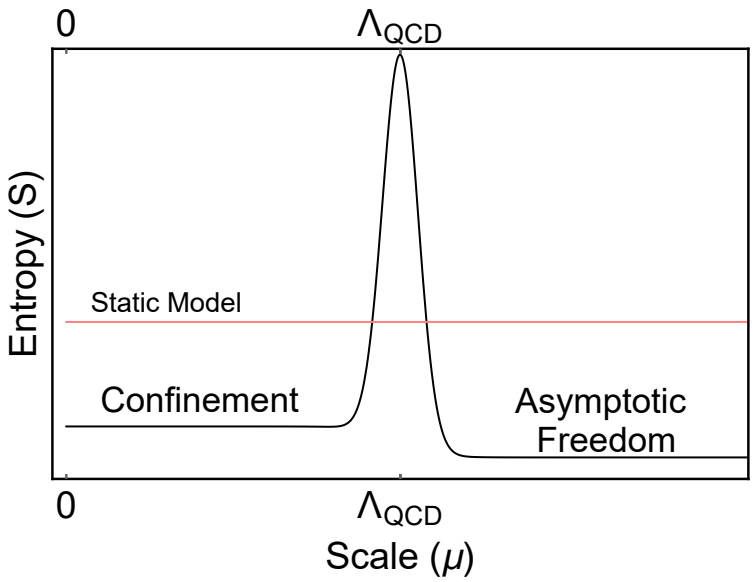

Figure 5.1: This shows a sketch of what the VS entropy of a ground state hadron in real QCD is expected to look like. The red line labeled "Static Model" shows what results a model built from only static properties would give, such as those of Chapters 2 and 3. At high energy scales where the quarks are asymptotically free, the entropy should be close to zero. Our results suggest that it will also be low in the confining phase as well. This implies that the region near Λ_{QCD} must have high entropy, or else the static model entropy would be much lower.

BIBLIOGRAPHY

[1]H. Yukawa, Proc. Phys. Math. Soc. Jap. **17**, 48–57 (1935).

[2]A. Deur, S. J. Brodsky, and G. F. De Téramond, Rept. Prog. Phys. **82**, 10.1088/1361-6633/ab0b8f (2019), arXiv:1807.05250 [hep-ph].

[3]M. Srednicki, *Quantum field theory* (Cambridge University Press, Jan. 2007).

[4]D. J. Gross and F. Wilczek, Phys. Rev. Lett. **30**, edited by J. C. Taylor, 1343–1346 (1973).

[5]H. D. Politzer, Phys. Rev. Lett. **30**, edited by J. C. Taylor, 1346–1349 (1973).

[6]C. W. Bauer et al., (2022), arXiv:2204.03381 [quant-ph].

[7]J. Goldstone, A. Salam, and S. Weinberg, Phys. Rev. **127**, 965–970 (1962).

[8]Y. Nambu and G. Jona-Lasinio, Phys. Rev. **122**, edited by T. Eguchi, 345–358 (1961).

[9]M. Gell-Mann, R. J. Oakes, and B. Renner, Phys. Rev. **175**, 2195–2199 (1968).

[10]H. Leutwyler and J. Stern, Annals Phys. **112**, 94 (1978).

[11]G. 't Hooft, Nucl. Phys. B **72**, edited by J. C. Taylor, 461 (1974).

[12]G. 't Hooft, Nucl. Phys. B **75**, 461–470 (1974).

[13]E. Witten, Nucl. Phys. B **160**, 57–115 (1979).

[14]C. G. Callan Jr., N. Coote, and D. J. Gross, Phys. Rev. D **13**, 1649 (1976).

[15]E. Witten, Riv. Nuovo Cim. **43**, 187–227 (2020), arXiv:1805.11965 [hep-th].

[16]C. H. Bennett, G. Brassard, S. Popescu, B. Schumacher, J. A. Smolin, and W. K. Wootters, Phys. Rev. Lett. **76**, 722–725 (1996), arXiv:quant-ph/9511027.

[17]P. M. Hayden, M. Horodecki, and B. M. Terhal, Journal of Physics A: Mathematical and General **34**, 6891–6898 (2001), arXiv:quant-ph/0008134.

[18]S. R. Beane and P. Ehlers, Mod. Phys. Lett. A **35**, 2050048 (2019), arXiv:1905.03295 [hep-ph].

[19]A. Aprahamian et al., (2015).

[20]C. Alexandrou et al., Phys. Rev. Lett. **119**, 142002 (2017), arXiv:1706.02973 [hep-lat].

[21]H.-W. Lin et al., Phys. Rev. **D98**, 094512 (2018), arXiv:1806.10604 [hep-lat].

[22]J. Liang et al., Phys. Rev. **D98**, 074505 (2018), arXiv:1806.08366 [hep-ph].

[23]A. Kovner and M. Lublinsky, Phys. Rev. D **92**, 034016 (2015), arXiv:1506.05394 [hep-ph].

[24]D. E. Kharzeev and E. M. Levin, Phys. Rev. D **95**, 114008 (2017), arXiv:1702.03489 [hep-ph].

[25]E. A. Kuraev, L. N. Lipatov, and V. S. Fadin, Sov. Phys. JETP **45**, [Zh. Eksp. Teor. Fiz.72,377(1977)], 199–204 (1977).

[26]I. I. Balitsky and L. N. Lipatov, Sov. J. Nucl. Phys. **28**, [Yad. Fiz.28,1597(1978)], 822–829 (1978).

[27]P. A. Dirac, Rev.Mod.Phys. **21**, 392–399 (1949).

[28]J. B. Kogut and D. E. Soper, Phys. Rev. **D1**, 2901–2913 (1970).

[29]S. R. Beane, Annals Phys. **337**, 111–142 (2013), arXiv:1302.1600 [nucl-th].

[30]A. Belitsky and A. Radyushkin, Phys.Rept. **418**, 1–387 (2005), arXiv:hep-ph/0504030 [hep-ph].

[31]K. Hornbostel, in Workshop on "From Fundamental Fields to Nuclear Phenomena", Boulder, Colorado, September 20-22 (1990), pp. 2–17.

[32]S. J. Brodsky and G. F. de Teramond, Phys. Rev. Lett. **96**, 201601 (2006), arXiv:hep-ph/0602252 [hep-ph].

[33]X.-d. Ji, J.-P. Ma, and F. Yuan, Nucl. Phys. **B652**, 383–404 (2003), arXiv:hep-ph/0210430 [hep-ph].

[34]X.-d. Ji, J.-P. Ma, and F. Yuan, Phys. Rev. Lett. **90**, 241601 (2003), arXiv:hep-ph/0301141 [hep-ph].

[35]X.-d. Ji, J.-P. Ma, and F. Yuan, Eur. Phys. J. **C33**, 75–90 (2004), arXiv:hep-ph/0304107 [hep-ph].

[36]S. Weinberg, Phys.Rev. **177**, 2604–2620 (1969).

[37]S. Weinberg, Phys.Rev.Lett. **22**, 1023–1025 (1969).

[38]S. Weinberg, (1994), arXiv:hep-ph/9412326 [hep-ph].

[39]J.-L. Gervais and B. Sakita, Phys.Rev.Lett. **52**, 87 (1984).

[40]R. F. Dashen and A. V. Manohar, Phys.Lett. **B315**, 425–430 (1993), arXiv:hep-ph/9307241 [hep-ph].

[41]R. F. Dashen, E. E. Jenkins, and A. V. Manohar, Phys. Rev. D **49**, [Erratum: Phys.Rev.D 51, 2489 (1995)], 4713 (1994), arXiv:hep-ph/9310379.

[42]A. Casher and L. Susskind, Phys.Rev. **D9**, 436–460 (1974).

[43]L. Susskind and M. Burkardt, (1994), arXiv:hep-ph/9410313 [hep-ph].

[44]S. R. Beane and P. Ehlers, (2019).

[45]R. D. Carlitz and J. Kaur, Phys. Rev. Lett. **38**, [Erratum: Phys. Rev. Lett.38,1102(1977)], 673 (1977).

[46]Y. V. Kovchegov and E. Levin, *Quantum chromodynamics at high energy*, Vol. 33 (Cambridge University Press, 2012).

[47]M. Tanabashi et al. (Particle Data Group), Phys. Rev. **D98**, 030001 (2018).

[48]J. J. Ethier, N. Sato, and W. Melnitchouk, Phys. Rev. Lett. **119**, 132001 (2017), arXiv:1705.05889 [hep-ph].

[49]S. R. Beane, D. B. Kaplan, N. Klco, and M. J. Savage, Phys. Rev. Lett. **122**, 102001 (2019), arXiv:1812.03138 [nucl-th].

[50]D. de Florian and W. Vogelsang, Phys. Rev. **D99**, 054001 (2019), arXiv:1902.04636 [hep-ph].

[51]C. Alexandrou, S. Bacchio, M. Constantinou, J. Finkenrath, K. Hadjiyiannakou, K. Jansen, G. Koutsou, H. Panagopoulos, and G. Spanoudes (Extended Twisted Mass Collaboration), Phys. Rev. D **101**, 094513 (2020).

[52]S. Boffi and B. Pasquini, Riv. Nuovo Cim. **30**, 387–448 (2007), arXiv:0711.2625 [hep-ph].

[53]C. Lorce and B. Pasquini, Phys. Rev. D **84**, 014015 (2011), arXiv:1106.0139 [hep-ph].

[54]R. Peschanski and S. Seki, Phys. Lett. B **758**, 89–92 (2016), arXiv:1602.00720 [hep-th].

[55]A. Florio and D. E. Kharzeev, Phys. Rev. D **104**, 056021 (2021), arXiv:2106.00838 [hep-th].

[56]D. E. Kharzeev, Phil. Trans. A. Math. Phys. Eng. Sci. **380**, 20210063 (2021), arXiv:2108.08792 [hep-ph].

[57]K. Zhang, K. Hao, D. Kharzeev, and V. Korepin, Phys. Rev. D **105**, 014002 (2022), arXiv:2110.04881 [quant-ph].

[58]R. Peschanski and S. Seki, Phys. Rev. D **100**, 076012 (2019), arXiv:1906.09696 [hep-th].

[59]A. Kovner, M. Lublinsky, and M. Serino, Phys. Lett. B **792**, 4–15 (2019), arXiv:1806.01089 [hep-ph].

[60]N. Armesto, F. Dominguez, A. Kovner, M. Lublinsky, and V. Skokov, JHEP **05**, 025 (2019), arXiv:1901.08080 [hep-ph].

[61]C. Akkaya and A. Kovner, Phys. Lett. B **808**, 135670 (2020), arXiv:1904.05477 [hep-th].

[62]H. Duan, C. Akkaya, A. Kovner, and V. V. Skokov, Phys. Rev. D **101**, 036017 (2020), arXiv:2001.01726 [hep-ph].

[63]D. E. Kharzeev and E. Levin, Phys. Rev. D **104**, L031503 (2021), arXiv:2102.09773 [hep-ph].

[64]S. Weinberg, Phys.Rev.Lett. **65**, 1177–1180 (1990).

[65]D. E. Soper, Phys. Rev. **D5**, 1956–1962 (1972).

[66]J. Pasupathy, Phys. Rev. **D2**, 357–361 (1970).

[67]C. Adolph et al., Physics Letters B **753**, 18–28 (2016).

[68]K. G. Wilson, Phys. Rev. D **10**, edited by J. C. Taylor, 2445–2459 (1974).

[69]T. Byrnes and Y. Yamamoto, Phys. Rev. A **73**, 022328 (2006), arXiv:quant-ph/0510027.

[70]K. Stannigel, P. Hauke, D. Marcos, M. Hafezi, S. Diehl, M. Dalmonte, and P. Zoller, Phys. Rev. Lett. **112**, 120406 (2014), arXiv:1308.0528 [quant-ph].

[71]E. Zohar, J. I. Cirac, and B. Reznik, Phys. Rev. A **88**, 023617 (2013), arXiv:1303.5040 [quant-ph].

[72]E. Zohar and M. Burrello, Phys. Rev. D **91**, 054506 (2015), arXiv:1409.3085 [quant-ph].

[73]D. Marcos, P. Widmer, E. Rico, M. Hafezi, P. Rabl, U. .-. Wiese, and P. Zoller, Annals Phys. **351**, 634–654 (2014), arXiv:1407.6066 [quant-ph].

[74]U.-J. Wiese, Nucl. Phys. A **931**, edited by P. Braun-Munzinger, B. Friman, and J. Stachel, 246–256 (2014), arXiv:1409.7414 [hep-th].

[75]L. García-Álvarez, J. Casanova, A. Mezzacapo, I. L. Egusquiza, L. Lamata, G. Romero, and E. Solano, Phys. Rev. Lett. **114**, 070502 (2015), arXiv:1404.2868 [quant-ph].

[76]V. Kasper, F. Hebenstreit, M. Oberthaler, and J. Berges, Phys. Lett. B **760**, 742–746 (2016), arXiv:1506.01238 [cond-mat.quant-gas].

[77]A. Mezzacapo, E. Rico, C. Sabín, I. L. Egusquiza, L. Lamata, and E. Solano, Phys. Rev. Lett. **115**, 240502 (2015), arXiv:1505.04720 [quant-ph].

[78]A. Bazavov, Y. Meurice, S.-W. Tsai, J. Unmuth-Yockey, and J. Zhang, Phys. Rev. D **92**, 076003 (2015), arXiv:1503.08354 [hep-lat].

[79]E. A. Martinez et al., Nature **534**, 516–519 (2016), arXiv:1605.04570 [quant-ph].

[80]S. P. Jordan, K. S. M. Lee, and J. Preskill, Quant. Inf. Comput. **14**, 1014–1080 (2014), arXiv:1112.4833 [hep-th].

[81]C. Muschik, M. Heyl, E. Martinez, T. Monz, P. Schindler, B. Vogell, M. Dalmonte, P. Hauke, R. Blatt, and P. Zoller, New J. Phys. **19**, 103020 (2017), arXiv:1612.08653 [quant-ph].

[82]M. C. Bañuls, K. Cichy, J. I. Cirac, K. Jansen, and S. Kühn, Phys. Rev. X **7**, 041046 (2017), arXiv:1707.06434 [hep-lat].

[83]K. Yeter-Aydeniz and G. Siopsis, Phys. Rev. D **97**, 036004 (2018), arXiv:1709.02355 [quant-ph].

[84]I. Raychowdhury and J. R. Stryker, Phys. Rev. Res. **2**, 033039 (2020), arXiv:1812.07554 [hep-lat].

[85]D. B. Kaplan and J. R. Stryker, Phys. Rev. D **102**, 094515 (2020), arXiv:1806.08797 [hep-lat].

[86]N. Klco and M. J. Savage, Phys. Rev. A **99**, 052335 (2019), arXiv:1808.10378 [quant-ph].

[87]A. Macridin, P. Spentzouris, J. Amundson, and R. Harnik, Phys. Rev. A **98**, 042312 (2018), arXiv:1805.09928 [quant-ph].

[88]K. Yeter-Aydeniz, E. F. Dumitrescu, A. J. McCaskey, R. S. Bennink, R. C. Pooser, and G. Siopsis, Phys. Rev. A **99**, 032306 (2019), arXiv:1811.12332 [quant-ph].

[89]A. Alexandru, P. F. Bedaque, S. Harmalkar, H. Lamm, S. Lawrence, and N. C. Warrington (NuQS), Phys. Rev. D **100**, 114501 (2019), arXiv:1906.11213 [hep-lat].

[90]D. Luo, J. Shen, M. Highman, B. K. Clark, B. DeMarco, A. X. El-Khadra, and B. Gadway, Phys. Rev. A **102**, 032617 (2020), arXiv:1912.11488 [quant-ph].

[91]S. P. Jordan, K. S. M. Lee, and J. Preskill, Science **336**, 1130–1133 (2012), arXiv:1111.3633 [quant-ph].

[92]F. M. Surace, P. P. Mazza, G. Giudici, A. Lerose, A. Gambassi, and M. Dalmonte, Phys. Rev. X **10**, 021041 (2020), arXiv:1902.09551 [cond-mat.quant-gas].

[93]N. Klco, J. R. Stryker, and M. J. Savage, Phys. Rev. D **101**, 074512 (2020), arXiv:1908.06935 [quant-ph].

[94]A. Mil, T. V. Zache, A. Hegde, A. Xia, R. P. Bhatt, M. K. Oberthaler, P. Hauke, J. Berges, and F. Jendrzejewski, Science **367**, 1128–1130 (2020), arXiv:1909.07641 [cond-mat.quant-gas].

[95]J. F. Haase, L. Dellantonio, A. Celi, D. Paulson, A. Kan, K. Jansen, and C. A. Muschik, Quantum **5**, 393 (2021), arXiv:2006.14160 [quant-ph].

[96]A. F. Shaw, P. Lougovski, J. R. Stryker, and N. Wiebe, Quantum **4**, 306 (2020), arXiv:2002.11146 [quant-ph].

[97]M. C. Bañuls et al., Eur. Phys. J. D **74**, 165 (2020), arXiv:1911.00003 [quant-ph].

[98]D. E. Kharzeev and Y. Kikuchi, Phys. Rev. Res. **2**, 023342 (2020), arXiv:2001.00698 [hep-ph].

[99]M. Kreshchuk, W. M. Kirby, G. Goldstein, H. Beauchemin, and P. J. Love, Phys. Rev. A **105**, 032418 (2022), arXiv:2002.04016 [quant-ph].

[100]S. P. Jordan, K. S. M. Lee, and J. Preskill, (2014), arXiv:1404.7115 [hep-th].

[101]M. Kreshchuk, S. Jia, W. M. Kirby, G. Goldstein, J. P. Vary, and P. J. Love, Phys. Rev. A **103**, 062601 (2021), arXiv:2011.13443 [quant-ph].

[102]Z. Davoudi, I. Raychowdhury, and A. Shaw, Phys. Rev. D **104**, 074505 (2021), arXiv:2009.11802 [hep-lat].

[103]N. Mueller, A. Tarasov, and R. Venugopalan, Nucl. Phys. A **1005**, edited by F. Liu, E. Wang, X.-N. Wang, N. Xu, and B.-W. Zhang, 121889 (2021), arXiv:2001.11145 [hep-th].

[104]A. Ciavarella, N. Klco, and M. J. Savage, Phys. Rev. D **103**, 094501 (2021), arXiv:2101.10227 [quant-ph].

[105]J. Barata, N. Mueller, A. Tarasov, and R. Venugopalan, Phys. Rev. A **103**, 042410 (2021), arXiv:2012.00020 [hep-th].

[106]D. M. Kurkcuoglu, M. S. Alam, J. A. Job, A. C. Y. Li, A. Macridin, G. N. Perdue, and S. Providence, (2021), arXiv:2108.13357 [quant-ph].

[107]C. W. Bauer, M. Freytsis, and B. Nachman, Phys. Rev. Lett. **127**, 212001 (2021), arXiv:2102.05044 [hep-ph].

[108]Z. Davoudi, N. M. Linke, and G. Pagano, Phys. Rev. Res. **3**, 043072 (2021), arXiv:2104.09346 [quant-ph].

[109]Y. Y. Atas, J. Zhang, R. Lewis, A. Jahanpour, J. F. Haase, and C. A. Muschik, Nature Commun. **12**, 6499 (2021), arXiv:2102.08920 [quant-ph].

[110]S. A Rahman, R. Lewis, E. Mendicelli, and S. Powell, Phys. Rev. D **104**, 034501 (2021), arXiv:2103.08661 [hep-lat].

[111]E. Zohar, J. I. Cirac, and B. Reznik, Phys. Rev. Lett. **109**, 125302 (2012), arXiv:1204.6574 [quant-ph].

[112]E. Zohar, J. I. Cirac, and B. Reznik, Phys. Rev. Lett. **110**, 125304 (2013), arXiv:1211.2241 [quant-ph].

[113]D. Banerjee, M. Dalmonte, M. Muller, E. Rico, P. Stebler, U. .-. Wiese, and P. Zoller, Phys. Rev. Lett. **109**, 175302 (2012), arXiv:1205.6366 [cond-mat.quant-gas].

[114]D. Banerjee, M. Bögli, M. Dalmonte, E. Rico, P. Stebler, U. .-. Wiese, and P. Zoller, Phys. Rev. Lett. **110**, 125303 (2013), arXiv:1211.2242 [cond-mat.quant-gas].

[115]L. Tagliacozzo, A. Celi, P. Orland, and M. Lewenstein, Nature Commun. **4**, 2615 (2013), arXiv:1211.2704 [cond-mat.quant-gas].

[116]L. Bombelli, R. K. Koul, J. Lee, and R. D. Sorkin, Phys. Rev. D **34**, 373–383 (1986).

[117]M. Srednicki, Phys. Rev. Lett. **71**, 666–669 (1993), arXiv:hep-th/9303048.

[118]C. G. Callan Jr. and F. Wilczek, Phys. Lett. B **333**, 55–61 (1994), arXiv:hep-th/9401072.

[119]C. Holzhey, F. Larsen, and F. Wilczek, Nucl. Phys. B **424**, 443–467 (1994), arXiv:hep-th/9403108.

[120]P. Calabrese and J. L. Cardy, J. Stat. Mech. **0406**, P06002 (2004), arXiv:hep-th/0405152.

[121]P. Calabrese and J. Cardy, J. Phys. A **42**, 504005 (2009), arXiv:0905.4013 [cond-mat.stat-mech].

[122]S. Ryu and T. Takayanagi, Phys. Rev. Lett. **96**, 181602 (2006), arXiv:hep-th/0603001.

[123]S. Ryu and T. Takayanagi, JHEP **08**, 045 (2006), arXiv:hep-th/0605073.

[124]V. Simak, M. Sumbera, and I. Zborovsky, Phys. Lett. B **206**, 159–162 (1988).

[125]L. Lello, D. Boyanovsky, and R. Holman, JHEP **11**, 116 (2013), arXiv:1304.6110 [hep-th].

[126]S. Seki, I. Y. Park, and S.-J. Sin, Phys. Lett. B **743**, 147–153 (2015), arXiv:1412.7894 [hep-th].

[127]C. M. Ho and S. D. H. Hsu, Mod. Phys. Lett. A **31**, 1650110 (2016), arXiv:1506.03696 [hep-th].

[128]A. Bialas and W. Czyz, Phys. Rev. D **61**, 074021 (2000), arXiv:hep-ph/9909209.

[129]B. Reznik, Found. Phys. **33**, 167–176 (2003), arXiv:quant-ph/0212044.

[130]M. R. Atayan et al. (EHS/NA22), AIP Conf. Proc. **828**, edited by V. Simak, M. Sumbera, S. Todorova-Nova, and B. Tomasik, 124–129 (2006), arXiv:hep-ex/0506029.

[131]K. Kutak, Phys. Lett. B **705**, 217–221 (2011), arXiv:1103.3654 [hep-ph].

[132]B. Muller and A. Schafer, Int. J. Mod. Phys. E **20**, 2235–2267 (2011), arXiv:1110.2378 [hep-ph].

[133]V. Balasubramanian, M. B. McDermott, and M. Van Raamsdonk, Phys. Rev. D **86**, 045014 (2012), arXiv:1108.3568 [hep-th].

[134]R. Peschanski, Phys. Rev. D **87**, 034042 (2013), arXiv:1211.6911 [hep-ph].

[135]T.-C. L. Hsu, M. B. McDermott, and M. Van Raamsdonk, JHEP **11**, 121 (2013), arXiv:1210.0054 [hep-th].

[136]J. Berges, S. Floerchinger, and R. Venugopalan, Nucl. Phys. A **982**, edited by F. Antinori, A. Dainese, P. Giubellino, V. Greco, M. P. Lombardo, and E. Scomparin, 819–822 (2019), arXiv:1812.08120 [hep-th].

[137]X. Feal, C. Pajares, and R. A. Vazquez, Phys. Rev. C **99**, 015205 (2019), arXiv:1805.12444 [hep-ph].

[138]Z. Tu, D. E. Kharzeev, and T. Ullrich, Phys. Rev. Lett. **124**, 062001 (2020), arXiv:1904.11974 [hep-ph].

[139]P. Castorina, A. Iorio, D. Lanteri, and P. Lukeš, Int. J. Mod. Phys. E **30**, 2150010 (2021), arXiv:2003.00112 [hep-ph].

[140]G. S. Ramos and M. V. T. Machado, Phys. Rev. D **101**, 074040 (2020), arXiv:2003.05008 [hep-ph].

[141]E. Gotsman and E. Levin, Phys. Rev. D **102**, 074008 (2020), arXiv:2006.11793 [hep-ph].

[142]C. Robin, M. J. Savage, and N. Pillet, Phys. Rev. C **103**, 034325 (2021), arXiv:2007.09157 [nucl-th].

[143]J. Berges, S. Floerchinger, and R. Venugopalan, JHEP **04**, 145 (2018), arXiv:1712.09362 [hep-th].

[144]G. S. Ramos and M. V. T. Machado, Phys. Rev. D **102**, 034019 (2020), arXiv:2007.09744 [hep-ph].

[145]G. Iskander, J. Pan, M. Tyler, C. Weber, and O. K. Baker, Phys. Lett. B **811**, 135948 (2020), arXiv:2010.00709 [hep-ph].

[146]V. Andreev et al. (H1), Eur. Phys. J. C **81**, 212 (2021), arXiv:2011.01812 [hep-ex].

[147]Y. Afik and J. R. M. de Nova, Eur. Phys. J. Plus **136**, 907 (2021), arXiv:2003.02280 [quant-ph].

[148]G. R. Germano and F. S. Navarra, (2020), arXiv:2011.08912 [hep-ph].

[149]G. R. Germano and F. S. Navarra, Phys. Rev. D **105**, 014005 (2022), arXiv:2110.12028 [hep-ph].

[150]M. Li and A. Kovner, JHEP **05**, 036 (2020), arXiv:2002.02282 [hep-ph].

[151]X. Feal, C. Pajares, and R. Vazquez, Phys. Rev. C **104**, 044904 (2021), arXiv:2012.02894 [hep-ph].

[152]N. Klco and M. J. Savage, Phys. Rev. Lett. **127**, 211602 (2021), arXiv:2103.14999 [hep-th].

[153]E. Shuryak and I. Zahed, Annals Phys. **396**, 1–17 (2018), arXiv:1707.01885 [hep-ph].

[154]H. Duan, in 28th International Workshop on Deep Inelastic Scattering and Related Subjects (July 2021), arXiv:2107.10812 [hep-ph].

[155]S. R. Beane, R. C. Farrell, and M. Varma, Int. J. Mod. Phys. A **36**, 2150205 (2021), arXiv:2108.00646 [hep-ph].

[156]V. Skokov, PoS **HardProbes2020**, 180 (2021).

[157]M. Hentschinski and K. Kutak, Eur. Phys. J. C **82**, 111 (2022), arXiv:2110.06156 [hep-ph].

[158]H. Duan, A. Kovner, and V. V. Skokov, Phys. Rev. D **105**, 056009 (2022), arXiv:2111.06475 [hep-ph].

[159]N. Klco, D. H. Beck, and M. J. Savage, (2021), arXiv:2110.10736 [quant-ph].

[160]I. Low and T. Mehen, Phys. Rev. D **104**, 074014 (2021), arXiv:2104.10835 [hep-th].

[161]A. Cervera-Lierta, J. I. Latorre, J. Rojo, and L. Rottoli, SciPost Phys. **3**, 036 (2017), arXiv:1703.02989 [hep-th].

[162]W. Gong, G. Parida, Z. Tu, and R. Venugopalan, (2021), arXiv:2107.13007 [hep-ph].

[163]G. Dvali and R. Venugopalan, Phys. Rev. D **105**, 056026 (2022), arXiv:2106.11989 [hep-th].

[164]G. S. Ramos and M. V. T. Machado, Phys. Rev. D **105**, 094009 (2022), arXiv:2203.10986 [hep-ph].

[165]A. Dumitru and E. Kolbusz, Phys. Rev. D **105**, 074030 (2022), arXiv:2202.01803 [hep-ph].

[166]Y. Liu, M. A. Nowak, and I. Zahed, Phys. Rev. D **105**, 114027 (2022), arXiv:2202.02612 [hep-ph].

[167]Y. Liu, M. A. Nowak, and I. Zahed, Phys. Rev. D **105**, 114028 (2022), arXiv:2203.00739 [hep-ph].

[168]Y. Afik and J. R. M. de Nova, (2022), arXiv:2203.05582 [quant-ph].

[169]Y. Liu, M. A. Nowak, and I. Zahed, (2022), arXiv:2205.06724 [hep-ph].

[170]M. Hentschinski, K. Kutak, and R. Straka, (2022), arXiv:2207.09430 [hep-ph].

[171]O. K. Baker and D. E. Kharzeev, Phys. Rev. D **98**, 054007 (2018), arXiv:1712.04558 [hep-ph].

[172]Y. Hagiwara, Y. Hatta, B.-W. Xiao, and F. Yuan, Phys. Rev. D **97**, 094029 (2018), arXiv:1801.00087 [hep-ph].

[173]D. Neill and W. J. Waalewijn, Phys. Rev. Lett. **123**, 142001 (2019), arXiv:1811.01021 [hep-ph].

[174]V. Balasubramanian, A. Bernamonti, B. Craps, T. De Jonckheere, and F. Galli, JHEP **12**, 094 (2016), arXiv:1609.03991 [hep-th].

[175]V. Balasubramanian, B. Craps, T. De Jonckheere, and G. Sárosi, JHEP **01**, 190 (2019), arXiv:1806.02871 [hep-th].

[176]J. Erdmenger and M. Gerbershagen, JHEP **03**, 082 (2020), arXiv:1910.05352 [hep-th].

[177]J. D. Bjorken, Phys. Rev. **179**, 1547–1553 (1969).

[178]R. P. Feynman, Phys. Rev. Lett. **23**, edited by L. M. Brown, 1415–1417 (1969).

[179]J. D. Bjorken and E. A. Paschos, Phys. Rev. **185**, 1975–1982 (1969).

[180]R. K. Ellis, H. Georgi, M. Machacek, H. D. Politzer, and G. G. Ross, Nucl. Phys. B **152**, 285–329 (1979).

[181]J. C. Collins, D. E. Soper, and G. F. Sterman, Adv. Ser. Direct. High Energy Phys. **5**, 1–91 (1989), arXiv:hep-ph/0409313.

[182]M. Diehl, Phys. Rept. **388**, 41–277 (2003), arXiv:hep-ph/0307382.

[183]X.-d. Ji, Phys. Rev. Lett. **91**, 062001 (2003), arXiv:hep-ph/0304037.

[184]X.-d. Ji, J.-p. Ma, and F. Yuan, Phys. Rev. D **71**, 034005 (2005), arXiv:hep-ph/0404183.

[185]E. Witten, Annals Phys. **128**, 363 (1980).

[186]R. F. Dashen, E. E. Jenkins, and A. V. Manohar, Phys. Rev. D **51**, 3697–3727 (1995), arXiv:hep-ph/9411234.

[187]D. B. Kaplan and M. J. Savage, Phys. Lett. B **365**, 244–251 (1996), arXiv:hep-ph/9509371.

[188]D. B. Kaplan and A. V. Manohar, Phys. Rev. C **56**, 76–83 (1997), arXiv:nucl-th/9612021.

[189]H. C. Pauli and S. J. Brodsky, Phys. Rev. D **32**, 2001 (1985).

[190]S. J. Brodsky, H.-C. Pauli, and S. S. Pinsky, Phys. Rept. **301**, 299–486 (1998), arXiv:hep-ph/9705477.

[191]K. Hornbostel, S. J. Brodsky, and H. C. Pauli, Phys. Rev. D **41**, 3814 (1990).

[192]K. Hornbostel, "THE APPLICATION OF LIGHT CONE QUANTIZATION TO QUANTUM CHROMODYNAMICS IN (1+1)-DIMENSIONS", Other thesis (Dec. 1988).

[193]W. Donnelly, Class. Quant. Grav. **31**, 214003 (2014), arXiv:1406.7304 [hep-th].

[194]A. V. Manohar, in Les Houches Summer School in Theoretical Physics, Session 68: Probing the Standard Model of Particle Interactions (Feb. 1998), pp. 1091–1169, arXiv:hep-ph/9802419.

[195]F. Lenz, M. Thies, K. Yazaki, and S. Levit, Annals Phys. **208**, 1–89 (1991).

[196]M. Engelhardt, Nucl. Phys. B **440**, 543–554 (1995), arXiv:hep-ph/9412314.

[197]S. J. Brodsky, in 58th Scottish Universities Summer School in Physics (SUSSP58): A NATO Advanced Study Institute and EU Hadron Physics 13 Summer Institute (Nov. 2004), pp. 121–173, arXiv:hep-ph/0412101.

[198]T. Heinzl, Lect. Notes Phys. **572**, edited by H. Latal and W. Schweiger, 55–142 (2001), arXiv:hep-th/0008096.

[199]M. Burkardt, Nucl. Phys. A **504**, 762–776 (1989).

[200]D. Pirjol and T.-M. Yan, Phys. Rev. D **57**, 1449–1486 (1998), arXiv:hep-ph/9707485.

[201]D. Pirjol and T.-M. Yan, Phys. Rev. D **57**, 5434–5443 (1998), arXiv:hep-ph/9711201.

[202]T. D. Cohen and R. F. Lebed, Phys. Rev. D **67**, 096008 (2003), arXiv:hep-ph/0301219.

[203]H. Collins and H. Georgi, Phys. Rev. **D59**, 094010 (1999), arXiv:hep - ph / 9810392 [hep-ph].

[204]S. Capstick and W. Roberts, Prog. Part. Nucl. Phys. **45**, S241–S331 (2000), arXiv:nucl-th/0008028 [nucl-th].

Appendix A

ALGORITHM DETAILS & YOUNG'S ORTHOGONAL BASIS

In this appendix, we will explain some of the details of the algorithm used to generate the DLCQ Hamiltonian, as well as the other algorithms needed to obtain the entanglement entropies. A suitable computational basis in DLCQ is the Fock state basis containing the finite set of states with a given total momentum and flavor content, where states are labeled by the momenta, flavors, and color charges of each quark in a state. Doing calculations in this basis is fairly straightforward, but since physical quantities are always calculated using color singlet states using this basis would be incredibly inefficient due to the large number of color charged states that ultimately do not contribute to any quantities of interest. We would rather restrict our computational basis to the subset of color singlet Fock states to improve the efficiency of the calculation.

A convenient way to construct color singlets from a Fock state with n_q quarks and $n_{\bar{q}}$ antiquarks is to organize them both into the n_q-dimensional and $n_{\bar{q}}$-dimensional irreducible representations (irreps) of $SU(N_c)$, and then unite the irreps for the quarks and antiquarks that are dual to each other, which is guaranteed to produce exactly one singlet per quark-antiquark irrep combination. The irreps of $SU(N_c)$ can be organized and parametrized using Young tableaux, and the number of copies of a given irrep that is formed from n quarks is equal to the number of ways that the tableau for that irrep can be formed from n boxes, which is in turn equal to the dimension of the irrep of the symmetric group S_n corresponding to the same tableau. Furthermore, operations in color space can be implemented through permutations that swap the color indices of the creation operators within the color singlet states. These permutations can be written as matrices that can be derived from the tableaux, in a basis known as Young's orthogonal basis. Thus we can exploit the structural similarities

between the irreps of $SU(N_c)$ and S_n, which are encoded into Young tableaux, to implement operations in color space via matrix operations in the symmetric group. The vast majority of this appendix will be devoted to describing how this is done.

The implementation of the Hamiltonian and density matrices can be separated into three broad categories. The kinetic term of the Hamiltonian is two-quark operator the conserves momentum and flavor, so it can be implemented by simply adding a factor of $n_p \frac{m_q^2}{k}$ for each quark and antiquark in the state to the relevant diagonal element of the Hamiltonian. The potential in the Hamiltonian as well as the density matrices for mesons and 2-color baryons are composed of four-quark operators, which can be broken down into a product of two-quark color singlet operators that may not conserve momentum or flavor. Finally, we also have six-quark operators needed for the 3-color baryon density matrices, but these can also be broken down into two-quark color singlet operators. Thus we can get everything we need by focusing on the actions of general two-quark color singlet operators on our Fock state basis. These come in four different types: operators of the form $b_a^\dagger b_a$, $d_a^\dagger d_a$, $d_a b_a$, and $b_a^\dagger d_a^\dagger$, where a is the color index that is implicitly being summed over.

The action of singlet operators of the form $b_a^\dagger b_a$ or $d_a^\dagger d_a$ can be implemented by simply changing the momentum and flavor indices of the Fock state to reflect the removal and addition of one particle, followed by the application of a permutation matrix in color space. The matrix stems from having to restore the normal ordering of the creation operators, which necessitates a permutation of the color indices. Since the action of these operators in color space amounts to a simple permutation matrix, they do not mix states in different irreps. Some simplifications can be made along the diagonal terms of the Hamiltonian matrix since they map states onto themselves. In this case only one permutation matrix is applied instead of two since the best a four-quark operator made only of $b_a^\dagger b_a$ or $d_a^\dagger d_a$ can do on the diagonal is swap two creation operators around. Details on the construction of the permutation matrices are given in the next section. For color singlet operators of the form $d_a b_a$, a more involved color matrix is applied to reflect that the $SU(N_c)$ irreps get truncated by the operator. Details on the construction of that matrix are given in another section

below. Singlet operators of the form $b_a^\dagger d_a^\dagger$ can be obtained from Hermitian conjugation of $d_a b_a$.

A.1 Permutation Matrices in Young's Orthogonal Basis

Young's orthogonal basis is a vector basis for the symmetric group in which the permutation matrices are rendered orthogonal. The orthogonality is of vital importance as it corresponds to the unitarity of the operators that swap quark and antiquark creation operators. The systematic method for deriving these permutation matrices from Young tableaux is detailed here. First, for a given Young tableau, we write out all the ways that the boxes of a tableau can be numerically labeled from 1 to n, where n is the number of boxes in the tableau. Each numbered tableau represents one of the color singlet basis vectors in the irrep represented by the tableau. The labeling is ordered such that the upper-left most box is always labeled 1, each following numerical label must be to the right of and below other labeled boxes, unless it is in the same column or row as the first box. This is essentially counting and labeling the distinct ways in which a given tableau can be assembled from n individual boxes, such that we are always assembling valid tableau of sizes ranging from 1 to n along the way. The number of distinct ways to form a tableau is same as the dimension of the S_n irrep represented by the tableau.

Now that we have our basis states organized and labeled, we can use this to derive the orthogonal permutation matrices. To get the permutation matrices that swap elements i and $i+1$, where i ranges from 1 to $n-1$, we can get the nonzero elements from the positions of boxes i and $i+1$ in the numbered tableaux. The diagonal elements are given by $\pm 1/d$, where d is the length under the taxicab metric between boxes i and $i+1$, and the sign is positive(negative) when $i+1$ is to the right(left) of and/or above(below) i. The off-diagonal elements are only non-zero when the two numbered tableau involved nearly identical except that boxes i and $i+1$ are swapped. The value of these elements are given by $\sqrt{(d^2-1)/d}$, using the value d corresponding to the labeled tableau involved. The permutations that swap elements i and $i+1$ form a multiplicative basis for all other permutations, so all of the

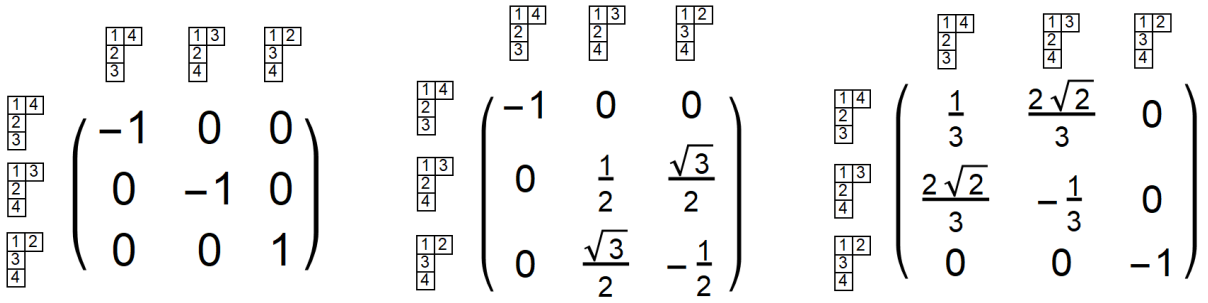

Figure A.1: The three permutation matrices T_{12}, T_{23}, and T_{34} for the antifundamental irrep of S_4 written in Young's orthogonal basis. The numbered Young tableaux correspond to the basis elements of the vector space and are required to derive these matrices as described in Appendix A.

other permutation matrices can be formed from products of the above matrices. In practice, the only permutations that are needed are ones that either swap two different elements and leave the rest alone or ones that cycle the order of a string of adjacent elements forward or back by one step.

Examples of this process are given in Fig. A.1. For T_{12} on the left, all of the diagonal elements are ± 1 since boxes 1 and 2 in the numbered tableaux representing the basis states are always adjacent to each other. The first two are negative since box 2 is always found under box 1, while the third is positive because its corresponding tableau has box 2 to the right of box one. All of the off diagonal elements involving this state are equal to 0.

For T_{23} in the middle, we need to look at the relative positions of boxes 2 and 3. In the first tableau, box 3 is directly below box 2, so $d = 1$ and the sign of the diagonal element is negative, so the diagonal element is -1 and all off-diagonal elements involving this state are 0. The remaining two tableaux are related by a swap of boxes 2 and 3, so they will have the same value of d, with one diagonal element positive and one negative, with off-diagonal elements between them given by $\sqrt{(d^2-1)/d}$. For these tableaux, boxes 2 and 3 are two boxes apart since they are separated by box 1, so $d = 2$, and since the first of the two

tableaux has box 3 above and to the right of box 2, the diagonal elements are $+1/2$ followed by $-1/2$, with off diagonal elements given by $\sqrt{(2^2-1)/2} = \sqrt{3/2}$.

For T_{34} on the right, boxes 3 and 4 are relevant. The first two tableaux are related by a swap of boxes 3 and 4, so their off-diagonal elements will be non-zero. There are two boxes between boxes 3 and 4, so $d = 3$ and therefore the off-diagonal elements are given by $\sqrt{(3^2-1)/3} = 2\sqrt{2/3}$. The first tableau has box 4 above and to the right of box 3, so the diagonal elements are $+1/3$ followed by $-1/3$. Finally, the last tableau has boxes 3 and 4 adjacent to each other with box 4 below box 3, so the last remaining nonzero element is the third diagonal, which is given by -1.

A.2 Transformation from standard basis

To further convince the reader that Young's orthogonal basis is a valid choice of basis for color singlet Fock states, we can take a look at how this basis is related to a more naive but more intuitive choice of defining the color singlet Fock states. If we assume that we have a number of quarks n and an equal number of antiquarks, we can define all color singlet states of this type using the form

$$|n, \mathcal{P}_n\rangle = \delta_{a_1 \ldots a_n; \mathcal{P}_n[b_1 \ldots b_n]}\ b^\dagger_{1,a_1} \ldots b^\dagger_{n,a_n} d^\dagger_{1,b_1} \ldots d^\dagger_{n,b_n} |0\rangle\,, \tag{A.1}$$

where $\delta_{a_1 \ldots a_n; b_1 \ldots b_n} = \delta_{a_1 b_1}\delta_{a_2 b_2} \ldots \delta_{a_n b_n}$ and $\mathcal{P}_n$ is some permutation of n elements. We also assume that each quark and antiquark operator is distinguishable from all others by quantum numbers other than color. This set of states is unnormalized, not orthogonal, and if the number of colors is less than n it is overcomplete. However, this basis does have the advantage that an operator $\mathcal{T}_b(\mathcal{P}_n)$ which permute the quark creation operators by a permutation $\mathcal{P}_n$ has the effect

$$\mathcal{T}_b(\mathcal{P}_n)\,|n, \mathcal{P}'_n\rangle = (-1)^{n-\ell(\mathcal{P}_n)}\,|n, \mathcal{P}_n.\mathcal{P}'_n\rangle\,, \tag{A.2}$$

where $\ell(\mathcal{P}_n)$ gives the number of disjoint cycles in the permutation $\mathcal{P}_n$, including 1-cycles corresponding to particles that do not get moved. Likewise, the similar operator $\mathcal{T}_d(\mathcal{P}_n)$ that

permutes the antiquark operators gives

$$\mathcal{T}_d(\mathcal{P}_n)\,|n,\mathcal{P}'_n\rangle = (-1)^{n-\ell(\mathcal{P}_n)}\left|n,\mathcal{P}'_n.\mathcal{P}_n^{-1}\right\rangle. \tag{A.3}$$

The overlap of two states in this basis is given by

$$\langle n,\mathcal{P}_n|\,|n,\mathcal{P}'_n\rangle = \delta_{a_1\ldots a_n;(\mathcal{P}_n^{-1}.\mathcal{P}'_n)[a_1\ldots a_n]} = N_c^{\ell(\mathcal{P}_n^{-1}.\mathcal{P}'_n)}. \tag{A.4}$$

In contrast, states corresponding to Young's orthogonal basis form a complete orthonormal basis. They are labeled by the state $|\lambda;u_\lambda,v_\lambda\rangle$, where λ refers one of the irreducible representations of the symmetric group S_n and both u_λ and v_λ are vector space indices for the irrep λ. The effects of the permutation operators are

$$\mathcal{T}_b(\mathcal{P}_n)\,|\lambda;u_\lambda,v_\lambda\rangle = (-1)^{n-\ell(\mathcal{P}_n)}(T_{\mathcal{P}_n})_{u'_\lambda u_\lambda}\,|\lambda;u'_\lambda,v_\lambda\rangle\,,\quad \mathcal{T}_d(\mathcal{P}_n)\,|\lambda;u_\lambda,v_\lambda\rangle = (-1)^{n-\ell(\mathcal{P}_n)}(T_{\mathcal{P}_n})_{v'_\lambda v_\lambda}\,|\lambda;u_\lambda,v'_\lambda\rangle\,, \tag{A.5}$$

where $T_{\mathcal{P}_n}$ is the permutation matrix for irrep λ written in Young's orthogonal basis, which was discussed earlier in this appendix. The Fock states can be written in terms of this basis by

$$|n,\mathcal{P}_n\rangle = \sum_\lambda \sum_{u_\lambda,v_\lambda=1}^{d_\lambda} \sqrt{\mathcal{D}_\lambda}\;(T_{\mathcal{P}_n})_{u_\lambda v_\lambda}\,|\lambda;u_\lambda,v_\lambda\rangle\,, \tag{A.6}$$

where λ is summed over the irreducible representations of the symmetric group S_n, d_λ is the dimension of the irrep λ, $\mathcal{D}_\lambda$ is the dimension of the irrep λ, u_λ and v_λ are vector indices for the irrep λ, and $T_{\mathcal{P}_n}$ is the permutation matrix in Young's orthogonal basis discussed above corresponding to the irrep λ.

To see how this works, consider the actions of $\mathcal{T}_b(\mathcal{P}_n)$ and $\mathcal{T}_d(\mathcal{P}_n)$ on the right side of the equation. Permuting the quarks gives

$$\begin{aligned}(-1)^{n-\ell(\mathcal{P}_n)}\mathcal{T}_b(\mathcal{P}_n)\,|n,\mathcal{P}'_n\rangle &= \sum_\lambda \sum_{u_\lambda,v_\lambda=1}^{d_\lambda} \sqrt{\mathcal{D}_\lambda}\;(T_{\mathcal{P}'_n})_{u_\lambda v_\lambda}(T_{\mathcal{P}_n})_{u'_\lambda u_\lambda}\,|\lambda;u'_\lambda,v_\lambda\rangle \\ &= \sum_\lambda \sum_{u_\lambda,v_\lambda=1}^{d_\lambda} \sqrt{\mathcal{D}_\lambda}\;(T_{(\mathcal{P}_n.\mathcal{P}'_n)})_{u_\lambda v_\lambda}\,|\lambda;u_\lambda,v_\lambda\rangle = |n,\mathcal{P}_n.\mathcal{P}'_n\rangle\,,\end{aligned} \tag{A.7}$$

so this matches. The antiquark permutation gives

$$(-1)^{n-\ell(\mathcal{P}_n)}\mathcal{T}_d(\mathcal{P}_n)\,|n,\mathcal{P}'_n\rangle = \sum_\lambda \sum_{u_\lambda,v_\lambda=1}^{d_\lambda} \sqrt{\mathcal{D}_\lambda}\;(T_{\mathcal{P}'_n})_{u_\lambda v_\lambda}(T_{\mathcal{P}_n})_{v'_\lambda v_\lambda}\,|\lambda;u_\lambda,v'_\lambda\rangle$$
$$= \sum_\lambda \sum_{u_\lambda,v_\lambda=1}^{d_\lambda} \sqrt{\mathcal{D}_\lambda}\;(T_{(\mathcal{P}'_n.\mathcal{P}_n^{-1})})_{u_\lambda v_\lambda}\,|\lambda;u_\lambda,v_\lambda\rangle = \left|n,\mathcal{P}'_n.\mathcal{P}_n^{-1}\right\rangle, \tag{A.8}$$

so this also matches. Finally, the overlap is given by

$$\langle n,\mathcal{P}_n|\,|n,\mathcal{P}'_n\rangle = \sum_\lambda \sum_{u_\lambda,v_\lambda=1}^{d_\lambda} \mathcal{D}_\lambda\;(T_{\mathcal{P}_n})_{u_\lambda v_\lambda}(T_{\mathcal{P}'_n})_{u_\lambda v_\lambda}$$
$$= \sum_\lambda \mathcal{D}_\lambda\;\mathrm{Tr}\left[T_{(\mathcal{P}_n^{-1}.\mathcal{P}'_n)}\right] = \sum_\lambda \mathcal{D}_\lambda\;\chi_\lambda(\mu(\mathcal{P}_n^{-1}.\mathcal{P}'_n)), \tag{A.9}$$

where $\chi_\lambda(\mu)$ is the character associated with the irrep λ and the conjugacy class μ and $\mu(\mathcal{P}_n))$ is the conjugacy class of the partition $\mathcal{P}_n$.

To prove that $\sum_\lambda \mathcal{D}_\lambda\,\chi_\lambda(\mu(\mathcal{P}_n)) = N_c^{\ell(\mathcal{P}_n)}$, we will need to introduce the Frobenius formula for calculating the values of characters. We start with the polynomial given by

$$P_n(\vec{x},\mu) = A_n(\vec{x})\prod_{k=1}^{\ell(\mu)}\left(\sum_{i=1}^{N_c} x_i^{\mu_k}\right) = \sum_{\alpha_1,\ldots,\alpha_{N_c}=1}^{N_c+n-1} c_{\alpha_1\ldots\alpha_{N_c}}(\mu)\prod_{i=1}^{N_c} x_i^{\alpha_i}, \tag{A.10}$$

$$A_n(\vec{x}) = \prod_{i=1}^{N_c}\prod_{j=i+1}^{N_c}(x_i - x_j) = \sum_{a_1,\ldots,a_{N_c}=1}^{N_c+n-1} \epsilon_{a_1\ldots a_{N_c}}\prod_{i=1}^{N_c} x_i^{N_c-a_i}, \tag{A.11}$$

where $\vec{x}$ is a N_c-element vector of variables, μ_k is the kth element of the integer partition of n corresponding to the conjugacy class μ, $\ell(\mu)$ is the length of this partition, and $\epsilon_{a_1\ldots a_{N_c}}$ is the Levi-Civita tensor with $\epsilon_{1\ldots N_c} = +1$. The Frobenius formula states that the polynomial $P_n(\vec{x},\mu)$ is a generator of the characters in the sense that

$$c_{\alpha_1>\alpha_2>\ldots>\alpha_{N_c}}(\mu) = \chi_\lambda(\mu), \quad \lambda_i = \alpha_i - n + i, \tag{A.12}$$

where λ_i is the length of the ith row of the tableau associated with the irrep λ, so that the second equation above gives a connection between the α_i's and the irrep λ of the character.

From the formulas of $P_n(\vec{x},\mu)$ and $A_n(\vec{x})$ above, we can see that both polynomials are antisymmetric under any exchange of two of the x_i variables, so we can go a step further and say that

$$c_{\alpha_1\ldots\alpha_{N_c}}(\mu) = -\chi_\lambda(\mu)\epsilon_{\alpha_1\ldots\alpha_{N_c}}. \tag{A.13}$$

To connect this back to our original expression $\sum_\lambda \mathcal{D}_\lambda\ \chi_\lambda(\mu)$, we will need an explicit expression for $\mathcal{D}_\lambda$. It can be written as

$$\mathcal{D}_\lambda = \prod_{i=1}^{N_c} \frac{(N_c+\lambda_i-i)!}{(N_c-i)!}\frac{d_\lambda}{n!}, \tag{A.14}$$

where $d_\lambda = \chi_\lambda(\mathbb{1})$ is the dimension of the irrep λ, equivalent to the character of the irrep under the conjugacy class of the identity matrix. We can then show that our original expression is equivalent up to a constant to the quantity

$$\begin{aligned}
P_n(\vec{\nabla},\mathbb{1})P_n(\vec{x},\mu) &= \left(\sum_{\beta_1,\ldots,\beta_{N_c}=1}^{N_c+n-1} c_{\beta_1\ldots\beta_{N_c}}(\mathbb{1})\prod_{j=1}^{N_c}\nabla_j^{\beta_j}\right)\sum_{\alpha_1,\ldots,\alpha_{N_c}=1}^{N_c+n-1} c_{\alpha_1\ldots\alpha_{N_c}}(\mu)\prod_{i=1}^{N_c}x_i^{\alpha_i}\\
&= \sum_{\alpha_1,\ldots,\alpha_{N_c}=1}^{N_c+n-1} c_{\alpha_1\ldots\alpha_{N_c}}(\mathbb{1})c_{\alpha_1\ldots\alpha_{N_c}}(\mu)\left(\prod_{i=1}^{N_c}(\alpha_i)!\right)\\
&= \sum_{\alpha_1,\ldots,\alpha_{N_c}=1}^{N_c+n-1} d_\lambda\ \chi_\lambda(\mu)(\epsilon_{\alpha_1\ldots\alpha_{N_c}})^2\left(\prod_{i=1}^{N_c}(N_c+\lambda_i-i)!\right)\\
&= n!(N_c)!\left(\prod_{i=1}^{N_c}(N_c-i)!\right)\left(\sum_\lambda \mathcal{D}_\lambda\ \chi_\lambda(\mu)\right).
\end{aligned} \tag{A.15}$$

On the other hand, if we use the other definition of P_n for this expression, we get

$$P_n(\vec{\nabla},\mathbb{1})P_n(\vec{x},\mu) = A_n(\vec{\nabla})\left(\sum_{i=1}^{N_c}\nabla_i\right)^n\left(A_n(\vec{x})\prod_{k=1}^{\ell(\mu)}\left(\sum_{i=1}^{N_c}x_i^{\mu_k}\right)\right). \tag{A.16}$$

Since $A_n(\vec{x})$ is a product of differences between pairs of variables and $\left(\sum_{k=1}^{N_c}\nabla_k\right)(x_i-x_j)=0$ for any pairing of indices i and j, we have that $\left(\sum_{i=1}^{N_c}\nabla_i\right)A_n(\vec{x})=0$. Also, if we expand the product $\prod_{k=1}^{\ell(\mu)}\left(\sum_{i=1}^{N_c}x_i^{\mu_k}\right)$, each term in the sum will have exactly n factors of x variables, so

the derivatives $\left(\sum_{k=1}^{N_c} \nabla_k\right)^n \prod_{k=1}^{\ell(\mu)} \left(\sum_{i=1}^{N_c} x_i^{\mu_k}\right)$ is equal to the $n!$ times the number of terms in the polynomial. Thus we have

$$P_n(\vec{\nabla}, \mathbb{1}) P_n(\vec{x}, \mu) = \left(A_n(\vec{\nabla}) A_n(\vec{x})\right) n! N_c^{\ell(\mu)}. \tag{A.17}$$

The remaining polynomial and derivative term gives

$$\begin{aligned} A_n(\vec{\nabla}) A_n(\vec{x}) &= \sum_{b_1,\ldots,b_{N_c}=1}^{N_c+n-1} \epsilon_{b_1 \ldots b_{N_c}} \prod_{j=1}^{N_c} \nabla_j^{N_c - b_j} \left(\sum_{a_1,\ldots,a_{N_c}=1}^{N_c+n-1} \epsilon_{a_1 \ldots a_{N_c}} \prod_{i=1}^{N_c} x_i^{N_c - a_i} \right) \\ &= \sum_{a_1,\ldots,a_{N_c}=1}^{N_c+n-1} \left(\epsilon_{a_1 \ldots a_{N_c}}\right)^2 \prod_{i=1}^{N_c} (N_c - a_i)! = (N_c)! \prod_{i=1}^{N_c} (N_c - i)!. \end{aligned} \tag{A.18}$$

Now, with our two different expressions for $P_n(\vec{\nabla}, \mathbb{1}) P_n(\vec{x}, \mu)$ we obtain the relation

$$\frac{1}{n!(N_c)! \prod_{i=1}^{N_c}(N_c - i)!} P_n(\vec{\nabla}, \mathbb{1}) P_n(\vec{x}, \mu) = \sum_{\lambda} \mathcal{D}_\lambda \ \chi_\lambda(\mu) = N_c^{\ell(\mu)}, \tag{A.19}$$

Thus we can finally show that the overlap of the Fock states is given by

$$\langle n, \mathcal{P}_n | \, | n, \mathcal{P}'_n \rangle = \sum_{\lambda} \mathcal{D}_\lambda \ \chi_\lambda(\mu(\mathcal{P}_n^{-1}.\mathcal{P}'_n)) = N_c^{\ell(\mu(\mathcal{P}_n^{-1}.\mathcal{P}'_n))} \tag{A.20}$$

when we assume it can be written in terms of the Young's orthogonal basis states.

We can also show what the Young's orthogonal basis states are in terms of the Fock states. To derive this, we will need to find a closed form for the quantity

$$S_{u_\lambda u_\Lambda, v_\lambda v_\Lambda} = \sum_{\mathcal{P}_n} (T_{\mathcal{P}_n})_{u_\lambda v_\lambda} (T_{\mathcal{P}_n})_{u_\Lambda v_\Lambda}, \tag{A.21}$$

where $T_{\mathcal{P}_n}$ is the permutation matrix in Young's orthogonal basis for a permutation $\mathcal{P}_n$ and an irrep λ or Λ. Since we are summing over all permutations and the $T_{\mathcal{P}_n}$ are orthogonal, we can show that

$$\begin{aligned} (T_{\mathcal{P}_n})_{u_\lambda u'_\lambda} S_{u'_\lambda u_\Lambda, v_\lambda v_\Lambda} &= \sum_{\mathcal{P}'_n} (T_{\mathcal{P}_n.\mathcal{P}'_n})_{u_\lambda v_\lambda} (T_{\mathcal{P}'_n})_{u_\Lambda v_\Lambda} \\ &= \sum_{\mathcal{P}''_n} (T_{\mathcal{P}''_n})_{u_\lambda v_\lambda} (T_{\mathcal{P}_n^{-1}.\mathcal{P}''_n})_{u_\Lambda v_\Lambda} = S_{u_\lambda u'_\Lambda, v_\lambda v_\Lambda} (T_{\mathcal{P}_n})_{u'_\Lambda u_\Lambda}. \end{aligned} \tag{A.22}$$

Likewise, we also have

$$(T_{\mathcal{P}_n})_{v_\lambda v'_\lambda} S_{u_\lambda u_\Lambda, v'_\lambda v_\Lambda} = S_{u_\lambda u_\Lambda, v_\lambda v'_\Lambda} (T_{\mathcal{P}_n})_{v'_\Lambda v_\Lambda}. \tag{A.23}$$

If we view $T_{\mathcal{P}_n}$ as a matrix not just for a specific irrep but as a block diagonal matrix over all irreps, then these formulas tell us that S commutes with all of the $T_{\mathcal{P}_n}$'s as a matrix over the u and v indices separately. The only way that this is possible is if S has the form

$$S_{u_\lambda u_\Lambda, v_\lambda v_\Lambda} = \alpha_\lambda \ \delta_{\lambda\Lambda} \ \delta_{u_\lambda u_\Lambda} \delta_{v_\lambda v_\Lambda}. \tag{A.24}$$

for some yet to be determined constant α_λ. In other words, the tensor S is zero unless the two irreps are the same, in which case it is proportional to the outer product of the identity matrix in that irrep with itself.

To find this constant, we can take the sum over the diagonal elements of S using its definition and by the form above. On one hand, the sum over the diagonal elements of S is just $\alpha_\lambda d_\lambda^2$, where d_λ is the dimension of the irrep λ. On the other hand, the original definition of S gives us a sum that looks like

$$\sum_{u_\lambda, v_\lambda} \sum_{\mathcal{P}_n} (T_{\mathcal{P}_n})_{u_\lambda v_\lambda} (T_{\mathcal{P}_n})_{u_\lambda v_\lambda} = \sum_{u_\lambda} \sum_{\mathcal{P}_n} 1 = n! \ d_\lambda, \tag{A.25}$$

where n corresponds to the symmetric group S_n and we used the fact that the matrix $T_{\mathcal{P}_n}$ is orthogonal. Thus we have that

$$S_{u_\lambda u_\Lambda, v_\lambda v_\Lambda} = \sum_{\mathcal{P}_n} (T_{\mathcal{P}_n})_{u_\lambda v_\lambda} (T_{\mathcal{P}_n})_{u_\Lambda v_\Lambda} = \frac{n!}{d_\lambda} \ \delta_{\lambda\Lambda} \ \delta_{u_\lambda u_\Lambda} \delta_{v_\lambda v_\Lambda}. \tag{A.26}$$

From here, it is relatively easy to achieve the original goal of writing a Young's orthogonal basis state in terms of Fock states. We have that

$$\sum_{\mathcal{P}_n} (T_{\mathcal{P}_n})_{u_\lambda v_\lambda} |n, \mathcal{P}_n\rangle = \sum_{\Lambda} \sum_{u_\Lambda, v_\Lambda} \sqrt{\mathcal{D}_\Lambda} \left(\sum_{\mathcal{P}_n} (T_{\mathcal{P}_n})_{u_\lambda v_\lambda} (T_{\mathcal{P}_n})_{u_\Lambda v_\Lambda} \right) |\Lambda; u_\Lambda, v_\Lambda\rangle = \sqrt{\mathcal{D}_\lambda} \, \frac{n!}{d_\lambda} \, |\lambda; u_\lambda, v_\lambda\rangle \,. \tag{A.27}$$

Thus the Young's orthogonal basis state can be written as

$$|\lambda; u_\lambda, v_\lambda\rangle = \frac{d_\lambda}{n! \sqrt{\mathcal{D}_\lambda}} \sum_{\mathcal{P}_n} (T_{\mathcal{P}_n})_{u_\lambda v_\lambda} |n, \mathcal{P}_n\rangle \,. \tag{A.28}$$

So far, we have discussed Fock states with an equal number of quarks and antiquarks, which are directly relevant to forming an orthonormal basis for mesons. This basis conversion can also be used for baryons as well, by attaching a Levi-Civita tensor to one of the quarks and treating it as a fully antisymmetrized collection of $N_c - 1$ antiquarks.

A.3 Action of $d_c b_c$ type operators in Young's orthogonal basis

The goal of this subsection is to illustrate how to find the matrix element $\langle \lambda, u_\lambda v_\lambda | \, d_{j,c} b_{i,c} \, | \Lambda, u_\Lambda v_\Lambda \rangle$, where $|\Lambda, u_\Lambda v_\Lambda\rangle$ is a Young's orthogonal basis state composed of n distinct quarks and antiquarks for an irrep Λ in S_n, $|\lambda, u_\lambda v_\lambda\rangle$ is a Young's orthogonal basis state composed of the same quarks and antiquarks except for the ith quark and the jth antiquark for an irrep λ in S_{n-1}, and $d_{j,c} b_{i,c}$ annihilates quark i and antiquark j with an implicit sum over the color index c. To simplify things, we can use permutation matrices to move the ith quark and the jth antiquark to their respective nth positions in the Fock state so that the annihilation operators always manipulate the nth color indices. This means that as far as the color structures are concerned the matrix element is numerically equivalent to

$$\langle \lambda, u_\lambda v_\lambda | \, d_{j,c} b_{i,c} \, | \Lambda, u_\Lambda v_\Lambda \rangle = (-1)^{i+j} \left(\prod_{k=i}^{n-1} T_{k,k+1} \right)_{u_\Lambda u'_\Lambda} \left(\prod_{l=j}^{n-1} T_{l,l+1} \right)_{v_\Lambda v'_\Lambda} \langle \lambda, u_\lambda v_\lambda | \, d_{n,c} b_{n,c} \, | \Lambda, u'_\Lambda v'_\Lambda \rangle \,, \tag{A.29}$$

where $T_{k,k+1}$ is the permutation matrix in the Λ irrep of S_n that swaps the color indices of operators k and $k+1$. This is helpful because it gives us the explicit i and j dependence of the matrix element relative to the choice where $i = j = n$.

To find the remaining matrix element, it will be most convenient to find the action of $d_{n,c} b_{n,c}$ on Fock states, and then change the basis to Young's orthogonal basis. The permutation $\mathcal{P}_n$ in S_n can either be written as $p_{n-1} \otimes \mathbf{1}$, meaning that it is a permutation p_{n-1} in S_{n-1} that does not move element n, or if $\mathcal{P}_n(i) = n$ it can be written in the form $\mathcal{P}_n = T_{in}.(p_{n-1} \otimes \mathbf{1})$, where T_{in} swaps the elements i and n. In the former case the operator simply annihilates the nth quark and antiquark and so

$$d_{n,c} b_{n,c} \, | n, p_{n-1} \otimes \mathbf{1} \rangle = (-1)^{n-1} N_c \, | n, p_{n-1} \rangle \,, \tag{A.30}$$

where the factor of N_c comes from the sum over the color index c. For the latter case, when the n quark and antiquark operators get annihilated, their color indices get matched together so that the resulting permutation moves $i \to n \to p_{n-1}(i)$. Thus we get

$$d_{n,c}b_{n,c}\left|n, T_{in}.(p_{n-1}\otimes \mathbf{1})\right\rangle = (-1)^{n-1}\left|n, p_{n-1}\right\rangle . \tag{A.31}$$

A Young's orthogonal basis matrix acted upon by the operator becomes

$$\begin{aligned} d_{n,c}b_{n,c}\left|\Lambda, u_\Lambda v_\Lambda\right\rangle &= \frac{d_\Lambda}{n!\sqrt{\mathcal{D}_\Lambda}}\sum_{\mathcal{P}_n}(T_{\mathcal{P}_n})_{u_\Lambda v_\Lambda} d_{n,c}b_{n,c}\left|n, \mathcal{P}_n\right\rangle \\ &= \frac{(-1)^{n-1}d_\Lambda}{n!\sqrt{\mathcal{D}_\Lambda}}\left(N_c\sum_{p_{n-1}}(T_{p_{n-1}\otimes\mathbf{1}})_{u_\Lambda v_\Lambda} + \sum_i\sum_{p_{n-1}}(T_{in}.T_{p_{n-1}\otimes\mathbf{1}})_{u_\Lambda v_\Lambda}\right)\left|n-1, p_{n-1}\right\rangle \\ &= (-1)^{n-1}\frac{d_\Lambda}{n!}\sum_\lambda\sqrt{\frac{\mathcal{D}_\lambda}{\mathcal{D}_\Lambda}}\sum_{u'_\Lambda}\sum_{u_\lambda, v_\lambda}\left(N_c\delta_{u_\Lambda u'_\Lambda} + \sum_{i=1}^{n-1}(T_{in})_{u_\Lambda u'_\Lambda}\right) \\ &\times\left(\sum_{p_{n-1}}(T_{p_{n-1}\otimes\mathbf{1}})_{u'_\Lambda v_\Lambda}(T_{p_{n-1}})_{u_\lambda v_\lambda}\right)\left|\lambda; u_\lambda, v_\lambda\right\rangle . \end{aligned} \tag{A.32}$$

Thus the remaining matrix element is

$$\left\langle\lambda, u_\lambda v_\lambda\right| d_{n,c}b_{n,c}\left|\Lambda, u_\Lambda v_\Lambda\right\rangle = (-1)^{n-1}\frac{d_\Lambda}{n!}\sqrt{\frac{\mathcal{D}_\lambda}{\mathcal{D}_\Lambda}}\sum_{u'_\Lambda}\mathcal{R}_{u_\Lambda u'_\Lambda}\mathcal{S}_{u_\lambda u'_\Lambda, v_\lambda v_\Lambda}, \tag{A.33}$$

with

$$\mathcal{S}_{u_\lambda u_\Lambda, v_\lambda v_\Lambda} = \sum_{p_{n-1}}(T_{p_{n-1}})_{u_\lambda v_\lambda}(T_{p_{n-1}\otimes\mathbf{1}})_{u_\Lambda v_\Lambda}. \tag{A.34}$$

and

$$\mathcal{R}_{u_\Lambda u'_\Lambda} = \left(N_c\delta_{u_\Lambda u'_\Lambda} + \sum_{i=1}^{n-1}(T_{in})_{u_\Lambda u'_\Lambda}\right). \tag{A.35}$$

For the first tensor $\mathcal{S}$, we can see that it is very similar to the tensor S given in Eq. ((A.26)). This new tensor has the similar property

$$(T_p)_{u_\lambda u'_\lambda}\mathcal{S}_{u'_\lambda u_\Lambda, v_\lambda v_\Lambda} = \mathcal{S}_{u_\lambda u'_\Lambda, v_\lambda v_\Lambda}(T_{p\otimes\mathbf{1}})_{u'_\Lambda u_\Lambda} \tag{A.36}$$

for a permutation p in S_{n-1}, with a similar equation for the v indices. As with the tensor S, these relations imply that $\mathcal{S}$ is a direct product of two matrices, so that

$$\mathcal{S}_{u_\lambda u_\Lambda, v_\lambda v_\Lambda} = \beta_{\lambda\Lambda}(M_{\lambda\Lambda})_{u_\Lambda u_\lambda}(M_{\lambda\Lambda})_{v_\Lambda v_\lambda}. \tag{A.37}$$

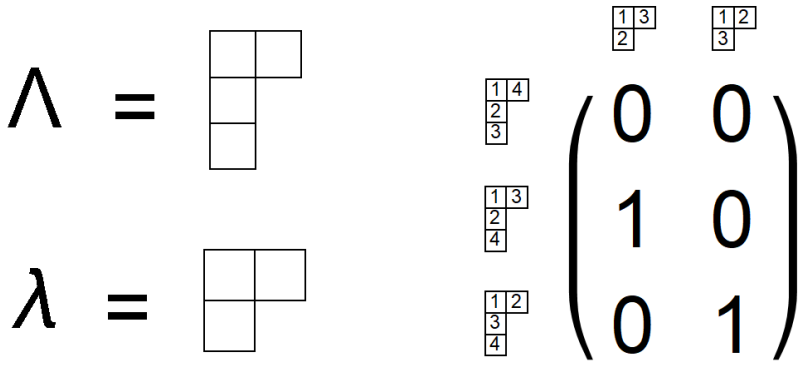

Figure A.2: The matrix $M_{\lambda\Lambda}$ where Λ is the antifundamental irrep of S_4 and λ is the mixed symmetry irrep of S_3, all written in Young's orthogonal basis. The numbered Young tableaux correspond to the basis elements of the vector space and are required to derive this matrix as described in Appendix A. Note that the only nonzero elements occur when the numbered tableau on the left matches the numbered tableau on top with box 4 removed.

for some matrix $M_{\lambda\Lambda}$ with the property

$$T_{p\otimes\mathbf{1}}.M_{\lambda\Lambda} = M_{\lambda\Lambda}.T_p. \tag{A.38}$$

This implies that the matrix $M^T_{\lambda\Lambda}.M_{\lambda\Lambda}$ is proportional to the identity in the smaller basis. Since we define $M_{\lambda\Lambda}$ through $\mathcal{S}$ using an undetermined constant $\beta_{\lambda\Lambda}$, we can choose $M_{\lambda\Lambda}$ to be defined such that $M^T_{\lambda\Lambda}.M_{\lambda\Lambda} = \mathbb{1}$ exactly. This also implies that the rows of the matrix $M_{\lambda\Lambda}$ are orthonormal vectors, which means that the matrix $M_{\lambda\Lambda}.M^T_{\lambda\Lambda}$ is a projection operator in the larger basis.

Looking at the way that Young's orthogonal matrices are constructed, we can see that the matrix $M_{\lambda\Lambda}$ is actually a section of the identity matrix in the larger space, where the ones appear where the numbered tableau on the smaller basis is the same as the numbered tableau in the larger basis with box n removed, as seen in Fig. A.2.

To find $\beta_{\lambda\Lambda}$, we can once again take traces of the tensor $\mathcal{S}$ to get

$$\sum_{u_\lambda, u_\Lambda} \mathcal{S}_{u_\lambda u_\Lambda, u_\lambda u_\Lambda} = \beta_{\lambda\Lambda}\ d_\lambda = \sum_\mu d_\mu\ \chi_\lambda(\mu)\chi_\Lambda(\nu), \tag{A.39}$$

where d_λ is the dimension of the smaller irrep λ, μ is one of the conjugacy classes of the permutations in S_{n-1}, ν is the conjugacy class in S_n such that if μ corresponds to a permutation p, then ν corresponds to $p \otimes \mathbf{1}$, the characters $\chi_\lambda(\mu)$ and $\chi_\Lambda(\nu)$ originate from traces of permutation matrices, and d_μ is the dimension of the conjugacy class μ, equivalent to the number of matrices in the conjugacy class μ. The character $\chi_\Lambda(\nu)$ can be written in terms of the characters $\chi_\lambda(\mu)$ by using the Frobenius formula. The polynomial corresponding to the conjugacy class ν can be written in terms of the smaller ones for μ by

$$F_n(\mathbf{x}, \nu) = F_{n-1}(\mathbf{x}, \mu)\left(\sum_{i=1}^n x_i\right). \tag{A.40}$$

This implies that $\chi_\Lambda(\nu) = \sum_{i=1}^n \chi_{\lambda_i}(\mu)$, where λ_i is the irrep obtained from taking the tableau associated with Λ and removing one box from row i. The character will be equal to zero if λ_i does not correspond to a valid tableau. Finally, we note that $\chi_\lambda(\mu)$ is orthogonal as a vector in the irreps λ, and if that vector is normalized it will also be orthonormal in the conjugacy classes μ. The normalization factor is equal to $(n-1)!/d_\mu$ for a class μ in S_{n-1}. Thus we can put this all together to get

$$\beta_{\lambda\Lambda} = \frac{1}{d_\lambda}\sum_\mu \sum_{i=1}^n d_\mu\ \chi_\lambda(\mu)\chi_{\lambda_i}(\mu) = \frac{(n-1)!}{d_\lambda}\sum_{i=1}^n \delta_{\lambda_i\lambda}. \tag{A.41}$$

This tells us that the tensor $\mathcal{S}$ is zero unless the tableau for the irrep Λ is the same as λ except for one extra box. We now have that, when the tensor $\mathcal{S}$ is nonzero, it is equal to

$$\mathcal{S}_{u_\lambda u_\Lambda, v_\lambda v_\Lambda} = \sum_{p_{n-1}} (T_{p_{n-1}})_{u_\lambda v_\lambda}(T_{p_{n-1}\otimes\mathbf{1}})_{u_\Lambda v_\Lambda} = \frac{(n-1)!}{d_\lambda}(M_{\lambda\Lambda})_{u_\Lambda u_\lambda}(M_{\lambda\Lambda})_{v_\Lambda v_\lambda}. \tag{A.42}$$

The other tensor $\mathcal{R}$ is a matrix that can be shown to commute with any permutation of the form $p \otimes \mathbf{1}$ since that permutation will only rearrange the indices i in the sum over matrices that defines $\mathcal{R}$. This implies that the matrix $M_{\lambda\Lambda}^T.\mathcal{R}.M_{\lambda\Lambda}$ is proportional to the identity

since it commutes with every permutation matrix in S_{n-1}. Also, it can be shown using the definition of $\mathcal{S}$ as a sum over permutations that $(\mathcal{R}.M_{\lambda\Lambda}) \otimes M_{\lambda\Lambda} = M_{\lambda\Lambda} \otimes (\mathcal{R}.M_{\lambda\Lambda})$, which further indicates that $\mathcal{R}.M_{\lambda\Lambda}$ is proportional to $M_{\lambda\Lambda}$. It turns out that the proportionality constant is given by

$$\mathcal{R}.M_{\lambda\Lambda} = (N_c + \Lambda_a - a)M_{\lambda\Lambda}, \tag{A.43}$$

where a is the row of the tableau for Λ that is different from the tableau for λ and Λ_a is the ath value of the permutation corresponding to Λ. This factor is equal to the N_c dependent factor coming from the box in Λ that is not in λ when determining the dimension of the $SU(N_c)$ irrep corresponding to Λ.

Putting all of this together and using the formulas for the dimensions d_λ and $\mathcal{D}_\lambda$ to simplify things, we find that

$$\begin{aligned}\langle \lambda, u_\lambda v_\lambda |\, d_{n,c} b_{n,c} \,| \Lambda, u_\Lambda v_\Lambda \rangle &= (-1)^{n-1} \sqrt{\frac{\mathcal{D}_\lambda}{\mathcal{D}_\Lambda}} \frac{d_\Lambda}{n\ d_\lambda} (N_c + \Lambda_a - a)(M_{\lambda\Lambda})_{u_\lambda u_\Lambda} (M_{\lambda\Lambda})_{v_\lambda v_\Lambda} \\ &= (-1)^{n-1} \sqrt{\frac{\mathcal{D}_\Lambda}{\mathcal{D}_\lambda}} (M_{\lambda\Lambda})_{u_\Lambda u_\lambda} (M_{\lambda\Lambda})_{v_\Lambda v_\lambda},\end{aligned} \tag{A.44}$$

where we have used that $\frac{\mathcal{D}_\Lambda}{\mathcal{D}_\lambda} = \frac{d_\Lambda}{d_\lambda} \frac{1}{n} (N_c + \Lambda_a - a)$. Thus the full matrix element for any operator $d_{j,c} b_{i,c}$ is given by

$$\langle \lambda, u_\lambda v_\lambda |\, d_{i,c} b_{j,c} \,| \Lambda, u_\Lambda v_\Lambda \rangle = (-1)^{n-1+i+j} \sqrt{\frac{\mathcal{D}_\Lambda}{\mathcal{D}_\lambda}} \left(\left(\prod_{k=i}^{n-1} T_{k,k+1} \right) . M_{\lambda\Lambda} \right)_{u_\Lambda u_\lambda} \left(\left(\prod_{l=j}^{n-1} T_{l,l+1} \right) . M_{\lambda\Lambda} \right)_{v_\Lambda v_\lambda} . \tag{A.45}$$

A.4 Near-degeneracy and scale factors in basis states

So far, we have exclusively worked with Fock states that have completely distinguishable quarks and antiquarks. In practice, though, many of the basis states will have nearly degenerate quarks in them, meaning that there are multiple quarks that share all quantum numbers except for color charge. In those cases, the basis has to be truncated into one where the nearly degenerate quarks are antisymmetrized. We can do this by working in the full, non-degenerate basis and then truncate the result using the appropriate change of basis

matrices for the states involved in the matrix element. Care must be taken when taking this approach with four-quark and six-quark operators, as the intermediate color singlet states formed by applying part of the full operator may have a higher degree of near-degeneracy that either of the two basis states in the matrix element. If this is not avoided or accounted for, then the result will have extra contributions from states that should not exist. This can be avoided by either finding an alternative way of calculating the matrix elements, as can be done for certain diagonal elements, or by carefully ordering the two-quark color singlet operators so that intermediate states alway have less antisymmetry than the basis states corresponding to the matrix element.

Like the permutation matrices, these projection matrices can be built from the labeled tableau. The procedure for doing this is to first note which quarks and antiquarks need to have their color indices antisymmetrized. Then, we group up all of the labeled tableau that are identical up to permutations of the numerical labels that are antisymmetrized. If a labeled tableau from the full basis does not match a tableau from the reduced basis up to antisymmetrized permutations, then the matrix element between those two tableau must be zero. Finally, we calculate the nonzero elements of the projection matrix using the distances d as defined above between all pairs of boxes that are antisymmetrized. The non-zero elements are found by taking a factor of $1/\sqrt{n!}$ coming from the change in normalization, where n is the number of near-degenerate quarks, and then multiplying a factor of $\mp\sqrt{1 \mp 1/d}$ for every pair within each group of antisymmetrized boxes, where $\pm d$ is defined as it is above for a pair of boxes.

Examples of these projection matrices are given in Fig. A.3. The first example shows the matrix needed when quarks 2 and 3 are antisymmetrized, with the two relevant 4-box tableaux derived in the first of the direct products shown on the left. The second example shows the matrix needed when particles 2, 3, and 4 are all antisymmetrized, with the single relevant 4-box tableau derived in the other direct product shown on the left.

For the first matrix on the left, we first need to group each of the numbered tableau in the full basis with one of the tableau in the reduced basis to see which elements must be

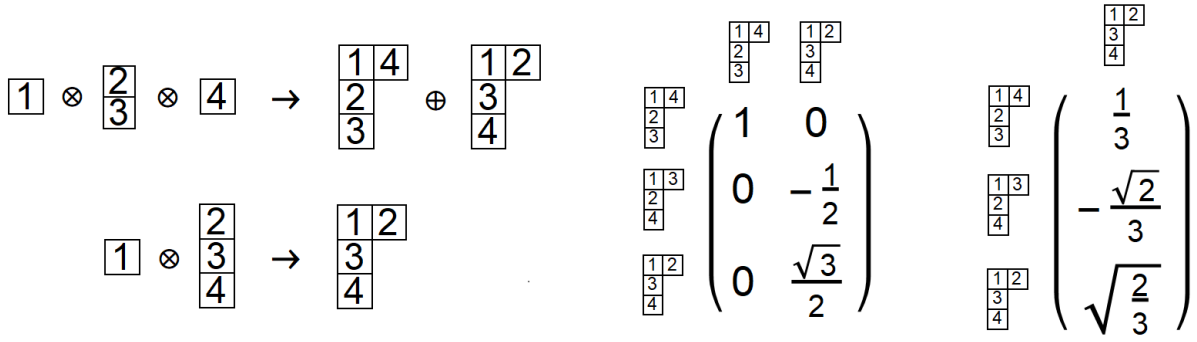

Figure A.3: Two change of basis matrices for the antifundamental irrep of S_4 written in Young's orthogonal basis. The first matrix changes from Young's orthogonal basis to a basis where particles 2 and 3 are antisymmetrized, as illustrated by the first direct product. The second matrix changes from Young's orthogonal basis to a basis where particles 2,3, and 4 are antisymmetrized, as illustrated by the second direct product. The numbered Young tableaux correspond to the basis elements of the vector space and are required to derive these matrices as described in Appendix A.

zero. The first tableau in both bases are identical, and no other tableau match them up to permutations of boxes 2 and 3, so the first column must be all zeros except for the first one. The remaining two tableaux in the full basis match the second tableau in the reduced basis up to a permutation of boxes 2 and 3, so only the first element in the second column is guaranteed to be zero. For the first tableau, we have between boxes 2 and 3 a value $\pm d = -1$, so the value of the first element in the matrix is $\mp\sqrt{(1 \mp 1/d)/n!} = +\sqrt{(1+1)/2!} = 1$. The values of d between boxes 2 and 3 for the remaining two tableaux are $\pm d = 2$ and $\pm d = -2$, so the remaining two elements of the matrix are $-\sqrt{(1-1/2)/2!} = -1/2$ and $+\sqrt{(1+1/2)/2!} = \sqrt{3}/2$.

For the second matrix on the right, there is only one state in the reduced basis, and all three tableaux in the full basis match it up to permutations in boxes 2, 3, and 4, so all elements of the matrix can be nonzero. To find these elements, we need the values of d between boxes 2 and 3, between 2 and 4, and between 3 and 4 for each of the tableaux in the full basis. For the first element and tableau, we have $\pm d_{23} = -1, \pm d_{24} = 2, \pm d_{34} = 3$, so the value of the element is given by

$$(\mp)_{23}(\mp)_{24}(\mp)_{34}\sqrt{(1 \mp 1/d_{23})(1 \mp 1/d_{24})(1 \mp 1/d_{34})/n!} = +\sqrt{(1+1)(1-1/2)(1-1/3)/3!} = 1/3. \tag{A.46}$$

For the next one, we have $\pm d_{23} = 2, \pm d_{24} = -1, \pm d_{34} = -3$, so the matrix element is $-\sqrt{(1-1/2)(1+1)(1+1/3)/3!} = -\sqrt{2}/3$. Finally, the last one has $\pm d_{23} = -2, \pm d_{24} = -3, \pm d_{34} = -1$, which becomes $+\sqrt{(1+1/2)(1+1/3)(1+1)/3!} = \sqrt{2/3}$.

Finally, there will also be a scale factor needed to account for changes in normalization and degeneracy factors. Each creation operator added to a state incurs a factor given by the square root of the near-degeneracy of the added state *after* the operator is applied, while for any annihilation operator we get the square root of the near-degeneracy *before* the state is removed. This is because the near-degeneracy of states needs to be normalized by an extra factor of $1/\sqrt{g!}$, where g is the number of near-degenerate copies of a specific type of quark or antiquark, so when a new state with the same quantum numbers is added we get a state

that is $\sqrt{g+1}$ times bigger than its normalized counterpart. For annihilation operators, this means that the norm is initially off by $1/\sqrt{g}$, but the annihilation operator will also generate g copies of this state since it fails to anticommute with each copy of the quark, so we get an over all factor of $\sqrt{g}$.

Appendix B

QUARK MODEL CHIRAL STATES

B.1 Representations of $\mathbf{S}_3$

Here we will review some necessary aspects of the $\mathbf{S}_3$ representation theory [203, 204]. There are three irreducible representations: the one-dimensional symmetric representation S, the one-dimensional antisymmetric representation A, and the two-dimensional mixed representation $M = (M_\rho, M_\varphi)$. The mixed representations are defined via

$$\mathcal{P}_{12} M_\rho = -M_\rho \quad , \quad \mathcal{P}_{12} M_\varphi = -M_\varphi \; ; \tag{B.1}$$

$$\mathcal{P}_{13} M_\rho = \frac{1}{2} M_\rho - \frac{\sqrt{3}}{2} M_\varphi \quad , \quad \mathcal{P}_{13} M_\varphi = -\frac{\sqrt{3}}{2} M_\rho - \frac{1}{2} M_\varphi \; , \tag{B.2}$$

where $\mathcal{P}_{ab}$ permutes elements a and b. The tensor products of the irreducible representations are given by

$$S \otimes S = S \quad , \quad S \otimes A = A \quad , \quad A \otimes A = S \; ; \tag{B.3}$$

$$S \otimes M = M \quad , \quad A \otimes M = M \quad , \quad M \otimes M = S \oplus A \oplus M \; . \tag{B.4}$$

It is useful to think of the action of $\mathbf{S}_3$ on the states of definite isospin and the states of definite helicity separately and then form the baryonic product state. The product rules for combining mixed representations are

$$S = \frac{1}{\sqrt{2}} (M_\rho M_\rho + M_\varphi M_\varphi) \tag{B.5}$$

$$A = \frac{1}{\sqrt{2}} (M_\rho M_\varphi - M_\varphi M_\rho) \tag{B.6}$$

$$M_\rho = \frac{1}{\sqrt{2}} (M_\rho M_\varphi + M_\varphi M_\rho) \tag{B.7}$$

$$M_\varphi = \frac{1}{\sqrt{2}} (M_\rho M_\rho - M_\varphi M_\varphi) \; . \tag{B.8}$$

B.2 Helicity states

Spin is not a good quantum number however the third component of spin, helicity, is a good quantum number and it is expected that each state of definite helicity is a linear combination of states of definite spin. There is a single $\lambda = +\frac{3}{2}$ state. This state is in the S representation of $\mathbf{S}_3$ and is denoted

$$|\xi^S_{3/2}\rangle \;=\; |\uparrow\uparrow\uparrow\rangle \;. \tag{B.9}$$

The most general $\lambda = +\frac{1}{2}$ state is

$$\alpha_1|\downarrow\uparrow\uparrow\rangle + \alpha_2|\uparrow\downarrow\uparrow\rangle + \alpha_3|\uparrow\uparrow\downarrow\rangle \;, \tag{B.10}$$

where the α's are mixing angles. In general, this decomposes into $S \oplus M$ of $\mathbf{S}_3$. Application of the rules of the previous section yields the normalized helicity states

$$|\xi^S_{1/2}\rangle \;=\; \frac{1}{\sqrt{3}}\left(|\downarrow\uparrow\uparrow\rangle + |\uparrow\downarrow\uparrow\rangle + |\uparrow\uparrow\downarrow\rangle\right) \;; \tag{B.11}$$

$$|\xi^\varphi_{1/2}\rangle \;=\; \frac{1}{\sqrt{6}}\left(2|\uparrow\uparrow\downarrow\rangle - |\uparrow\downarrow\uparrow\rangle - |\downarrow\uparrow\uparrow\rangle\right) \;; \tag{B.12}$$

$$|\xi^\rho_{1/2}\rangle \;=\; \frac{1}{\sqrt{2}}\left(|\uparrow\downarrow\uparrow\rangle - |\downarrow\uparrow\uparrow\rangle\right) \;. \tag{B.13}$$

The negative helicity states are

$$|\xi^S_{-3/2}\rangle \;=\; |\downarrow\downarrow\downarrow\rangle \;; \tag{B.14}$$

$$|\xi^S_{-1/2}\rangle \;=\; \frac{1}{\sqrt{3}}\left(|\uparrow\downarrow\downarrow\rangle + |\downarrow\uparrow\downarrow\rangle + |\downarrow\downarrow\uparrow\rangle\right) \;; \tag{B.15}$$

$$|\xi^\varphi_{-1/2}\rangle \;=\; -\frac{1}{\sqrt{6}}\left(2|\downarrow\downarrow\uparrow\rangle - |\downarrow\uparrow\downarrow\rangle - |\uparrow\downarrow\downarrow\rangle\right) \;; \tag{B.16}$$

$$|\xi^\rho_{-1/2}\rangle \;=\; -\frac{1}{\sqrt{2}}\left(|\downarrow\uparrow\downarrow\rangle - |\uparrow\downarrow\downarrow\rangle\right) \;. \tag{B.17}$$

With this choice of phases, the $|\xi^S_\lambda\rangle$ states form a spin quartet, and the $|\xi^\varphi_\lambda\rangle$ and $|\xi^\rho_\lambda\rangle$ states form independent spin doublets. This has not been assumed but rather is a consequence of the $\mathbf{S}_3$ symmetry.

B.3 Isospin states

Isospin is a good symmetry. There are two **2** representations given by

$$|\phi_p^\varphi\rangle = \frac{1}{\sqrt{6}}\left(2|u\,u\,d\rangle - |u\,d\,u\rangle - |d\,u\,u\rangle\right) ; \tag{B.18}$$

$$|\phi_n^\varphi\rangle = -\frac{1}{\sqrt{6}}\left(2|d\,d\,u\rangle - |d\,u\,d\rangle - |u\,d\,d\rangle\right) , \tag{B.19}$$

and

$$|\phi_p^\rho\rangle = \frac{1}{\sqrt{2}}\left(|u\,d\,u\rangle - |d\,u\,u\rangle\right) ; \tag{B.20}$$

$$|\phi_n^\rho\rangle = -\frac{1}{\sqrt{2}}\left(|d\,u\,d\rangle - |u\,d\,d\rangle\right) . \tag{B.21}$$

There is a single **4** representation given by

$$|\phi^S_{\Delta^{++}}\rangle = |u\,u\,u\rangle ; \tag{B.22}$$

$$|\phi^S_{\Delta^{+}}\rangle = \frac{1}{\sqrt{3}}\left(|u\,u\,d\rangle + |u\,d\,u\rangle + |d\,u\,u\rangle\right) ; \tag{B.23}$$

$$|\phi^S_{\Delta^{0}}\rangle = \frac{1}{\sqrt{3}}\left(|d\,d\,u\rangle + |d\,u\,d\rangle + |u\,d\,d\rangle\right) ; \tag{B.24}$$

$$|\phi^S_{\Delta^{-}}\rangle = |d\,d\,d\rangle . \tag{B.25}$$

B.4 Chiral states

The chiral states are readily constructed as products of the helicity and isospin states. The $\lambda = \pm\frac{1}{2}$ states in the **2** of isospin which transform irreducibly with respect to $\mathbf{S}_3$ are:

$$|S_N,\lambda\rangle = \frac{1}{\sqrt{2}}\left(|\phi_N^\rho\rangle|\xi_\lambda^\rho\rangle + |\phi_N^\varphi\rangle|\xi_\lambda^\varphi\rangle\right) ; \tag{B.26}$$

$$|A_N,\lambda\rangle = \frac{1}{\sqrt{2}}\left(|\phi_N^\rho\rangle|\xi_\lambda^\varphi\rangle - |\phi_N^\varphi\rangle|\xi_\lambda^\rho\rangle\right) ; \tag{B.27}$$

$$|M_N^\rho,\lambda\rangle = \frac{1}{\sqrt{2}}\left(|\phi_N^\rho\rangle|\xi_\lambda^\varphi\rangle + |\phi_N^\varphi\rangle|\xi_\lambda^\rho\rangle\right) ; \tag{B.28}$$

$$|M_N^\varphi,\lambda\rangle = \frac{1}{\sqrt{2}}\left(|\phi_N^\rho\rangle|\xi_\lambda^\rho\rangle - |\phi_N^\varphi\rangle|\xi_\lambda^\varphi\rangle\right) ; \tag{B.29}$$

$$|\bar{M}_N^\rho,\lambda\rangle = |\phi_N^\rho\rangle|\xi_\lambda^S\rangle ; \tag{B.30}$$

$$|\bar{M}_N^\varphi,\lambda\rangle = |\phi_N^\varphi\rangle|\xi_\lambda^S\rangle . \tag{B.31}$$

Now defining

$$|O_N^{\rho,\varphi},\lambda\rangle \;=\; \frac{1}{\sqrt{2}}\left(|M_N^{\rho,\varphi},\lambda\rangle \;+\; |\bar{M}_N^{\rho,\varphi},\lambda\rangle\right)\;; \tag{B.32}$$

$$|N_N^{\rho,\varphi},\lambda\rangle \;=\; \frac{1}{\sqrt{2}}\left(|M_N^{\rho,\varphi},\lambda\rangle \;-\; |\bar{M}_N^{\rho,\varphi},\lambda\rangle\right) \tag{B.33}$$

it is straightforward to show, using the results of the previous section that $|A_N,\frac{1}{2}\rangle$, $|O_N^{\rho},\frac{1}{2}\rangle$, and $|O_N^{\varphi},\frac{1}{2}\rangle$ transform as $(\mathbf{2},\mathbf{1})$, $|A_N,-\frac{1}{2}\rangle$, $|O_N^{\rho},-\frac{1}{2}\rangle$, and $|O_N^{\varphi},-\frac{1}{2}\rangle$ transform as $(\mathbf{1},\mathbf{2})$ and $|S_N,\frac{1}{2}\rangle$, $|N_N^{\rho},\frac{1}{2}\rangle$, and $|N_N^{\varphi},\frac{1}{2}\rangle$ transform as $(\mathbf{2},\mathbf{3})_{\mathbf{2}}$, $|S_N,-\frac{1}{2}\rangle$, $|N_N^{\rho},-\frac{1}{2}\rangle$, and $|N_N^{\varphi},-\frac{1}{2}\rangle$ transform as $(\mathbf{3},\mathbf{2})_{\mathbf{2}}$. The $\lambda=\pm\frac{3}{2}$ states in the $\mathbf{2}$ of isospin which transform irreducibly with respect to $\mathbf{S}_3$ are:

$$|P_N^{\rho},\lambda\rangle \;=\; |\phi_N^{\rho}\rangle|\xi_\lambda^S\rangle\;; \tag{B.34}$$

$$|P_N^{\varphi},\lambda\rangle \;=\; |\phi_N^{\varphi}\rangle|\xi_\lambda^S\rangle\;. \tag{B.35}$$

The $|P_N^{\rho},\frac{3}{2}\rangle$ states transform as $(\mathbf{1},\mathbf{2})$ and the $|P_N^{\rho},-\frac{3}{2}\rangle$ states transform as $(\mathbf{2},\mathbf{1})$. The $\lambda=\pm\frac{1}{2}$ states in the $\mathbf{4}$ of isospin which transform irreducibly with respect to $\mathbf{S}_3$ are:

$$|S_\Delta,\lambda\rangle \;=\; |\phi_\Delta^S\rangle|\xi_\lambda^S\rangle\;; \tag{B.36}$$

$$|Q_\Delta^{\varphi},\lambda\rangle \;=\; |\phi_\Delta^S\rangle|\xi_\lambda^{\varphi}\rangle\;; \tag{B.37}$$

$$|Q_\Delta^{\rho},\lambda\rangle \;=\; |\phi_\Delta^S\rangle|\xi_\lambda^{\rho}\rangle\;. \tag{B.38}$$

The $|S_\Delta,\frac{1}{2}\rangle$, $|Q_\Delta^{\varphi},\frac{1}{2}\rangle$ and $|Q_\Delta^{\rho},\frac{1}{2}\rangle$ states transform as $(\mathbf{2},\mathbf{3})_{\mathbf{4}}$, and $|S_\Delta,-\frac{1}{2}\rangle$, $|Q_\Delta^{\varphi},-\frac{1}{2}\rangle$ and $|Q_\Delta^{\rho},-\frac{1}{2}\rangle$ states transform as $(\mathbf{3},\mathbf{2})_{\mathbf{4}}$. Finally, the $\lambda=\pm\frac{3}{2}$ states in the $\mathbf{4}$ of isospin which transform irreducibly with respect to $\mathbf{S}_3$ are:

$$|S_\Delta,\lambda\rangle \;=\; |\phi_\Delta^S\rangle|\xi_\lambda^S\rangle\;. \tag{B.39}$$

the $|S_\Delta,\frac{3}{2}\rangle$ states transform as $(\mathbf{1},\mathbf{4})$ and the $|S_\Delta,-\frac{3}{2}\rangle$ states transform as $(\mathbf{4},\mathbf{1})$. Note that the states $|S_N,\lambda\rangle$, $|A_N,\lambda\rangle$ and $|Q_\Delta^{\rho,\varphi},\lambda\rangle$ for $\lambda=\pm\frac{1}{2}$ and the states $|S_\Delta,\lambda\rangle$ for $\lambda=\pm\frac{1}{2},\pm\frac{3}{2}$ are spin eigenstates, whereas the states $|N_N^{\rho,\varphi},\lambda\rangle$ and $|O_N^{\rho,\varphi},\lambda\rangle$ for $\lambda=\pm\frac{1}{2}$ and $|P_N^{\rho,\varphi},\lambda\rangle$ for

$\lambda = \pm\frac{1}{2}$ transform reducibly. In particular,

$$\hat{S}^+|N_N^{\rho,\varphi}, -\tfrac{1}{2}\rangle = -\tfrac{1}{2}\left(|O_N^{\rho,\varphi}, \tfrac{1}{2}\rangle - 3|N_N^{\rho,\varphi}, \tfrac{1}{2}\rangle\right) ; \tag{B.40}$$

$$\hat{S}^+|O_N^{\rho,\varphi}, -\tfrac{1}{2}\rangle = \tfrac{1}{2}\left(3|O_N^{\rho,\varphi}, \tfrac{1}{2}\rangle - |N_N^{\rho,\varphi}, \tfrac{1}{2}\rangle\right) ; \tag{B.41}$$

$$\hat{S}^+|P_N^{\rho,\varphi}, -\tfrac{3}{2}\rangle = \sqrt{\tfrac{3}{2}}\left(|O_N^{\rho,\varphi}, -\tfrac{1}{2}\rangle - |N_N^{\rho,\varphi}, -\tfrac{1}{2}\rangle\right) ; \tag{B.42}$$

$$\hat{S}^+|N_N^{\rho,\varphi}, \tfrac{1}{2}\rangle = -\sqrt{\tfrac{3}{2}}|P_N^{\rho,\varphi}, \tfrac{3}{2}\rangle ; \tag{B.43}$$

$$\hat{S}^+|O_N^{\rho,\varphi}, \tfrac{1}{2}\rangle = \sqrt{\tfrac{3}{2}}|P_N^{\rho,\varphi}, \tfrac{3}{2}\rangle . \tag{B.44}$$

In summary, the states of definite isospin and chiral symmetry can be expressed in terms of the states transforming irreducibly with respect to $\mathbf{S}_3$ as

$$\begin{aligned}
|(\mathbf{2},\mathbf{1}), \tfrac{1}{2}\rangle_{A,\rho,\phi} &\equiv \{|A_N, \tfrac{1}{2}\rangle, |O_N^{\rho}, \tfrac{1}{2}\rangle, |O_N^{\varphi}, \tfrac{1}{2}\rangle\} ; \\
|(\mathbf{2},\mathbf{3})_{\mathbf{2}}, \tfrac{1}{2}\rangle_{S,\rho,\phi} &\equiv \{|S_N, \tfrac{1}{2}\rangle, |N_N^{\rho}, \tfrac{1}{2}\rangle, |N_N^{\varphi}, \tfrac{1}{2}\rangle\} ; \\
|(\mathbf{1},\mathbf{2}), \tfrac{3}{2}\rangle_{\rho,\phi} &\equiv \{|P_N^{\rho}, \tfrac{3}{2}\rangle, |P_N^{\varphi}, \tfrac{3}{2}\rangle\} ; \\
|(\mathbf{2},\mathbf{3})_{\mathbf{4}}, \tfrac{1}{2}\rangle_{S,\rho,\phi} &\equiv \{|S_\Delta, \tfrac{1}{2}\rangle, |Q_\Delta^{\rho}, \tfrac{1}{2}\rangle, |Q_\Delta^{\varphi}, \tfrac{1}{2}\rangle\} ; \\
|(\mathbf{1},\mathbf{4}), \tfrac{3}{2}\rangle &\equiv |S_\Delta, \tfrac{3}{2}\rangle,
\end{aligned} \tag{B.45}$$

and

$$\begin{aligned}
|(\mathbf{1},\mathbf{2}), -\tfrac{1}{2}\rangle_{A,\rho,\phi} &\equiv \{|A_N, -\tfrac{1}{2}\rangle, |O_N^{\rho}, -\tfrac{1}{2}\rangle, |O_N^{\varphi}, -\tfrac{1}{2}\rangle\} ; \\
|(\mathbf{3},\mathbf{2})_{\mathbf{2}}, -\tfrac{1}{2}\rangle_{S,\rho,\phi} &\equiv \{|S_N, -\tfrac{1}{2}\rangle, |N_N^{\rho}, -\tfrac{1}{2}\rangle, |N_N^{\varphi}, -\tfrac{1}{2}\rangle\} ; \\
|(\mathbf{2},\mathbf{1}), \tfrac{3}{2}\rangle_{\rho,\phi} &\equiv \{|P_N^{\rho}, -\tfrac{3}{2}\rangle, |P_N^{\varphi}, -\tfrac{3}{2}\rangle\} ; \\
|(\mathbf{3},\mathbf{2})_{\mathbf{4}}, -\tfrac{1}{2}\rangle_{S,\rho,\phi} &\equiv \{|S_\Delta, -\tfrac{1}{2}\rangle, |Q_\Delta^{\rho}, -\tfrac{1}{2}\rangle, |Q_\Delta^{\varphi}, -\tfrac{1}{2}\rangle\} ; \\
|(\mathbf{4},\mathbf{1}), -\tfrac{3}{2}\rangle &\equiv |S_\Delta, -\tfrac{3}{2}\rangle.
\end{aligned} \tag{B.46}$$

B.5 $SU(4)$ *states*

The 64 chiral states listed in Eqs. (B.45) and (B.46) must map onto states obtained by placing the three quarks in the fundamental of $SU(4)$. The available states then transform in the

product: $\mathbf{4}\otimes\mathbf{4}\otimes\mathbf{4}=\mathbf{4}_A\oplus\mathbf{20}_S\oplus\mathbf{20}_M^{\rho}\oplus\mathbf{20}_M^{\varphi}$ where these irreducible $SU(4)$ representations in turn decompose to the spin-isospin states:

$$\begin{aligned}
&\mathbf{4}_A:\ {}^{\mathbf{2}}N\ ;\\
&\mathbf{20}_S:\ {}^{\mathbf{2}}N\oplus{}^{\mathbf{4}}\Delta\ ;\\
&\mathbf{20}_M^{\rho,\varphi}:\ {}^{\mathbf{2}}N\oplus{}^{\mathbf{4}}N\oplus{}^{\mathbf{2}}\Delta\ .
\end{aligned}\tag{B.47}$$

It is a simple matter to find the relation between the chiral states and the $SU(4)$ states:

$$|\mathbf{4}_A,{}^{\mathbf{2}}N,\tfrac{1}{2}\rangle\ =\ |(\mathbf{2},\mathbf{1})\,,\,\tfrac{1}{2}\rangle_A\ ;\tag{B.48}$$

$$\begin{aligned}
|\mathbf{20}_S,{}^{\mathbf{2}}N,\tfrac{1}{2}\rangle\ &=\ |(\mathbf{2},\mathbf{3})_{\mathbf{2}}\,,\,\tfrac{1}{2}\rangle_S\ ;\\
|\mathbf{20}_S,{}^{\mathbf{4}}\Delta,\tfrac{1}{2}\rangle\ &=\ |(\mathbf{2},\mathbf{3})_{\mathbf{4}}\,,\,\tfrac{1}{2}\rangle_S\ ;\\
|\mathbf{20}_S,{}^{\mathbf{4}}\Delta,\tfrac{3}{2}\rangle\ &=\ |(\mathbf{1},\mathbf{4})\,,\,\tfrac{3}{2}\rangle\ ;
\end{aligned}\tag{B.49}$$

$$\begin{aligned}
|\mathbf{20}_M^{\rho,\varphi},{}^{\mathbf{2}}N,\tfrac{1}{2}\rangle\ &=\ \tfrac{1}{\sqrt{2}}\left(|(\mathbf{2},\mathbf{1})\,,\,\tfrac{1}{2}\rangle_{\rho,\varphi}\ +\ |(\mathbf{2},\mathbf{3})_{\mathbf{2}}\,,\,\tfrac{1}{2}\rangle_{\rho,\varphi}\right)\ ;\\
|\mathbf{20}_M^{\rho,\varphi},{}^{\mathbf{4}}N,\tfrac{1}{2}\rangle\ &=\ \tfrac{1}{\sqrt{2}}\left(|(\mathbf{2},\mathbf{1})\,,\,\tfrac{1}{2}\rangle_{\rho,\varphi}\ -\ |(\mathbf{2},\mathbf{3})_{\mathbf{2}}\,,\,\tfrac{1}{2}\rangle_{\rho,\varphi}\right)\ ;\\
|\mathbf{20}_M^{\rho,\varphi},{}^{\mathbf{4}}N,\tfrac{3}{2}\rangle\ &=\ |(\mathbf{1},\mathbf{2})\,,\,\tfrac{3}{2}\rangle_{\rho,\phi}\ ;\\
|\mathbf{20}_M^{\rho,\varphi},{}^{\mathbf{2}}\Delta,\tfrac{1}{2}\rangle\ &=\ |(\mathbf{2},\mathbf{3})_{\mathbf{4}}\,,\,\tfrac{1}{2}\rangle_{\rho,\varphi}\ .
\end{aligned}\tag{B.50}$$

Appendix C

IRREDUCIBLE CHIRAL TENSORS

C.1 N *in a* $(\mathbf{2},\mathbf{1})$ *or a* $(\mathbf{1},\mathbf{2})$

Here the positive helicity baryon states transforming as $(\mathbf{2},\mathbf{1})$ or $(\mathbf{1},\mathbf{2})$ will be constructed. We have a $\lambda = +\frac{1}{2}$ state transforming as $(\mathbf{2},\mathbf{1})$ and a $\lambda = +\frac{3}{2}$ state transforming as $(\mathbf{1},\mathbf{2})$. The negative helicity states are then obtained by acting with the $\mathcal{Y}$ operator as in Eq. (3.39).

Consider the field operator S_L that creates a state that transforms as $(\mathbf{2},\mathbf{1})$ under $SU(2)_L \otimes SU(2)_R$; that is,

$$S_L^a \to (L)_b^a \, S_L^b \ . \tag{C.1}$$

This isodoublet is assigned particle content

$$S_1 = p_S \quad , \quad S_2 = n_S \ . \tag{C.2}$$

The field operator creates the isodoublet state $|S_L^a\,,\,\lambda\rangle = |(\mathbf{2},\mathbf{1})^a\,,\,\lambda\rangle$, where $\lambda = \frac{1}{2}$ or $-\frac{3}{2}$. The transformation property of the field operator S_L is expressed algebraically as

$$[\,\tilde{Q}_L^\alpha\,,\,S_L^a\,] \;=\; S_L^b (T^\alpha)^{ba} \quad , \quad [\,\tilde{Q}_R^\alpha\,,\,S_L^a\,] \;=\; 0 \ . \tag{C.3}$$

Acting with these commutators on the vacuum state then gives

$$\tilde{Q}^\alpha |S_L^a\,,\,\lambda\rangle \;=\; (T^\alpha)^{ba} |S_L^b\,,\,\lambda\rangle \quad , \quad \tilde{Q}_5^\alpha |S_L^a\,,\,\lambda\rangle \;=\; -(T^\alpha)^{ba} |S_L^b\,,\,\lambda\rangle \ . \tag{C.4}$$

Note that both charges annihilate the vacuum state. The axial charges can then be read off; with the axial charge defined as

$$g_A \;\equiv\; \langle\, p_S\,,\,\tfrac{1}{2}\,|\left(\tilde{Q}_5^1 + i\tilde{Q}_5^2\right)|n_S\,,\,\tfrac{1}{2}\,\rangle \;=\; \langle\, p_S\,,\,\tfrac{1}{2}\,|\,2\tilde{Q}_5^3\,|p_S\,,\,\tfrac{1}{2}\,\rangle \ , \tag{C.5}$$

one finds $g_A = -1$. It is now straightforward to construct the state that transforms as $(\mathbf{2},\mathbf{1})$ in the chiral basis. The $(\mathbf{2},\mathbf{1})$ state of opposite helicity can be obtained by acting with the normality operator. Equivalently one constructs the field operator S_R that creates a state that transforms as $(\mathbf{1},\mathbf{2})$ under $SU(2)_L \otimes SU(2)_R$; that is, $|S_R^a\,,\,\lambda'\rangle = |(\mathbf{1},\mathbf{2})^a\,,\,\lambda'\rangle$, where $\lambda' = -\frac{1}{2}$ or $\frac{3}{2}$. Algebraically this operator satisfies

$$[\,\tilde{Q}_R^\alpha\,,\,S_R^a\,] \;=\; S_R^b (T^\alpha)^{ba} \quad , \quad [\,\tilde{Q}_L^\alpha\,,\,S_R^a\,] \;=\; 0\;. \tag{C.6}$$

Proceeding as above one then finds, for instance, $g_A = 1$.

C.2 Δ *in a* $(\mathbf{1},\mathbf{4})$

Here the positive helicity baryon states transforming as $(\mathbf{1},\mathbf{4})$ will be constructed. We have a $\lambda = +\frac{3}{2}$ state transforming as $(\mathbf{1},\mathbf{4})$. The negative helicity states are then obtained by acting with the $\mathcal{Y}$ operator as in Eq. (3.39).

We introduce the field D which transforms as $(\mathbf{1},\mathbf{4})$ under $SU(2)_L \otimes SU(2)_R$ and creates the isoquartet state $|D^{abc}\,,\,\frac{3}{2}\rangle = |(\mathbf{1},\mathbf{4})^{abc}\,,\,\frac{3}{2}\rangle$. The transformation property is

$$D_{abc} \to (R)_a^{a'}\,(R)_b^{b'}\,(R)_c^{c'}\,D_{a'b'c'} \quad . \tag{C.7}$$

D is symmetric under the interchange of all of the right-handed indices and therefore transforms like $S_R S_R S_R$. Using the results of the previous section it follows that D satisfies the algebraic constraints

$$[\,\tilde{Q}^\alpha\,,\,D^{abc}\,] \;=\; [\,\tilde{Q}_5^\alpha\,,\,D^{abc}\,] \;=\; (T^\alpha)^{da} D^{dbc} \;+\; (T^\alpha)^{db} D^{adc} \;+\; (T^\alpha)^{dc} D^{abd}\;. \tag{C.8}$$

It is then easy to work out the isospin transformation properties and find the particle content

$$\begin{aligned} &D_{111} = \Delta_D^{++} \quad , \quad \frac{1}{\sqrt{3}}\,(D_{112} + D_{121} + D_{211}) = \Delta_D^{+} \\ &\frac{1}{\sqrt{3}}\,(D_{122} + D_{221} + D_{212}) = \Delta_D^{0} \quad , \quad D_{222} = \Delta_D^{-}\;. \end{aligned} \tag{C.9}$$

Defining

$$\mathcal{H}_{\Delta\Delta} \;\equiv\; -3\sqrt{3}\langle\,\Delta_D^{++}\,,\,\tfrac{3}{2}\,|\,\left(\tilde{Q}_5^1 \,+\, i\tilde{Q}_5^2\right)|\Delta_D^{+}\,,\,\tfrac{3}{2}\,\rangle\;, \tag{C.10}$$

then gives $\mathcal{H}_{\Delta\Delta} = -3$.

C.3 N *and* Δ *in a* $(\mathbf{2},\mathbf{3})$

Here the positive helicity baryon states transforming as $(\mathbf{2},\mathbf{3})$. We have a $\lambda = +\frac{1}{2}$ state transforming as $(\mathbf{2},\mathbf{3})$. The negative helicity states are then obtained by acting with the $\mathcal{Y}$ operator as in Eq. (3.39).

It is straightforward to embed an N state and a Δ state into a single irreducible representation of $SU(2)_L \otimes SU(2)_R$, the $(\mathbf{2},\mathbf{3})$. There are several ways to do this. Consider the field operator Γ_R^α which transforms as $(\mathbf{1},\mathbf{3})$ and therefore satisfies the algebraic constraints

$$[\,\tilde{Q}_R^\alpha\,,\,\Gamma_R^\beta\,] \;=\; i\epsilon^{\alpha\beta\gamma}\Gamma_R^\gamma \quad , \quad [\,\tilde{Q}_L^\alpha\,,\,\Gamma_R^\beta\,] \;=\; 0\;. \tag{C.11}$$

The tensor $t_a^\alpha = S_a^L\Gamma_R^\alpha$ with one fundamental and one adjoint index therefore transforms as $(\mathbf{2},\mathbf{1})\otimes(\mathbf{1},\mathbf{3}) = (\mathbf{2},\mathbf{3})$, and satisfies the algebraic constraints

$$\begin{aligned}
[\,\tilde{Q}^\alpha\,,\,t_a^\beta\,] &= (T^\alpha)_{ba}t_b^\beta \;+\; i\epsilon^{\alpha\beta\gamma}t_a^\gamma \\
[\,\tilde{Q}_5^\alpha\,,\,t_a^\beta\,] &= -(T^\alpha)_{ba}t_b^\beta \;+\; i\epsilon^{\alpha\beta\gamma}t_a^\gamma\;.
\end{aligned} \tag{C.12}$$

This representation has mixed transformation properties under isospin, transforming as $\mathbf{2}\oplus\mathbf{4}$. The states of definite isospin are easily found to be

$$\begin{aligned}
\frac{1}{\sqrt{3}}\left(-it_2^1 + t_2^2 - it_1^3\right) &= p_t \\
\frac{1}{\sqrt{3}}\left(-it_1^1 - t_1^2 + it_2^3\right) &= n_t
\end{aligned} \tag{C.13}$$

for the $\mathbf{2}$ and

$$\begin{aligned}
\frac{1}{\sqrt{2}}\left(-it_1^1 + t_1^2\right) &= \Delta_t^{++} \\
\frac{1}{\sqrt{6}}\left(-it_2^1 + t_2^2 + 2it_1^3\right) &= \Delta_t^{+} \\
\frac{1}{\sqrt{6}}\left(it_1^1 + t_1^2 + 2it_2^3\right) &= \Delta_t^{0} \\
\frac{1}{\sqrt{2}}\left(it_2^1 + t_2^2\right) &= \Delta_t^{-}
\end{aligned} \tag{C.14}$$

for the **4**. One then finds obtains

$$g_A \;=\; \frac{5}{3} \;\;,\;\; \mathcal{C}_{\Delta N} \;=\; -2 \;\;,\;\; \mathcal{H}_{\Delta\Delta} \;=\; -3 \quad , \tag{C.15}$$

where

$$\mathcal{C}_{\Delta N} \;\equiv\; -\sqrt{\frac{3}{2}} \langle\, \Delta_t^{++} \,,\, \tfrac{1}{2} \,|\, \left(\tilde{Q}_5^1 + i\tilde{Q}_5^2 \right) |p_t \,,\, \tfrac{1}{2} \,\rangle \;. \tag{C.16}$$

Appendix D

PRINCIPAL VALUES IN DLCQ

This appendix elaborates on our choice of principle value for the momentum space potentials in 1+1d QCD. For a more general definition of the principle value given by

$$\left(\mathscr{P}\left[\frac{-1}{(n_2-n_3)^2}\right]\delta_{n_1+n_2,n_3+n_4}\right)_{n_1=n_4,n_2=n_3}=f_{n_1}+f_{n_2}. \tag{D.1}$$

The parts of the potential that require a principle value are given by

$$\begin{aligned}V_B=&-\frac{\xi^2 n_p}{2N_c}\sum_{n_1,n_2,n_3,n_4}\mathscr{P}\left[\frac{-1}{(n_2-n_3)^2}\right]\delta_{n_1+n_2,n_3+n_4}\\&*\left(b^\dagger_{a,f,n_1}b^\dagger_{b,g,n_2}b_{a,g,n_3}b_{b,f,n_4}-\frac{1}{N_c}b^\dagger_{a,f,n_1}b^\dagger_{b,g,n_2}b_{b,g,n_3}b_{a,f,n_4}+(b\to d)\right),\end{aligned} \tag{D.2}$$

$$\begin{aligned}V_M=&\frac{\xi^2 n_p}{N_c}\sum_{n_1,n_2,n_3,n_4}\mathscr{P}\left[\frac{-1}{(n_2-n_3)^2}\right]\delta_{n_1+n_2,n_3+n_4}\\&*\left(b^\dagger_{a,f,n_1}d^\dagger_{a,g,n_2}d_{b,g,n_3}b_{b,f,n_4}-\frac{1}{N_c}b^\dagger_{a,f,n_1}d^\dagger_{b,g,n_2}d_{b,g,n_3}b_{a,f,n_4}\right).\end{aligned} \tag{D.3}$$

When the incoming and outgoing momenta are the same, then we have

$$\begin{aligned}(V_B)_0=&-\frac{\xi^2 n_p}{2N_c}\sum_{n_1,n_2}(f_{n_1}+f_{n_2})\\&*\left(b^\dagger_{a,f,n_1}b^\dagger_{b,g,n_2}b_{a,g,n_2}b_{b,f,n_1}-\frac{1}{N_c}b^\dagger_{a,f,n_1}b^\dagger_{b,g,n_2}b_{b,g,n_2}b_{a,f,n_1}+(b\to d)\right),\end{aligned} \tag{D.4}$$

$$\begin{aligned}(V_M)_0=&\frac{\xi^2 n_p}{N_c}\sum_{n_1,n_2}(f_{n_1}+f_{n_2})\\&*\left(b^\dagger_{a,f,n_1}d^\dagger_{a,g,n_2}d_{b,g,n_2}b_{b,f,n_1}-\frac{1}{N_c}b^\dagger_{a,f,n_1}d^\dagger_{b,g,n_2}d_{b,g,n_2}b_{a,f,n_1}\right).\end{aligned} \tag{D.5}$$

With $F_q = \sum_n (f_n) b^\dagger_{a,f,n} b_{a,f,n}$ and $F_{\bar{q}} = \sum_n (f_n) d^\dagger_{a,f,n} d_{a,f,n}$, these potentials become

$$(V_B + V_M)_0 = \frac{\xi^2 n_p}{N_c^2} \left(N_c U_0 + (N_q - N_{\bar{q}})(F_q - F_{\bar{q}}) - F_q - F_{\bar{q}} \right). \tag{D.6}$$

$$\begin{aligned} U_0 = & \sum_{n_1,n_2} (f_{n_1} + f_{n_2}) \left(b^\dagger_{a,f,n_1} d^\dagger_{a,g,n_2} d_{b,g,n_2} b_{b,f,n_1} \right) \\ & - \sum_{n_1,n_2} f_{n_1} \left(b^\dagger_{a,f,n_1} b^\dagger_{b,g,n_2} b_{a,g,n_2} b_{b,f,n_1} + (b \to d) \right) \end{aligned} \tag{D.7}$$

The state vector for a set of quarks and antiquarks ψ in a color singlet α is given by

$$|\psi, \alpha\rangle = T^\alpha_{\{a_i\},\{a_j\}} \prod_i \left(b^\dagger_{a_i,f_i,n_i} \right) \prod_j \left(d^\dagger_{a_j,f_j,n_j} \right) |0\rangle , \tag{D.8}$$

where $|0\rangle$ is the light-cone vacuum. The operator U_0 acting on this state gives

$$\begin{aligned} U_0 |\psi, \alpha\rangle = & \left(\sum_I f_{n_I} \left(\sum_J T^{\Delta_{IJ}(\alpha)}_{\{a_i\},\{a_j\}} - \sum_{I' \neq I} T^{X^b_{II'}(\alpha)}_{\{a_i\},\{a_j\}} \right) \right. \\ & \left. + \sum_J f_{n_J} \left(\sum_I T^{\Delta_{IJ}(\alpha)}_{\{a_i\},\{a_j\}} - \sum_{J' \neq J} T^{X^d_{JJ'}(\alpha)}_{\{a_i\},\{a_j\}} \right) \right) \\ & * \prod_i \left(b^\dagger_{a_i,f_i,n_i} \right) \prod_j \left(d^\dagger_{a_j,f_j,n_j} \right) |0\rangle , \end{aligned} \tag{D.9}$$

where

$$T^{\Delta_{IJ}(\alpha)}_{\{a_i\},\{a_j\}} = \sum_A \left(T^\alpha_{\{a_i\},\{a_j\}} \right)_{a_I = a_J = A} \delta_{a_I, a_J}, \tag{D.10}$$

$$T^{X^b_{II'}(\alpha)}_{\{a_i\},\{a_j\}} = \left(T^\alpha_{\{a_i\},\{a_j\}} \right)_{a_I \leftrightarrow a_{I'}}, \tag{D.11}$$

$$T^{X^d_{JJ'}(\alpha)}_{\{a_i\},\{a_j\}} = \left(T^\alpha_{\{a_i\},\{a_j\}} \right)_{a_J \leftrightarrow a_{J'}}. \tag{D.12}$$

Since T^α corresponds to an $SU(N_c)$ color singlet, the Δ_{IJ} piece summed over the antiquark

indices can be written as

$$\begin{aligned}
\sum_J T^{\Delta_{IJ}(\alpha)}_{\{a_i\},\{a_j\}} &= \sum_J \sum_{b_I,b_J} \left(T^{\alpha}_{\{a_i\},\{a_j\}}\right)_{a_I=b_I,a_J=b_J} \delta_{b_I,b_J}\delta_{a_I,a_J} \\
&= \sum_J \sum_{b_I,b_J} \left(T^{\alpha}_{\{a_i\},\{a_j\}}\right)_{a_I=b_I,a_J=b_J} (2(T^A)_{a_I,b_I}(T^A)_{a_J,b_J} + \frac{1}{N_c}\delta_{a_I,b_I}\delta_{a_J,b_J}) \\
&= \sum_{I'\neq I} \sum_{b_I,b'_I} \left(T^{\alpha}_{\{a_i\},\{a_j\}}\right)_{a_I=b_I,a'_I=b'_I} 2(T^A)_{a_I,b_I}(T^A)_{a'_I,b'_I} + \sum_{b_I,c_I} 2(T^A)_{a_I,b_I}(T^A)_{b_I,c_I} \left(T^{\alpha}_{\{a_i\},\{a_j\}}\right)_{a_I=c_I} \\
&\quad + \frac{1}{N_c} N_{\bar{q}} T^{\alpha}_{\{a_i\},\{a_j\}} \\
&= \sum_{I'\neq I} \left(T^{\alpha}_{\{a_i\},\{a_j\}}\right)_{a_I\leftrightarrow a'_I} + (N_c - \frac{1}{N_c}(N_q - N_{\bar{q}}))T^{\alpha}_{\{a_i\},\{a_j\}} \\
&= \sum_{I'\neq I} T^{X^b_{II'}(\alpha)}_{\{a_i\},\{a_j\}} + (N_c - B)T^{\alpha}_{\{a_i\},\{a_j\}}. \qquad \text{(D.13)}
\end{aligned}$$

Similarly, the Δ_{IJ} piece summed over the quark indices can be written as

$$\sum_I T^{\Delta_{IJ}(\alpha)}_{\{a_i\},\{a_j\}} = \sum_{J'\neq J} T^{X^d_{JJ'}(\alpha)}_{\{a_i\},\{a_j\}} + (N_c + B)T^{\alpha}_{\{a_i\},\{a_j\}}. \qquad \text{(D.14)}$$

The expressions in parenthesis above can then be written as

$$\left(\sum_J T^{\Delta_{IJ}(\alpha)}_{\{a_i\},\{a_j\}} - \sum_{I'\neq I} T^{X^b_{II'}(\alpha)}_{\{a_i\},\{a_j\}}\right) = (N_c - B)T^{\alpha}_{\{a_i\},\{a_j\}} \qquad \text{(D.15)}$$

$$\left(\sum_I T^{\Delta_{IJ}(\alpha)}_{\{a_i\},\{a_j\}} - \sum_{J'\neq J} T^{X^d_{JJ'}(\alpha)}_{\{a_i\},\{a_j\}}\right) = (N_c + B)T^{\alpha}_{\{a_i\},\{a_j\}}. \qquad \text{(D.16)}$$

Therefore, U_0 acting on a color singlet vector is given by

$$\begin{aligned}
U_0 \left|\psi,\alpha\right\rangle &= \left(\sum_I f_{n_I}(N_c - B) + \sum_J f_{n_J}(N_c + B)\right)\left|\psi,\alpha\right\rangle \\
&= \left((F_q + F_{\bar{q}})N_c - (F_q - F_{\bar{q}})B\right)\left|\psi,\alpha\right\rangle . \qquad \text{(D.17)}
\end{aligned}$$

and the forward scattering part of the potentials are given by

$$\begin{aligned}
(V_B + V_M)_0 \left|\psi,\alpha\right\rangle &= \frac{\xi^2 n_p}{N_c^2}\left((F_q + F_{\bar{q}})N_c^2 - (F_q - F_{\bar{q}})N_c B + N_c B(F_q - F_{\bar{q}}) - F_q - F_{\bar{q}}\right)\left|\psi,\alpha\right\rangle \\
&= \xi^2 n_p \left(1 - \frac{1}{N_c^2}\right)(F_q + F_{\bar{q}})\left|\psi,\alpha\right\rangle . \qquad \text{(D.18)}
\end{aligned}$$

Thus even with a fairly general expression for the principle value the contribution to the Hamiltonian will be fairly simple, and this is what allows the V_2 term to be subsumed into the principle value of the momentum space potential.

Appendix E

PDFS IN DLCQ

The null plane field operator is written in terms of creation and annihilation operators by

$$q(y) = \int_0^\infty \frac{dk}{2\pi\sqrt{2k}} \left(b(k)e^{-iky} + d^\dagger(k)e^{iky}\right) \tag{E.1}$$

$$b(k) = \sqrt{2k}\int_{-\infty}^{\infty} dy\ q(y)e^{iky} \tag{E.2}$$

$$d(k) = \sqrt{2k}\int_{-\infty}^{\infty} dy\ q^\dagger(y)e^{iky} \tag{E.3}$$

The PDF is defined as

$$f_q(x) = \frac{1}{4\pi}\int_{-\infty}^{\infty} dy\ e^{-ixPy}\left\langle P\right| q^\dagger(y)q(0)\left|P\right\rangle \tag{E.4}$$

$$f_{\bar{q}}(x) = \frac{1}{4\pi}\int_{-\infty}^{\infty} dy\ e^{-ixPy}\left\langle P\right| q(y)q^\dagger(0)\left|P\right\rangle \tag{E.5}$$

After discretization, we have

$$q(y) = \sqrt{\frac{a}{2\pi}}\sum_{n=1/2}^{\infty}\left(b_n e^{-iany} + d_n^\dagger e^{iany}\right) \tag{E.6}$$

$$b_n = \sqrt{\frac{a}{2\pi}}\int_{-\pi/a}^{\pi/a} dy\ q(y)e^{iany} \tag{E.7}$$

$$d_n = \sqrt{\frac{a}{2\pi}}\int_{-\pi/a}^{\pi/a} dy\ q^\dagger(y)e^{iany} \tag{E.8}$$

and

$$f_q(n) = \int_{-\pi/a}^{\pi/a} dy\ e^{-iany} \langle K| q^\dagger(y)q(0) |K\rangle$$
$$= \langle K| b_n^\dagger b_n |K\rangle \tag{E.9}$$
$$f_{\bar{q}}(n) = \int_{-\pi/a}^{\pi/a} dy\ e^{-iany} \langle K| q(y)q^\dagger(0) |K\rangle$$
$$= \langle K| d_n^\dagger d_n |K\rangle \tag{E.10}$$

with $\langle K|\ K'\rangle = \delta_{KK'}$ and $\{b_m^\dagger, b_n\} = \{d_m^\dagger, d_n\} = \delta_{mn}$.